CHARACTERISTICS OF A TRANSFERRED-ARC PLASMA

A

THESIS

by

M. TANJU MEHMETOĞLU, B.Sc., M.Sc.

Department of Chemical Engineering - McGill University

Under the Supervision of Dr. W.H. Gauvin

Submitted to the Faculty of Graduate Studies
and Research of McGill University in partial
fulfillment of the requirements for the
degree of Doctor of Philosophy

McGill University
MONTREAL, Canada

March 1980

ABSTRACT

The basic characteristics of a transferred arc argon plasma were determined. A cathode assembly suitable for transferring the electric arc to a molten metal bath or to a cooled anode was designed and constructed to produce the plasma in open air. It included provision for the injection of secondary gas into the arc column.

The measured electrical characteristics indicated that the sustained voltage depended strongly on the arc length and much less on current. The inlet gas velocity past the cathode tip was determined to be an important operating parameter, rather than the volumetric gas flowrate.

The measurement of the axial and radial profiles of temperature was effected with ± 8% accuracy by a novel diagnostic technique based on the determination of the variations in the outputs of a two-wavelength pyrometer that views a small section of the plasma, as the latter is swept rapidly by a blocking element. Temperatures up to 18,500 K were observed on the axis of the plasma column.

A sweeping microprobe was used to measure the axial and radial profiles of velocity. Velocities up to 190 m/s were recorded. The presence of a relatively colder flow surrounding the plasma column was detected. Mass and energy balances performed by taking this flow into account agreed with the measured input rates.

RÉSUMÉ

Les caractéristiques d'une colonne de plasma d'argon créée par un arc transféré ont été établies. Le montage d'une cathode capable de transférer un arc électrique à une anode refroidie ou à un bain anodique de métal en fusion a été construit pour permettre l'opération du système à l'air ouvert. Il était aussi possible d'injecter un gaz secondaire dans la colonne de plasma.

La mesure des caractéristiques électriques du plasma indique que la tension entre les deux électrodes dépend fortement de la longueur de l'arc et beaucoup moins du courant. Il a aussi été établi que la vitesse d'écoulement du gaz au niveau de la pointe de la cathode est un paramètre très important, et non le taux volumétrique de l'écoulement.

La mesure des profiles de température axiaux et radiaux a été effectuée avec une précision de ± 8% au moyen d'une nouvelle technique diagnostique basée sur la détermination des variations des signaux émanant d'un pyromètre optique à deux longueurs d'onde focusé sur une petite section de la colonne de plasma, tandis que celle-ci est rapidement traversée par une lame de bloquage. Des températures allant jusqu'à 18 500 K ont été observées sur l'axe du plasma.

Un microtube de pitot, traversant le plasma rapidement, a été employé pour déterminer les profiles axiaux et radiaux de la vitesse. Des vitesses allant jusqu'à 190 m/s ont été observées.

La présence d'un écoulement de gas relativement froid a été détectée autour de la colonne de plasma. Quand cet écoulement est inclus, les bilans de masse et d'énergie s'accordent avec leurs valeurs respectives à l'entrée du système.

To my parents

ACKNOWLEDGEMENTS

The author wishes to express his gratitude to all those who contributed both directly and indirectly to the work presented in this thesis.

To the members of the Plasma Technology Group, in particular, to Professor R.J. Munz, for his assistance in the design of the cathode assembly, to Drs. N.N. Sayegh and O. Biceroglu for many useful discussions and suggestions, and to fellow graduate students H.Y. Choi and G. Vannier-Moreau and to summer student, S. Pohlad, for their help in the experimental work.

To the members of his Research Group, Professor J.R. Grace and Dr. B.Z. Uysal for many useful suggestions.

To fellow graduate student E. Bayramlı for his assistance in the use of the shadow graph.

To Mr. A. Krish and the staff of the Chemical Engineering Workshop for prompt construction of essential items of the equipment.

To Mr. F. Kitzinger and the staff of the Instrumentation Department of the Noranda Research Centre, in particular Mr. V. Labuc, for their suggestions and assistance in the construction

of the electronic components of the equipment.

To Dr. W. Dutton and Mr. I. Eljarbo of the Noranda Research Centre for their generous help in the minicomputer programming.

To Mrs. Barbra E. Toivanen for her patience and excellent typing of the manuscript, and to Mr. I. Sabadin for the preparation of the drawings.

To the rest of his family for their understanding, patience and encouragement, and to his friends for making his stay in Montreal a pleasant one.

TABLE OF CONTENTS

EXPERIMENTAL SECTION

APPENDICES

LIST OF FIGURES

APPENDICES

LIST OF TABLES

GENERAL INTRODUCTION

GENERAL INTRODUCTION

The applications of plasma technology to high-temperature heterogeneous systems are attracting increasing attention, due to the availability of efficient, large-scale plasma generators, and to the inherent simplicity of the processing technique. Early attempts to use plasmas as high-enthalpy sources for the processing of finely-divided materials centered on the use of d.c. plasma jets or R.F. induction torch. More recently, increasing attention has been devoted to the use of transferred arcs, in which the anode consists of a bath of the molten metallic product. This approach provides a number of significant advantages, chief among which are the use of the anodic energy dissipation to maintain the bath at very high temperatures and the provision of additional residence time to complete the conversion of the particles which have not undergone sufficient treatment under the action of the plasma column alone. This is particularly important when a very high degree of conversion is necessary. The design and optimization of plasma reactors for such processes requires a sound knowledge of the basic plasma characteristics, such as temperature and velocity under different operating conditions of current, arc

length and sheath gas flow rate. Precise diagnostic techniques to determine plasma characteristics are, therefore, a necessity for fundamental studies.

The general aim of this thesis was to develop simple but accurate diagnostic techniques and to use them for the determination of the basic characteristics of a transferred arc plasma.

In accordance with current practice, this thesis has been written as a number of individual sections, which are complete in themselves. The two main sections of the thesis are:

i) A review of the pertinent literature in the field of plasmas and measurement techniques.

ii) A report of the experimental determinations of the basic characteristics of a transferred arc argon plasma.

LITERATURE REVIEW

INTRODUCTION

The review of the literature presented here is divided into two parts: a description of plasma phenomena and of plasma generating devices, and a survey of plasma diagnostic methods. The first part will be concerned with plasmas in general, the methods for plasma generation as well as their particular characteristics, and the applications of plasma technology in chemical and metallurgical processes. A short review of the studies on plasma transport properties will also be given because of their relevance to the present work.

The second part will describe the various techniques used in plasma diagnostics. This part of the review will be limited to the determination of the two major plasma flow parameters, namely the temperature and the velocity fields. A stronger emphasis will be placed on the measurement of temperature because of its importance in this work. A brief review of the methods used for the inversion of lateral measurements to radial measurements will be presented also. Finally, a brief background on jet entrainment will be given.

I. PLASMA PHENOMENA AND PLASMA DEVICES

GENERAL

A review of the plasma generating devices and of their operation and characteristics can be found in several books and review articles that have recently appeared. Amongst the books, the ones by Baddour and Timmins (1967), by Gerdeman and Hecht (1972), by Hollahan and Bell (1974) and more recently by Howatson (1976) are the most pertinent. Of the review articles, those of Landt (1970), Wurzel and Polak (1970), Sayce (1971, 1976), Waldie (1972 a,b), Bonet (1976), Wilks (1976), Rykalin (1976, 1977), Hamblyn (1977) and Aubreton and Fauchais (1978) are the most relevant to this thesis. The interested reader is also referred to the Ph.D. thesis of Munz (1974) in which an extensive review of plasma devices, both those which are useful in small laboratory experiments, and those which are considered for commercial operations, can be found.

The following section is intended to provide a summary of the available information which is pertinent to the present work.

DEFINITION OF PLASMA

The term "plasma" refers to a mass of gas in which enough atoms are ionized for the free charges to have significant effects. It is on the average neutral because the number density of the positive charges is equal to that of the negative ones. The plasma

may also contain neutral particles (atomic or molecular) or may be fully ionized in which case all the particles are charged. The ions may be singly or multiply charged. Unlike gas in its normal state, the ionized form is an electrical conductor and is thus influenced by magnetic and electric fields.

An important parameter is the degree of ionization, which is the percentage of those gaseous atoms or molecules initially present that has been decomposed into charged carriers. When the plasma contains neutral particles, the degree of ionization is less than one.

From the point of view of the universe, the plasma state is actually by far the most common form of matter [up to 99 per cent in the universe (A. Kettani and M.F. Hoyaux, 1973)] and thus is often referred to as "the fourth state of matter." It is also the most energetic state and is the source of the highest continuously controllable temperatures available today. It has the conductive properties of metallic materials; however, it is a compressible fluid and obeys the laws of fluid mechanics as well as those of electromagnetics.

Plasmas are present in such diverse devices as fluorescent and neon lamps as well as in the huge machines for the study of controlled nuclear fusion. They are broadly classified as cold plasmas (operating under vacuum) and hot or thermal plasmas (operating at or above atmospheric pressures). The energy

distribution between the electrons, atoms and ions is more uniform in the latter which makes it possible to characterize them in terms of transport and energy-temperature relationships.

Thermal plasmas formed by electrical discharges typically have temperatures between 2,500 and 30,000 K and ionization levels greater than 0.1% (Howatson, 1976) and are at atmospheric pressure. They are those most relevant to high-temperature chemical and metallurgical processing, and for the purpose of this thesis, further discussion of plasmas will be limited to this type.

PLASMA DEVICES

Classically, plasmas are generated between electrodes that carry the current to the plasma region. These types of plasmas are generally known as "Arc Plasmas." On the other hand, it is also possible to generate plasmas without electrodes (Electrodeless Plasma Generators) as in inductance or capacitance-generated plasmas from a high-frequency source. In the following section, these two categories will be discussed in the order of increasing relevance to this study.

Electrodeless Plasma Generators

In these types of generators, the energy is transferred from the high frequency source to the gas by either a coil or a set of capacitor plates, resulting in an inductive or capacitive coupling between the electric and magnetic fields. The ionization

is maintained once started, provided sufficient power is supplied. The absence of electrodes avoids contamination of the plasma system with the possible evaporation or erosion of the electrode material, and permits the use of even quite corrosive gases like chlorine as plasma-forming gases (Biceroglu, 1978).

Induction torches are more commonly employed in plasma studies than the capacitance types. Following their first description in 1961 (Reed, 1961), the induction torches have been used in such broad applications as light sources, spheroidization, crystal growing and chemical synthesis. The review paper by Eckert (1974) contains a full description of such applications. In the McGill Plasma Laboratory, radio-frequency induction torches have been used both for chemical reaction and for heat-mass transfer studies (Munz, 1974), (Sayegh, 1977), (Biceroglu, 1978), (Vannier-Moreau, 1980) as well as a source for laser-doppler anemometry improvement studies (Ho, 1976).

The plasma produced by induction torches generally shows two clearly distinguished regions: the fireball in the region of the coil [with temperatures ranging from 7,000 to 11,000 K and velocities from 50 to 250 m/s for argon (Eckert, 1974), (Lesinski et al, 1979)] and the plasma tailflame region below this fireball, [temperatures typically around 2,000 to 5,000 K, and velocities around 6-12 m/s (Sayegh, 1977)]. The temperatures may be raised somewhat by operation at pressures above ambient and the velocity

of the tailflame may be increased by the use of a constricting nozzle. The power efficiency of induction torches is considerably lower than that of electrode devices similar in size (Sayce, 1971), (Harry and Hobson, 1975). This is due to the energy losses associated with the various steps involved in the generation of high frequencies. The radiation losses are also greater due to the larger volume of the plasma generated. In addition, the capital cost per operating kilowatt is quite higher than for most of the dc arc systems.

If it is desired to introduce solids or gases into an induction torch, two approaches are possible. One method is to inject them directly into the fireball. Although the temperatures are highest here, the presence of upward recirculation flow (caused by magnetic pumping which will be explained in detail later on) poses several difficulties. A study on the mixing of an argon plasma fireball and a surrounding sheath of hydrogen or air by Dundas (1970) showed that very little mixing occurred between the two flows. As pointed out by Boulos (1975), forced throughput of powders or gas does not aid in entraining the particles. In addition, the added heat load causes instabilities in plasma generation as found by Huska (1966), Warren and Shimizu (1965) and Charles et al (1970). Solids or gases may be injected more successfully into the tailflame of the plasma. However, the temperatures in that region are lower and thus this scheme is only advantageous for the treatment of solids which might otherwise

evaporate at higher temperatures, or where it is desired to maintain a composition in the tailflame which would generate too much heat if introduced into the fireball (Reed, 1967).

In summary, it would appear that the electrodeless plasma torches are only suitable for laboratory use for basic kinetic or heat transfer studies in which elimination of the contamination from the electrodes is essential and precise control of the plasma is desirable.

Arc Plasmas

The common feature in all arc plasmas is the presence of electrodes. Unless one of the electrode materials is to be used as a reactant, the electrodes are well cooled and the constriction necessary to stabilize the arc and to attain high temperatures is achieved either by surrounding the arc by cold walls (wall-stabilized plasmas), or by surrounding the arc with a cold liquid or gas which is forced to flow into the arc (or is convected into it by natural processes) and provides the species which constitute the thermal plasma. Although it is possible to classify arc plasmas in several ways according to the method of stabilization (Baddour and Timmins, 1967), to the configuration of the electrodes (Freeman, 1969), to the method of ignition (Hellund, 1961), to the nature of the power supply (Hamblyn, 1977), or to the current which they carry (Howatson, 1976), in this review, for simplicity, they will be discussed under two headings: stationary arc plasmas

and transferred arc plasmas. While the former will be briefly reviewed for the sake of completeness, the latter will be dealt with in greater detail since the transferred arc plasma is the focus of attention in this thesis.

Stationary-Arc Plasmas

The most widely accepted version of this type is the dc-jet plasma torch in which the plasma-forming gas flows between an inner conical cathode and a surrounding nozzle-shaped anode. The arc struck between the electrodes ionizes the gas and is blown through the nozzle by the plasma-forming gas as a high temperature jet [about 13,000 K in the core, with argon (Freeman, 1968), (Lewis and Gauvin, 1973)]. Basic dc torches have been modified in a number of ways to provide more stable and efficient operation. The recent review paper by Hamblyn (1977) gives an excellent account of these attempts. When applied to the processing of solid particles, the dc torch (and the stationary configuration in general) suffers from great limitations.

These limitations arise from the following reasons:

1. A great percentage of the power is lost into the anode nozzle cooling, thus reducing the efficiency, defined as the ratio of the power transferred to gas to the total power input to the generator (Sayce, 1977).

2. Injection of particles into the arc, if increased beyond a certain level, leads to instabilities and excessive electrode erosion. Injection of particles outside the torch directly into the plasma jet leaving the anode orifice is inefficient since many of the particles simply bounce off the boundary (Tylko, 1972).

3. The high velocities encountered in the dc jet give the particles very short times of residence (Boulos and Gauvin, 1974), (Bhattacharrya and Gauvin, 1975). The temperature of the jet decays very rapidly (Lewis and Gauvin, 1973) and is not sufficiently high to compensate for these low residence times.

4. Product collection and recovery is a problem in these plasma systems.

Transferred-Arc Plasma

This type of plasma has only recently begun to attract attention and differs from the stationary version in a number of ways. In transferred-arc devices, the arc is formed between rather widely-separated electrodes. The greatest dissipation of electrical energy here is at the anode face. If the anode is made the work piece (as in the case of metal cutting) or the reactant, the energy efficiency can be made quite high since the anode is

not water-cooled. In most cases, the arc has to pass through a constricting nozzle. This nozzle may remain disconnected at a floating potential or alternatively may have a small current flowing through it (Tylko, 1972), (Mercure et al, 1977).

The presence of this nozzle and of convective currents (which arise due to magneto-hydrodynamic forces) tends to constrict the transferred arc. As a consequence of this, the arc is almost parallel over most of its length and is characterized by a high temperature and high velocity together with a high current density (Stojanoff, 1968). In addition to the factors common in all the aforementioned devices that influence the operating characteristics (power input, thermal losses, chemical and physical nature and flow rate of the gas), the transferred-arc plasma characteristics (temperature and velocity, in particular) are also influenced by the arc length and the degree of the arc constriction (Sheer et al, 1969, 1974).

For the ignition of the arc, a low current pilot arc between the cathode and the nozzle can be used (Mercure et al, 1977), or alternatively, the main anode can be brought very close to the cathode and a high-frequency arc can be struck between them (Sayce, 1976).

The basic design of the transferred arc discussed above has been the object of attempts to refine it, from the point of view of improved industrial applications. As mentioned earlier, the

diameter of a transferred arc tends to remain narrow and the plasma column thus exhibits high thermal gradients. One possibility of overcoming these disadvantages lies in the expansion of the plasma column. Such an idea is by no means new and indeed its principle was described by Weizel and Rompe in 1949 and Finkelnburg and Maecker in 1956, not to mention others. Basically, it states that an electrical discharge may be stabilized along a linear path and expanded centrifugally by a hollow cylinder which surrounds the arc column and rotates around it. In this way, the viscous drag forces interact with the boundary of the arc column expanding it radially outward. Audsley et al (1967) and Whyman (1967) used this principle in their cylindrically-expanded, rotating-wall, direct current plasma furnaces. The cathode geometry that can be used for such a system has been described by Bryant et al (1969). When expanded, it was argued, the plasma region would create low gradients of temperature, velocity and viscosity. Though the solid particles were fed by gravity through a hollow cathode, their design utilized magneto-hydrodynamic streaming to carry the powder into the arc column. Tylko (1972) criticized the above configurations as being very difficult to scale-up and described a transferred-arc furnace in which the plasma column itself is mechanically rotated around a ring electrode acting as the anode. The feedstocks were injected through two diametrically opposed ports pointing to the top of the supposedly conical plasma column generated by a circularly-oscillating

cathode (the so-called Precessive Expanded Plasma). The applicability of this design to heterogeneous reaction systems is being studied by Tetronics in collaboration with the Foster-Wheeler Corp. in Farrington, England, but it is now recognized that a continuous conical-shape sheet of plasma is not formed by this technique. Another method for expansion of the plasma column is to use an external rotating magnetic field (Maniero et al, 1966). In spite of its apparent attractiveness, this approach has not received much attention.

From the information given so far, it is obvious that the design of the torch must be closely coupled with that of the reactor itself. Sayce (1977), Hamblyn (1977) and more recently Aubreton and Fauchais (1978) have described several different forms of plasma reactors that use the transferred-arc mode. They unanimously agree that the systems in which an arc is struck between the cathode and a molten feed, (serving as the anode) are often far more thermally efficient than non-transferred plasma jets. They further recognize that the use of a transferred-arc system can enable economies to be made in the quantities of gas consumed, and can also permit the heating of reactive gases using electrode systems which are essentially non-consumable. They also suggest that high-value, high-temperature materials processing operations in the future will utilize either of the two following feed stock injection techniques: injection of the powdered feed near the cathode constriction, or tangential injection directed

towards the reactor's walls such that the feed will eventually move down as a molten film along the walls.

The cathode design in transferred arcs is undoubtedly very important, whichever injection technique is preferred, due to the fact that maximum penetration of the particles and/or the plasma forming gas into the primary energy dissipation zone within the arc column is required for maximum conversion and minimum cooling of the molten anode. Recently, workers in the field have displayed a great deal of ingenuity and creativity to this end. As Gauvin et al (1980) have pointed out, the bulk of the work in this field is being done in or for industrial concerns and is thus not necessarily reported in the literature. Nonetheless, the design approach of Sheer et al (1969) has probably laid down the underlying principles for all subsequent designs. Their design consisted of a central, water-cooled conical cathode tip surrounded by a closely-spaced conical nozzle so that the plasma-forming gas was injected as a thin, relatively high speed film into the arc column, very close to the cathode tip. Little material loss was observed from the cathode since, they claimed, it was cooled by convection. They called this configuration the Fluid Convective Cathode (FCC). It was found that if the gas impinged on the arc column in the contraction zone, the gas would preferentially enter the column. (The electromagnetic pumping utilized in this technique will be discussed later in greater detail). Measurements have shown that up to 80% of the gas so injected will enter into

the column. In a later publication, Sheer et al (1974) described a double shroud FCC for injecting reactive gases into the arc column. While a non-reactive gas (argon) is fed through the inner nozzle to protect and cool the cathode, the reactive gases are fed through the outer shroud. They used this design for arc vaporization of refractory powders injected through the outer shroud. An interesting observation they reported was that thermophoretic forces put a lower limit to the size of particles to be entrained. They have not, however, conducted a study as to determine the change in the plasma characteristics due to secondary gas and/or particle injection, as well as the extent of the penetration of this injection.

In summary, it would appear that the use of transferred arcs in metallurgical materials processing is advantageous over the other possible techniques for the following reasons:

1. The injected gases and particles are heated directly by the arc in a minimum volume of gas at very high temperatures. Higher thermal efficiencies and much higher particle loadings are therefore possible.

2. The product may be collected as a molten bath in which case the anodic energy dissipation (a significant loss in non-transferred arcs), is used to heat the molten product.

3. Scale-up is simple since cathode cooling will be sufficient even at higher particle inputs, and anode erosion, which is a problem for other torches, is eliminated.

4. Although complete conversion of all particles in their flight in the arc is desirable, it is not essential since the unreacted particles will be further treated in the molten bath where they are retained over much longer residence times than are possible for in-flight contacting treatments.

ELECTRIC FEATURES OF ARC PLASMAS

The electric arc can be described as a discharge sustaining quite large currents (in some applications, thousands of amperes) maintained by a comparatively low voltage. Further, the voltage-current characteristic curve is of the falling type and the current density of the arc can be very high (hundreds of A/cm^2) resulting in much greater power density than other types of electrical discharges, (e.g., Townsend dark discharge, normal glow discharge). However, the characteristic that is often cited as the most distinguishing feature is the low voltage drop in the region of the cathode. Figure 1 shows a schematic representation of the conventional arc, displaying in addition the spatial distribution of voltage and current density along the length of the arc. As can be seen, the voltage drop across the discharge

FIGURE 1

THE SPATIAL DISTRIBUTION OF
VOLTAGE AND CURRENT DENSITY
ALONG THE LENGTH OF THE ARC

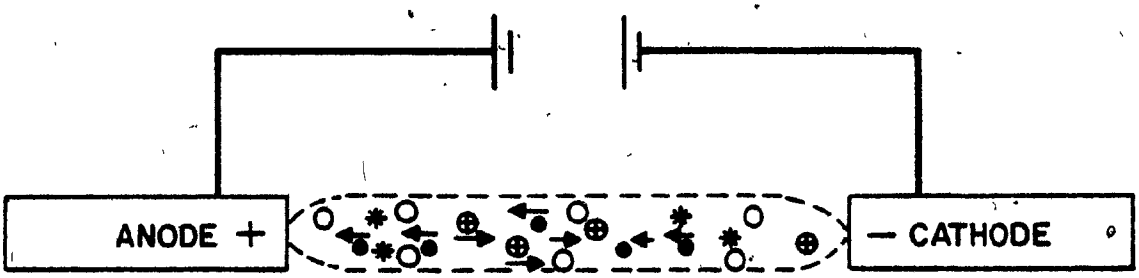

O NEUTRAL MOLECULES
⊕ POSITIVE ION
● ELECTRON
✱ EXCITED MOLECULES

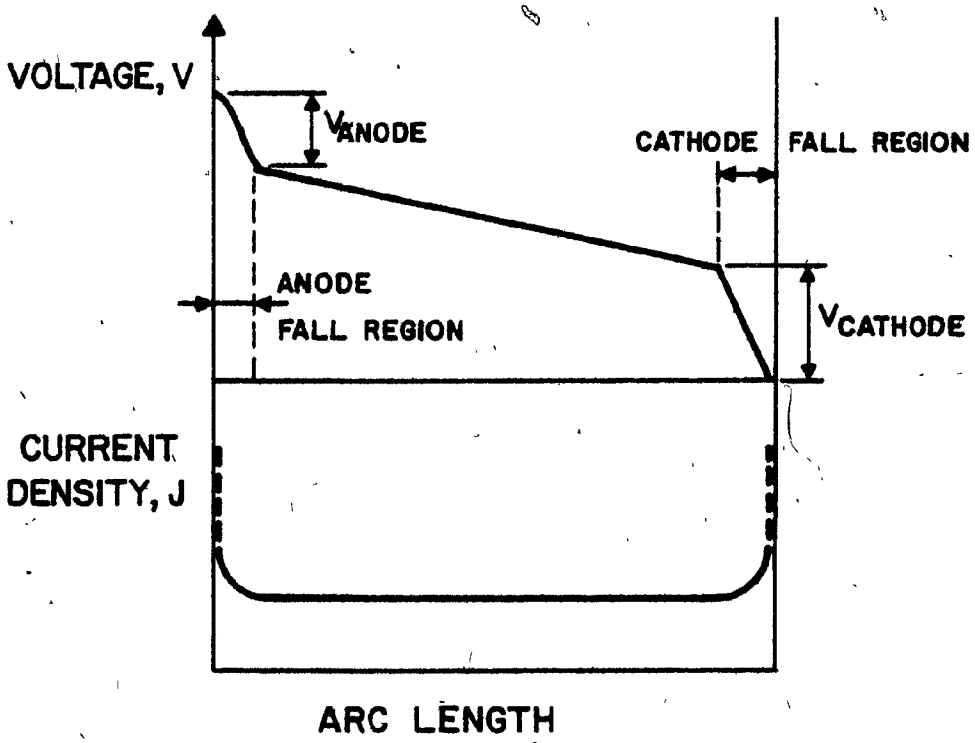

consists of three portions: the cathode fall, the column potential drop and the anode fall. The cathode drop potential (V_c) is somewhat greater than the anode drop (V_a), which may be absent altogether (Somerville, 1959). Usually, V_c is of the order of ten volts, comparable to the ionization potential of the plasma gas. Between the two electrodes, in the region referred to as "The Positive Column" for historical reasons, the voltage decreases almost linearly, implying reasonably uniform conditions. The value of this voltage gradient depends on current, arc length, material and shape of cathode and on the velocity of the cold shielding gas. Stojanoff (1968) reports a maximum value of 10 V/cm for a 3 cm-long argon arc plasma.

The physical picture behind the existence of these three regions can be better understood if one looks to the three transfers that must be effected when current is to be passed between two electrodes in a gas:

a. The current must be transferred across the gas-cathode junction.

b. The current must be conducted through the body of the gas. This requires that the normally neutral gas must be made conducting by the introduction of charge carriers, or by their creation within it, or both.

c. Finally, the current must be transferred across the anode-gas junction.

It is evident from this physical picture that in the positive column, the properties are not much influenced by the processes taking place at the electrodes while in the electrode fall regions, the properties of the system are either strongly modified, or completely determined, by the electrode processes.

The detailed mechanisms operating at the anode fall region and cathode fall region are not well understood, and even for particular types of arcs, it is exceptional that a given theory be granted the agreement of the majority of researchers, to say nothing of unanimity. Somerville (1959), Hoyaux (1968) and Howatson (1976) present descriptions of these theories. The Ph.D. thesis of Choi (1980) is also recommended for the critical review of the models used to explain the electrode fall phenomena.

On the other hand, the positive column is much better understood. It is also much more important for the purpose of the present work and for this reason, the mechanisms active in the positive column and the governing equations will be discussed briefly in the following sections.

Energy Transfer Mechanism

This section is based on the texts of Somerville (1959), Hellund (1961) and Hoyaux (1968), and summarizes the mechanism by which electrical energy is transferred into thermal energy in the gas.

The arc column conducts because of the presence of charge carriers of both signs. It is important to note that the number densities of electrons and positive ions are always approximately equal (quasi-neutrality) and in this aspect of charge distribution, the plasma is closely similar to a metal conductor. The main carrier, by which the external electric supply feeds power to the arc column, however, is the electron constituent of the plasma. This can be understood as follows.

The arc-current density (j) can be written as the sum of the electron and ion currents in the form:

$$j = n_e e v_e + n_i e v_i \ (A/cm^2) \qquad (1)$$

Typical values of the electron and ion number density (n_e and n_i) are $10^{12} - 10^{13}$/cc (Hellund, 1961), (Olsen, 1959). Values of the electron and ion drift velocities (v_e and v_i) depend on the gas pressure, temperature, and on the nature of the gas. Olsen (1959) reports values between 0.5 to 2.5 x 10^5 cm/sec for v_e for atmospheric argon plasma. The ion drift velocity is smaller by a factor of the order of several hundreds (Somerville, 1959), due to their greater mass. Thus, it remains true that the current is carried substantially by electrons.

After the gap between the electrons is bridged by some means, say by a high-frequency, high-voltage gap, the chain of events which occur is as follows: the high voltage between cathode

and anode causes local ionization of the gas. Electrons near the cathode are accelerated toward the anode by the electric field, acquiring a sufficient amount of energy to cause ionization of any atom of gas with which they collide. (It must be noted that in such collisions, only a very small fraction of the electron's energy is lost - proportional to the ratio of electron to particle mass). The ionization produces a further electron and an ion. The new electron is accelerated toward the anode, repeating the ionization process. The ion drifts toward the cathode and on impact liberates another electron to start a new chain reaction.

On the other hand, ions also pick up energy from the field and pass this energy along to the neutral molecules. As emphasized previously, the ions do not pick up energy from the field as readily as electrons due to their greater mass. Hence, the electrons will always be at the highest temperature in the arc plasma, the ions much cooler, and the neutral molecules at the lowest temperature. As a direct consequence of such an energy exchange mechanism, in any arc plasma there is not a strictly thermal equilibrium between the various constituents. The degree of departure depends on the gas pressure and temperature. Many plasmas, however, are in a state which does not differ very much from ideal equilibrium. One denotes this state with the term "Local Thermodynamic Equilibrium" (LTE). The state of LTE will be discussed in the second part of the literature survey because of its importance in the definition of the plasma temperature.

A certain fraction of the energy input is lost as radiation to the surroundings. This is due to the fact that some of the charges of opposite signs come together, giving up energy in the form of radiation by charge coalescence. This loss increases rapidly with pressure and according to Hellund (1961), is the principal effect at pressures greater than 10^7 N/m^2. This subject will also be discussed further in the subsequent sections.

Apart from the fraction of the input energy lost as radiation and as electrode losses, part of the electrical energy is used to accelerate the gas in ordered motion, away from the electrodes. This is caused by the magneto-dynamic effect of the electric field on the ionized gas. This effect constitutes the magneto-hydrodynamic streaming, which is the subject of the next section.

MHD Streaming in Arc Plasmas

Magneto-hydrodynamics, MHD, is the science dealing with moving conducting fluids in electromagnetic fields. With reference to plasma physics, the word has often a more restrictive meaning, notably that the plasma is regarded as a unique fluid in which charge separations are disregarded. MHD theories are useful in explaining the pressure gradients that exist near the electrodes [termed as "magnetic pressure" or "Maecker Effect" (Somerville, 1959)]. This effect, in turn, is the basis of several designs aimed at drawing the gaseous and/or solid reactants into the

primary energy dissipation zone of the arc plasma (Whyman, 1967), (Bryant et al, 1969), (Bhattacharrya and Gauvin, 1976), (Sheer et al, 1969). The following review is intended to be a brief summary of the information given by Hoyaux (1968), Howatson (1976), and Bhattacharrya and Gauvin (1976).

Historically, when streams of particles were first observed coming from one or both of the electrodes, they were thought to be caused by rapid vaporization of the electrodes (Somerville, 1959, reference 130). It is only after Maecker (1955) that they were attributed to the compressive forces exerted on the arc by its own magnetic field.

The imposed electric field in the arc column creates a continuous discharge resulting in a high current flow which gives rise to its self-magnetic field. A force, called the Lorentz force, will be created and in the steady state, this force is balanced by a gradient in the pressure P of the current carrying particles, so that in general,

$$\vec{J} \times \vec{B} = \nabla P \qquad (2)$$

In cylindrical coordinates, taking z axis as the axis of symmetry, the radial pressure gradient is:

$$\partial P/\partial r = J_z B_\theta$$

where J_z is the axial component of $\vec{J}$ and B_θ the azimuthal $\vec{B}$. In

other words, a cylindrical plasma carrying an axial current of density $\underline{J}_z$ which produces the azimuthal flux density $\underline{B}_\theta$ creates an inward direct pressure gradient.

Since $\underline{B}$ can be related to $\underline{J}$ using Ampere's Law, one can integrate the above equation to find the profile of pressure caused by a given distribution of current. Based on the average current density of $I/\pi R^2$, the pressure distribution can be obtained as (Bhattacharrya and Gauvin, 1976):

$$P = 10^{-7}\ I^2/\pi R^2 [1-(r/R)^2] \tag{3}$$

The average pressure is defined as follows:

$$P_{av} = (1/\pi R^2) \int_0^R P(2\pi r)\ dr \tag{4}$$

The radial streaming velocity may be calculated from the r-momentum equation. Neglecting the viscous forces and assuming the radial velocity has no gradient in the z-direction, one can obtain:

$$\bar{V} = (2P_{av}/\rho)^{1/2} \tag{5}$$

The maximum velocity $\underline{V}_{max}$ on the axis will be:

$$V_{max} = 2\ I^2/\pi\rho R^2 \tag{6}$$

If the arc diameter is constricted anywhere more than the average (as it always is at the point of attachment to electrodes, for example) then the current density and consequently the magnetic pressure will be higher at that point causing the plasma streaming

(Maecker, 1955). Even though the pressure differential is only of the order of 10^3 N/m^2 or less, a streaming velocity sets in along the axis away from the points of greater constriction. Velocities due to this MHD pumping are typically of the order of 100 m/sec, for a stagnant surrounding [Reed (1960), Goldman (1963), Freeman (1968), and Bhattacharrya and Gauvin (1976)]. It has been claimed that whether or not there is a superimposed gas flow, this MHD streaming would appear to control the flow, near the electrodes (Freeman, 1968).

In induction plasmas, the Lorentz force produces a similar magnetic compression around the sides of the fireball. The streaming is from the centre of the fireball towards both ends (Boulos, 1975) and consequently opposes the entrainment of any solid feed from upstream or back injection from downstream, to the hottest zone of the flame. It is observed that the magnetic force is much higher in arc plasmas than induction plasmas. The magnetic pressure in an induction device (Chase, 1971) is typically of the order of 0.15 N/m^2 (streaming velocity = 38.73 m/s at 15,000°K), whereas in a high-current dc arc it could easily be 2.5 N/m^2 (streaming velocity = 158 m/s at 15,000°K) (Bhattacharrya and Gauvin, 1976).

It is evident from this review that the magnetic pinch force is an important parameter in the design of arc plasma devices where injection of gaseous and/or solid reagents is required.

Though the magnitude of this excess magnetic pressure has little effect on the total volume of plasma, its influence on the circulation due to MHD streaming is significant. It can be concluded that since this force is very predominant near the cathode of an arc plasma, the MHD streaming of the gas can be advantageously employed in drawing the gas and/or solid reactants into the primary energy dissipation zone.

Theory of the Arc Plasma

The physics of the electric arc is an extremely complicated mixture of different kinds of phenomena: electrical, mechanical, thermal, radiative, etc. It is probably because of this complexity that although the theory of the arc plasma has received considerable attention, even the best known models are strictly limited as far as their validity is concerned and may not be applied in an indisputed manner to industrial devices. Nevertheless, in this section an attempt will be made to summarize the information given in the texts of Hoyaux (1968), Kettani and Hoyaux (1973), and Howatson (1976), basically for two reasons: (i) to help in the interpretation of the results of this thesis and (ii) to lay down some guidelines for future theoretical analyses of the transferred arc plasma, which has not yet been done, to the best knowledge of the author.

Similarly to the molecular and continuum approaches that can be used in deriving the governing equations of motion in fluid

mechanics, one can divide the analysis of plasma behaviour into two entirely different approaches. One is the individual particle motion and the other consists in viewing the plasma as a continuum. The second one is generally known as the magneto-hydrodynamic approach. There is, however, a basic need for establishing criteria as to permit the choice of circumstances in which one or the other approach can be safely used.

The first criterion is the fraction of particles which exist in the ionized state in thermal equilibrium and is given by the Saha equation:

$$n_e n_i / n_a = (2\pi mkT)^{3/2}/h^3 \cdot [2U'(T)/U(T)] \cdot \exp(-eV_i/kT) \qquad (7)$$

The Saha equation can be used to estimate the degree of ionization in any hot gas, whether or not carrying a discharge, for which equilibrium can be safely assumed. The variations of the degree of ionization, $X[= n_i/(n_i + n_a)]$, with $\underline{T}$ is shown in Figure 2 for atmospheric argon (Howatson, 1976).

Before one can state that a plasma regime exists at all, it must be possible to show that the Debye radius which describes the ordering of electrons about an ion is much less than the dimensions of the plasma. Therefore, the following condition defines the limits of validity of application of the term plasma state:

$$(4\pi kT/n_e e^2)^{1/2} \ll L \qquad (8)$$

FIGURE 2

EQUILIBRIUM IONIZATION FOR ARGON
ACCORDING TO THE SAHA EQUATION

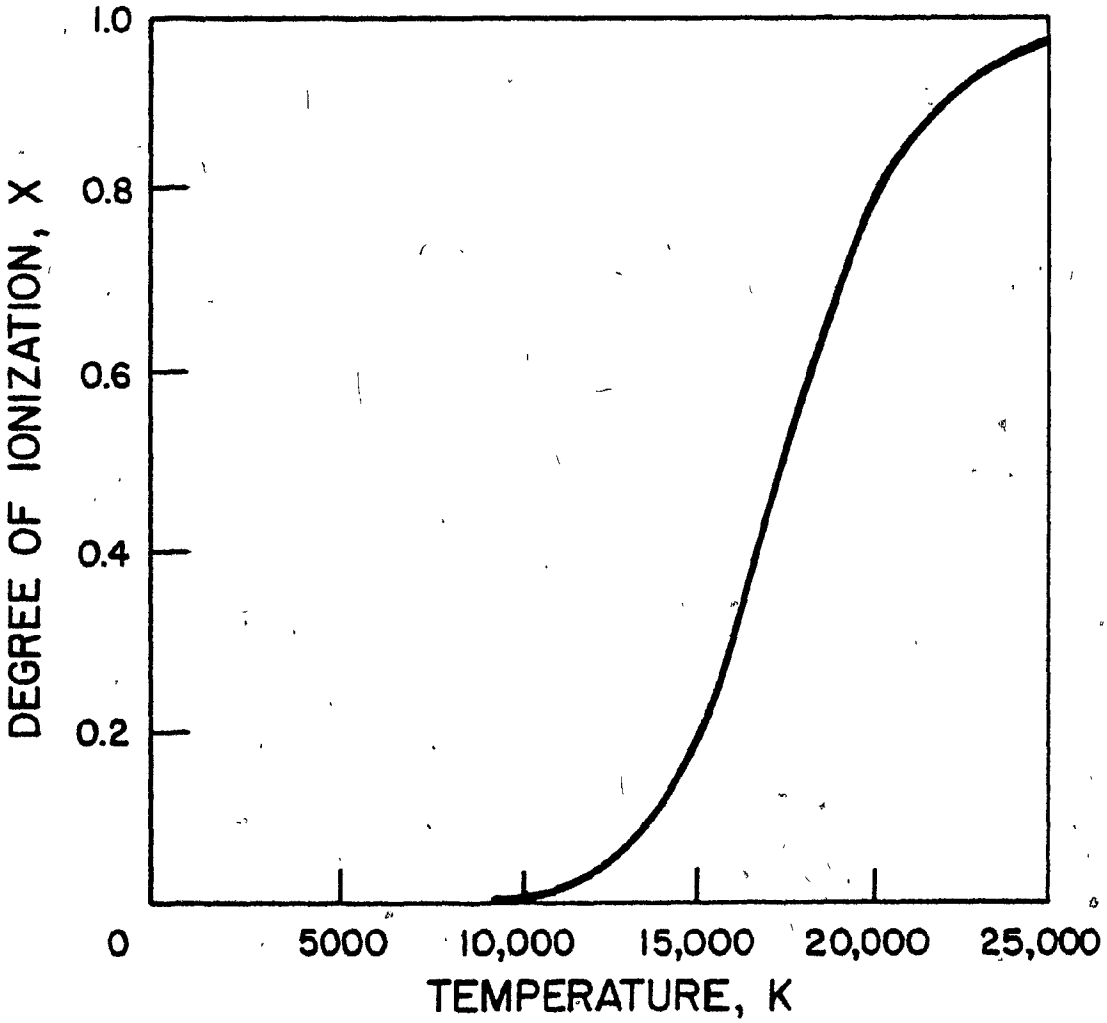
DEGREE OF IONIZATION, X
1.0
0.8
0.6
0.4
0.2
0
5000
10,000
15,000
20,000
25,000
TEMPERATURE, K

Here L is the smallest plasma dimension, generally taken as the radius of the column. (It is interesting to note that there is a weak parallelism between Equation (8) and the Knudsen number used in fluid mechanics).

For the high pressure arc plasmas under investigation in this thesis, the above two criteria suggest that MHD simplifications can be used in defining the governing equations [Kettani and Hoyaux (1973), Howatson (1976)].

In the magneto-hydrodynamics approach, the behaviour of the plasma can be described in terms of Maxwell's equations and those of fluid mechanics.

a. Maxwell's Equation

These equations express the relationship between electric and magnetic fields in a medium. Since these fields are functions of space and time, there will be a need for four relationships. These relationships are concerned with the conservation of electric charge, magnetic charge and Faraday's Law of induction of electromotive force, and Ampere's Law which defines the magnetic field originating in electric currents. These equations can be written in vector notation as follows:

$$\nabla \cdot \vec{D} = q \qquad (9)$$

$$\nabla \cdot \vec{B} = 0 \qquad (10)$$

$$\nabla \times \vec{E} = -\partial \vec{B}/\partial t \qquad (11)$$

$$\nabla \times \vec{H} = \vec{J} + \partial \vec{D}/\partial t \qquad (12)$$

b. The Material Equations

These relate the flux densities to the field vectors and the current to the electric field (generalized Ohm's Law):

$$\vec{D} = \epsilon \vec{E} \qquad (13)$$

$$\vec{B} = \mu^* \vec{H} \qquad (14)$$

$$\vec{J} = \sigma(\vec{E} + \vec{c} \times \vec{B}) + q\vec{c} \qquad (15)$$

c. Equation of State

$$P = nkT \qquad (16)$$

d. Conservation of Mass

$$\partial \rho/\partial t + \nabla \cdot (\rho \vec{c}) = 0 \qquad (17)$$

or:

$$\partial \rho/\partial t + \partial(\rho U_i)/\partial X_i = 0 \qquad (17')$$

e. Conservation of Electrical Charge

$$\partial q/\partial t + \nabla \cdot \vec{J} = 0 \tag{18}$$

or:
$$\partial q/\partial t + \partial j_i/\partial X_i = 0 \tag{18'}$$

f. Momentum Transport Equation

$$\rho \, D\vec{c}/Dt = \vec{J} \times \vec{B} - \nabla : \underline{T} + q\vec{E} + \rho \, \nabla \vec{G} \tag{19}$$

or, neglecting the effects of electric and gravimetric fields, for cylindrical symmetry (Bird et al, 1960),

$$\partial/\partial t(\rho U_i) + \partial/\partial X_i(\rho U_i U_j) = \partial P_{ji}/\partial X_j + (j \times B)_i \tag{20}$$

where:

$$P_{ji} = -\delta_{ij} P + \eta \left(\partial U_j/\partial X_i + \partial U_i/\partial X_j\right) - 2/3 \cdot \eta \, \delta_{ij} \, \partial U_k/\partial X_k \tag{21}$$

g. Energy Conservation Equation

For constant pressure, steady state conditions, neglecting viscous dissipation:

$$\sigma \vec{E}^2 + \nabla \cdot (\kappa \nabla T) - \rho C_p \, \vec{c} \cdot \nabla T = 0 \tag{22}$$

In this form, the equation represents the modified

form of the Elenbaas-Heller Equation for convective and forced flow. In general, one must also introduce the radiative power term. With this addition, for cylindrical plasma, Equation (22) takes the form:

$$S(T) + \rho C_p (U_i \partial T/\partial X_i + U_j \partial T/\partial X_j) = \partial/\partial X_i (\kappa \partial T/\partial X_i) + \sigma E^2 \qquad (23)$$

The above set of equations has been used by several workers to theoretically analyze different forms of electric arcs. In most cases, radiation, self-magnetic pinch force and convective terms are neglected, and axisymmetric, steady-state, laminar flow is assumed (Topham, 1971), (Cohen and Whitman, 1976), (Gvozdetskii and Zrazhevskii, 1975). In the cases when the radiative terms was not neglected, (Topham, 1978) empirical relations were used. Herman et al (1974) used experimental temperature distribution in a cascade arc to obtain the radial profile of the radiative power. All of these analyses suffer from the difficulty of assigning empirical equations to variations of $\underline{\sigma}$, $\underline{\eta}$ and $\underline{\kappa}$ with temperature. The calculation of these parameters will be discussed in the next section. To conclude this section, it must be noted that, to the author's best knowledge, there exists no theoretical analysis of a transferred arc "burning" in a jet of gas which emerges from a converging annular nozzle and impinges on a flat surface (anode), as used in the present study.

PLASMA TRANSPORT PARAMETERS

The transport parameters that will be discussed in this section are the viscosity, the thermal conductivity and the electric conductivity. While the methods and results for viscosity will be dealt with in detail because of its relevance to the present work, only references for the other two will be given, for completeness.

The literature on the estimation of viscosity for partially-ionized argon is rather extensive. However, it can be divided into two, depending on whether theoretical or measured intensive parameters are used. In the theoretical studies, the rigorous kinetic theory of Chapman and Enskog (Bird et al, 1960) is generally accepted as the base. Amdur and Mason (1958) and Svehla (1962) used this technique by ignoring ionization. It is also possible to use the simple kinetic theory, by considering a partially ionized argon plasma to be a mixture of atoms, ions and electrons, as done by Kimura and Kanzawa (1965). Devoto (1967, a, b), Drellishak (1963), Ahtye (1965), Mathur and Thodos (1963), and Kanzawa and Kimura (1967) used the rigorous method for binary mixtures (atom and ion in this case), developed by Hirschfelder et al (1954).

On the other hand, one can calculate the viscosity from the measured quantities. The complexity of the analysis varies considerably, but basically the simplified form of the momentum

equation written as:

$$-dP/dz = 1/r \cdot [d/dr(r \cdot \eta \cdot dU_z/dr)] \quad (24)$$

is used together with the axial static pressure gradient and velocity profile to deduce viscosity. Bahador and Soo (1966), Kanzawa and Kimura (1967), Stojanoff (1968), Schreiber et al (1970), and Asinovsky et al (1976) used this method of analysis.

The values of argon viscosities at one atmosphere obtained by different workers are plotted in Figure 3 for comparison. It can be concluded that the results of Devoto (1967) can be used safely for $8,000 < T < 20,000$ K.

For the thermal and electrical conductivity, in addition to the already referred studies, the works of Oster (1961), Knopp and Cambel (1966) and Emmons (1967) are noteworthy. The theoretical results of Devoto (1967) are again recommended because of their agreement with experimental measurements of Stojanoff (1968).

PLASMA APPLICATIONS

The last twenty years have seen a considerable amount of research in the field of thermal plasma processing. The recent review articles by Rykalin (1976), Sayce (1972, 1977), Hamblyn (1977), and by Aubreton and Fauchais (1978) cover much of the progress to date. In spite of the large number of patents which

FIGURE 3

ARGON VISCOSITY AS A FUNCTION OF TEMPERATURE

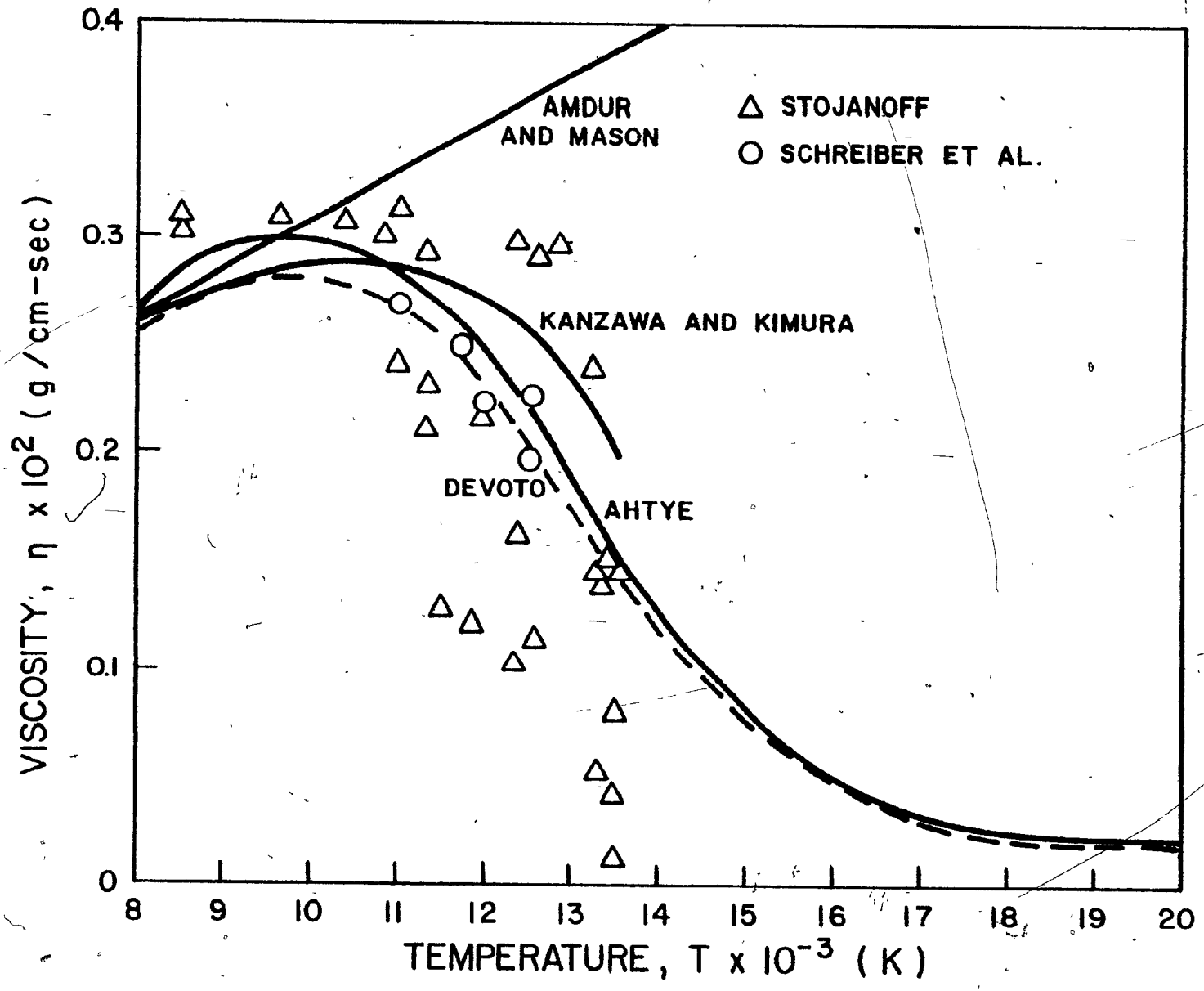
0.4
0.3
0.2
0.1
0
VISCOSITY, η x 10² (g / cm-sec)
8
9
10
11
12
13
14
15
16
17
18
19
20
TEMPERATURE, T x 10⁻³ (K)
AMDUR AND MASON
STOJANOFF
SCHREIBER ET AL.
KANZAWA AND KIMURA
DEVOTO
AHTYE

resulted from these investigations, very few commercial applications have been developed. Before reviewing the latter, it is appropriate to list the chemical and metallurgical operations in which plasmas may be employed, with the most important references:

a. Cutting and Welding

[Ton (1975), Howatson (1976), Glickstein (1976)].

b. Spheroidization and Plasma Spraying

[Gold et al (1979), Borer (1978), Welch (1972), Fisher (1972)].

c. Melting

[Bhat (1972), Borodachyov et al (1977), Asada and Adachi (1971), Magnolo (1964)].

d. Evaporation

[Sheer et al (1974), Bonet et al (1974), Angier et al (1973), Everest et al (1973)].

e. Pyrolysis

[Sheer et al (1979), Garratt and Littewood (1979)].

f. Gas-Solid Reactions

[Thurnsfield and Davies (1974), Rains and Kadlec 1970), Landt (1970), Sayce and Selton (1972), Biceroglu (1978), Fey et al (1979), Heberlein et al (1979), Munz and Gauvin (1975)].

g. Gas-Solid-Solid Reactions

[Sheer and Korman (1956), Matsumato et al (1970, 1971, 1974), Mac Rae et al (1976), Foster-Wheeler/

Tetronics (1979), Pickles et al (1976), Goldberger (1963)].

Up to very recently, the use of plasmas as chemical reactors on a commercial scale was limited to three processes: the production of acetylene (Landt, 1970), that of titanium oxide (Arkless and Cleaver, 1966), and the dissociation of zircon and sand into zirconia and silica [Wilks et al (1974), Thorpe and Wilks (1971)]. Very recently, however, a trend has been observed for the production of ferro-alloys via the plasma route. A very impressive example of this trend is the 20-ton/hour, 19.8 MW plasma steel-melting furnace developed by East German workers [Fiedler, 1976), Borodachyov et al (1977), Esser et al (1974)]. Their design utilizes three plasma arcs transferred to the metal bath, and claims very high thermal and electrical efficiencies together with easy control. Bethlehem Steel Corp. of USA [Gold et al (1975), Mac Rae (1976)], Foster-Wheeler/Tetronics of England (F-W/T, 1979) and Daido Steel Co. of Japan (Asada and Adachi, 1971), all have large capacity reactors in operation, or on the eve of operation, for production of ferro-alloys and specialty steel.

From these attempts it can be predicted that one of the major thrusts for plasma technology in the future will be the gradual replacement of electric arc furnaces by their plasma counterparts. On the other hand, plasmas have a potential domain of industrial application for the production of high unit value,

high purity metals, metallic compounds and refractory materials.

CONCLUSION

The literature on plasma technology discussed in this section indicates that the experience with large-scale plasma operations seems to have improved the prospects for their industrial commercialization considerably. Because of their advantages over the other plasma devices, the transferred arc plasmas will play a very important role in these applications. However, before the design of a plasma system can be undertaken, it is imperative that a much better understanding of the fundamental principles underlying the operation of transferred arc plasmas first be obtained. Only then can the vast amount of kinetic data already existing about high-temperature reactions yielding a product of high unit value be used for the effective design and control of plasma reactors.

II. PLASMA DIAGNOSTIC METHODS

GENERAL

In one sense, plasma diagnostics are coexistent with the whole of plasma research. It is difficult to think of a plasma experiment which does not incorporate different means of sampling and/or monitoring plasma properties. Indeed, one can say that progress in plasma research can be assessed by the development of its measurement techniques and the adequacy of the accompanying

theoretical analysis. Because of this importance, therefore, it is not surprising that plasma diagnostics are not the domain of a single science only, but rather have a somewhat interdisciplinary character, borrowing their methods from many branches of physics, mathematics and engineering.

The domain of plasma diagnostics is, in turn, very broad; it includes the measurement of the microscopic properties such as electron and ion densities, and macroscopic properties like electrical and magnetic fields. From a chemical engineering point of view, however, the temperature and velocity of the plasma stream are the basic parameters required for the study, design and control of the plasma systems. Thus, for the purpose of this thesis, the meaning of plasma diagnostics is narrowed greatly to include only these two parameters.

In this section, various diagnostic techniques used to determine the temperature and velocity of the plasma are discussed. The texts by Lochte-Holtgreven (1968), Taurin (1966), Huddlestone and Leonard (1965), Herzfeld (1962), Howatson (1976) and Kettani and Hoyaux (1973) were used as primary sources of information.

TEMPERATURE

Definitions and Techniques

1. Meaning of Temperature

A knowledge of the temperature of the plasma is essential for the study of the physical and chemical processes occurring in a plasma. To fully appreciate this property, one has to understand the physical definition and interpretation of the temperature of a gas in general.

It is convenient to distinguish between the definition of temperature as a thermodynamic concept, and the interpretations of temperature in terms of atomistic processes of energy transfer. A widely accepted definition of temperature is the one given by Taurin (1966) based on the concepts of a thermodynamic state and thermal equilibrium, as summarized below.

An isolated thermodynamic system left undisturbed for a sufficient time will maintain constant values of its state variables (such as pressure and volume). Such an isolated system is said to be in "thermal equilibrium." When two isolated systems, both in thermal equilibrium, but with different values of state variables are brought in contact, either no change in state variables is observed (in which case the two systems are said to be in equilibrium with each other); or the state variables of both systems change, and following a transfer of energy, both systems

come to equilibrium again, each with its own new set of values of the state variables. Thus, it is evident that thermodynamic systems can be grouped in classes, such that the members in a certain class are in equilibrium with each other. Such a grouping of thermodynamic systems into classes defines a variable which has a certain common value for all systems in a class, but different values for other classes of similar systems. This variable is said to be "Temperature."

A gas consists of molecules - monatomic, diatomic, polyatomic. A plasma contains ions and electrons in addition. Each of these gas particles has a certain degree of freedom attached to it (for example, excitation and ionization, for an ion). Each degree of freedom of the gas particles can be regarded as a thermodynamic system, and each such system has a temperature. Under normal ambient conditions, these degrees of freedom are in equilibrium and therefore one would expect the same temperature to be given whatever experimental technique is used. This is not necessarily true when considering plasma temperatures, since the various degrees of freedom have different relaxation times. As a consequence of this, in cooling of a gas from say 10,000 K to 1,000 K, the different degrees of freedom can get "out of step" and it is possible to simultaneously assign to a gas "temperatures" differing by several orders of magnitude.

In order to explain this situation, the various

interpretation of temperature and the main experimental techniques appropriate to each interpretation is outlined in the following sections based on the texts of Taurin (1966) and Lochte-Holtgreven (1968). This is followed by a discussion of the concept of equilibrium and diagnostic techniques. Finally, based on this comparison, some fundamental definitions required for the technique used in this thesis are given.

ii. The Translation (Kinetic) Temperature

The kinetic (translation) temperature of a gas is a measure of the mean kinetic energy of the gas particles. In the kinetic theory of gases (Moore, 1961), it is shown that the fraction of particles (Δn) of a gas at absolute temperature T having a velocity between v and $v + \Delta v$, is given by the Maxwellian Law:

$$\Delta n = n\, 4\pi\, (m/2\pi kT)^{3/2}\, \exp(-mv^2/2kT)\, v^2\, \Delta v \qquad (25)$$

where n is the total number of particles with mass m, and k is Boltzmann's constant; the mean particle kinetic energy $\bar{E}$ is related to temperature as follows:

$$\bar{E} = (1/2)\, m\bar{v}^2 = (3/2)\, k\, T^* \qquad (26)$$

where $\bar{v}^2$ is the mean square velocity of the distribution defined by Equation (25). The kinetic temperature T^* may be defined as that temperature which satisfies Equation (26), and thus is an index of

the kinetic energy of the gas. Note that the kinetic temperature T* is an interpretation of the quantity T which appears in Equation (25).

A common technique of measuring kinetic temperature is to allow a solid (or liquid) device to come to thermal equilibrium with the gas and to compare a change in some property of the device with the translation temperature of the gas. Typical devices are thermocouples, mercury-in-glass thermocouples and resistance gauges (Herzfeld, 1962). These devices are susceptible to large errors because the assumption that the device temperature and the gas temperature are equal is not always true. In thermocouples, for example, a correction has to be made to account for the heat losses from the junction by radiation and conduction through the support. Bradley and Mathew (1968) presented a model for obtaining actual gas temperatures from thermocouple readings. The largest limitation of these techniques is the restriction on the gas temperature level (less than 2,500 K). Chu and Gottschlich (1968), Polyakov et al (1978) and Chevela et al (1975) used thermocouples in the regions of the plasma where the kinetic temperatures were below 2,500 K.

iii. Rotation-Vibration Temperature

A diatomic molecule consists of two atoms, the nuclei of which are affected by intermolecular forces in such a way that the nuclei vibrate about equilibrium positions along the internuclear axis. At the same time, the nuclei rotate about their common centre

of mass while the electrons describe orbits about the individual atoms. The total energy of the molecule can be assumed to be composed of the contributions of the electronic energy, vibrational energy and rotational energy. The distribution of this energy is governed by the Maxwell-Boltzmann Law and it is therefore possible to define the rotation-vibration temperature as directly proportional to the mean rotation-vibration energy. The rotation-vibration temperature is determined from the measurements of the intensity of the molecular bands. This requires the knowledge of electronic transition probabilities of diatomic bands. The experimental determinations of the latter are scarce and contain uncertainties (Lochte-Holtgreven, 1968). Therefore, the method to evaluate temperatures of plasmas from the intensities of the bands (rotation-vibration temperature) is applicable in very few cases only. Smith and Churchill (1965) and Morgan and Nicholls (1970) used this method for argon-nitrogen mixtures and both could only claim an accuracy of ±20% for their results.

iv. Electron Excitation Temperature

An atom can acquire energy in the form of electronic excitation. This gain in potential energy occurs when energy gained by collision causes an orbital electron of the atom to be relocated in an orbit of higher energy value. The electron in this higher energy state may subsequently make a spontaneous transition to a lower level with the emission of a photon of

light having an energy equal to the difference in the energies of the upper and lower level. The frequency of the photon is proportional to this energy. The intensity of the radiation is a function of the concentration of the excited state which in turn is a function of the temperature. This temperature is referred to as "Electron Excitation Temperature." The measurement of intensity of emitted radiation from a gas forms the basis of spectroscopic temperature measurement (Taurin, 1966) and the several techniques employed in spectroscopic diagnostics will be discussed later.

v. Electron Temperature

In the same manner as in the case of translation (kinetic) temperature, one can assign a temperature T_e which is proportional to the mean kinetic energy of translation of the electrons. It is usually estimated from the variation in the current drawn from a wire as the voltage bias of the wire is changed. This is the basis of the Langmuir Probe and various aspects of this technique have been discussed at length by Huddlestone and Leonard (1965), Lochte-Holtgreven (1968) and Howatson (1976). For high pressure plasmas, use of Langmuir probes is not recommended (Schott, 1968).

vi. Equilibrium

The system of interest in this thesis is a transferred arc argon plasma which consists of argon atoms, argon ions and electrons. Following the previous interpretations of temperature, one can

consider two translation temperatures (for atoms and ions), two electronic excitation temperatures (for atoms and ions) and one electron temperature for electrons. These temperatures will be equal if a state of complete thermodynamic equilibrium is attained in the plasma. Actually, on a formal basis, it is improper to talk about "Temperature" unless all the degrees of freedom of a gas are in mutual equilibrium. On the other hand, a true thermodynamic equilibrium can exist in a system only when it is completely isolated and does not exchange mass, momentum, or energy with the surroundings. In such a system, the total energy content is constant and the energy distributions for the various states are determined by a unique temperature. Each mechanism of energy exchange in the system is exactly balanced by its reverse (Aller, 1963). A laboratory plasma system like the one used in this thesis exchanges energy with the surrounding by emitting radiation, and hence cannot be in complete thermodynamic equilibrium. Relaxation of the strict definition of equilibrium is therefore necessary, if the concept of temperature is ever to be invoked.

It has been shown that temperature is a constant of equilibrium and in this view a temperature gradient, (an inevitable consequence of energy loss to surrounding) is a contradiction in terms. However, if temperature is regarded merely as a property of an energy distribution, which can vary in space, then the idea of varying temperature can be accepted; moreover, if the distribution is not changing too quickly in space or time it will

remain close to the equilibrium form at every point (Howatson, 1976). So one is led to the idea of "Local Thermal Equilibrium" or LTE. Thus, for a plasma exhibiting LTE, the velocity distribution of the atoms, ions and electrons is Maxwellian, the distribution of population densities of excited atomic states is Boltzmannian, and the distribution of atoms and ions obeys the Saha equation at each point in the system (Lochte-Holtgreven, 1968). The radiation field, however, is not black body (given by the Planck function), but is a line spectrum characteristic of the element and is determined by the Einstein relation. A gradient in the local temperature may exist, but the relative change must be sufficiently small so that a particle subjected to such a change has time to equilibrate. Then, steady-state distributions are established at each location in the plasma, and the local temperature specifying these distributions has meaning. The change in temperature, in effect, is continuous. Thus, the system can be subjected to a directional flow of heat, mass and change, although at each point there is a restriction on the amount transferred such that it must be small in comparison to the total content of the system. Similarly, there could be a time restriction on the interval of measurements in terms of the relaxation time of the species. In plasmas, LTE will prevail as long as collisional rate processes among particles not directly connected with radiation energy transfer are predominant, the radiation rate processes being small in comparison. Then, the distribution functions will be determined

by particle collisions which tend to equilibrate the various forms of energy distribution (Sampson, 1965).

LTE in argon plasmas has been the subject of many studies. Representative of the theoretical studies is the work of Greim (1963). Olsen (1963), Bober and Tankin (1970), and Niimura et al (1974) are amongst the workers who investigated LTE experimentally. Olsen (1963) independently measured the excitation temperatures of argon atoms and argon ions and found them to agree in his atmospheric pressure plasma. The conclusion, which always seems to be reached for plasmas at atmospheric pressure and above (Preston, 1976), is that the system is very close to equilibrium and that approximately the same temperature can be assigned to translation, electronic excitation, and ionization. In the cases where departures from LTE are observed (Niimura et al, 1974), it is generally restricted to the electrode regions and to the arc periphery. As stated by Taurin (1966), the importance of non-equilibrium in spectroscopic temperature measurements has sometimes been exaggerated. A spectroscopic anomaly which might be caused by non-equilibrium will often turn out to be caused by self-absorption, severe temperature gradients, or the use of incorrect spectroscopic constants in calculating the temperature.

Before concluding this section, the work of Dundas and Thorpe (1969) on the effect of electron concentration, gas pressure and ratio of electric field strength has to be mentioned. They

found that at high electron density (>10^{13}/mm^3) electron and translation temperatures agree, but at lower concentrations, the electron temperature can be an order of magnitude higher. The same effect appears with decrease of pressure. At high ratios of electric field strength to gas pressure [>1(v/mm)/(mm Hg)] the electron temperature can be two orders of magnitude higher than the translation temperature.

DIAGNOSTIC TECHNIQUES FOR PLASMA TEMPERATURE

Temperature measurements in plasmas can be made either with the aid of insertion probes, or by optical methods, or by a combination of both.

1. Probe Techniques

In all diagnostic techniques which depend on the insertion of a material probe into the plasma, there is always an irreducible, though in many cases small, disturbance of the local plasma conditions. These methods, however, more than make up for this disadvantage by (directly) yielding local information, usually with good spatial resolution. In many cases, also, an upper bound can be placed on the disturbance caused by the probe.

The various probes used in the measurement of high temperatures can be classified into three categories, according to Grey (1965): pneumatic devices, heat-flux gauges and calorimetric sampling probes. The pneumatic probe relies on the application of

the continuity equation to a sample of the unknown gas continuously flowing through two sonic orifices. The temperature of the gas at the stagnation point can be determined from (Simmonds and Glawe, 1959):

$$T_1 = (C_1A_1/C_2A_2)^2 \cdot T_2(P_1/P_2)^2 \cdot C_3 \qquad (27)$$

This requires that the pressures of each constriction ($\underline{P}_1$ and $\underline{P}_2$), the temperature at the downstream constriction ($\underline{T}_2$), the area and discharge coefficients of the constrictions ($\underline{A}_1$ and $\underline{C}_1$) and the value of $\underline{C}_3$ (which is a known function of the ratio of the specific heats) are known.

This method has several drawbacks in that it needs pre-calibration of the nozzles, ideal isentropic flow must take place at each nozzle, a certain degree of suction is required when the total pressure is low, and the nozzle ratio must not change between calibration and actual operation. Since the nozzle ratio is a function of the fourth power of the nozzle diameters, slight expansion effects in the first nozzle (expected when measuring high temperatures) can cause errors of the order of 10% in the stagnation temperature (Grey, 1965).

Heat-flux gauges measure the heat transfer rates across a calorimeter surface (usually normal to the flow velocity) at a known or measured stagnation pressure. The plasma enthalpy or temperature is deduced from the heat flux with the application of a

theoretical analysis. Thus, a prerequisite for this method is calibration or knowledge of the relation between the heat transfer rate and the gas temperature. The main sources of error in this technique are inaccuracies in estimating heat transfer to or from the insulating jacket and the finite area of the gauge face required for adequate resolution, which reduces the validity of stagnation-point heat transfer assumption (Grey, 1965).

Calorimetric methods determine the local enthalpy of the gas by cooling a small amount of sample of the hot gas and measuring the amount of heat transferred and the final temperature of the gas. Grey et al (1962, 1964) developed a probe called "tare-measurement calorimetric probe" capable of measuring gas temperatures up to 15,000 K. The change in coolant temperature was observed for the case when the valve in the gas sample line was closed and when it was open. The difference was a measure of the heat lost by the gas sample which in turn gave the gas temperature. The accuracy of this method depends heavily on duplicating the flow conditions near the probe tip in the flow and no-flow cases.

In a later paper, Grey (1968) describes two other geometries of calorimetric probes. He first points out that the above method can be used only in large heat flux environments. Its principle disadvantage, he maintains, is lack of sensitivity at lower heat flux conditions caused by small differences between two large numbers (tare and actual measurements). For lower heat-flux conditions,

the fully-isolated non-tare measurement probe was recommended. This has an insulation section between the cooling jacket and the calorimetric part. The enthalpy measurement is then obtained directly without the need of a tare measurement. However, in very low ambient pressure conditions, such as those encountered in most hypersonic flows, the gas sample energy is so small that the coolant flow rate cannot be reduced sufficiently to produce a measurable temperature difference. Moreover, the stagnation pressure is too low to drive an adequate amount of sample gas through the probe. Under these conditions, the sharp-inlet shock-swallowing probe was recommended.

Katta et al (1973) used an improved, double-jacketed non-tare probe, designed by Grey, for axial temperature measurements in argon and helium plasma jets, in the range of 2,000 to 13,000 K. At the high temperature level (12,000 K), the probe measurements agreed with the spectroscopic data reported in the literature, while the values in the lower range were confirmed by thermocouple readings. They concluded that the probe was capable of good accuracy (5% error estimated), but great care had to be exercised in the setting up of the coolant flow rates, making its use rather time-consuming. Its vulnerability to an aggressive gaseous environment was also noted.

Smith and Churchill (1965) measured plasma jet temperature both spectroscopically and by a calorimetric probe. Their results showed that reliable enthalpy data could not be obtained by using a

sampling probe due to its dependency on the sampling rate. At too low sampling rates, the sample is drawn only from the cold region near the probe and at too high sampling rates a greater portion of the gas which normally flows past the outside of the probe is drawn through the sampling probe. Both of these effects result in a lower than actual enthalpy value. Differences up to 4,000 K were found between the temperatures obtained by the two techniques. This discrepancy was also observed by Chludzinski (1964). Similar results to those of Smith and Churchill were obtained by Hare (1972). His results also showed that in regions where both thermocouples and enthalpy probes could be used to measure the temperature, the thermocouple always indicated significantly higher temperatures. This view, however, was contradicted by the results of Incropera and Leppert (1967) who measured radial temperature and velocity profiles in a dc argon plasma jet, using both calorimeter and spectrophotometer. They claimed that, as long as the flow conditions are duplicated for actual and tare measurements (they did not say how), both results agreed within a few per cents. Spectroscopic methods were found to be more accurate over 12,000 K. Below 10,000 K, they agreed with Hare's findings that uncertainties with probe measurement rise to excessively high values. They suggest, however, that more reliable results can be obtained by choosing a suitable cooling flow rate.

ii. Optical Techniques

The spectroscopic techniques, which group together a relatively large number of different methods, are the most important ones of the optical techniques used for plasma temperature measurements. Spectroscopic temperature measurements based on Line Emission and Continuum Emission will be mentioned only in this section.

a. Line Emission

As mentioned earlier, an electron is an excited state can make a spontaneous transition to an orbit of lower energy value by emitting radiation. Such a process between quantized states results in a characteristic spectral line. The volume emission coefficient for this line depends upon the number of downward transitions per second, which is expressed in terms of the concentration of atoms in the higher excited energy level N_n and the probability per second for the transition of interest A_{nm} (known as the Einstein's spontaneous transition probability), and upon the energy associated with the particular transition, which is related to the wavelength λ by:

$$E_n - E_m = hc/\lambda \qquad (28)$$

where, E_n, E_m = Energy of upper level n and lower level m respectively, with respect to the ground level, h = Planck's constant and c = speed of light.

The Einstein relation then for the line emission coefficient is (Lochte-Holtgreven, 1968):

$$\varepsilon_{line} = (1/4\pi\lambda)\ hc\ N_n\ A_{nm} \tag{29}$$

Equation (29) does not depend on the existence of any equilibrium condition and only involves constants of the particular species. If LTE conditions prevail, a Boltzmann distribution can be assigned to the populations of the excited states, and the number density of atoms in the upper state $\underline{N}_n$ is related to that of atoms in the lower state $\underline{N}_o$ by:

$$N_n = N_o \cdot (g_n/g_o) \cdot \exp(-(E_n - E_o)/kT) \tag{30}$$

where, g_n, g_o = statistical weight of the upper and lower energy levels, k = Boltzmann's constant and T = temperature.

Summing up the discrete energy levels of the excited atomic states up to the ionization energy, with the energy of the lowest level taken as zero, the Boltzmann distribution becomes:

$$N_n = N_a (q_n/U_a)\ \exp(-E_n/kT) \tag{31}$$

where $\underline{N}_a$ is the total number density of atoms and $\underline{U}_a$, the internal partition function of the atom defined as:

$$U_a = \sum_i g_i\ \exp(-E_i/kT) \tag{32}$$

The atomic number density is obtained from the Saha equation and the ideal gas law. The partition functions for atoms

and ions have been calculated by various workers (Olsen, 1961, 1963), (Drellishak et al, 1963). The equation for the line emission coefficient becomes:

$$\varepsilon_{line} = (1/4\pi\lambda)\ hc \cdot g_n A_{nm} (N_a/U_a)\ \exp(-E_n/kT) \qquad (33)$$

The values of the transition probabilities, A_{nm}, are different for each spectral line. In practice, for atoms like argon, they must be determined experimentally. Two experimental approaches are possible. One is seeding hydrogen into the argon plasma. Since the transition probabilities for hydrogen lines are known from quantum mechanics, one can determine the plasma temperature. The argon transition probabilities are then calculated from the observed argon line intensities. The other technique, known as the Fowler-Milne method, uses only the observed argon spectra. This method will be described in the following section. Adcock and Plumtree (1964) summarized various determinations of argon transition probabilities. For some lines, the values found by different workers differ by as much as a factor of 2.

"Single-Line" Temperature Determination

Equation (33) can be used to determine plasma temperatures from the measurements of ε_{line}, if the transition probability of the line is known. The calculation is by trial and error, however, since U_a and N_a are functions of the temperature. In practice, it is somewhat easier to use tabulated values of U_a and N_a at the

desired pressure and temperature, and prepare a plot of ε_{line} as a function of temperature. Under certain circumstances, a single line can be used for temperature determination even if the transition probability is not known. This method, known as the Larenz or the Fowler-Milne method, makes use of the fact that the intensity of a line goes through a maximum as the temperature is increased. While the exponentral term in Equation (33) increases with temperature, N_a decreases. The net result is that an intensity maximum exists, say at about 15,000 K. Now if the plasma source contains temperature gradients, and if the temperature is known to be above 15,000 K at some point, the position of the maximum intensity in the spectroscopic measurement corresponds to 15,000 K. The relative values of emission coefficients then give the temperature distribution and transition probabilities. This method of plasma temperature measurement has been used by Olsen (1963), Knopp et al (1962), Gottschlich (1966), Meubus (1969), and Incropera and Leppert (1967), to list a few. The temperature determination from this method suffers from the fact that the maximum of $\varepsilon(T)$ is not sharp. Therefore, unless the temperature gradient in the plasma either in space or in time is very large, temperatures can be determined with poor accuracy only (Lochte-Holtgreven, 1968).

"Multi-Line" Temperature Determination

By comparing the intensities of two (or more) spectral lines, temperatures can be determined from relative, rather than

absolute, values of emission coefficients and transition probability. If two lines, belonging to the same atomic species, are considered, their emission coefficient ratio is given as:

$$\varepsilon_{line_1}/\varepsilon_{line_2} = A_1 g_1 \lambda_2/(A_2 g_2 \lambda_1) \cdot \exp[-(E_1-E_2)/kT] \qquad (34)$$

Thus, the partition functions U_1 and the number densities of particles in the ground state N_1 appearing in Equation (35) cancel out.

As pointed out by Welch (1972), the accuracy of the temperature determination depends on the energy difference $(E_1 - E_2)$ as can be seen in the following equation obtained by differentiating Equation (34):

$$\Delta T/T = kT/(E_1-E_2) \cdot \Delta(\varepsilon_1/\varepsilon_2)/(\varepsilon_1/\varepsilon_2) \qquad (35)$$

Unfortunately, in many cases the energy difference $(E_1 - E_2)$ is below 2ev and in addition, the uncertainties in the values of the transition probabilities magnify in the ratio (Chuang, 1965). Accuracy may be improved by averaging measurements of 2-line pairs. This averaging can be done also by plotting the log $(\varepsilon_1/\varepsilon_2)$ against $(E_1 - E_2)$ for several pairs, in which case a straight line will be obtained whose slope yields the temperature. But for increased accuracy, the range of $(E_1 - E_2)$ should be as large as possible.

A complete list of all the workers that used the "multi-line" technique will not be given here since they are numerous.

The work of Adcock and Plumtree (1964) is quite representative. It is generally preferred over the single line technique since the validity of LTE can also be checked from log-log plot (Richter, 1965). However, a high degree of reproducibility of the plasma source is required in order to collect the large amount of spectroscopic data necessary to reduce the random uncertainties in the log-log fitting procedure and hence yield an accurate resultant temperature (Preston, 1977). This may explain the scatter observed in the results of various investigators including Carleton (1970), Glickstein (1976) and Tidwell (1972).

The requirement of large energy differences of the upper level ($E_1 - E_2$) leads to the use of lines from different ionization stages. Here again the number of atomic species cancels, but the sum of states $\underline{U}$ cancels no longer. In addition, the transition probabilities of the lines are required and the argument of Chuang holds here again. It is interesting to note that Welch (1972) in his Ph.D. thesis, used lines from different ionization stages but mistakingly cancelled the partition functions, $\underline{U}_1$.

b. Continuum Emission

In the radiation emitted by a plasma, the discrete spectral lines are superimposed on a continuous spectrum. Continuum emission results from transitions involving free electrons whose energy is unquantized. There are two types of electron transitions: free-free (or bremsstrahlung) which results when the electron undergoes

an acceleration in the field of another charged particle, and free-bound (or recombination) which results when the electron is captured into the orbit.

For the free-free transition, assuming a Maxwellian velocity distribution of electrons with a temperature T_e, the emission coefficient follows from Kramers' calculation as (Richter, 1968):

$$\varepsilon_{ff}(\nu,T_e) = C_1 N_e/T_e^{1/2} \cdot \sum_1^z z^2 N_z \exp(-h\nu/kT_e) \qquad (36)$$

where, $C_1 = 16\ \pi e^6/(3c^3(6\pi m^3 k)^{1/2}) = 5.44 \times 10^{-39}$ cgs units. N_e = electron density, N_z = density of ions at level z, z = nuclear charge (z = 1 for singly ionized, etc.).

Equation (36) is, strictly speaking, only valid for hydrogen-like atoms. To apply to argon radiation, a factor $G_z(\nu,T_e)$, called Gaunt factor, is introduced. Karzas and Latter (1961) have calculated $G_z(\nu,T_e)$ quantum-mechanically.

On the other hand, the emission coefficient for the recombination or free-bound radiation is given by:

$$\varepsilon_{fb}(\nu,T_e) = C_1\ N_e/T_e^{1/2} \sum z^2 N_z\ g_z/U_z \cdot \zeta_z(\nu,T_e)$$
$$[1 - \exp(-h\nu/k\ T_e)] \qquad (37)$$

Here, again, $\zeta_z(\nu,T_e)$ is a factor which takes deviations from hydrogen-like behaviour into consideration, and is generally known as Biberman factor (Biberman and Norman, 1960). The value of this factor, which depends much on the frequency ν, and rather little

on temperature T_e, was later re-calculated by Schlüter (1964) and experimentally determined by Schulz-Gulde (1970).

Taking free-bound and free-free transitions together, the continuous radiation of plasma is described by:

$$\varepsilon(\nu,T_e) = c_1 N_e/(T_e^{1/2}) \cdot \sum_z z^2 N_z [G_z(\nu,T_e)\exp(-h\nu/kT_e) + \zeta_z(\nu,T_e)\, g_z/U_z \cdot (1-\exp(-h\nu/kT_e))] \quad (38)$$

At high frequences $(h\nu/kT_e) >> 1$, the continuum is reduced to the recombination continuum (Venugopalan, 1972):

$$\varepsilon(\nu,T_e) = c_1 \Sigma z^2 N_e N_z/T_e^{1/2} \cdot \zeta_z(\nu,T_e) \quad (39)$$

(where, for simplicity, g_z/U_z is taken as 1).

At low frequencies $(h\nu/kT_e) << 1$, the continuum radiation is emitted by the free-free transition:

$$\varepsilon(\nu,T_e) = c_1 \Sigma z^2\, N_e N_z/T_e^{1/2}\, G_z(\nu,T_e) \quad (40)$$

Equation (38) or its simplified forms Equations (39) and (40) (as in most cases) can be used for temperature determination. It has two important advantages over the diagnostics based on line emissions: it is easier to correct for the optically thick plasmas (where plasma absorbs some of its own radiation), and it can be used even when the plasma is out of equilibrium, provided that the electron velocity distribution is Maxwellian (Venugopalan, 1972). However, on the average, the continuum emission coefficient is about an order

of magnitude lower than the strong line emission coefficients (measured at the same wavelength) and thus integration over a wide wavelength range is required, introducing the possibility of interference from other sources of radiation (Huddlestone and Leonard, 1965). Most workers used continuum emission measurements as a check for LTE (by comparing with line emission), rather than as a diagnostics tool by itself.

To be able to use continuum emission for the above purposes, the values of $G_z(\nu,T_e)$ and $\zeta_z(\nu,T_e)$ must be known. As stated by Schulz-Gulde (1970), an accuracy of 20 to 25% can be expected for their values, which change between 1 and 2 for most of the visible range. It is thus not very surprising to see that Olsen (1961) obtained very good agreement between temperatures obtained from line emission and continuum emission measurements, although he assumed unity for the correction factors. In his later works (1962 and 1963a) Olsen used Fowler-Milne (or Larenz) method (i.e., on a normalized basis) for the continuum emission temperature determination and thus ignored the temperature dependence of the correction factors. A value of 2.3 was obtained for the whole term in square brackets in Equation (38) for 5535 A° (Olsen, 1963b). This value was confirmed by the measurements of Bott (1966). Schulz-Gulde (1970) experimentally determined the value of $\zeta(\nu,T_e)$ and found very close agreement with the results of Schlüter (1965), in the spectral range from 2600 to 7000 A°. He assumed a value of 1.7 for $G_z(\nu,T_e)$ in the range of his calculations. This assumption

is in agreement with Schnapauff (1968) who reported very small variation of $G_z(\nu,T_e)$ with wavelength and temperature. Lapworth (1977) and Preston (1977) also used the values of Schlütter and Schnapauff for $\zeta_z(\nu,T_e)$ and $G_z(\nu,T_e)$, respectively. All of the above workers only considered single ionization of argon (i.e., $z = 1$ and $N_z = N_e$), although the doubly-ionized levels do become important above 12,000 K (Olsen, 1962). This assumption further simplifies Equation (38) since $q_z \approx U_z$ for single ionization.

iii. Miscellaneous Techniques

A third possible way of measuring plasma temperatures is the combination of the probe and optical techniques. A good example of this technique, which has been demonstrated by Stojanoff (1966, 1968) and Sheer et al (1969), is the transient Fiber Optics Probe. The basic motivation was to eliminate the limitations of the side-on spectrophotometric techniques. (These limitations are the subject of the next section). The probe essentially consisted of a thin stainless steel tube (i.d. 1.5 mm) with a cap or blocking shield beyond the end of the tube. The purpose of the cap was to block off the radiation from all plasma source points outside the small volume between the cap and the end of the tube. Into the far end of the probe tube, a fiber optics bundle was inserted to transmit the radiation incident on the entrance surface of the bundle inside the probe to a monochromator tuned to a certain argon line (6965 A°). The probe was driven through the plasma with a high

speed traverse mechanism (750 cm/sec). A linear potentiometer coupled with the drive shaft indexed the position. The output of the monochromator was fed to an oscilloscope horizontally driven by the potentiometer. The radial intensities were first converted into the emission coefficient and then by comparing with the theoretical values, actual temperatures were determined. The most important questions arising from the application of such an immersion type optical probe for plasma diagnostics are the plasma perturbations, the possible influence of the plasma velocity on the flow pattern in the sampling gas (as observed by Stojanoff, 1966), and the limited resolution due to the finite volume of the sampling volume. The possible loss of the plasma radiation in the fiber optics by absorption is also another restriction of the above technique.

In addition to the above techniques, various methods exist for measuring mean temperatures, such as attenuation of microwaves (Herzfeld, 1962), velocity of sound (Hersfeld, 1962), (Carnevale et al, 1961), electron beam excitation (Muntz, 1961), and density of radioactive vapor (Ecker, 1951). Recently, Cabannes et al (1970) used separate determinations of gas velocity and impact pressure to infer plasma temperatures from the Bernoulli equation. Anestos and Hendricks (1974) injected small macroscopic particles into the plasma and measured the charge acquired by them to determine the plasma temperature. Laser methods had also been used for plasma temperature determination (Jelyashevich et al, 1977).

COMPARISON OF THE PLASMA TEMPERATURE DIAGNOSTIC TECHNIQUES

The probe techniques mentioned earlier are applicable for temperatures below 10,000 K. They have a limited resolution because of their finite size, and the great care required in setting the coolant rate makes their use time-consuming. The steep temperature gradients and the small size of the transferred-arc plasma considered in this thesis necessitates better techniques than the probe techniques. Thermocouples, on the other hand, are limited to a useful maximum of about 2,500 K (Kubanek and Gauvin, 1967), and are subject to frequent burn-out due to oxygen contamination.

The spectroscopic temperature measurements (e.g., excitation temperature measurement) require a spectrophotometer. This equipment is large, non-portable and expensive. The measurements are time-consuming and the data resolution, as will be discussed in the next section, are lengthy and rely on several assumptions. These limitations can be eliminated if spectroscopic principles are combined with probing techniques, as done by Stojanoff (1968).

The other miscellaneous techniques mentioned give a mean value across the sampling path. The inability to resolve the steep gradients which can exist in a plasma, like transferred-arc, restricts the applicability of these techniques.

INVERSION OF LATERAL INTENSITY MEASUREMENTS TO RADIAL DISTRIBUTION

The optical systems used in plasma diagnostics detect the radiant energy coming from a range of depths. The spectral intensity of this radiation, I_λ, is related to emission coefficient, ε_λ, (line or continuum) by:

$$I_\lambda = \int \varepsilon_\lambda \, dl \tag{41}$$

where dl is the incremental length in the direction of observation through the source. Equation (41) is written on the assumption that the radiation source (plasma) is "optically thin," that is, the self-absorption of the radiation emitted by the source is negligible. (The validity of this assumption for atmospheric plasmas will be discussed at the end of this section). In the case of a cylindrical, symmetric plasma, the intensities measured along the chords (lateral intensities) passed through the plasma can be converted into true radial emission coefficients by the mathematical technique known as the Abel Inversion Technique. The geometry associated with this plasma is shown in Figure 4.

With the new notation, the specific intensity observed at any chord position x in a plane of constant z (direction of plasma flow) is:

$$I_\lambda(x,z) = \int_{-y_o}^{y_o} \varepsilon_\lambda(r,z) \, dy \tag{42}$$

FIGURE 4

GEOMETRY OF THE SPECTROGRAPHIC OBSERVATIONS

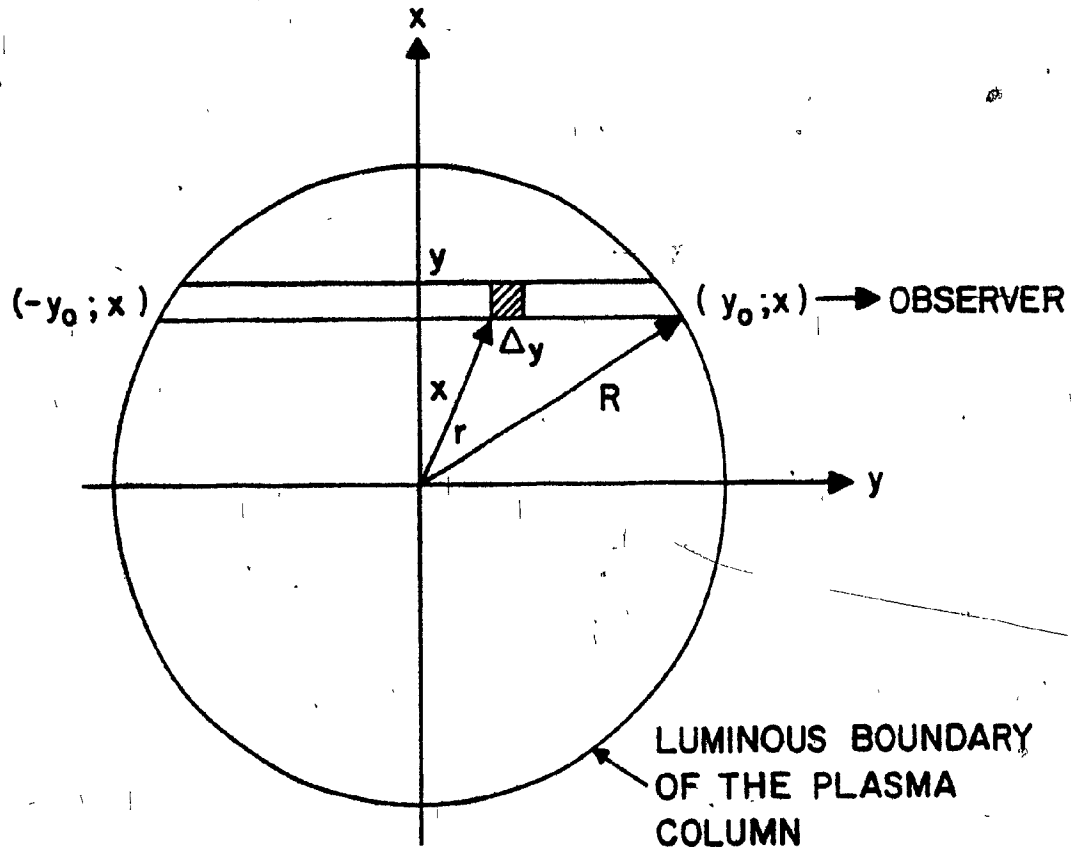
x
y
$(-y_0 ; x)$
$(y_0 ; x)$
OBSERVER
Δ_y
x
r
R
y
LUMINOUS BOUNDARY
OF THE PLASMA
COLUMN

The observed specific intensity $\underline{I_\lambda}(x,z)$ represents an integral of the emission through the plasma because of the gradient of $\underline{\varepsilon_\lambda}$ (i.e., temperature). At constant $\underline{x}$:

$$dy = rdr\ /y \tag{43}$$

and since

$$y^2 = r^2 - x^2 \tag{44}$$

one can write Equation (42) as:

$$I_\lambda(x,z) = 2 \int_x^R \varepsilon_\lambda(r,z) rdr/(r^2 - x^2)^{1/2} \tag{45}$$

in which $\underline{R}$ is the radius beyond which $\underline{\varepsilon_\lambda(r,z)}$ vanishes. This Equation (45) is a form of the Abel integral equation which can be analytically inverted as (Perry, 1973):

$$\varepsilon_\lambda(r,z) = -1/\pi \cdot \int_r^R (dI_\lambda/dx)dx/(x^2 - r^2)^{1/2} \tag{46}$$

Since it is not convenient to express the measured $\underline{I_\lambda(x,z)}$ as an analytical function, Equation (46) must be solved by numerical methods.

Several numerical methods have been developed for this inversion (Nestor and Olsen, 1960), (Bockasten, 1961), (Barr, 1962), (Pearce, 1960), (Maldonado et al, 1965), (Bohn et al, 1967). Following Lochte-Holtgreven (1968), the different methods used can be classified into four groups as follows:

1. Graphical integration

2. a) Expansion of the Integral Equation (41) as a set of linear equations given by:

$$I_\lambda(x_k,z) = \sum_{i=k}^{N} a_{ik}\, \varepsilon_\lambda\,(r_i,z) \tag{47}$$

b) Or, using an inverse matrix:

$$\varepsilon_\lambda(r_i,z) = \sum_{i=k}^{N} b_{ik}\, I_\lambda\,(x_k,z) \tag{48}$$

3. Expansion of the Integral Equation (46) into a set of linear equations:

$$\varepsilon_\lambda(r_i,z) = \sum_{i=k}^{N} \beta_{ik}\, I'_\lambda\,(x_k,z) \tag{49}$$

4. Approximation of $\underline{I(x,z)}$ by polynominals

Berge and Richter (1966) showed that method (1) is too tedious and not very accurate; method (2a) needs subsequent inversion, so that method (2b) is to be preferred. With method (3), which has been used by Nestor and Olsen (1960), and Bockasten (1961), difficulties arise near the axis and edges where $\underline{I'_\lambda(x,z)}$ is rather small. In addition, as discussed by Barr (1962), when the derivative is obtained, the noise in the data is amplified. The curve fitting technique (4) can be done in approximation with different analytical expressions. Macdonado et al (1965) used this technique for circularly-symmetric sources, and later extended it for asymmetric sources (1966). However, as readily admitted by the authors, because of the various parameters involved, the method is

computationally very complex and time-consuming.

Barr (1962) showed that when using method (3), if the order of differentiation and integration is reversed, important improvements can be achieved in the accuracy of the inversion. The expression resulting is the Equation (48). He has tabulated the values of the coefficients b_{1k} for $N<20$. His method is used in this investigation for comparison of the techniques and is described in Appendix (A).

It must be noted that the methods (2) are recursive in character; thus, the numerical errors are summing up. The resulting error is not only of an experimental nature but depends furthermore strongly on the plasma profile and on the number of divisions (observations) used. In addition, in each interval, $I(x)$ has to be approximated by a polynomial (a necessity in method (3) also) which further causes some errors.

Whichever method is used for inversion, the evaluated radial distribution may deviate from the true distribution for a number of additional reasons. First, one has to choose a certain number of intervals and the assumption that $\varepsilon(r)$ is constant throughout the subintervals of integration and independent of θ (i.e., circular symmetry) does not satisfy the real conditions in many plasmas. In addition, in most cases, due to the fluctuations encountered in the plasma radiation, only a time average of the function $I_\lambda(x,z)$ can be measured. Thus $I'_\lambda(x,z)$ is the derivative

of an average quantity. [At this point, if one refers back to the equations given for the relations between intensity of radiation and temperature, it will be seen that temperatures obtained from these averaged intensities will be weighted averages that can often deviate from simple averages (Burns, 1964)].

Before closing this section on inversion of intensity into emission coefficient, it is appropriate to discuss briefly the important assumption that the plasma is optically thin. A body of gas in which the total absorption approaches unity in a certain direction is said to be "Optically Thick." Most gas discharges at ordinary pressure, however, are optically thin, except for absorption lines and limited regions outside the visible spectrum. Self-absorption at a certain wavelength can be checked in two ways: (a) by using the temperature distribution obtained from spectral lines known to be least absorbed, the distribution of emission coefficients and then that of intensity can be calculated, neglecting absorption. These are then compared with the measured values (Olsen, 1963). Or, (b) by reflecting the radiation back upon itself through the hot gas or plasma by means of a concave mirror. The intensity of the direct radiation plus the reflected radiation will then be very nearly twice as great as the direct radiation alone (after allowing for reflection losses at the mirror) for all optically thin lines [Lapworth, (1974), Knopp et al (1962)]. When selecting the wavelengths to be used for diagnostics, it is important that the absorption characteristics of

the plasma is taken into consideration. Knopp et al (1962), Olsen (1963), Morris et al (1964), Evans and Tankin (1967) and Lapworth (1974) provide useful guidelines for this purpose. Lochte-Holtgreven (1968) gave detailed analyses of the cases when the plasma is not optically thin.

CONCLUSION

A single method of gas temperature measurement is by no means available which can be used for the wide range of temperatures existing in a plasma, without corrections or without questions as to the validity of the results.

Calorimetric probes and thermocouples can measure temperatures up to 10,000 K only and their applicability in plasmas is further limited because of poor resolution and associated uncertainties. Above 10,000 K, spectroscopic methods are probably the most useful although they suffer from the assumptions associated with the data analysis. In addition, because of turbulence and intrinsic plasma fluctuations, the spectroscopically measured temperatures are inescapably weighted averages (Burns, 1964) that can often deviate considerably from simple averages and therefore yield spurious values. These considerations, together with the general difficulty of handling spectrometers, dictate that a reliable diagnostic technique combining the merits of the probe and spectroscopic methods is required, with the chief advantages of relative simplicity and lack of dependence on source symmetry. The

development and test of such a method is one of the major objectives of this thesis.

GAS VELOCITY

Following Trokham (1968), the existing methods for measuring the velocity of plasma flows can be classified into three groups: kinematic methods based on the time of flight of tracers; dynamic methods based on the interactions between the flow and an inserted probe or an electric or magnetic field, and physical methods based on the quantitative assessment of phenomena occurring in the tested zone of the flow and which are a function of its velocity.

Tracer methods pose some difficulties in obtaining local measurements and in interpreting the results. The presence and method of introduction of the tracer may also disturb the plasma. The probe techniques, on the other hand, are simple and give good resolution despite the fact that they disturb the plasma. In most cases, however, these disturbances are small. Physical methods are the least accurate of the three, since they are indirect methods.

When determining the plasma velocity by the tracer method, one can either create tracers in the flow or inject tracer particles into the flow. Chen (1968) followed the downstream motion of an intense plasma "drop" produced by a giant-pulse laser beam by means of a streak-drum camera. Buoyancy effects and shock wave formation

effects were calculated to be negligible. Freeman et al (1962) determined the velocity of propogation of the luminous details in the plasma jet by the time required to transit between photo-multiplier stations located along the jet axis. They found that the plasma fluctuations could be ascribed to temperature fluctuations and to pressure waves. They were not able to interpret their results in terms of plasma velocity.

Desai et al (1968) measured the velocity distribution in an argon plasma by injecting boron nitride particles. The radial position of the particles was determined by using a three dimensional photographic technique. Chase (1971), Lewis and Gauvin (1973) and Waldie (1975) also used similar techniques to obtain flow visualization and gas velocities. While Desai assumed the particles moved at the gas velocity, the latter assumed Stokesian flow around the particles and thus deduced the plasma gas velocity from the particle velocities.

Gold (1975) described an opto-electronic method in which the optically and temporally-resolved measurements of the plasma luminosity was used to determine the velocity of the injected particles as well as the plasma. Sodium chloride particles were injected into the flame and the velocity was then deduced from following the propagation of increased intensity. The results obtained are not very accurate since it was not possible to determine the exact radial position of the particles.

Meubus (1974) used hydrogen as a tracer and was able to determine the concentration profiles spectroscopically. These profiles together with temperature field were used in a simplified material balance to determine argon velocity profiles. The argon flow rate determined by integrating this profile showed 20% deviation from the actual value.

Bowman (1972) dropped a line of ball bearings through a horizontal arc and recorded the horizontal deflection of the spheres (about 3 mm in diameter). Multiple drops through repeated arcs enabled a deflection curve to be compiled. The radial variation of the aerodynamic drag on the balls could be determined by using Abel inversion. By iterative techniques, the plasma velocity distribution was then determined. The results are questionable due to the disturbing influence of the balls within the plasma as well as the difficulty of assigning a temperature for drag coefficient determination.

Pressure probes are probably the most universally-applied devices for the measurement of gas velocity. The subject of pressure probes is extensively covered in the literature (Folsom, 1956), (Chue, 1975), (Becker, 1974, 1975). However, the bulk of the work has been carried out for isothermal flows and none of the above reviews deal with measurements in high-temperature flows, where the presence of a cooler probe disturbs not only the velocity field, but also the temperature field.

Grey et al (1962) used a water-cooled probe to measure the impact pressures in an argon jet. Bernoulli's equation for incompressible and inviscid fluids was then used to determine the velocity distribution. This probe could also be used as a calorimetric probe. Other users of this method included Katta et al (1973) and Gol'dfarb et al (1967). In a study on heat and mass transfer between a plasma jet and a gaseous coolant, Smith and Churchill (1965) also used a water-cooled probe to measure the gas velocity; however, they modified the Bernoulli's equation to take the density variation into account. In the same laboratory, Carleton (1970) carried out a semi-theoretical analysis for the stagnation pressure at the tip of a cold hemispherical probe. In his analysis, the stagnation streamline is divided into two regions. The flow region near the free stream is considered to be isentropic, inviscid and compressible, and the region next to the probe surface to be laminar, viscous and incompressible. The expression arrived at can be written as:

$$\Delta P = \rho_g U_g^2/2 + \rho_g U_g^4/(8\gamma P_g) + 2\bar{\mu} U_g / R(1 + 0.55/\sqrt{Re}) \qquad (50)$$

where $Re = U R \bar{\rho} / \bar{\mu}$.

The first term represents the conventional Bernoulli dependency on velocity, the second accounts for compressibility and the last one represents a correction for the effect of viscous forces near the probe. The first two terms were evaluated at the free-stream temperature and the third term at the temperature

corresponding to the mean enthalpy of the gas. Thus, the temperature correction was due to viscous effects and not density changes. Maximum correction of 3% for compressibility and 14% for the viscosity term was obtained by Carleton.

Hare (1972) studied the effect of the pitot tube tip temperature on velocity measurements in flames at temperatures in excess of 1500°C. It was found that the heat flux between the gas and the tube affected the pitot tube measurements for temperatures above 1000°C. No quantitative description was, however, given for this phenomenon. He recommended that for temperatures above 5000°C, the equation suggested by Carleton could be used safely.

All of the above workers used water-cooled probes and thus the sizes of their probes were comparable with the sizes of the plasmas used. To reduce the disturbances on the plasma, it is desirable to use miniaturized probes. However, below a certain diameter, it is not possible to cool the probes. A solution has been suggested by Barkan and Whitman (1966) who used a transient uncooled pitot tube. A high response time pressure transducer (<0.001 sec) was connected to a small (<0.15 mm o.d.) uncooled, pitot tube which was swept through the plasma (≈0.015 sec). This principle was later used by Sheer et al (1969) who connected the outlet of the pressure transducer and of the linear displacement transducer (which, in turn, was connected to the drive mechanism) to an oscilloscope which gave the stagnation pressure distribution

directly. A Pace-Wianco model P105 D variable reluctance transducer with a sensitivity of 0.001 psi was used. The traverse speed used was determined from the cold flow measurements. These workers also investigated the possible sources of errors. They concluded that the assumption of incompressibility, probe ablation effects, variation with temperature of the gas specific heat ratio, existence of radial and axial pressure gradients, and departure from adiabatic deceleration in the tube have negligible effect on the results. For viscosity effects, however, a correction had to be made following Barker (1922). With this correction, the Bernoulli's equation takes the form of:

$$\Delta P = 1/2 \cdot \rho U^2 + 3/2 \mu U/a \qquad (51)$$

This correction for low Reynolds number flows has also been suggested by Hurd et al (1953), MacMillan (1954), Schowalter and Blaker (1961), Sherman (1953) and Folsom (1956). Chue (1975) and Sayegh and Gauvin (1979) used a pressure coefficient, whose value depended on Reynolds number, to include the effect of viscosity.

The work of Kimura and Kanzawa (1963) is also interesting. The streaming velocity in an arc was evaluated by measurement of the drag on a small plate swept across the arc. The plate was attached to the diaphragm of a capacitance-type pressure sensor. The error in the measured stream velocity was calculated to be 17%.

Amongst the physical methods used for velocity determinations

in plasmas, the ones that are based on utilizing the Doppler effect are the most common. Bohn et al (1967) measured the Doppler shifts of spectral lines in an argon plasma jet with an interferometer. These were then converted into velocity profiles. Laser-Doppler anemometry is another technique that can be included in this group of methods. This technique is based on the accurate determination of particle velocities by measuring the Doppler shift of optical radiation scattered by moving particles. The use of this technique in plasma is somewhat restricted by several factors such as the method of seeding, material of the particles, cooling effect of the particle and most importantly, how accurately the particles can follow the plasma flow (Gouesbet and Grehan, 1979), (Todorovic et al, 1976). A preliminary study has been carried out in these laboratories and was discussed in more detail by Ho (1976).

Some workers tried to model the flow characteristics of plasmas. Gottschlich et al (1966) proposed a model where the axial velocity of a plasma jet was calculated from the temperature profile by a simple energy balance. The flow was assumed to be axisymmetric and unidirectional. Viscous energy dissipation and effects of radiation was neglected. The uncertainty in the thermal conductivity was reported to be the principal limitation. Meubus and Parent (1969) described a flow model where the luminous profile equation, temperature distribution and gas flow rate were used in the energy equation to determine the velocity distribution. The estimated error was of the order of 25%. Strachan and Barrault

(1976) and Topham (1971) also solved the energy equation using the experimental values of arc current, electric field, radius and radiation losses. No experimental verification was given in both cases.

CONCLUSION

As in the case of gas temperature measurements, the selection of the technique for plasma velocity depends on the range involved and the accuracy required. The transient uncooled pitot tube seems to be the most appropriate for measurements in a transferred arc plasma, basically due to its good spatial resolution and simplicity. On the other hand, laser-doppler anemometry appears to be the candidate for future applications.

III. JETS

In this section, a summary of the work on jets which is of immediate interest to this thesis will be given. Forstall and Shapiro (1950) and more recently Ferri (1964) provided extensive reviews on jets. The books by Abramovich (1963) and Birkhoff and Zarantonello (1957) are two standard texts on this subject.

Characteristics of Free Jets

According to Abramovich, when a tangential separation surface arises during the motion of a fluid, the flow of fluid on either side of this surface is called a jet. Any jet is divided

into three regions, namely the potential core, the transition region or the developing region, and the fully-developed region where the jet characteristics are independent of its source.

In most jets, the potential core region shows constant values of concentration, temperature and velocity, along the centre line. In the developing region, these three variables show a rapid decay with axial distance. In near isothermal circular jets, the decay has an inverse relationship with distance from the virtual origin of the jet (X):

$$U_m = c_1/X \tag{52}$$

$$T_m - T_o = c_2/X \tag{53}$$

$$C_m - C_o = c_3/X \tag{54}$$

where c_1, c_2 and c_3 are constants.

The validity of these expressions for plasma jets, where large changes in density (or velocity) result due to gas cooling, is doubtful. Indeed, Grey and Jacobs (1964) observed that a heated jet decays much more rapidly than an isothermal jet. Lemoine (1969) obtained an inverse square decay for the centreline gas velocity in an argon plasma jet. O'Connor et al (1966) found that centreline values of concentration decayed more rapidly than enthalpy, which decayed more rapidly than velocity. Lewis and Gauvin (1973), however, noted that the normalized profiles of velocity and

temperature are remarkably similar, with 90% of the decay occurring within a distance of ten nozzle diameters. The concentration decay was found to be slower than the velocity and temperature decays.

The radial profiles in the core region of isothermal jets can be expressed as (Warren, 1957):

$$U_r = U_m \qquad r < r_i \tag{55}$$

$$U_r = U_m \exp[-0.693(r^2-r_i^2)/(r^2_{1/2}-r_i^2)] \qquad r > r_i \tag{56}$$

In the developing region, the radial profiles may be represented by a Gaussian distribution (Abramovich, 1963):

$$U_r = U_m \exp[-0.693(r/r_{1/2})^2] \tag{57}$$

[where, for temperature or concentration profiles, U_r is replaced with ΔT or ΔC (difference between the values at a given distance in the jet and the outer boundary) and U_m with ΔT_o or ΔC_o (the corresponding difference at the centreline of the jet)].

O'Connor et al (1966) found that the radial profiles of velocity, enthalpy and concentration are similar at various axial stations of a plasma jet in the developing region and can be well represented by a Gaussian curve. They also observed a departure of the jet boundaries from the conical shape of isothermal jets. The curvature of their results, however, was in the opposite direction to that of Grey and Jacobs (1964). Another disagreement between their results is that the latter noted that concentration

spreads more rapidly than enthalpy which, in turn, spreads more rapidly than momentum. The fact that enthalpy spreads more rapidly than momentum has been also reported by Corrsin and Uberoi (1949) who studied circular jets of heated air, and more recently by Kubanek and Gauvin (1968), and Katta and Gauvin (1973).

Jet Entrainment

In addition to work concerned with free jets, some studies of entrainment in free jets are also pertinent to this thesis.

The majority of the work in this field is done with stagnant environment. Donald and Singer (1959) observed that the entrained fluid enters the jet at right angles. They found an empirical expression relating the entrainment capacity to kinematic viscosity and axial distance from the nozzle. Their results, however, are strictly for isothermal jets and even for this case the results are doubtful since they predict the same entrainment rates for the potential core and developed regions ($X/d_o > 15$). Ricou and Spalding (1961) developed a new technique for measuring total entrainment in axially-symmetric gas jets of various densities. They correlated their results as:

$$m_i = m_o[0.32\ X/d_o(\rho_1/\rho_2)^{1/2}-1] \qquad (58)$$

where m_i is the entrained mass flux and m_o the initial mass flow rate of the jet. These workers also noted that buoyancy effects increased the entrainment rate but were unable to reach a firm

conclusion. Hill (1972) confirmed that the rate of entrainment is constant in the fully developed region but found that the local entrainment rate, which is independent of the nozzle Reynolds number, is a strong fuction of axial distance in the core region. He did not correlate his results however.

CONCLUSION

There is a lack of agreement between several workers on the variation of jet parameters. This disagreement could possibly be explained by the complexity of the plasma jet systems and difficulties encountered in the experimental techniques.

The radial distributions of properties follow a Gaussian curve in plasma jets. The axial variation, on the other hand, shows an inverse square decay, with concentration decaying faster than temperature and temperature decaying faster than velocity.

The applicability of the limited data on the entrainment in isothermal free jets to plasma conditions is doubtful because of the presence of the bouyancy effects and magneto-hydrodynamic forces.

NOMENCLATURE

NOMENCLATURE

A_{nm}	–	Einstein's spontaneous transition probability
A_1, A_2	–	Nozzle cross-sectional area, Equation (27)
a	–	Coefficient, Equation (47)
a	–	Inside radius of pitot-tube, Equation (51)
$\vec{B}$	–	Magnetic flux density (vector)
b	–	Coefficient, Equation (48)
C	–	Concentration
c	–	Speed of light
$\vec{c}$	–	Total macroscopic drift velocity of the plasma
C_p	–	Heat capacity at constant pressure
$\vec{D}$	–	Electric flux density (vector)
d_o	–	Jet nozzle diameter
$\vec{E}$	–	Electric field strength (vector)
e	–	Electronic charge
E_n	–	Energy of level n with respect to the ground level
$\vec{G}$	–	Gravitational field (vector)

G_z	-	Gaunt factor
g_n	-	Statistical weight of the level n
$\vec{H}$	-	Magnetic field strength (vector)
h	-	Plank's constant
I	-	Intensity of radiation, Equation (41) afterwards
I	-	Current
$\vec{J}$	-	Current density (vector)
k	-	Boltzmann constant
m	-	Mass of electron
N	-	Number of observations in Abel Inversion Technique
n	-	Number of atoms
n_e, n_i, n_a	-	Electron, ion and atom densities, respectively
N_n	-	Concentration of atoms in the excited state n
P	-	Pressure
q	-	Total change
R	-	Radius
r	-	Radial distance
$r_{1/2}$	-	Radius at which property has half the centreline value
Re	-	Reynolds number, uD/ν
r_i	-	Radius of the edge of jet core

$S(T)$	-	Radiative power
T	-	Temperature
t	-	Time
$\underline{\underline{T}}$	-	Pressure tensor of the entire plasma
U	-	Free-Stream velocity
$U(T)$	-	Partition function
v_i	-	Ionization potential
$\vec{V}$	-	Streaming velocity
v_e, v_i	-	Electron and ion drift velocities, respectively
X	-	Distance from the virtual origin of the jet Equation (52)
X	-	Coordinate
z	-	Nuclear charge

Greek Letters

λ	-	Wavelength
ν	-	Frequency (or Kinematic viscosity)
ζ_z	-	Biberman factor
β	-	Coefficient, Equation (49)
ε	-	Emission coefficient
ρ	-	Density

ε - Permitivity of the medium, Equation (13)

μ^* - Permeability of the medium, Equation (14)

σ - Electrical conductivity, Equation (15)

δ_{ij} - Kronecker delta

η - Dynamic viscosity

$\bar{\mu}$ - Average viscosity

κ - Thermal conductivity

γ - Euler's constant

Subscripts

m - Property at the jet axis

o - Property outside the jet boundary

r - In r-direction

θ - In θ-direction

z - In z-direction

i - In i-direction

j - In j-direction

REFERENCES

REFERENCES

Abramovich, G.N., "The Theory of Turbulent Jets," MIT Press, (1963).

Adcock, B.D. and Plumtree, W.E.G., "On Excitation Temperature Measurements in a Plasma Jet, and Transition Probabilities for Argon Lines," J. Quant. Spect. Radiat. Transfer, 4, 29-39, (1964).

Ahtye, W.F., "A Critical Evaluation of Methods for Calculating Transport Coefficients of Partially and Fully Ionized Gases," NASA Technical Note, D-2611, Washington, (1965).

Aller, L.H., "Astrophysics: The Atmospheres of the Sun and Stars," 2nd. ed., The Roland Press Co., N.Y., (1963).

Amdur, I. and Mason, E.A., "Properties of Gases at Very High Temp.," The Physics of Fluids, 1, (5), 370, (1958).

Anestos, T.C. and Hendricks, C.D., "Injection of Small Macroscopic Particles into Plasmas as a Diagnostic Technique," Journal of Applied Physics, 45, (3), 1176, (1974).

Angier, D.J., Cahn, R.P., Sheer, C. and Korman, S., "Synthesis of Submicron Powders by Arc Vaporization," Intern. Symp. on Plasma Chem., Kiel, Germany, (1973).

Arkless, K. and Cleaver, D., to Tioxide International, Oxidation Process, British Pat. 4,035,191, (1966).

Asada, C. and Adachi, T., "On Plasma Induction Melting," in 3rd. Inter. Symp. on Electroslag and Other Special Melting Tech., ed. by G.K. Bhat and Simkovich, A., (June 1971).

Asinovsky, E.I., Pakhomov, E.P. and Yantsev, I.M., "Argon Plasma Viscosity Measurements," IEE Conf. Pub. no. 143, 376-378, (1976).

Aubreton, J. and Fauchais, P., "Les Fours à Plasma," Rev. Gen. Therm. Fr., no. 200-201, p. 681, (1978).

Audsley, A., "Thermal Plasmas: Their Control and Use," Chem. Eng., 190-192, Sept., (1967).

Baddour, R.F. and Timmins, R.S., "The Application of Plasmas to Chemical Processing," M.I.T. Press, (1967).

Bahador, M.N. and Soo, S.L., "Non Equilibrium Transport Phenomena of Partially Ionized Argon," Int. J. Heat-Mass Tr., 9, 17-34, (1966).

Barkan, P. and Whitman, A.M., "Stagnation Pressure Measurement in a Current Carrying Plasma," AIAA J., Tech. Notes, 4, (9), 1691, (1966).

Barker, M., (Miss), "On the Use of Very Small Pitot-Tubes for Measuring Wind Velocity," Proc. Roy. Soc. of London, 101, 435, (1922).

Barr, W.L., "Method for Computing the Radial Distribution of Emitters in a Cylindrical Source," J. of Opt. Soc. of America, 52, (8), 885, (1962).

Becker, H.A. and Brown, A.P.G., "Response of Pitot Tubes in Turbulent Streams," J. Fluid. Mech., 62, Part 1, 85-114, (1974).

Becker, H.A., Cho, S.H. and Dhanjal, M.S., "Response of Static Pressure Probes in Turbulent Flames," J. Fluid Mech., 63, Part 2, (1975).

Berge, O.E. and Richter, J., "AFSC Report 61, (052), 797, (1966), from Lochte-Holtgreven (1968), p. 185.

Bhat, G.K., "New Developments in Plasma Arc Melting," J. Vac. Sci. Technol., 9, (6), 1344, (1972).

Bhattacharyya, D. and Gauvin, W.H., "Modelling of Heterogeneous Systems in a Plasma Jet Reactor," AIChE Journal, 21, (5), 879, (1975).

Bhattacharyya, D. and Gauvin, W.H., "Application of Magnetic Pinch Force to Arc Plasma Processes," J. of Appl. Phys., 47, (11), 4863, (1976).

Biberman, L.M. and Norman, G.E., "On the Calculation of Photo Ionization Absorption in Atomic Gases," Optics and Spectroscopy, 8, 230, (1960).

Biceroglu, O., "Chlorination Kinetics of ZrO_2 in an RF Plasma Tailflame," Ph.D. Thesis, McGill University, (1978).

Bird, R.B., Stewart, W.E., Lightfoot, E.N., "Transport Phenomena," John Wiley, (1960).

Birkhoff, G. and Zarantonello, E.H., "Jets, Wakes and Cavities," Academic Press, (1957).

Bober, L. and Tankin, R.S., "Investigation of Equilibrium in An Argon Plasma," J. Quant. Spectrosc. Radiat. Transfer, 10, 991-1000, (1970).

Bockasten, K., "Transformation of Observed Radiances into Radial Distribution of the Emission of a Plasma," J. of Opt. Soc. of America, 51, (9), 943, (1961).

Bohn, W.L., Beth, M.U. and Nedder, G., "On Spectroscopic Measurements of Velocity Profiles and Non-Equilibrium Radial Temperatures in an Argon Plasma Jet," J. Quant. Spect. Radiat. Transfer, 7, 661, (1967).

Bonet, C. et al, "A Study of the Thermal Treatment of Refractories in a Fluidized Bed by Plasma Discharge," Rev. Int. Htes. Temp. et Refract. 11, 11-24, (1974).

Bonet, C., "Thermal Plasma Processing," C.E.P., p. 63, (December 1976).

Borer, W., "Large Scale Spheroidisation of Oxide Powders," discussed at Gordon Conference on Plasma Chemistry, (August 1978).

Borodachyov, A.S., Okorokov, G.N., Pozdeev, N.P., Tulin, N.A., (U.S.S.R.), and Fiedler, H., Muller, F. and Scharf, G., (G.D.R.), "Plasma Steel-Making Furnaces - Dev. and App. Experience," Proceedings of the World Electrotechnical Congress, Paper No. 4A-26, Session Iv, Moscow, U.S.S.R., (June 1977).

Bott, J.F., "Spectroscopic Measurement of Temperatures in an Argon Plasma Arc," The Physics of Fluids, 9, (8), 1540, (1966).

Boulos, M.I. and Gauvin, W.H., "Powder Processing in a Plasma Jet: A Proposed Model," Can. J. Chem. Eng., 52, 355, (1974).

Boulos, M.I., "Flow and Temp. Fields in the Fire-ball of an Inductively Coupled Plasma," Conf. Proceedings, Int. Round Table On Plasmas, Odeillo, France, (1975).

Bowman, B., "Measurement of Plasma Velocity Distributions in Free-Burning DC Arcs up to 2160A," J. Phys.D., Appl. Physics, 5, 1422, (1972).

Bradley, D. and Matthews, K.J., "Measurement of High Gas Temperature with Fine Wire Thermocouples," J. Mech. Eng. Sci., 10, (4), 299, (1968).

Bryant, J.W. and Whyman, D., "A Cathode Assembly for Feeding Powders into the Plasma of Expanded DC Arcs," J. of Sci. Inst., 7, Series 2, 779, (1969).

Burns, J., "Research on Effects of Arc Fluctuations on Spectroscopically Determined Temperatures in Arc Plasmas," Air Force Materials Lab., Res. and Technology Div., Air Force System Command, TDR-ML-TDR-64-243, (July 1964).

Cabannes, F., Chapelle, J., Czerichowski, A., Decroisette, M. et Zamarlick, J., Rev. Inst. Htes. Temp. et Refract., 7, 7, (1970).

Carleton, F.E., "Flow Patterns in a Confined Plasma Jet," Ph.D. Thesis, University of MIchigan, Ann Arbor, (1970).

Carnevale, E.H., Poss, H.L. and Yos, J.M., "Avco Corp., Tech. Rep. RAD-TR-61-13, (1961).

Charles, J.A., Davies, G.J., Jervis, R.M., Thrusfield, G., "Processing of Minerals in an Induction Coupled Plasma Torch," Trans. Inst. of Min. & Metall., 79, 54, (1970).

Chase, J.D., "Theoretical and Experimental Investigation of Flow and Pressure in Induction Plasmas," J. of Appl. Phys., 42, (12), 4870, (1971).

Chen, C.J., "Velocity Profile Measurement in Plasma Flows Using Tracers Produced by a Laser Beam," J. of App. Physics, 37, (8), 3092, (1966).

Chevela, O.B. et al, "Experimental Investigation of the Temperature of a Plasma Jet," Sav. Proi 2, No. 10, 1-3, (1975).

Chludzinski, G.R., "Energy Transfer to Solids in r.f. Generated Plasmas," Ph.D. Thesis, University of Michigan, Ann Arbor, (1964).

Choi, H.K., "Energy Distribution and Heat Transfer in an Argon Transferred-Arc Reactor," Ph.D. Thesis, McGill University, (1980).

Chu, T.K. and Gottschlich, C.F., "Temperature Measurement of an Alkali Metal-Seeded Plasma in an Electric Field," AIAA J., 6, (4), 114, (1968).

Chuang, H., "Uncertainties in the Measurements of the Plasma Temperature by the Relative Intensity Method," Appl. Optics, 4, 1589, (1965).

Chue, S.H., "Pressure Probes for Fluid Measurement," Prog. Aerospace Sci, 16, (2), 147, (1975).

Cohen, I.M. and Whitman, A.M., "The Two-Dimensional Constant Property Arc," J. of Appl. Physics, 47, (5), 1932, (1976).

Corrsin, S. and Uberoi, M.S., NACA Report 998, (1949).

Desai, S.V., Daniel, E.S. and Corcoran, W.H., "Use of Particles of Boron Nitride in the Measurement of the Velocity Distribution in Laminar Flow in an Argon Plasma Jet," Rev. of Scie. Inst., 39, (4), 612, (1968).

Devoto, R.S., "Transport Coeff. of Partially Ionized Argon," The Phys. of Fluids, 10, (2), 354, (1967a).

Devoto, R.S., "Simplified Expressions for the Transport Properties of Ionized Monatomic Gases," The Phys. of Fluids, 10, (10), 2105, (1967b).

Donald, M.B. and Singer, H., "Entrainment in Turbulent Fluid Jets," Transac. Inst. Ch. Eng., 37, 255, (1959).

Drellishak, K.S., AEDC-TDR-63-146, (August 1963).

Drellishak, K.S., Knopp, C.F. and Cambel, A.B., "Partition Functions and Thermodynamic Properties of Argon Plasma," The Physics of Fluids, 6, (9), 1280, (1963).

Dundas, P.H., "Induction Plasma Heating, Meas. of Gas Concentrations, Temp. and Stagnation Heads in a Binary Plasma System," NASA CR1527, NASA, Wash. D.C., (1970).

Ecker, G., A. Phys., 130, 585, (1951).

Eckert, H.W., "The Induction Arc: A State of the Art Review," HIgh T. Scie., 6, 99-134, (1974).

Emmons, H.W., "Arc Measurements of High Temp. Gas Properties," The Physics of Fluids, 10, (6), 1125, (1967).

Esser, F., et al, "Theory of Remelting and Melting-Down of Solid Metallic Charges in a Plasma Furnace - A contribution to Optimizing the Process of Plasma Primary Melting," Neue Hutte., 19, (10), 577-586, (1974).

Evans, D.L. and Tankin, R.S., "Measurement of Emission and Absorption of Radiation by an Argon Plasma," The Phys. of Fluids, 10, (6), 1137, (1967).

Everest, D.A., Sayce, I.G. and Selton, B., "Preparation of Ultrafine Silica Powders by Evaporation Using a Thermal Plasma," Symp. on Electrochem. Eng. (ed. J.D. Thornton) Vol. 2, p.2-108, Inst. of Chem. Eng., London, (1973).

Ferri, A., "Review of Problems in Application of Supersonic Combustion," J. of Roy. Aero. Soc., 68, 575, (1964).

Fey, M.G., Meyer, T.N. and Reed, W.H., "An Electric Arc Heater Process to Produce Solar Grade Silicon," Proceedings of 4th Intern. Symp. on Plasma Chemistry, V. 2., p. 708, Zurich, Switzerland, (August 1979).

Fiedler, H., "The State of Plasma Melting Technology in the GDR," Neue Hutte, 21, (2), 69-72, (1976).

Finkelnburg, W. and Maecker, H., "Hanbuch der Physik," 22, p. 244-254, Springer, Berlin, (1956).

Fisher, I.A., "Variables Influencing the Characteristics of Plasma Sprayed Coatings," Intern. Metall. Rev., 17, 117-129, (1972).

Folsom, R.G., "Review of the Pitot Tube," ASME Trans., 1448, (1956).

Forstall, W. and Shapiro, A.H., "Momentum and Mass Transfer in Coaxial Gas Jets," J. Appl. Mech., Trans. ASME, 17, 399, (1950).

Foster-Wheeler/Tetronics: News Features, "Plasma Process is Ready for Metal Revoery," Chem. Eng., 86, (4), 75, (1979).

Freeman, M.P., Sik, U.Li and Von Jaskowsky, W., "Velocity of Propogation and Nature of Luminosity Fluctuations in a Plasma Jet," J. of App. Physics, 33, 9, (1962).

Freeman, M.P., "Chemical Reactions in Electrical Discharges," Advan. Chem. Ser., 80, 406, (1968).

Freeman, M.P., "Chemical Research in Streaming Thermal Plasmas," in Advances in High Temperature Chemistry, Vol. 2, (1969), ed. L. Eyring, Academic Press.

Garratt, M.J. and Littlewood, K., "The Direct Production of Acetylene by Pyrolysis of Coal in Plasma Jets," Proceedings of Intern. Symp. on Plasma Chem., Vol. 2, p. 408, Zurich, Switzerland, (August 1979).

Gauvin, W.H., Kubanek, G.R. and Irons, G.A., "The Plasma Production of Ferromolybdenum - Process Development and Economics," J. of Metals, (1980), (in press).

Gerdeman, D.A. and Hecht, N.L., "Arc Plasma Technology in Materials Science," Springer-Verlag (1972).

Gold, D., "Velocity Measurement in an R.F. Induction Plasma," Int. Round Table on Plasmas, Odeillo (1975), paper IV-8.

Gold, R.G., Sandall, W.R., Cheplick, P.G. and Mac Rae, D.R., "Plasma Reduction of Iron Oxide with Hydrogen and Natural Gas at 100 kW and One Megawatt" in "Metal Slag-Gas Reactions and Processes," ed. by 2-A, Foroulis and Smeltzer W.W., The Electrochem. Soc., p. 969-981, (1975).

Gold, D., Bonet, C., Chauvin, G., Mathieu, A.C., "Spheroidisation of Alumino-Silicate Particles," Int. Symp. on Plasma Chem., Zurich, Switzerland, (August 1979).

Goldberger, W.M., "The Plasma Bed: Performance and Capabilities," Fluid-Particle Techno., Chem. E. Symp. Series, Vol. 62, (62), p. 42, (1963).

Gol'dfarb, V.M., Danskoi, A.V., Drevsin, S.V. and Klubnikin, V.S., "Investigation of Plasma Torch of High-Frequency Argon Burner," High Temp., 5, 495, (1967).

Goldman, K., "Electric Arcs in Argon," Physica, 29, 1024-1040, (1963).

Gottschlich, C.F., Enright, J.A. and Cadek, F.C., "Measurement of the Velocity Distribution in a Plasma Jet," AIAA Journal, 4, (6), 1085, (1966).

Gouesbet, G. and Grehan, G., "Laser-Doppler Systems for Plasma Diagnostics: A Review and Prospective Paper," 4th Int. Symp. on Plasma Chem., Vol. 2, p. 603, Zurich, Switzerland, (August 1979).

Glikstein, S.S., "Temperature Measurements in a Free-Burning Arc," Welding Research Supplement, 222-5, (1976).

Grey, J., Jacobs, P.F. and Sherman, M.P., "Calorimetric Probe for the Measurement of Extremely High Temperatures," Rev. Sci. Instrum., 33, (7), 738, (1962).

Grey, J. and Jacobs, P.F., "Experiments on Turbulent Mixing in a Partially Ionized Gas," AIAA Journal, 2, (3), 433, (1964).

Grey, J., "Thermodynamic Methods of High-Temperature Measurement," ISA Trans., 4, (2), 102, (1965).

Grey, J., "Proposed Method for Measuring Gas Enthalpy Using Calorimetric Probes," ASTM, Committee E-21 on Space Simulation, (1968).

Griem, H.R., "Validity of LTE in Plasma Spectroscopy," Physical Review, 131, (3), 1170, (1963).

Gvozdetskii, V.S. and Zrazhevskii, V.A., Numerical Solution of the Equation for Energy Balance of the Column of the Cylindrical Arc," Avt. Svarka, No. 6, p. 5-8, (1975).

Hamblyn, S.M.L., "A Review of Applications of Plasma Technology with Particular Reference to Ferro-Alloy Production," National Inst. for Metall., Rep. No. 1895, (1977).

Hare, A.L., "Some Problems Associated with using Cooled Probes to Characterize Flames of Temperatures in Excess of 1500°C," presented at 21st. Aerodynamics Panel Meeting, International Flame Res. Foundation, Ijmuiden, November 8, (1972).

Harry, J.E. and Hobson, L., "The Interaction of an Induction Coupled Discharge with a DC Arc," Int. Round Table on Study and Appl. of Transport Phenomena in Thermal Plasmas, Odeillo, France, (1975).

Heberlein, J.V.R., Lowry, J.F., Meyer, T.N. and Ciliberti, D.F., "The Reduction of Tetrachlorosilicane by Sodium at High Temperatures in a Laboratory Scale Experiment," Proceedings of 4th Intern. Symp. on Plasma Chemistry, Vol. 2, p. 716, Zurich, Switzerland, (August 1979).

Hellund, E.J., "The Plasma State," Reinhold, (1961).

Hermann, W., Kogelschatz, U., Ragaller, K., Schade, E., "Investigation of a Cylindrical Axially Blown, High Pressure Arc," J. Phys. D.: Appl. Phys. 7, 607, (1974).

Herzfeld, C.M., "Temperature, Its Measurements in Science and Industry," Reinhold, Vol. 3, Part 2, 3, (1962).

Hill, B.J., "Measurements of Local Entrainment in the Initial Region of Axisymmetric Turbulent Air Jets," J. Fluid Mech., 51, (4), 773, (1973).

Hirschfelder, J.O., Curtiss, C.F. and Bird, R.B., "Molecular Theory of Gases and Liquids," John Wiley & Sons, (1954).

Ho, T.H., "Laser-Doppler Anemometry and Its Application to High Temperature Reactors," M. Eng. Thesis, McGill University, (1976).

Hollahan, J.R. and Bell, A.T., "Techniques and Applications of Plasma Chemistry," John Wiley and Sons, (1974).

Howatson, A.M., "An Introduction to Gas Discharges," 2nd. ed., Permagon, (1976).

Hoyaux, M.F., "Arc Physics," Springer-Verlag, (1968).

Huddlestone, R.H. and Leonard, S.L., "Plasma Diagnostic Techniques," Academic Press, (1965).

Hurd, C.W., Chesky, K.P. and Shapiro, A.H., "Influence of Viscous Effects on Impact Tubes," J. of App.. Mech., 253, (June 1953).

Huska, P.A., "Characterization of Induction-Coupled Plasmas and Their Use for Direct Production of Molybdenum by Thermal Decomposition of Molybdenum Disulphide," Ph.D. Thesis, Lehigh University, Penn., 1966, (from Munz, 1974).

Incropera, F.P. and Leppert, G., "Investigation of Arc Jet Temperature Measurement Techniques," ISA Trans., 6, 35, (1967).

Jelyashevich, M.A., Kiselevskii, L.I. and Shimanovich, V.D., "Spectroscopic and Laser Methods for Dense Plasma Diagnostics," Symp. Int. de Chimie des Plasmas, Université de Limoges, (June 1977), Vol. 1, G3.

Kanzawa, A. and Kimura, I., "Measurements of Viscosity and Thermal Conductivity of Partially Ionized Argon Plasmas," AIAA J., 5, (7), 1315, (1967).

Karzas, W.J. and Latter, R., Astrophys. J. Supp., 6, 167, (1961).

Katta, S., "Local Heat Transfer to Spheres in a Plasma Jet," Ph.D. Thesis, McGill University, (1972).

Katta, S., Lewis, J.A. and Gauvin, W.H., "A Plasma Calorimetric Probe," Rev. Sci. Instrum. 44, (10), 1519, (1973)

Katta, S. and Gauvin, W.H., "The Effect of Local Gas Velocity and Temperature on Local Heat Transfer to a Sphere in a High-Temperature Jet," Can. J. of Ch. Eng., 51, 307, (1973).

Kettani, M.A. and Hoyaux, M.F., "Plasma Engineering," Butterworths, (1973).

Kimura, I. and Kanzawa, A., "Measurement of Stream Velocity in an Arc," AIAA J., 1, (2), 310, (1963).

Kimura, I. and Kanzawa, A., "Experiments on Heat Transfer to Wires in a Partially Ionized Argon Plasma," AIAA J., 3, (3), 476, (1965).

Knopp, C.F., Gottschlich, C.F. and Cambel, A.B., "The Spectroscopic Measurement of Temperature in Transparent Argon Plasma," J. Quant. Spectrosc. Radiat. Transfer., 2, 297, (1962).

Knopp, C.F. and Cambel, A.B., "Experimental Determination of the Thermal Conductivity of Atmospheric Argon Plasma," The Physics of Fluids, 9, 5, (1966).

Kubanek, G.K. and Gauvin, W.H., "Recent Developments in Plasma Jet Technology," Can. J. of Chem. Eng., 45, 251, (1967).

Kubanek, G.R., Gauvin, W.H., Irons, G.A. and Choi, H.K., "The Industrial Application of Plasmas to Metallurgical Processes," Conference Proceedings, 4th Int. Symp. on Plasma Chemistry, Zurich, Switzerland, (August 1979).

Kubanek, G.R. and Gauvin, W.H., The Chemical Engineer, 332, (1968).

Landt, U., "Developments - Inorg. Arc Plasma Chemistry," Angew Chem. Inst. Edit., 9, 10, (1970).

Lapworth, K.C., "Spectroscopic Temperature Measurement in High Temperature Gases and Plasmas," (Rev. Article), J. of Physics E : Scie. Inst., 7, 413, (1974).

Lapworth, K.C., Preston, R.C., Nettleton, D. and Brookes, C., "Standards and Measurements of High Temperatures at the National Physical Laboratory, U.K.," Symp. Int. de Chimie des Plasmas, Univ. de Limoges, (June 1977), Vol. 4, S.1.

Lemoine, A., Ph.D. Thesis, University of Nancy, France, (1969).

Lesinski, J., Lesinska, B.M., Fanton, J.C. and Boulos, M.I., "LDA Measurements under Plasma Conditions," Proceedings of 4th International Symposium on Plasma Chem., p. 786, Vol. 2, Zurich, Switzerland, (August 1979).

Lewis, J.A., "The Motion of Particles Entrained in a Plasma Jet," Ph.D. Thesis, McGill University, (1972).

Lewis, J.A. and Gauvin, W.H., "Motion of Particles Entrained in a Plasma Jet," AIChE J., 19, (5), 982, (1973).

Lochte-Holtgreven, W., "Plasma Diagnostics," North-Holland Pub. Co., (1968).

MacMillan, F.A., "Viscous Effects on Pitot Tubes at Low Speeds," J. of the Royal. Aero. Soc., 58, 570, (1954).

Mac Rae, D.R., Gold, R.G., Thompson, C.D. and Sandall, W.R., "Ferrovanadium Production by Plasma Carbothermic Reduction of Vanadium Oxide," 34th Electric Furnace Conference, St. Louis, Mo., (December 1976).

Maecker, H., Plasmatrömungen in Lichtbögen infolge Eigen magnetischer Kompression," Z. Physik, 141, 198, (1955).

Magnolo, G., "The Plasmarc Furnace," Can. Min. Metall. Bull., 57, 57-62, (1964).

Maldonado, C.D., Caron, A.P. and Olsen, H.N., "New Method for Obtaining Emission Coefficients from Emitted Spectral Intensities: Part I - Circularly Symmetric Light Source," J. of Opt. Soc. of America, 55, (10), 1247, (1965).

Manriero, D.A., Kienast, P.F. and Hirayama, G., Westinghouse Engineer, 26, (2), 67, (1966), (from Munz, 1974).

Mathur, G.P. and Thodos, G., "The Viscosity of Dissociated and Undissociated Gases for Temp. up to 10,000°K," AIChE J., 9, (5), 596, (1963).

Mathur, G.P. and Thodos, G., "The Thermal Conductivity and Diffusivity of Gases for Temp. up to 10,000°K," AIChE J., 11, (1), 164, (1965).

Matsumoto, O. and Shirato, Y., "Nitration of Zirconium Silicate by Means of a Nitrogen Plasma Jet," Denki Kagaku, 38, (3), 168, (1970).

Matsumoto, O. and Miyazaki, T., "Carburization of ZrO_2 by Means of Plasma Jet," Denki Kagoku, 39, (5), 388, (1971).

Matsumoto, O. and Saito, M., "Formation of Niobium Carbide by the Carborisation of Nb_2O_5 in an Argon Plasma Jet," High Temp. Science, 6, 135-141, (1974).

Mercure, H., Dimoff, K. and Jean, B., "The Need for a Systematic Study of Physical Processes within a Seeded DC Transferred Arc," IUPAC 3rd. International Symp. on Plasma Chemistry, (July 1977), Limoges, France.

Meubus, P. and Parent, J.R., "Temperature Distributions in a Helium Plasma," The Can. J. of Ch. Eng., 47, 536, (1969).

Meubus, P., "Hydrogen Concentration Profiles and Velocity Distributions in a Reducing Argon-Hydrogen Plasma," Can. J. of Chem. Eng., 52, 616, (1974).

Moore, W.J., "Physical Chemistry," Longmans-Green, (1961).

Morgan, F.J. and Nicholls, R.W., "Axial and Radial Temperature Profiles in a Weakly Ionized Argon Jet," Can. J. of Physics, 48, 1845, (1970).

Morris, J.C., Bach, G.R. and Yos, J.M., "Research on Radiation from Arc Heated Plasma," Office of Aerospace Res., U.S.A.F. ARL64-180, (1964).

Muntz, E.P., University of Toronto, UTIA Rep. No. 71, (1961).

Munz, R.J., "The Decomposition of Molybdenum Disulphide in an Induction Plasma Tailflame," Ph.D. Thesis, McGill University, (1974).

Munz, R.J. and Gauvin, W.H., "The Decomposition Kinetics of Molybdenite in an Argon Plasma," AIChE J., 21, (6), 1132, (1975).

Nestor, O.H. and Olsen, H.N., "Numerical Methods for Reducing Line and Surface Probe Data," SIAM Review, 2, (3), 200, (1960).

Niimura, M., Chan, P.W. and Churchill, R.J., "Non-Equilibrium in a Free-Burning Argon Arc Plasma," Air Force Cambridge Research Laboratories, AFCRL-TR-74-0638, Massachusetts, U.S.A., (1974).

O'Connor, T.J., Comfort, E.H. and Cass, L.A., "Turbulent Mixing of an Axisymmetric Jet of Partially Dissociated N_2 with Ambient Air," AIAAJ., 4, (11), 2026, (1966).

Olsen, H.N., "Thermal and Electrical Properties of an Argon Plasma," The Physics of Fluids, 2, (6), 614, (1959).

Olsen, H.N., "Partition Function Cutoff and Lowering of the Ionization Potential in an Argon Plasma," Physical Rev., 124, (6), 1703, (1961).

Olsen, H.N., "Determination of the Properties of an Optically Thin Argon Plasma," in "Temperature: Its Measurement and Control in Science and Industry," Vol. 3, ed. by Herzfeld, C.M. Reinhold Pub. Co., N.Y., (1962).

Olsen, H.N., "Measurement of Argon Transition Probabilities Using the Thermal Arc Plasma as a Radiation Source," J. Quant. Spect. Radiat. Transfer, 3, 59-76, (1963).

Olsen, H.N., "The Electric Arc as a Light Source for Quantitative Spectroscopy," J. Quant. Spect. Radiat. Transfer, 3, 305, (1963).

Oster, L., "Emission, Absorption and Conductivity of a Fully Ionized Gas at Radio Frequencies," Reviews of Modern Physics, 33, (4), 525, (1961).

Pearce, W.J., "Plasma Jet Temperature Measurements," in Optical Spectroscopic Methods of High Temperatures ed. by Dickerman, p. 125, (1960).

Perry, R.H. and Chilton, C.H., "Chemical Engineers Handbook" 5th Ed., McGraw-Hill, (1973).

Pickles, C.A., McLean, A., Alcock, C.B. and Segsworth, R.S., "Graphite Electrode Plasma Furnaces and Their Application for Iron and Steel Making," Adv. in Extractive Metall., the Inst. of Min. and Metall., London, 69-87, (1977).

Polyakov, S.P., Bulanyi, P.F. and Pisanko, S.N., "An Experimental Study of Influence of Degree of Swirling of a Plasma Air Jet and Introduction of Natural Gas into It On Temperature and Velocity Fields," Translation from Inzhenero-Fizichenskii Zhurnal, 34, (2), (1978).

Preston, R.C., "Spectroscopic Studies of a Plasma Temperature and Radiation Standard Based on a Wall Stabilized Arc," J. Quant. Spectrosc. Radiat. Transfer, 18, 337-360, (1977).

Rains, R.K. and Kadlec, R.H., "The Reduction of Al_2O_3 to Aluminum in a Plasma," Metallurgical Transac., 1, 1501, (1970).

Reed, T.B., "Induction Coupled Plasma Torch," J. Appl. Physics, 32, 821, (1961).

Reed, T.B., "Chemical Uses of Induction Plasma," in The Application of Plasmas to Chemical Processes, by Baddour and Timmins, Chp. 3, (1967).

Richter, J., "Radiation of Hot Gases," in Plasma Diagnostics ed. by W. Lochte-Holtgreven, 1968.

Ricou, F.P. and Spalding, D.B., "Measurements of Entrainment by Axisymmetric Turbulent Jets," J. Fluid Mech., 11, 21, (1961).

Rykalin, N.N., "Plasma Engineering in Metallurgy and Inorganic Materials Technology," Pure and Appl. Chem., 48, 179-194, (1976).

Rykalin, N.N., "Thermal Plasmas in Technology," paper presented at World Electrotech. Congress, Moscow, U.S.S.R., (July 1977), Section 0, No. 6.

Sampson, D.H., "Radiative Contributions to Energy and Momentum Transport in a Gas," Interscience Publishers, N.Y., (1965).

Sayce, I.G., "Plasma Processes in Extractive Metallurgy," Advances in Ext. Met. & Mining, The Inst. of Mining & Metall., paper No. 77, (1971).

Sayce, I.G. and Selton, B., "Special Ceramics," p. 157, ed. P. Popper, British Ceramic Research Ass., Stoke-on-Trent, (1972).

Sayce, I.G., "Some Applications of Thermal Plasmas to Material Processing," paper presented at World Electrotech. Congress, Moscow, U.S.S.R., Sect. 4A, No. 107, (July 1977).

Sayegh, N.N., "Variable Property Flow and Heat Transfer to Single Spheres," Ph.D. Thesis, McGill University, (1977).

Sayegh, N.N. and Gauvin, W.H., "Heat Transfer to a Stationary Sphere in a Plasma Flame," AIChE J., 25, (6), 1057, (1979).

Schott, L., in "Plasma Diagnostics", ed. by Lochte-Holtgreven, W., p. 668, (1968).

Schowalter, W.R. and Blaker, G.E., "On the Behaviour of Impact Tubes at Low Reynolds Numbers," Trans. of ASME, 28, 136, (1961).

Schlüter, D., "Die Berechnung der Uber gangs Wahrescheinlichkeiten von Senengrenzkontinua mit Anwendung auf die Schweren Edelgase," Z. für Astrophysik, 61, 67, (1965).

Schnapauff, R., "Measurements of Ar II Transition Prob. and Continuous Spectra of A and Ne," Z. Astrophys., 68, 431, (1968), (in German).

Schreiber, P.W., Hunter, A.M., Benedetlo, K.R., "Argon Plasma Viscosity Measurements," AIAA 3rd Fluid & Plasma Dynamics Conf., paper No. 70-775, Los Angeles, California, (1970).

Schulz-Gulde, E., "The Continuous Emission of Argon in the Visible Spectral Range," Z. Physik, 230, 449, (1970).

Sheer, C. and Korman, S., "The HIgh-Intensity Arc in Process Chemistry," in "Arcs in Inert Atmospheres and Vacuum," ed. by Kuhn, W.E., J. Wiley and Sons, p. 175, (1956).

Sheer, C., Korman, S., Stojanoff, C.G. and Tschang, P.S., "Diagnostic Study of the Fluid Transpiration Arc," AFOSR, Final Rep., 70-0195 TR, (1969).

Sheer, C. and Korman, S., "Arc Synthesis of Hydrocarbons," Adv. in Chem. Series, No. 131, p. 42, (1974).

Sheer, C., Korman, S., Angier, D.J., Cahn, R.P., "Arc Vaporization of Refractory Powders," Fine Particles, 2nd. Inter. Symp. of Electrochem. Soc., Boston, 1973, pub. by E. Soc., ed. by W.E. Kuhn, p. 133-152, (1974).

Sheer, C., Korman, S. and Dougherty, R.J., "Arc Gasification of Coal," Proceedings of Intern. Symp. on Plasma Chem., Vol. 1, p. 277, Zurich, Switzerland, (August 1979).

Sherman, F.S., "New Experiments on Impact-Pressure Interpretation in Supersonic and Subsonic Rarefied Air Streams," National Advisory Committee for Aeronautics, TN 2995, (1953).

Simmons, F.S. and Glawe, G.E., "Theory and Design of a Pneumatic Temperature Probe and Experimental Results Obtained in a High Temperature Gas Stream," NACA TN-3893, (January 1957).

Smith, D.L. and Churchill, S.W., "Mass and Energy Transfer Between a Confined Plasma Jet and a Gaseous Coolant," Tech. Report ORA, Project 05607, Dept. of Chem. and Metall. Eng., University of Michigan, Ann Arbor, (1965).

Somerville, J.M., "The Electric Arc," Methuen, (1959).

Stojanoff, C.G., "A Transient Fiber Optics Probe for Space Resolved Diagnostics of Dense Plasmas," AIAA J., 4, (10), 1766, (1966).

Stojanoff, C.G., "Eigenschaften eines durch Längsströmung stabilisierten Hochstrombogens und dessen Anwendung zur Bestimmung von Stoffwerten," Dr. Ing. Thesis, Stuttgart University, (1968).

Svehla, R.A., "Estimated Viscosities and Thermal Conductivities of Gases at High Temp." NASA Technical Report, R-132, Washington, (1962).

Taurin, R.H., "Spectroscopic Temperature Measurements," Elsevier, (1966).

Thorpe, M.L. and Wilks, P.H., Chem. Eng., (1971), 417.

Thurnsfield, G. and Davies, G.J., "Sulphide Processing in Induction Plasmas," Trans. Inst. Min. Metall., 83, C191-192, (1974).

Tidwell, E.D., "Transition Probabilities of Argon II," J. Quant. Spectrosc. Radiat. Transfer, 12, 431, (1972).

Todorovic, P.S., Jones, G.R. and Barrault, M.R., "Time Resolved Laser-Doppler Measurements in a High-Current Arc Plasma," J. Phys. D:Appl. Physics, 9, 423, (1976).

Ton, H., "Physical Properties of the Plasma-MIG Welding Arc," J. Phys.D:App. Phys., 8, 922, (1975).

Topham, D.R., "The Electric Arc in Constant Pressure Axial Gas Flow," J. Phys.D:Applied Phys., 4, 1114, (1971).

Topham, D.R., "Some Considerations of High Current Electric Arcs in Nozzle Flow," J. Phys. D:Appl. Physics, 11, 87, (1978).

Trokhan, A.M., Izmaritel'naya Tekhniska, 2, 5, (1968), (English Translation), (also in Inst. Soc. of America, No. 8, 1968).

Tylko, J.K., "Expanded Low Temperature Plasmas and Their Application," paper presented at the Conference of the Bulgarian State Committee for Science, November, (1972).

Vannier-Moreau, G., "Effect of Mass Transfer on Heat Transfer to Single Spheres in an R.F. Plasma Tailflame," M.Eng. Thesis, McGill University, (to be published).

Venugopalan, V.I., "Reactions Under Plasma Conditions," John Wiley, Pub., 1972.

Vurzel, F.B. and Polak, L.S., "Plasma Chemical Technology - The Future of the Chemical Industry, I and E Chem., 62, 6, (1970).

Waldie, B., "Review of Recent Work on the Processing of Powders in High Temp. Plasmas: Part 1, Chem. E., 92, (1972), Part 2, Chem. E., 188, (1972).

Waldie, B., "Velocity Measurements in and Around the Coil Region of an Induction Plasma," Int. Round Table on Plasmas, Odeillo, (1975), Paper IV-9.

Warren, W.R., Princeton University, Dept. Aero. Eng., Report 381, (1957), (cited in Lewis, 1972).

Warren, I.H. and Shimizu, H., "Applications of Plasma Technology in Extractive Metallurgy," Trans. Can. Inst. Min. & Metall., 58, 169-178, (1965).

Weizel, W. and Rompte, R., "Theorie Elektrischer Lichtbögen und Funker," Leipzig (1949), (from Tylko, 1972).

Welch, J.W., "An Analytical and Experimental Investigation of the Arc Plasma Metal Spraying Process," Ph.D. Thesis, Vanderbilt University, (1972).

Whyman, D., "A Rotating Wall dc Arc Plasma Furnace," J. Sci. Instr., 44, 525-530, (1967).

Wilks, P.H., Ravinder, P., Grant, C.L., Pelton, P.A., Downer, R.J. and Talbot, M.L., "Plasma Process for ZrO_2," Chem. Eng. World, 9, (3), 59, (1974).

Wilks, P.H., "The Current State and Future Directions of Industrial Plasma Chemistry," Pure and Appl. Chem., 48, 195-197, (1976).

EXPERIMENTAL SECTION

INTRODUCTION

The application of plasma technology to chemical and metallurgical processes has been receiving increasing attention in the last two decades. One promising application is in the field of beneficiation of mineral ores of high unit value. To date, however, most of the research in this field has been devoted to exploring the technical feasibility of effecting the desired reactions under plasma conditions, rather than optimizing and controlling the plasma system so as to make it economically viable (Sayce, 1977), (Gauvin et al, 1980). As a consequence of this and although plasma generators capable of continuous operation at a power of several megawatts are commercially available, the use of plasma reactors on a commercial scale is limited to a few processes: the production of acetylene, that of titanium oxide, the dissociation of zircon sand and the smelting operations in steel making. Rykalin (1976), Sayce (1972, 1977), Hamblyn (1977) and Aubreton and Fauchais (1978) have reviewed the use of plasmas for high-temperature heterogeneous systems and they have unanimously agreed that the transferred arc plasma in which an arc is struck between the cathode and a molten feed (acting as the anode) is often far

more thermally efficient than the non-transferred arc plasma (for example, r.f. plasmas and d.c. jet plasmas). The injection techniques used to introduce feed stocks into the primary heat dissipation zone of the plasmas, as reviewed in these articles, indicate that the cathode design in transferred arc plasmas is an integral part of the reactor design. In the past, workers in this field have obtained various patents on the cathode design. Nevertheless, the Fluid Convective Cathode (FCC) design of Sheer et al (1968) probably provided the basic design principles for most of them and stands as the only design suitable for scaling-up.

From a chemical engineering point of view, the temperature and velocity fields in the plasma column of a transferred arc are the most important parameters for the study, design and control of the plasma system. The Literature Review section showed that the transferred arc plasma has received little attention in this respect. The work of Stojanoff (1966, 1968), in which a 3-cm long transferred arc was diagnosed for the purpose of obtaining the transport properties of argon plasmas is a notable exception. Although this work demonstrated the effect of gas flow rate on temperature and velocity fields, it falls short of being a complete diagnostic study in that the effect of varying the arc length, which is probably the most important parameter as far as residence times of particles injected into the plasma column are concerned, was not studied. The scatter of the transport parameters obtained by the author (Figure

3, in the Literature Review section) and the large deviations from the theoretical values at high temperatures, raise serious doubts about the accuracy of his temperature and velocity profiles, probably linked to the inaccuracy of his diagnostic techniques.

The diagnostic techniques used for plasmas show a considerable diversity. For temperature measurements, either insertion probes, or optical methods, or a combination of both have been used. The calorimetric probe is the most commonly used type of the first group and was mainly developed by Grey and co-workers (1962, 1965, 1968). Other users of such devices have included Smith and Churchill (1965), Chludzinksi (1964), Incropera and Leppert (1967) and Katta et al (1973). The applicability of such techniques for transferred arc temperature measurements is restricted due to their measurement range (below 10,000 K), their limited resolution and their sensitivity to the settling of the coolant rate. The optical techniques, of which the spectroscopic techniques are the most important, suffer from the fact that the measurements are time consuming and that the data analysis (as in the Abel Inversion) require the assumption of circular symmetry of the plasma column (Lochte-Holtgreven, 1968). In addition, the spectroscopically-measured temperatures are inescapably weighted averages (Burns, 1964) that can often deviate considerably from simple averages and therefore yield spurious values. These limitations can be eliminated if spectroscopic principles are combined with probing techniques, as done by Stojanoff (1968).

For velocity measurements, again a variety of techniques can be used; however, the transient uncooled pitot tube seems to be the most appropriate for measurements in a transferred arc plasma, basically due to its good spatial resolution and simplicity. Following the recommendations of Sheer et al (1969), a correction, called Barker correction (Barker, 1922), has to be made for viscosity effects at low Reynolds numbers.

From the foregoing discussion, three main conclusions can be drawn. Of all the plasma generators, the transferred arc is the most suitable one for chemical and metallurgical applications and up to the present time there exists no complete study of the variations of the transferred arc plasma characteristics with the basic variables. In addition, the diagnostic techniques used in plasmas for velocity and temperature measurement are lacking in simplicity and reliability. Therefore, the work reported in this section represents an attempt to develop simple techniques for plasma diagnostics and to determine the basic plasma characteristics and their variations with operating variables in a transferred arc plasma.

To achieve these objectives, a cathode assembly suitable for transferring an arc to a molten metal bath or to a cooled anode and for the injection of a secondary gas into the plasma column had to be designed for operation in open air for ease of accessibility. The plasma thus produced was studied photographically and with

respect to its electrical characteristics and to heat losses in the initial part of the work. The techniques for these measurements were adopted from the literature and are well known. For temperature measurements, however, a novel technique was designed, tested and finally employed to obtain temperature mappings of the column under different operating conditions. Finally, the velocity measurements were carried out with the aid of an uncooled, transient pitot-tube, as already employed by some previous workers under similar conditions.

EXPERIMENTAL

APPARATUS

The apparatus used in the experimental work consisted of a power supply, a control console, and a transferred arc system including a cathode assembly, an anode assembly and a driving mechanism. A schematic drawing of the overall set-up is given in Figure 1.

The power supply was of the direct current, welding type, capable of providing a maximum power of 40 kW. It had a drooping volt-ampere curve and could be operated in the open circuit voltage range of 80-320 volts. In this work, following the manufacturer's recommendation, a 160-volt mode was employed. A high frequency arc starter facilitated the initial breakdown of the arc gap. The arc was ignited at about 90 amperes. All necessary power supply

FIGURE 1

SCHEMATIC DRAWING OF EQUIPMENT

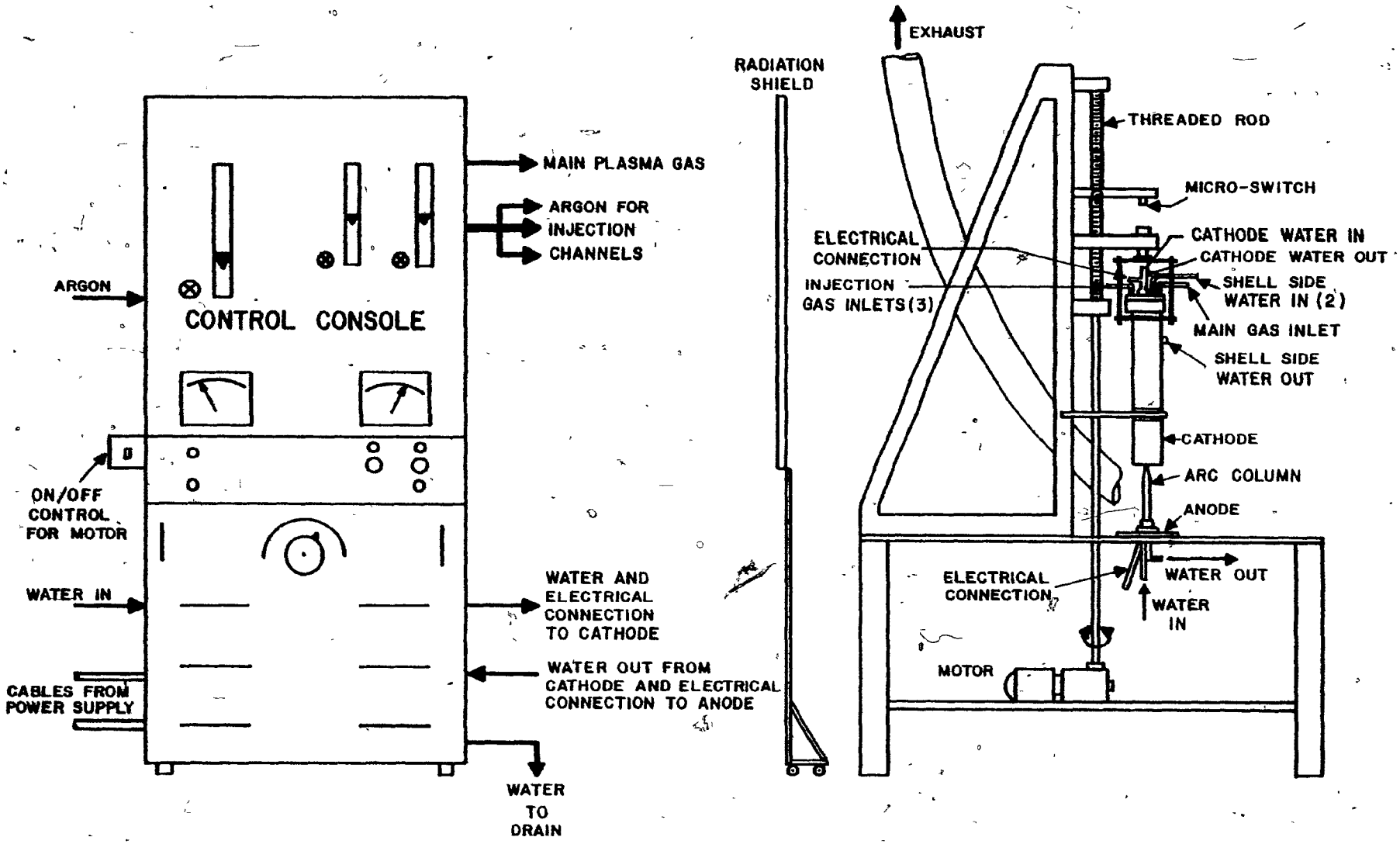
CONTROL CONSOLE
ARGON
MAIN PLASMA GAS
ARGON FOR INJECTION CHANNELS
ON/OFF CONTROL FOR MOTOR
WATER IN
WATER AND ELECTRICAL CONNECTION TO CATHODE
WATER OUT FROM CATHODE AND ELECTRICAL CONNECTION TO ANODE
CABLES FROM POWER SUPPLY
WATER TO DRAIN
RADIATION SHIELD
EXHAUST
THREADED ROD
MICRO-SWITCH
ELECTRICAL CONNECTION
CATHODE WATER IN
CATHODE WATER OUT
INJECTION GAS INLETS(3)
SHELL SIDE WATER IN (2)
MAIN GAS INLET
SHELL SIDE WATER OUT
CATHODE
ARC COLUMN
ANODE
ELECTRICAL CONNECTION
WATER OUT
WATER IN
MOTOR

adjustments and gas flow regulations were made through a Thermal Dynamics Model B60 control console. In particular, for the arc gap and gas conditions employed here, a continuous range of arc currents above 100 amperes was available by adjustment of a rheostat on this console. The console also contained safety interlocks to the power supply for the water and gas lines, to prevent operation under low water or gas pressures. A copper adapter was used to separate electrical and cooling water lines both at the exit and at the inlet of the console. A three-way splitter was employed at the carrier gas exit of the console. The main plasma forming gas and the injection gas flow rates were monitored by calibrated precision (2%) rotameters.

Argon gas, with a purity of 99.997%, was supplied from three cylinders joined to a common manifold and regulated by a two-stage pressure regulator.

A cathode assembly suitable for operation in the transferred arc mode and for injection of fine particles or of a secondary gas other than the main plasma-forming gas was designed. The cathode assembly is shown in Figure 2. A more detailed drawing and specification of its various components is given in Appendix B. A photograph of the unit is also shown in Figure 3. The cathode assembly consisted essentially of a water-cooled conical thoriated tungsten cathode tip surrounded by a water cooled brass nozzle. The injection gas was fed through three equally-spaced feed tubes, each

FIGURE 2

SCHEMATIC DIAGRAM OF THE CATHODE ASSEMBLY

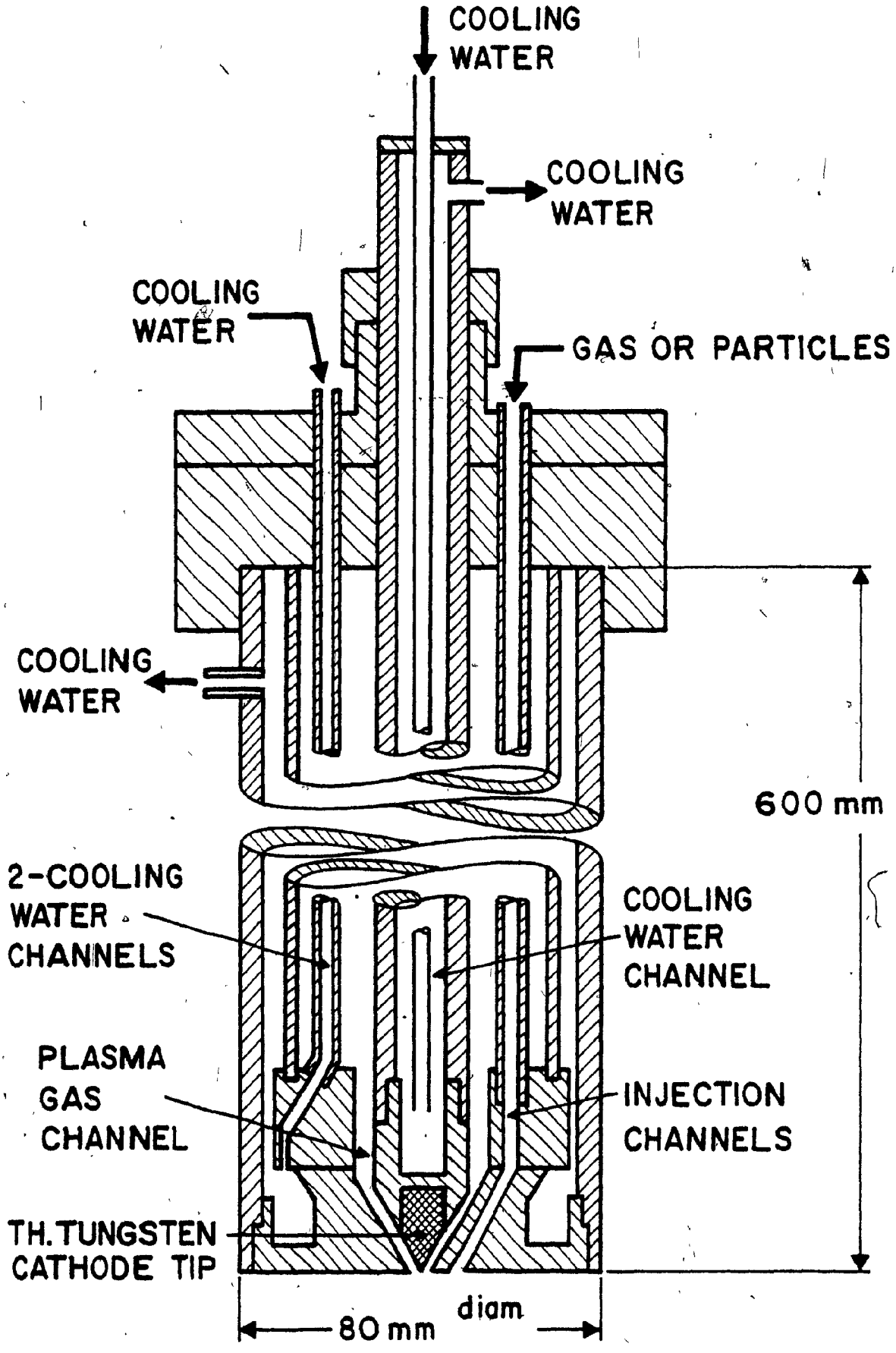
COOLING WATER
COOLING WATER
COOLING WATER
GAS OR PARTICLES
COOLING WATER
600 mm
2-COOLING WATER CHANNELS
COOLING WATER CHANNEL
PLASMA GAS CHANNEL
INJECTION CHANNELS
TH. TUNGSTEN CATHODE TIP
80 mm diam

FIGURE 3

PHOTOGRAPH OF THE CATHODE ASSEMBLY

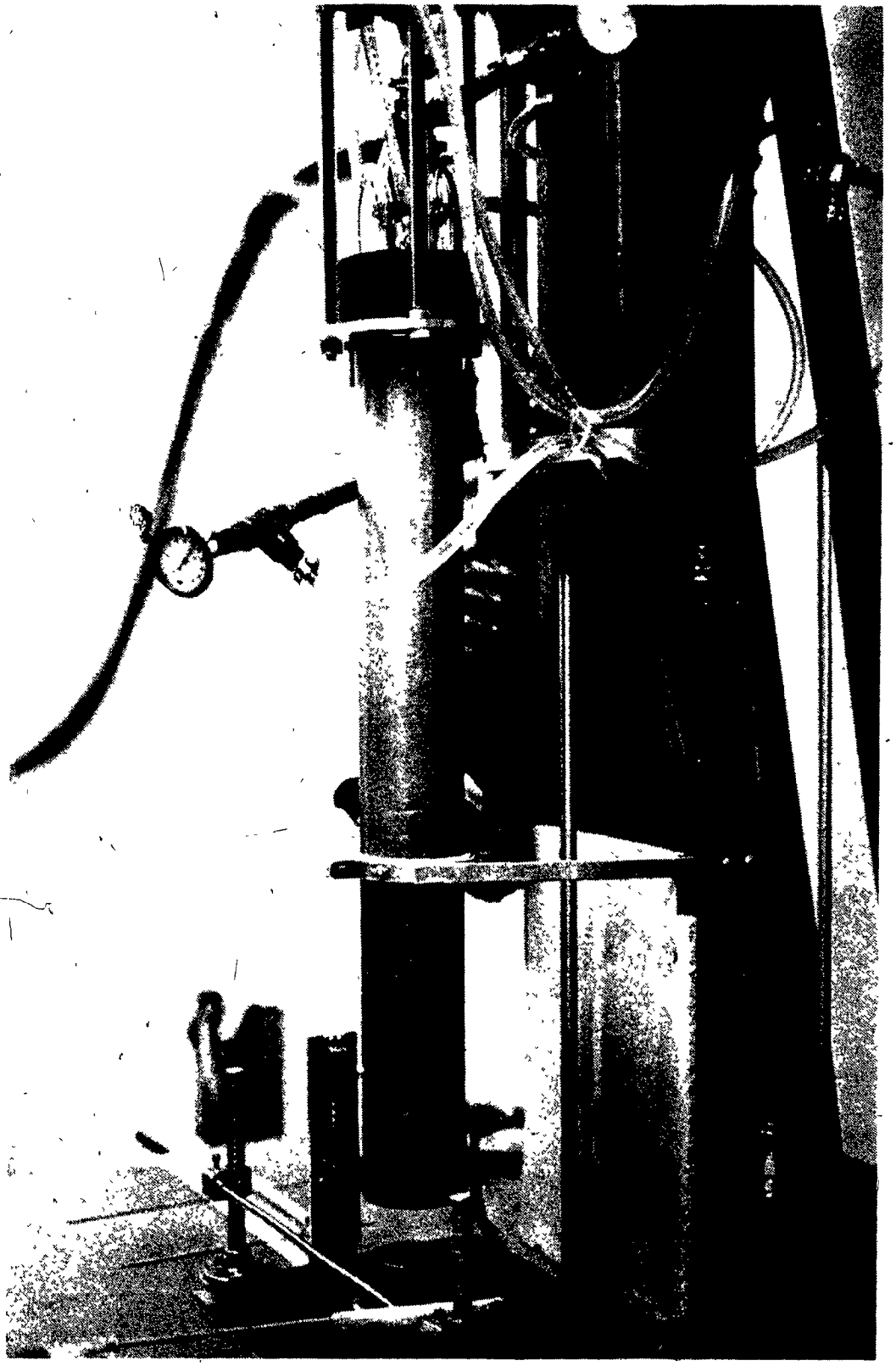

0.4 cm in diameter. Two different nozzles, one with an injection angle of 30° with the axis, and the other of 45°, were used. The angle of the injection channels and of the cathode tip was the same as the nozzle used. Nozzle diameters of 0.381 and 0.476 cm were used. The plasma gas was forced to pass through a narrow shroud, the width of which could be adjusted by moving the cathode tip up or down. The nozzle directed this thin, high velocity layer of gas so that it impinged on the arc column in the region of the contraction zone. It was expected that with this configuration, the component of input gas momentum parallel to the arc axis exerted a stabilizing influence on the entire arc column. The thin layer of plasma gas was intended to convectively cool the cathode tip and thus reduce the cooling requirements.

The cathode assembly was designed to be versatile in its operation: it could be used for injection of a gas and/or particles, and could be used in a closed system or in open air. The various parts and their connections were designed for easy dismantling, essentially for changing the brass nozzle and the thoriated tungsten cathode tip. Tight seals between the components were effected with O-rings and silicone sealant. The current-carrying cathode was insulated from the nozzle and the shell by employing electrically non-conducting materials (phenolic board and teflon) as the head cap and spacers. The purpose of the spacers was to act as gas distributors, to prevent the contact of the tubes with the cathode holder and also to help in the alignment of the cathode tip in the

nozzle. This alignment was further effected by the adjustment of the six (6) screws joining the end cap and the outer shell.

The thoriated tungsten tips used in the cathodes were prepared by modifying the standard electrodes commercially available from Thermal Dynamics. The tungsten pieces were removed from their original brass holders, ground to the desired angle and shape and then soldered to the new brass pieces. A photograph of the cathode tip and of the brass nozzle is given in Figure 4.

A remotely controlled driving mechanism was constructed to allow for the movement of the cathode assembly in a vertical direction within a distance of 20 cm. A motor-driven shaft was connected to a threaded rod which in turn drove the cathode unit. The connections between the rod and the unit were made of insulating materials so that the nozzle around the cathode tip, which was also insulated from the current-carrying cathode, was maintained at a floating potential. Two limiting microswitches, one movable and the other fixed, were employed to pre-adjust the arc length before start-up and to prevent the contact of the cathode and the anode units, respectively.

Several designs were attempted for the anode unit. The early models failed due to insufficient cooling. The final anode design, shown on Figure 5, consisted of three copper pieces: the anode holder (including the coolant lines and the electrical connections), the cap which was bolted to this holder, and the anode

FIGURE 4

PHOTOGRAPHS OF THE ANODE WITH PRESSURE HOLE

THE BRASS NOZZLE AND THE TUNGSTEN CATHODE TIP

FIGURE 5

SCHEMATIC DIAGRAM OF THE

ANODE ASSEMBLY

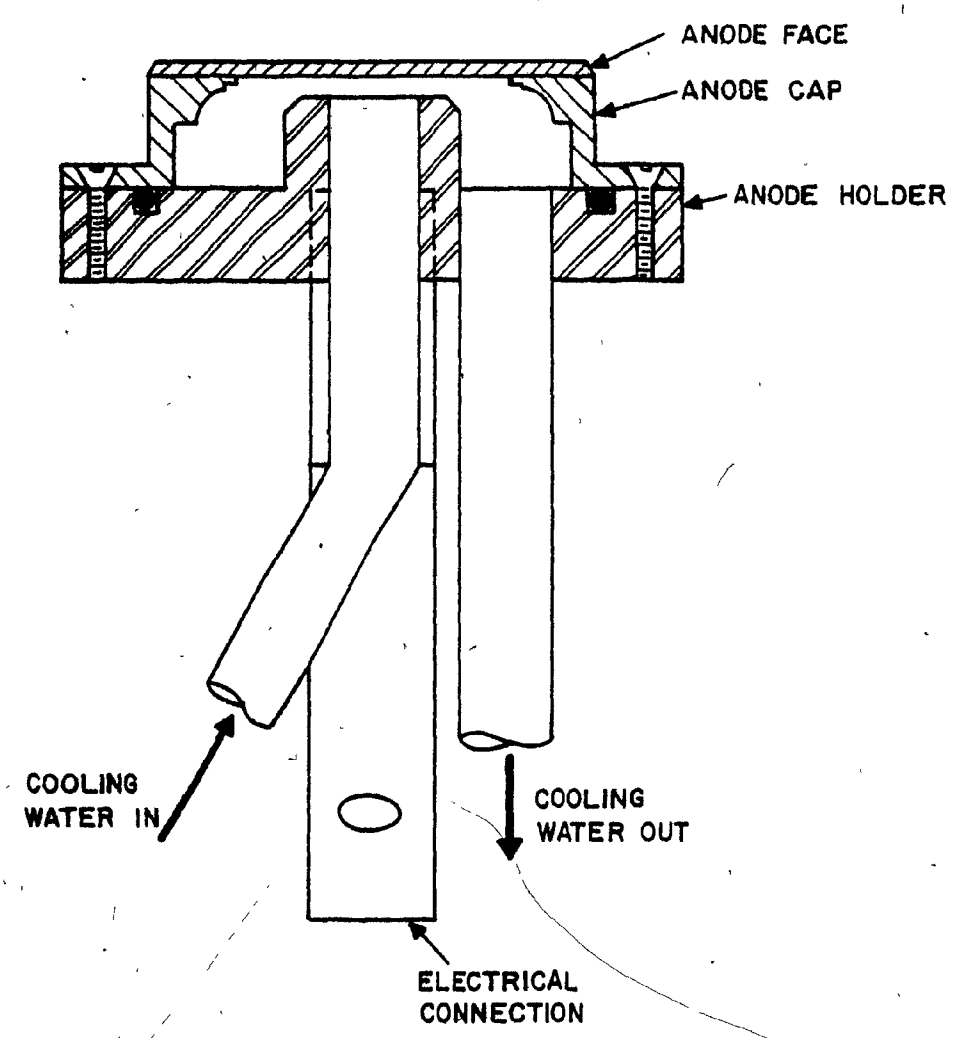
ANODE FACE
ANODE CAP
ANODE HOLDER
COOLING
WATER IN
COOLING
WATER OUT
ELECTRICAL
CONNECTION

face or arc attachment piece which was a 0.15878-cm (1/16-inch) thick, 5.715 cm in diameter flat disc, resting over the cap and soldered to it from inside. The O-ring between the cap and the holder was sealed against water leaks. With this design, the maximum cooling power was concentrated opposite the plasma stagnation point at the centre of the anode face. The width of the passage between the anode face and the coolant flange of the anode holder was 0.25 cm. This configuration directed the cooling water flow outward from the centre of the anode to the peripheral regions and thus assured arc symmetry. It was possible to replace the copper anode face whenever it was necessary by first removing the cap and then melting the solder inbetween.

In some parts of the experimental work, this anode was replaced with a pressure-tapped anode which consisted of a 0.3175-cm diameter stainless steel tube connected to a 0.079-cm (1/32-inch) hole on the anode face and leading to a manometer. This device was used to measure the stagnation pressure at the anode. A photograph of this anode is given in Figure 4.

The anode unit rested on a steel table which also held the cathode assembly and the cathode driving mechanism. A cooled copper plate was placed between the anode and the table to protect the latter from the hot effluent gases and from the radiation. A plexiglass sheet between the copper plate and the table, and a teflon sleeve between the anode and the copper plate were employed

for electrical insulation. Insulated screws were used to fix the position of the anode over the table.

MEASUREMENT TECHNIQUES AND INSTRUMENTATION

1. Electrical, Calorimetric and Photographic Characterizations

In the first part of the experimental work, the electrical characterization of the transferred arc plasma was carried out. For this purpose, the arc voltage was monitored as a function of various operating parameters. The voltmeter available on the control console was used for rough estimations. More precise and continuous measurements were possible by attaching leads to the anode and the cathode to a chart recorder. The arc current was measured with an ammeter via a precision shunt connected in series with the arc.

In addition to the voltage drop between the electrodes, the distribution of the voltage along the arc length with respect to an electrode was also measured. This was achieved by connecting a 0.1-mm tungsten wire to the positive end of an oscilloscope via a 100-kohm resistor. The negative terminal of the oscilloscope was connected to the cathode. The wire was then swept through the plasma, at various vertical positions, with a speed high enough to prevent thermal ablation of the wire.

To obtain the fractions of the input power lost to the different parts of the equipment, the cathode, the nozzle and the anode were used as calorimeters. The inlet and outlet water

temperatures were measured with bimetallic dial thermometers accurate to 0.25 K in the range 273-323 K. Provisions were made in the design of the equipment for immersion of the thermometer stems of about 10 cm in the fluid, in order to meet their calibration. Water flow rate to the above parts was metered separately, using precalibrated Brooks rotameters. Although different flow rates were tried to check the results and increase the accuracy, under normal conditions, the water flow rates used were as follows: 1.09 m^3/h for the anode, 0.041 m^3/h for the cathode and 0.095 m^3/h for nozzle, at 689 kPa.

To determine the effect of the operating conditions on the luminous plasma profile, still photographs of the plasma were taken using a 35 mm Minolta SRT-202 camera with a 100-mm lens. Due to the excessive brightness of the plasma, Kodak Tri-X Pan film with an ASA setting of 400 was used. Exposure time of 1/1000 second at f-22 was found satisfactory. The plasma column diameter at various distances from the cathode tip was determined from the negatives by using a Nikon shadowgraph at x50 magnification. The nozzle diameter was used as the reference.

2. Temperature Measurement Technique

A new electro-optical technique was developed for the measurement of plasma temperatures above 8000 K. The basic principle of this technique was to determine the total emission coefficients of the plasma at two wavelengths, as a function of radial position,

The radial temperature distribution was then obtained by comparing the ratio of the measured emission coefficients with the theoretically-calculated values.

The total emission coefficients of an argon plasma at the wavelengths of 4806 Å and 6965 Å as a function of temperature has been calculated. The detailed calculations and resulting graphs are presented in Appendix C. A regression analysis was carried out on the theoretical results (temperature-versus-ratio of the total emission coefficients at 4806 Å and 6965 Å), using a package statistical computer program, STATPK, of the McGill University Computing Centre, and the following expressions were found to fit the data best:

i) For $7{,}000\ K < T < 15{,}000\ K$

$$T = 10^{(4.3006 + 0.249 \log R)} \qquad (1)$$

ii) For $15{,}000\ K < T < 25{,}000\ K$

$$T = 10^{(4.228 + 0.089 \log R)} \qquad (2)$$

Where R = ratio of the total emission coefficients of 4806 Å and 6965 Å, respectively

The new experimental technique which utilized the above principle to yield the temperature profile of the transferred arc plasma consisted of a two-wavelength pyrometer, a metal plate (coupled to a linear motor) which varied the amount of plasma radiation seen by the pyrometer, a digital oscilloscope which stored radiation intensity signals, and an interface-minicomputer assembly which

processed the pyrometer signals (as stored on the oscilloscope) to yield plasma temperature profile curves. A block diagram of the complete system is given in Figure 6, and a photograph of the unit is shown in Figure 7.

The procedure by which the temperature profiles were obtained was as follows: before the experiment was initiated, the metal strip (opaque screen) was positioned between the 100 μm diameter aperture (through which the two-wavelength pyrometer views the plasma) and the plasma column. Thus, the pyrometer received no radiation from the plasma. Then, the experiment was started by pressing the command button of the linear motor's sweep generator. The linear motor carried the metal strip (2 mm by 0.6 mm; blackened to prevent reflection of radiation) through the plasma column at a constant velocity, away from the optical system. Thus, the radiating volume of the plasma that the pyrometer viewed increased from zero (at the beginning of the traverse), to a maximum when the strip completed its traverse. The intensity of the impinging radiation on the photocells placed behind two interference filters (tuned to 4806 Å and 6965 Å) was recorded by a digital storage oscilloscope triggered by the motion of the linear motor driving the metal strip. Figure 8(a) shows a schematic representation of such a recording. This recording is actually an integral of local emission coefficients, and the derivatives of these curves yielded the radial emission coefficient distribution, as shown in Figure 8(b). These values were then employed in Equation 1 (or 2, depending on the

FIGURE 6

BLOCK DIAGRAM OF COMPLETE TEMPERATURE

DIAGNOSTIC SYSTEM

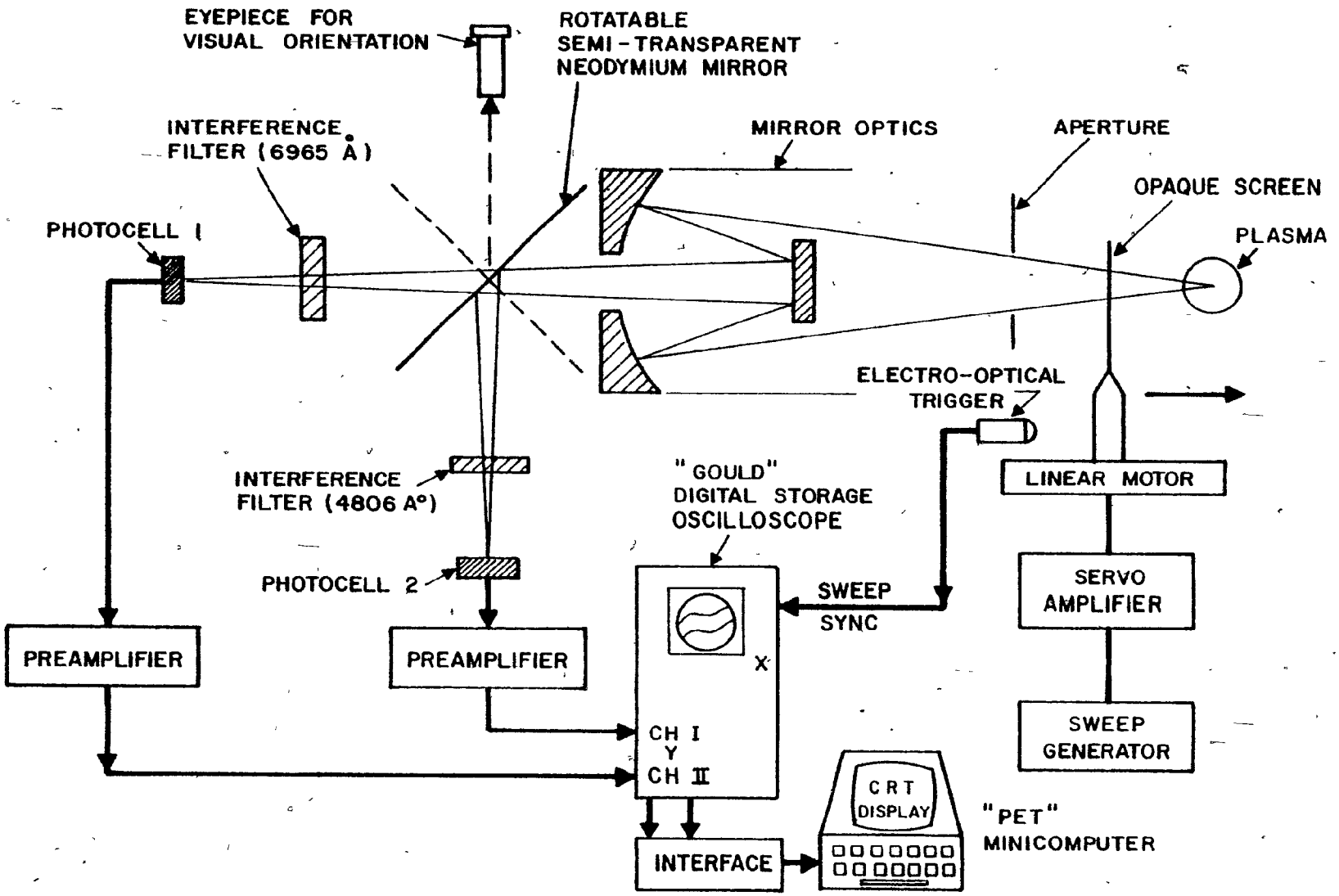
EYEPIECE FOR
VISUAL ORIENTATION
ROTATABLE
SEMI-TRANSPARENT
NEODYMIUM MIRROR
INTERFERENCE
FILTER (6965 Å)
MIRROR OPTICS
APERTURE
OPAQUE SCREEN
PLASMA
PHOTOCELL 1
ELECTRO-OPTICAL
TRIGGER
INTERFERENCE
FILTER (4806 A°)
"GOULD"
DIGITAL STORAGE
OSCILLOSCOPE
LINEAR MOTOR
PHOTOCELL 2
SWEEP
SYNC
SERVO
AMPLIFIER
PREAMPLIFIER
PREAMPLIFIER
X
CH I
Y
CH II
SWEEP
GENERATOR
CRT
DISPLAY
"PET"
MINICOMPUTER
INTERFACE

FIGURE 7

PHOTOGRAPH OF THE TEMPERATURE

DIAGNOSTIC SYSTEM

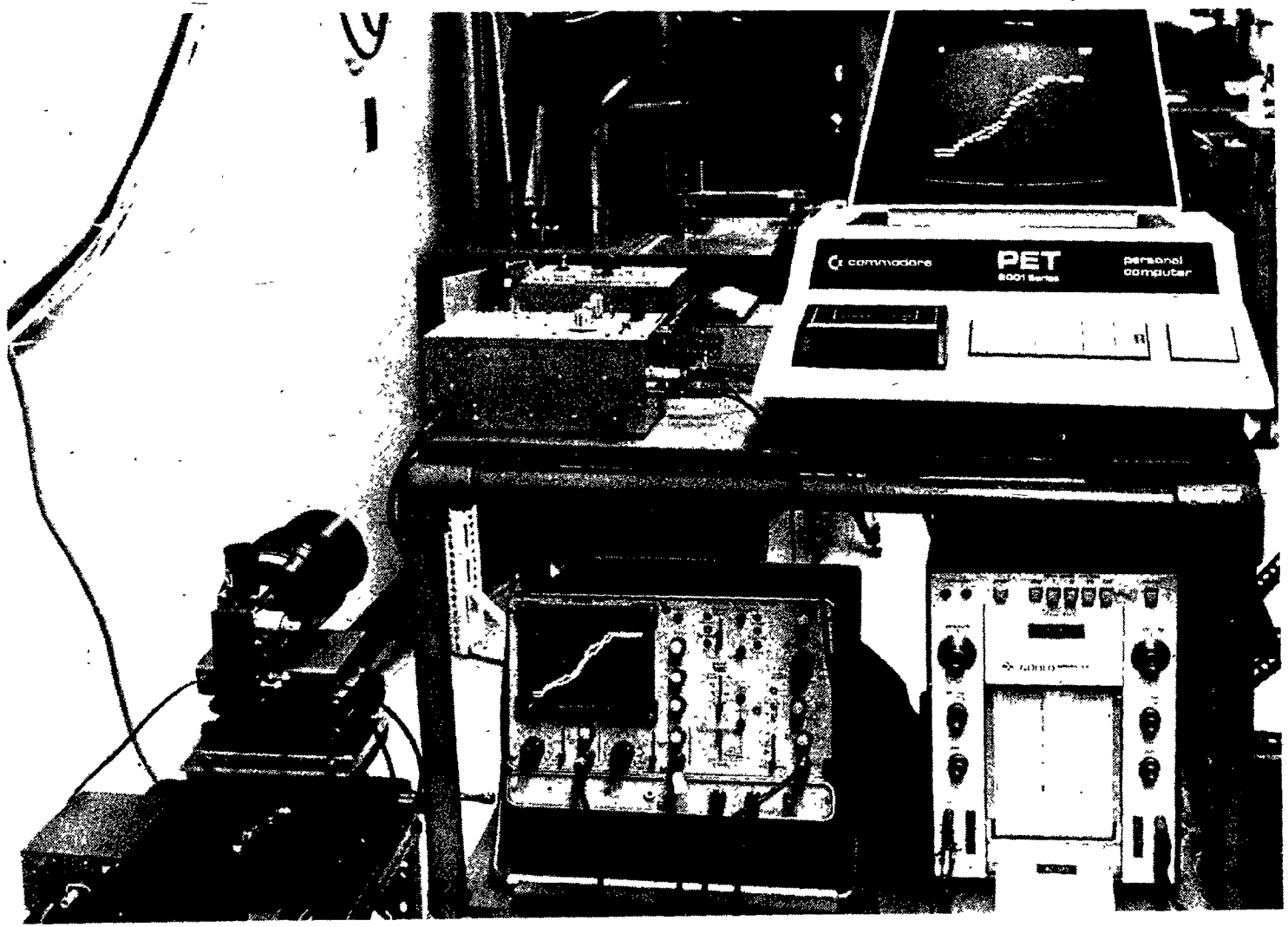
commodore
PET
8001 Series
personal
computer

FIGURE 8

(a) OSCILLOSCOPE RECORDING OF THE PHOTOCELL OUTPUTS AFTER THE TRAVERSE OF THE BLOCKING ELEMENT

(b) DERIVATIVES OF THE ABOVE OUTPUTS

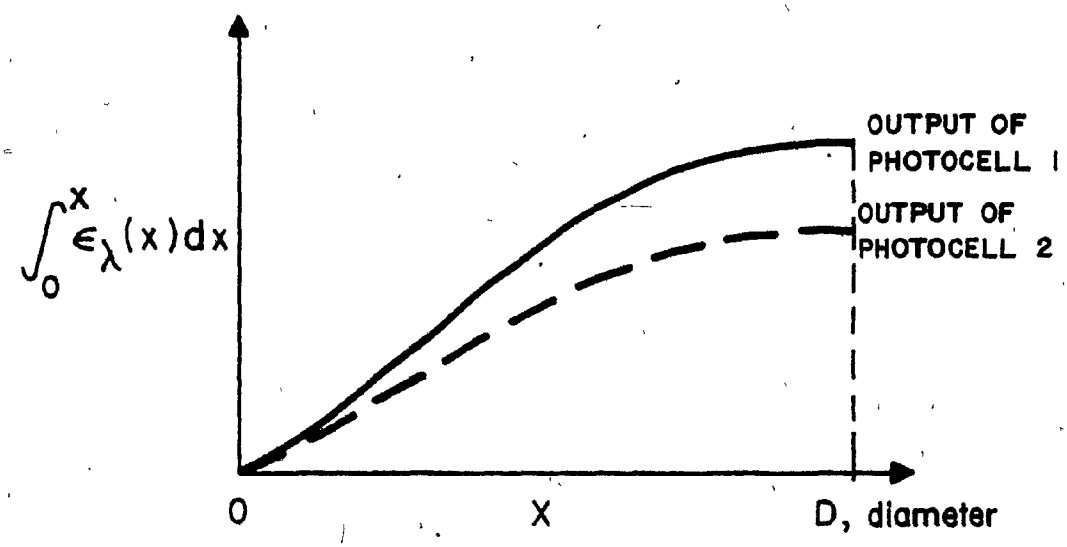
$\int_0^X \epsilon_\lambda(x)dx$
OUTPUT OF PHOTOCELL 1
OUTPUT OF PHOTOCELL 2
0
X
D, diameter

(a)

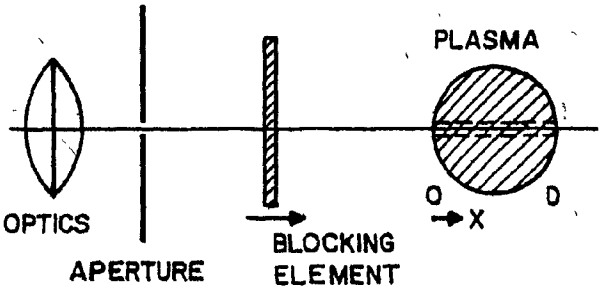
PLASMA
0
D
X
OPTICS
APERTURE
BLOCKING ELEMENT

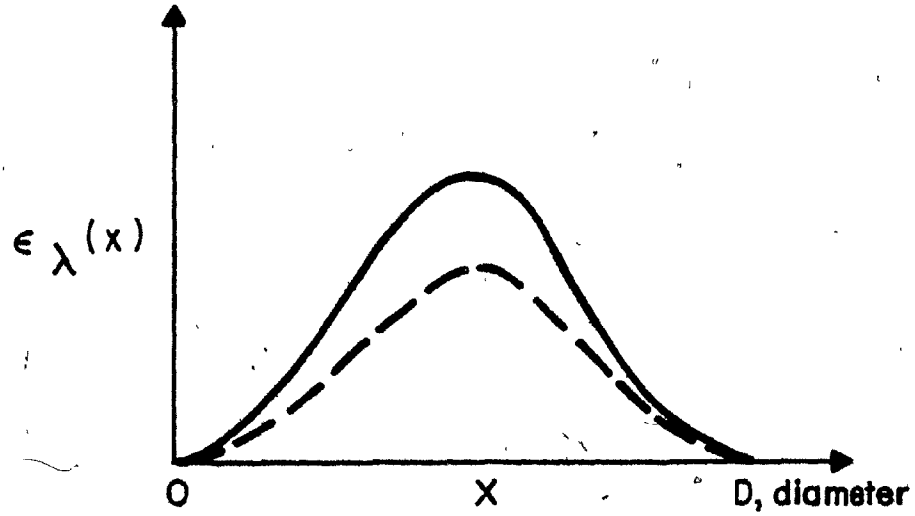
$\epsilon_\lambda(x)$
0
X
D, diameter

(b)

temperature) to obtain the local temperatures. An interface-mini-computer assembly was used to process the signals recorded on the oscilloscope to yield the plasma temperature profiles. The following is a detailed description of the individual sections making up the instrument.

1. Optical Sensing Head

The internal component arrangement of the optical head is shown in Figure 6. A high-quality four-element mirror optic assembly with an effective focal length of 700 mm (Questar 700) was used to focus onto a small spot of the plasma column (via a 100 μm-diameter aperture which was positioned 7 cm away from the axis of the plasma and ∿3 m away from the lens) and transferred the captured radiation onto photocells through the semi-transparent Neodymium mirror and interference filters inside the sensing head. The selection of a mirror optic was based on the recommendations of Ruffino (1976) who reported that glass components should be eliminated in the optical systems used in plasma spectroscopy due to aberrations and refraction problems.

The Neodymium mirror was mounted on a mechanical assembly which allowed rotation between two positions spaced at 90° apart. A positive detent mechanism was used to rotate the mirror, ensuring exact alignment in each mode of operation. The two mirror positions are shown in Figure 6 as a solid and a dashed line. The dashed position enabled visual orientation. In this mode, the incoming

radiation from the mirror optics was partially reflected toward the eyepiece, allowing the operator to focus on the portion of the plasma column to be measured. A welding filter No. 10 was attached to the eyepiece, to protect the eye from the intense radiation. The solid line represents the position of the mirror when a measurement was being performed.

As can be seen in the diagram, the incoming radiation was partially transmitted straight through to photocell No. 1 and partially reflected at an angle of 90° to photocell No. 2. Each photocell was illuminated through a precision interference filter which provided a sharp maximum transmission response at the selected wavelengths, 4806 Å and 6965 Å. The filters were specially made by Baird Co. System Components Division, and both had a bandwidth of 10 Å at half-peak transmittance. These particular wavelengths were selected for their isolation from other lines in the spectrum, their strong emission, and high upper energy levels. The negligible self-absorption of the argon plasma for these lines was also of primary importance. The photocells being employed (Centronic Silicon Photodetector, Type 05D5-1) were chosen for their spectral response at the above wavelengths, as well as their high rise time. They were not affected by fatigue also. The intensity of the impinging radiation on each photocell was converted to a voltage output which was amplified by an internal high-gain amplifier circuit.

The schematic diagram of the amplifier is shown in Figure

9. Two identical amplifier stages were used, the gain of which could be changed by a switch controlling both channels simultaneously. In addition, two zero control potentiometers were supplied to enable setting of the amplifier outputs to zero voltage when no radiation was present. The outputs of the two amplifiers were brought out of the sensing head by means of shielded coaxial cables and fed directly into the Y-axis input of the dual-channel digital storage oscilloscope.

The alignment of the optical system was made by connecting the output of the sensors alternatively, to the Y-coordinate input of an X-Y recorder which had a small light bulb attached to its pen. The X-axis of the recorder was driven by the time axis. When the image of the light bulb fell on the sensor, the output from the sensor increased causing the pen and the bulb to move up and to draw a peak. Then the sensors were switched and the output of the second sensor was recorded on the same spot of the graph paper. Alignment was checked by matching the two peaks obtained. This method was employed both for vertical and horizontal alignment. (The system was rotated 90° for vertical alignment).

The optical head was calibrated by focusing the system to a Tungsten Strip Lamp calibrated by the National Research Council of Canada at the wavelengths used in this work, for various currents.

FIGURE 9

CIRCUIT DIAGRAM OF OPTICAL HEAD AMPLIFIER

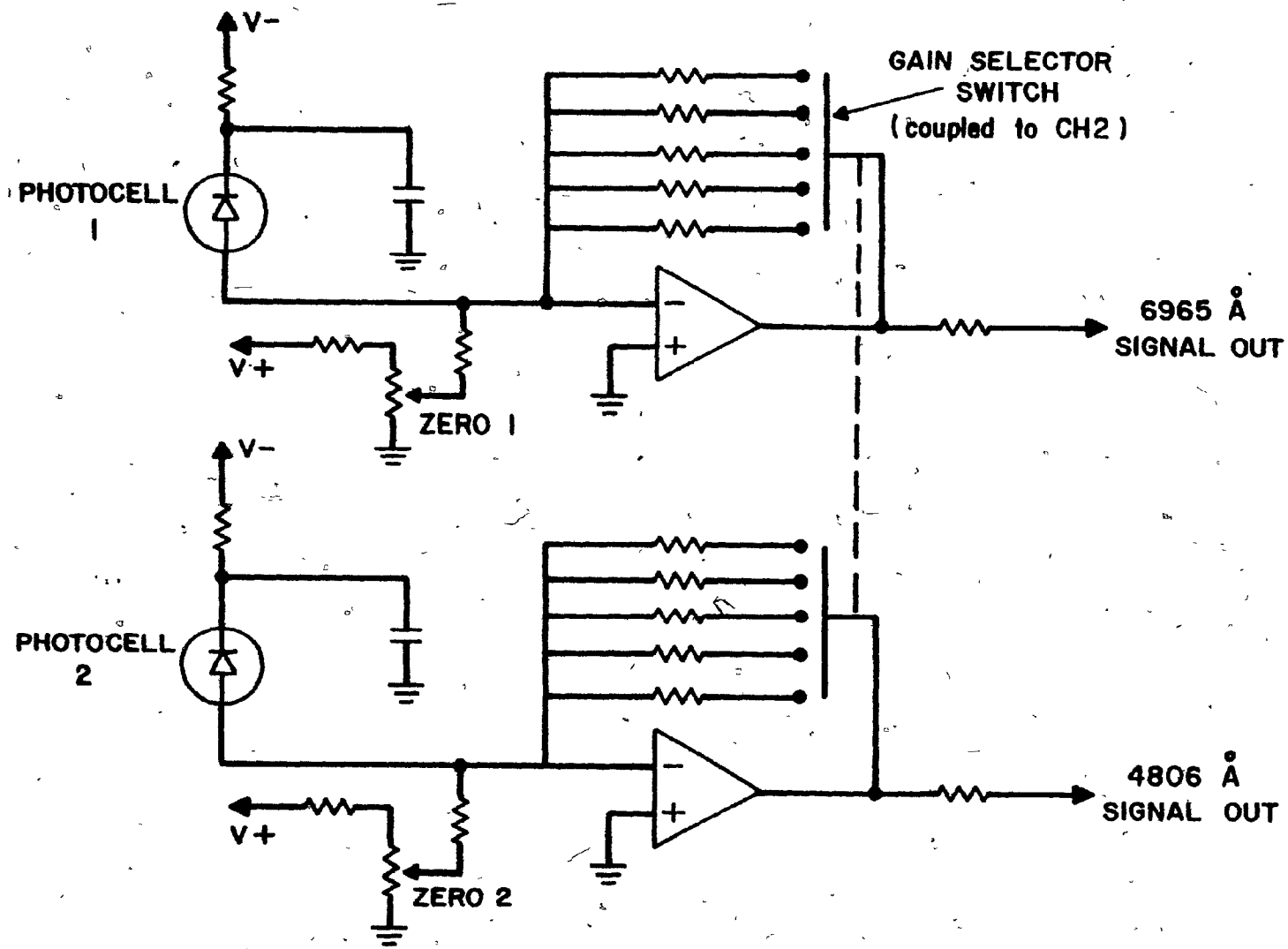
V-
GAIN SELECTOR
SWITCH
(coupled to CH2)
PHOTOCELL
1
6965 Å
SIGNAL OUT
V+
ZERO 1
V-
PHOTOCELL
2
4806 Å
SIGNAL OUT
V+
ZERO 2

ii) Linear Motor Drive Assembly

When performing the actual temperature profile measurement, it was necessary to move an opaque metallic plate, along the optical axis of the detector, through the plasma column in such a way as to vary the amount of incoming radiation from zero to maximum. To accomplish this, a voltage ramp generator and a servo-driven linear motor were used.

Figure 10 shows a block diagram of the complete drive assembly. A ramp generator was used to provide a linearly increasing voltage that rised from zero to one volt in a time span that was controlled by an external potentiometer. The rise time of the ramp could be varied from 0.3 to 5 seconds. The ramp waveform was fed to a servo amplifier which provided a control signal to drive the linear motor. The motor was a modified version of the kind used in fast chart recorders and provided a stable linear motion for the travelling metal plate. A tin plate, with the dimensions of 2mm by 0.6 mm by 3 cm was blackened with a spray-dye (Nextel Velvet Coating, 3 M Co.), specified to resist high temperatures ($\sim$200°C). A probe, one end connected to the drive mechanism of the linear motor and the other end having a latch mechanism, was built out of teflon and plexiglass to carry the tin plate. An optical trigger, consisting of a small infrared emitting diode and a photocell, was used to trigger the X-axis sweep of the oscilloscope just before the metal strip reached the plasma. This was later replaced by a mechanical

FIGURE 10

BLOCK DIAGRAM OF THE LINEAR MOTOR
AND OSCILLOSCOPE TRIGGER CIRCUITRY

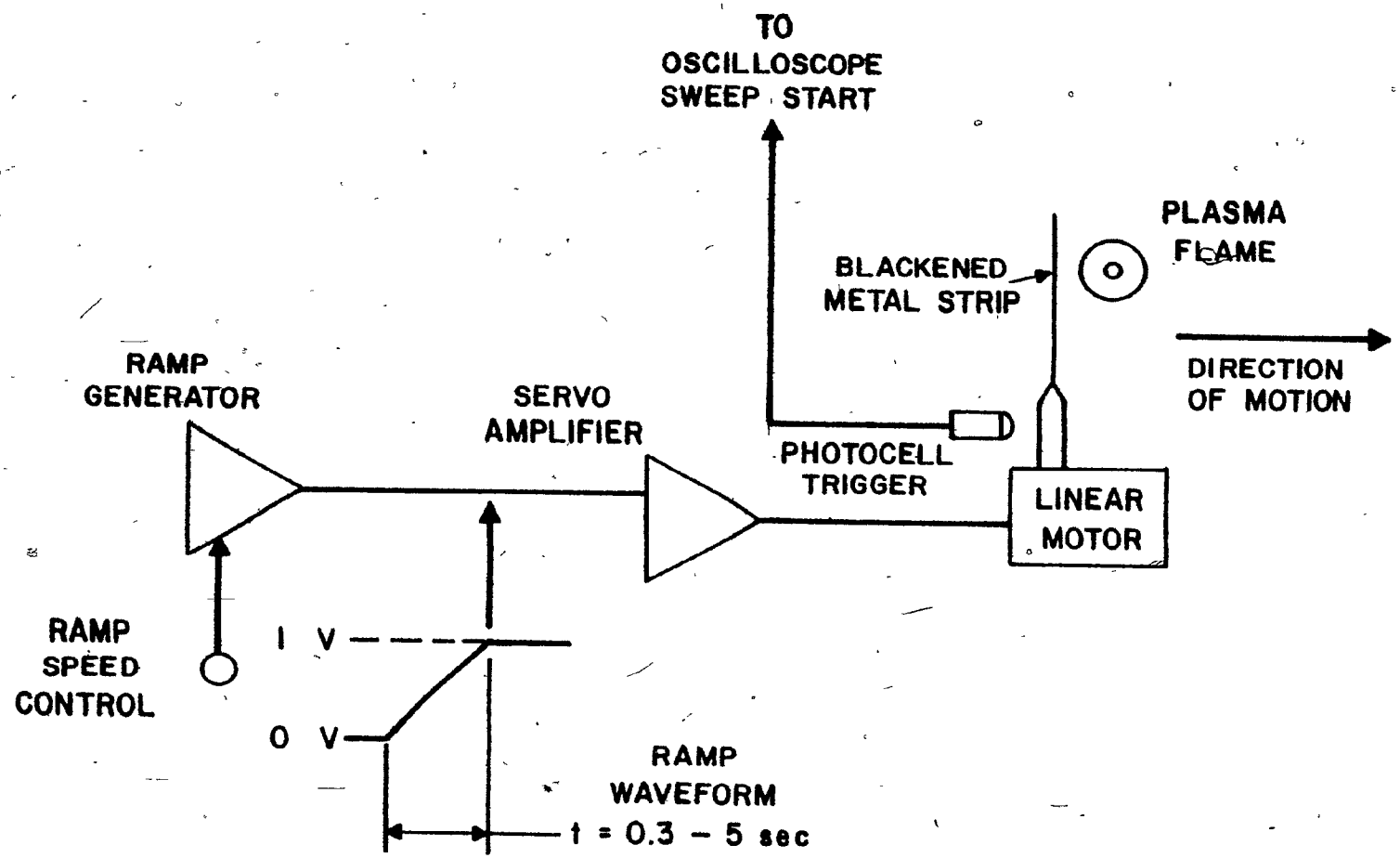
TO
OSCILLOSCOPE
SWEEP START
PLASMA
FLAME
BLACKENED
METAL STRIP
DIRECTION
OF MOTION
RAMP
GENERATOR
SERVO
AMPLIFIER
PHOTOCELL
TRIGGER
LINEAR
MOTOR
RAMP
SPEED
CONTROL
1 V
0 V
RAMP
WAVEFORM
t = 0.3 – 5 sec

trigger system consisting of a micro-switch.

iii) Oscilloscope-Computer Interface

The digital storage oscilloscope used (Gould-Brush, Advance Model 054000/4001, with Output Unit) stored the waveform information presented on the CRT display, by means of a 1024 byte x 8 bit memory. Each 8 bit word contained the voltage or Y-axis information for each individual sampled point of the waveform. Every complete sweep of the X-axis produced 1024 sampled points. The result was a digital picture of the CRT display stored in memory. The digital information contained therein was available at a user-accessible terminal in the oscilloscope. In order to accommodate two separate channels, the memory must be alternatively divided between the two incoming signals. Channel 1 was put into even-numbered memory locations and Channel 2 in odd-numbered spaces. The result was that each signal was sampled 512 times instead of the maximum 1024.

In order to retrieve the stored information, the oscilloscope user port provided two eight-bit output buses and two one-bit synchronization lines. One bus accessed even address (Channel 1) information, and the other bus presented odd address (Channel 2) data. Valid data on each bus was indicated when a momentary transition from a logical 1 to 0 occurs on its associated synchronization line. The entire memory was transferred in a succession of even and odd addresses, and output was initialized by means of a

pushbutton on the oscilloscope panel.

The PET 2001 (Commodore) minicomputer which was used to analyze the stored oscilloscope data had an 8-bit user-accessible input port. In order to accommodate the two output terminals of the oscilloscope, an interface circuit was necessary to alternatively switch the two 8-bit signals into the computer's input. A block diagram of how the interface performed this function is shown in Figure 11. The function of multiplexing the two signals into one line was performed by the solid-state switches shown in the diagram. The switches allowed signals to pass when their associated control lines went to a logic 1. For example, say the oscilloscope has just presented an 8-bit word at the "Channel 1 Data In" line (only one bit is shown for clarity), at the same time the Channel 1 Synchronization Signal will go from 1 to 0, flow through its associated pulse shaper, and latch the flip-flop so that the Channel 1 Control Line goes high. This puts the Channel 1 input data onto the output bus. Note that the Channel 2 Control Line is low and any data present at the Channel 2 input port will not affect the output. When the oscilloscope indicates that the Channel 2 data is ready, the Channel 2 Synchronization signal will momentarily go low, reversing the state of the flip-flop, causing the Channel 1 Control Line to go low, the Channel 2 Control Line to go high, and presenting the new data at the output port. The outputs of the two pulse shapers were also connected to an "OR" gate which provided a train of pulses to the computer indicating when successive channel data

FIGURE 11

BLOCK DIAGRAM SHOWING SIGNAL FLOW IN

OSCILLOSCOPE-COMPUTER INTERFACE

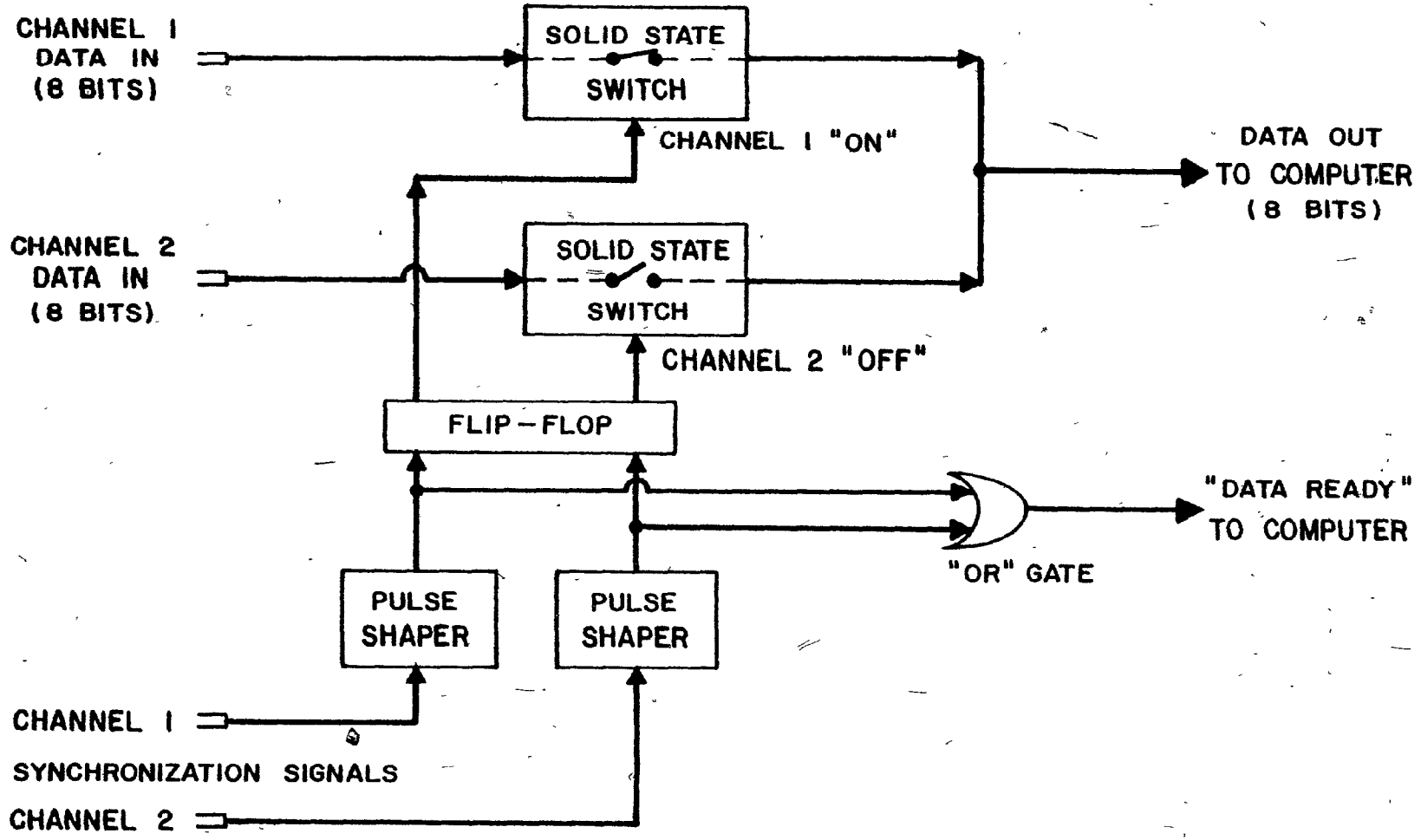
CHANNEL 1
DATA IN
(8 BITS)
SOLID STATE
SWITCH
CHANNEL 1 "ON"
DATA OUT
TO COMPUTER
(8 BITS)
CHANNEL 2
DATA IN
(8 BITS)
SOLID STATE
SWITCH
CHANNEL 2 "OFF"
FLIP-FLOP
"DATA READY"
TO COMPUTER
"OR" GATE
PULSE
SHAPER
PULSE
SHAPER
CHANNEL 1
SYNCHRONIZATION SIGNALS
CHANNEL 2

were being presented at the output. The computer had no way of knowing directly whether a data byte corresponded to Channel 1 or Channel 2. It simply assumed that the first "DATA READY" pulse corresponded to Channel 1, the second to Channel 2, and so forth until the whole memory was transferred by the oscilloscope. The pulse shapers which were used to interface the synchronization signals from the oscilloscope converted the latter's short duration (200 ns) pulses into a longer duration signal (10 ms) suitable for sensing by the computer. A detailed circuit diagram of the interface is shown in Figure 12.

A computer program, written in both BASIC and ASSEMBLER languages to operate on a Commodore PET minicomputer, was utilized to process the raw data. The objectives of the program, which are reproduced and explained in detail in Appendix D, were:

a. to transfer data as stored in the memory of the GOULD storage oscilloscope to the memory of the PET minicomputer;
b. to reproduce graphically the transferred data;
c. to smooth and differentiate the data by using the Convolution Integers Method, described by Savitzky and Golay (1964);
d. to plot the derivatives thus obtained;
e. to calculate the temperature at each data point using the ratio of the derivatives in Equations

FIGURE 12

CIRCUIT DIAGRAM OF OSCILLOSCOPE

COMPUTER INTERFACE

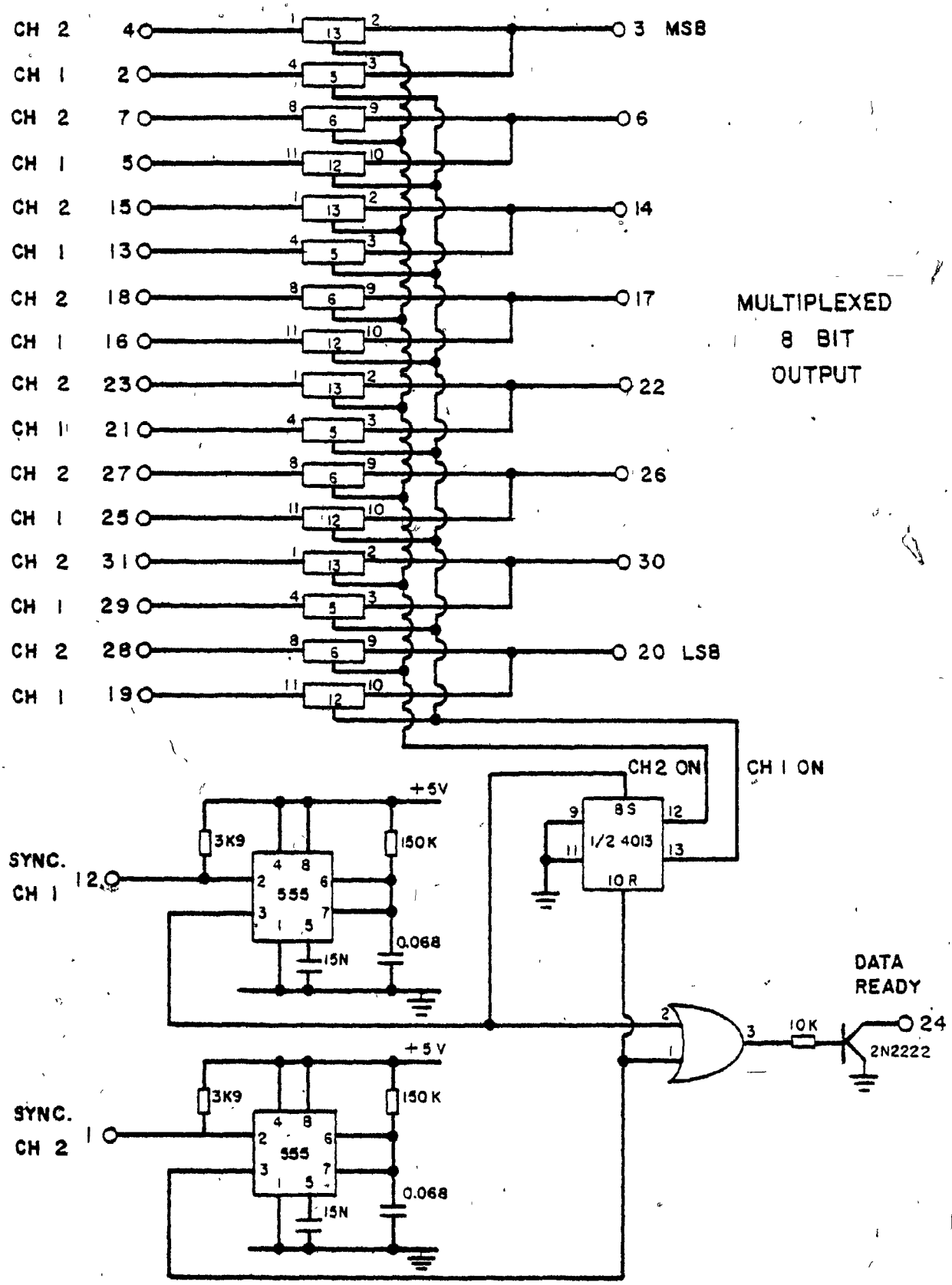
CH 2 4
CH 1 2
CH 2 7
CH 1 5
CH 2 15
CH 1 13
CH 2 18
CH 1 16
CH 2 23
CH 1 21
CH 2 27
CH 1 25
CH 2 31
CH 1 29
CH 2 28
CH 1 19
3 MSB
6
14
17
22
26
30
20 LSB
MULTIPLEXED
8 BIT
OUTPUT
CH2 ON
CH 1 ON
+5V
3K9
150K
SYNC.
CH 1
12
555
0.068
15N
8 S
1/2 4013
10 R
DATA
READY
10K
2N2222
24
SYNC.
CH 2
1

1 or 2;

f. to plot and tabulate the temperatures, as a function of radius (calculated from the speed of the linear motor and time-scale of the oscilloscope, both manually input to the mini computer);

3. Impact Pressure Measurement Technique

A dynamic pressure probe was developed to obtain direct flow field distributions in the transferred arc column. The probe involved in this work follows the design of Barkan and Whitman (1966). It consisted of a miniature pitot tube swept through the column. The pitot tube was connected to a pressure transducer which produced a signal proportional to the local dynamic pressure. The velocity and mass flow density were then derived from the dynamic pressure with the aid of the Bernoulli equation corrected for viscous effects.

The selection of the pressure transducer to be used in this work was based on the criteria of light weight, high sensitivity, high response time and resistance to shock, vibration and relatively high temperatures. The unit described by Barkan and Whitman involved a piezoelectrical pressure transducer with a sensitivity of ~0.5 psi. Sheer et al (1969), who tested this transducer in a free-burning arc, found it to be wholly inadequate. They suggested that the sensitivity requirement should be two orders of magnitude higher. They finally

adopted the Pace-Wianco Model P105D variable reluctance transducer, having a sensitivity <0.001 psi. In the light of this information, the various available pressure transducers on the market were checked, and eventually the Celesco Model P109D miniature variable reluctance differential pressure transducer was selected. This unit showed a sensitivity of <0.005 psi, and was much more insensitive to mechanical shock and vibration than any of the piezoelectric types available. The possibility of changing its stainless diaphragm was a definite improvement over the Pace-Wianco P105D user by Sheer et al.

A small stainless steel pitot tube, 1.5875-mm (1/16-inch) O.D., 0.508-mm I.D. by 3.75-cm long was connected to the transducer via teflon fittings to prevent arcing. The hook length was 0.6 cm, short enough to prevent the establishment of a cathode-anode discharge on the probe, but sufficient to avoid spurious pressure effects. The face of the transducer subjected to plasma radiation was shielded by an aluminum plate, acting as a heat sink. A thin teflon gasket placed in between provided the required thermal insulation. The transducer was firmly attached on a mounting assembly which was driven by the linear motor described in the previous section. Figure 13 shows a schematic representation of the pressure probe unit.

The electrical outlets of the transducer were connected to a demodulator (Model CD10 miniature carrier-demodulator, by Celesco)

FIGURE 13

SKETCH OF THE TRANSIENT

PRESSURE PROBE

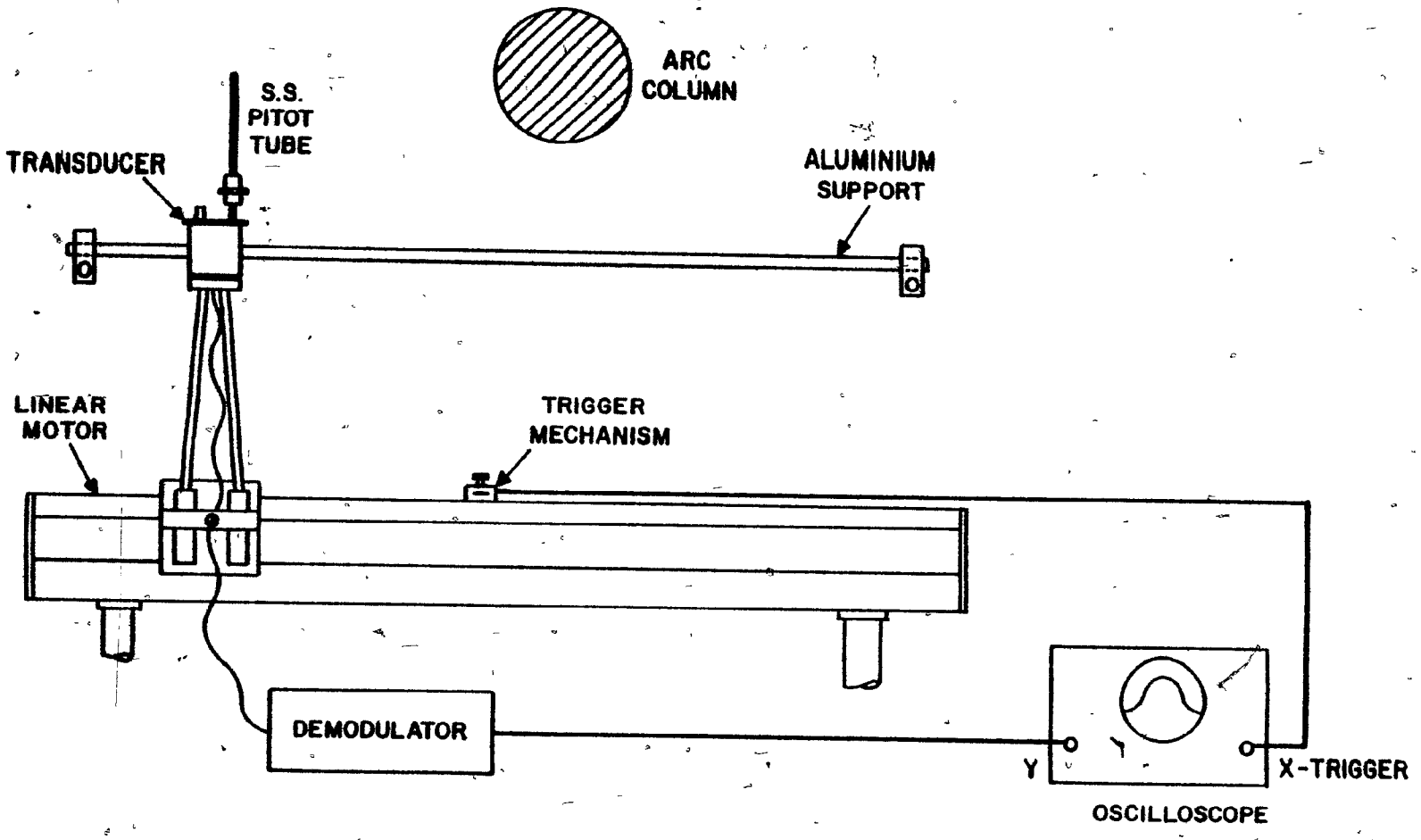
ARC
COLUMN
S.S.
PITOT
TUBE
TRANSDUCER
ALUMINIUM
SUPPORT
LINEAR
MOTOR
TRIGGER
MECHANISM
DEMODULATOR
Y
X-TRIGGER
OSCILLOSCOPE

whose output was displayed on a Gould-Brush digital storage oscilloscope. The same triggering system as in the temperature diagnostic system was also employed here. The transducer and the pitot tube were calibrated against an accurate alcohol manometer.

The selection of the diaphragm used in the pressure transducer was based on the preliminary measurements of impact pressure carried out with the anode having a stagnation pressure tap. Consequently, a diaphragm with a maximum measurement capacity of 0.1 psig was selected.

One of the important parameters in this work was the response time. A time-resolved calibration was made by directing a cold jet of air at the probe assembly, interposing a small metal strip (carried by the linear motor) in which a slot had been cut between the probe and the cold air jet. As the strip was moved back and forth by the linear motor (at a constant speed), square wave pulses of air were directed at the probe. For the probe employed in this investigation, a time constant of about 0.002 second was observed in this way.

To test the transient response of the system, the transducer and the pitot tube were mounted on the linear motor and transient measurements of the flow field of an argon jet issuing from a 2-cm I.D. pipe were made at different traverse speeds. The measurements were compared with the steady state (stationary) measurements. The

results are shown in Figure 14, from which it is seen that at traverse speeds around 20 cm/s, the transient response of the system was satisfactory. At this speed, the exposure time of the stainless steel tube to the hot plasma was short enough to avoid thermal damage of the portion immersed in the column.

The dynamic pressure data obtained were reduced to gas velocity by means of a simple relation derived as follows.

For an incompressible fluid and isentropic recovery of pressure in the tube, one can write:

$$\Delta P = 1/2\ \rho\ U^2 \qquad (3)$$

where ΔP = difference between the measured impact pressure and the free stream pressure

ρ = gas density

U = gas velocity

Because of the assumption of incompressibility, ρ may be taken as the free stream density. From the ideal gas law:

$$\rho = \rho_\infty = P_\infty / R\ T_\infty \qquad (4)$$

where the subscript ∞ denotes the free stream value.

Equation (3) (Bernoulli's Equation) assumes incompressibility as well as negligible viscous effects. For the flow regimes

FIGURE 14

COMPARISON OF TRANSIENT AND STEADY STATE PRESSURE PROBE MEASUREMENTS

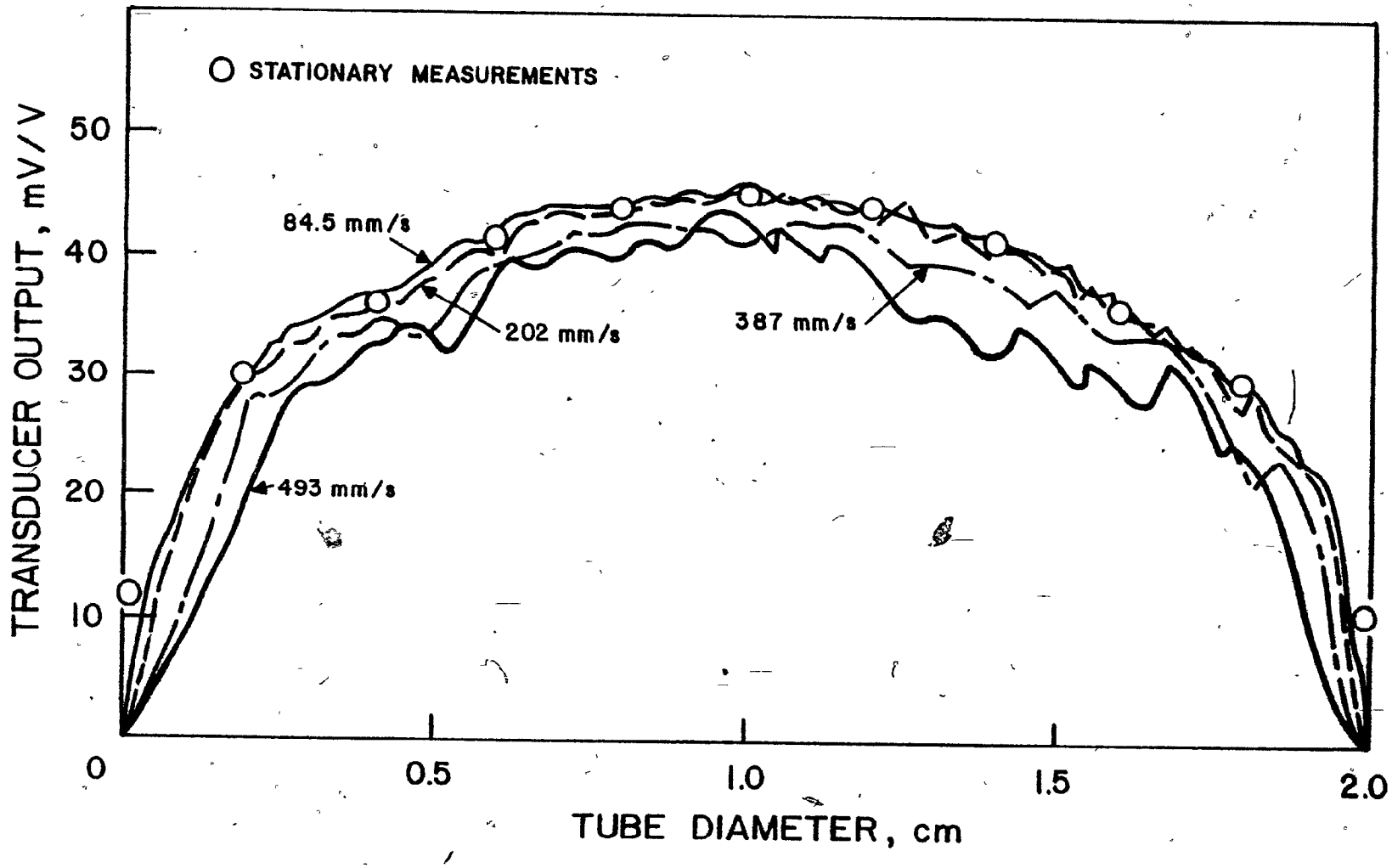
O STATIONARY MEASUREMENTS
84.5 mm/s
202 mm/s
387 mm/s
493 mm/s
TRANSDUCER OUTPUT, mV/V
50
40
30
20
10
0
0.5
1.0
1.5
2.0
TUBE DIAMETER, cm

involved, the maximum value of the Mach number was <0.13; thus the error involved in the assumption of imcompressibility was <1% (Shapiro, 1953). The viscous effects, however, could not be neglected for many of the flow conditions used in this work. It has been observed by several workers that at very low Reynolds number (∿20), the effect of gas viscosity is to increase the dynamic pressure developed in the pitot tube over that given by the Bernoulli Equation. Thus:

$$\Delta P = 1/2\ \rho\ U^2 + P' \qquad (5)$$

where P' = increase in dynamic pressure due to viscosity

Barker (1922) used Stokes' Law to derive an expression for P', as follows:

$$P' = 3/2\ \mu\ U/a \qquad (6)$$

where a = inside radius of pitot tube

μ = viscosity of the gas

Substituting Equation (6) in (5):

$$\Delta P = 1/2\ \rho\ U^2 + 3/2\ \mu\ U/a \qquad (7)$$

The experiments of Barker showed that there is a linear discrepancy between the measured values of the pressure and those obtained from Equation (7). The discrepancy can be taken into account

by a constant, whose value was calculated as 1.10022, by a linear fit in this work. Thus, the relationship between measured and theoretical values can be very closely expressed by:

$$\Delta P = 1.1\ \Delta P_{exp.} \tag{8}$$

where ΔP_{exp} = the experimentally determined pressure. Substituting Equation (8) in Equation (7) yields:

$$1.1\ \Delta P_{exp} = 1/2\ \rho\ U^2 + 3/2\ \mu\ U/a \tag{9}$$

Solving this equation for U, one obtains:

$$U = 1/2\ \{-3\nu/a + [(3\nu/a)^2 + 8.8\Delta P_{exp}/\rho]^{1/2}\} \tag{10}$$

where ν = kinematic viscosity (μ/ρ).

Both μ and ρ used in Equation (10) are functions of temperature. Following the results of Carleton (1970), the temperature used in the determination of viscosity and density was chosen to be that corresponding to the mean enthalpy of the pitot tube wall and free stream. Both μ and ρ were corrected for departures from the ideal gas law, using theoretically-derived relations between viscosity and compressibility versus temperature (Ahtye, 1965).

PROCEDURES

In this section, the procedures involved in operating the experimental system described in the previous section are explained. Included in this discussion are start-up and operation of the transferred-arc, precautionary safety measures, measurement of temperature and the procedure for impact pressure measurements.

1. Plasma Start-up and Operation

Prior to each run, the surface of the anode was cleaned with fine emery cloth. A plexiglass centering piece was then used to centre the anode (see Figure 15). After the position of the anode was fixed, the cathode assembly was lowered to about 2 mm away from the anode. The upper limiting microswitch was adjusted to predetermine the arc length. The cooling water to the various channels was turned on, and the desired flow rates were set and recorded. The argon cylinder outlet pressure was adjusted and the main power switch was turned on. First, the high-frequency start-up test knob was used to ensure that the electrodes were close enough to start the arc. The power to the electrodes was then engaged and argon flow rate was set to an arbitrary medium value. The arc was then ignited pressing the high-frequency ignition button. After the ignition, the motor that lifted the cathode was switched on immediately and the applied current was simultaneously increased. When the full arc length was reached, the argon flow rate was adjusted to the desired value and the current was again set. This sequence of steps

provided sufficient reproducibility of the torch operation and insured stability in the operation as indicated by the current and voltage. The excessive heating of the electrodes was also prevented. When the injection gas was to be fed, it was only introduced after the full arc length had been achieved, to ensure easy control of the current. Whenever a new operation condition was introduced, the voltmeter leads were connected to the oscilloscope and the voltage fluctuations were observed. The magnitude of these fluctuations was taken as the criterion for filtering the unstable conditions.

In most cases, the arc characteristics did not drift appreciably for the duration of a run, which sometimes was as long as half an hour. The voltage and current, and the various cooling water flow rates and temperatures were recorded at intermediate times during the course of a run.

It should be mentioned that the only controllable electrical parameter was the current applied. The arc voltage could not be specified, but depended on the argon flow rate and the arc current for a given electrode separation. Thus, a power level was specified when a current was selected for a given operating condition, and if the current control was not changed, the power level remained essentially constant.

2. Precautionary Safety Measures

Because of the high intensity radiation emitted by the arc column, several precautionary measures were necessary. The arc column was sufficiently bright to cause serious eye damage if viewed without eye protection. The arc column was observed directly only through an electrical welding helmet. A radiation shield with a welding filter window was placed between the assembly and the control console. A warning light was installed at the laboratory entrance to prevent persons from entering without proper eye protection. The table holding the assembly was carefully insulated from the current carrying parts and was never approached without welding gloves. The UV radiation from the plasma could also cause burns on the skin, and thus care was taken not to expose bare skin to the plasma radiation. During operation of the plasma, a build-up of ozone in the laboratory due to UV radiation emitted by the plasma could be detected. An exhaust fan was employed to eliminate this problem.

3. Temperature Measurements

For temperature measurements, it was very important to align the blocking metal strip, the aperture and the receiving optics. For this purpose, a Helium-Neon Laser was used. Prior to an experiment, the laser system was positioned such that the laser beam would pass through the axis of the plasma, at the vertical position where the temperature profile would be obtained. The

plexiglass centering device already mentioned was used for determining the axis and a cathetometer was employed for vertical leveling. The aperture, which consisted of a 100 μm-hole mounted on an aluminum bellows system, was then aligned according to the laser beam. The position of the optical system, which was placed on a precision laboratory jack, was also roughly adjusted. A dummy blocking metal strip was attached to the probe extending from the linear motor. Then the linear motor assembly and the aluminum rod support used to eliminate vibrations of the probe were aligned carefully so that the metal strip would be on line with the tiny laser beam during its complete traverse. This ensured that the blocking strip would sweep the plasma horizontally, at the vertical position where the temperature profile was desired. The speed of the linear motor was checked from the chart recorder which was connected to the servo-amplifier. Then the dummy blocking metal was replaced with a newly painted tin strip. Its position with respect to the electrodes was again checked using the cathetometer. The laser system and centering device were then removed. Figure 15 shows a sketch of the alignment system.

Prior to all these adjustments, the power supply of the sensor head had to be turned on to provide sufficient time for the warm-up of the amplifiers. An experiment was attempted only when the zero positions of the outputs of the two sensors were stabilized, as observed on the digital storage oscilloscope.

FIGURE 15

SKETCH OF THE ALIGNMENT SYSTEM

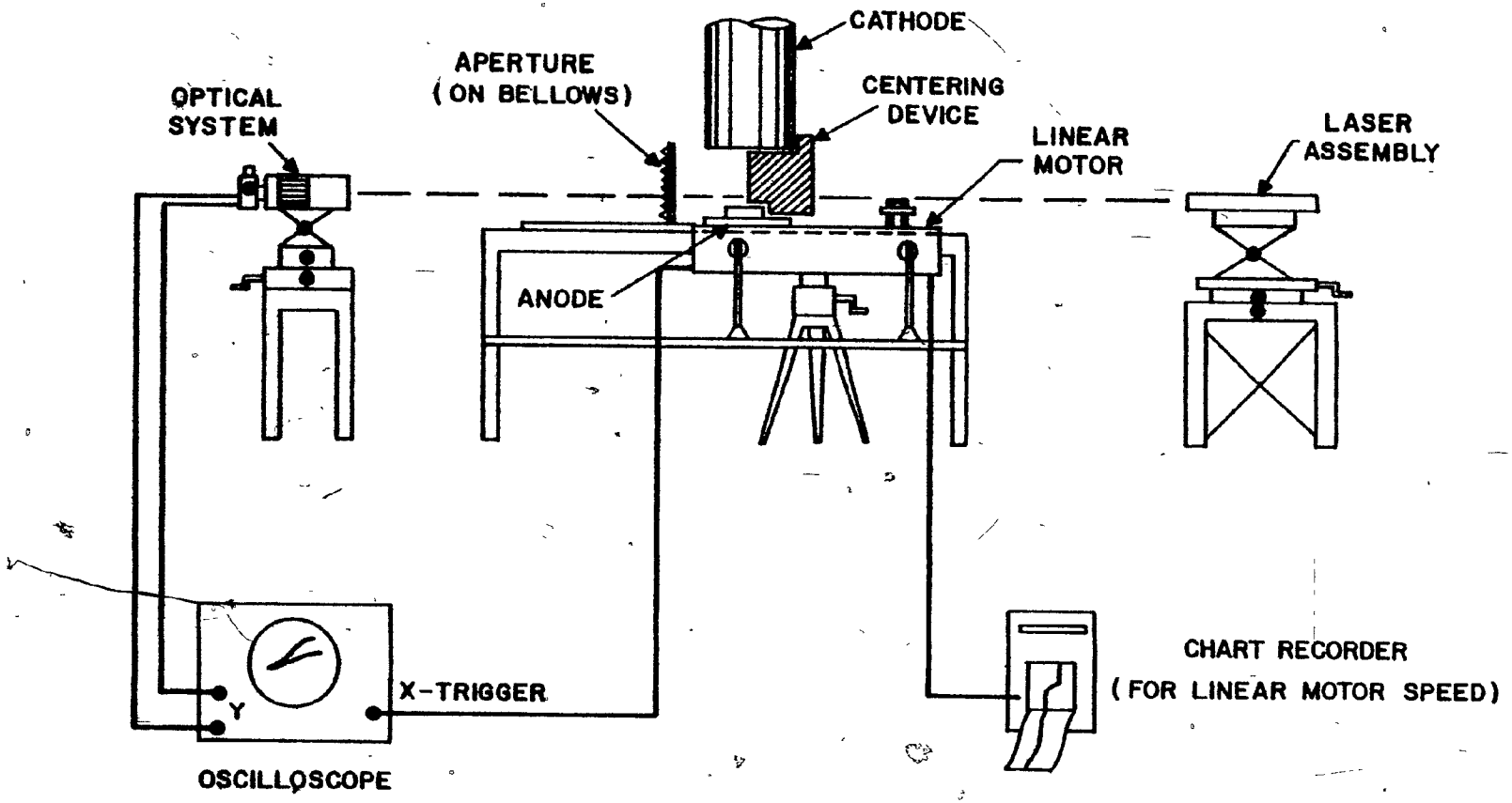
CATHODE
APERTURE
(ON BELLOWS)
CENTERING
DEVICE
OPTICAL
SYSTEM
LINEAR
MOTOR
LASER
ASSEMBLY
ANODE
X-TRIGGER
Y
OSCILLOSCOPE
CHART RECORDER
(FOR LINEAR MOTOR SPEED)

The transferred-arc plasma was then generated as previously explained. After the necessary adjustments had been made for a stable operation, the Neodymium mirror in the sensor head assembly was oriented such that the plasma could be viewed through the eyepiece. The bright spot of the aperture was focused and centered with respect to the cross-hair lines in the eyepiece, by adjusting the three-dimensional traversing mechanism on which the optical assembly was mounted.

The next step in the sequence was to adjust the sensitivity and the sweep rate of the oscilloscope such that the whole of the rising curve (or falling curve, depending on the direction of the traverse) resulting from the traverse would be captured on the screen. The oscilloscope was set to the external triggering-storage mode. Then the linear motor was turned on and, with the command of a pushbuttom, the metal strip was traversed through the plasma. Meanwhile, the speed of the linear motor and the voltage fluctuations of the plasma were recorded on chart recorders. The experiment was considered as valid if the outputs of the sensors showed little or no noise and if the voltage fluctuations were below acceptable levels.

Following shutdown of the plasma, the recorded data were transferred to the minicomputer. For this purpose, the minicomputer was first turned on (during an experiment, the minicomputer had to be turned off to protect it from the high-frequency noise of the

plasma starter). The BASIC program stored on a cassette was loaded and then run. The transfer button of the oscilloscope was pressed when the computer program requested so. The settings of the oscilloscope and the calculated linear motor speed were manually input, again when the program demanded. The authenticity of the transfer was checked visually from the reproduction on the CRT. Finally, the temperature-versus-radius-graph was transcribed on transparent sheets prepared to fit on the CRT screen.

4. Velocity

The impact pressure and temperature measurements had to be performed separately since they employed the same driving mechanism and storage oscilloscope. Generally, the impact pressure measurements followed temperature measurements and, to ensure reproducibility, the arc length, gas flow rate and arc current were carefully set and the arc voltage was closely monitored. The condition for reproducibility was set at <1% change in arc voltages.

Prior to an experiment, the pitot tube and transducer were placed on the drive mechanism and the linear motor's vertical position was adjusted such that the tip of the pitot tube would be at the vertical position in the arc where the profile was to be obtained. A cathetometer was used to effect this positioning. The speed of the linear motor was then checked and adjusted around 20 cm/s. After the pitot tube and transducer mounting assembly were brought to the rest position (about 10 cm away from the plasma

axis, to minimize heating due to radiation) the transferred arc plasma was generated and the transducer modulator was turned on. The oscilloscope was set to the storage mode and the linear motor was activated. When the response of the transducer was captured on the oscilloscope, it was transferred to the chart recorder (which already registered the speed of the linear motor), and the measurement was repeated with the direction of the traverse of the pitot tube reversed. After the second recording was captured, the plasma was shut off and the responses obtained in the forward and reverse traverses compared. The experiment was repeated if they showed any deviation. The condition of the pitot tube was checked to determine if the thermal ablation was appreciable.

The data read from the recorder were used, together with plasma temperatures, to obtain the gas velocity profile. These values were also converted into mass flow density using gas densities. The PET Minicomputer was employed for these calculations.

RESULTS AND DISCUSSION

The results of the experimental work are presented and discussed in this section. General observations on the behaviour of the transferred-arc plasma and on the electrodes are reported first. The electrical characteristics of the arc, namely the arc voltage and the voltage gradient as a function of a number of parameters, are then considered as a possible aid for prediction of the transferred arc behaviour. Calorimetric measurements made to describe the heat losses of the plasma are discussed. Measurements of the thermal condition of the plasma are presented. Velocity profiles obtained from impact pressure measurements are analyzed. Finally, the mass and energy balances are performed.

1 - General Observations

Before the specific details of the outcome of the various phases of this study are presented, it is important that some general observations on the behaviour of the transferred arc plasma be reported. Such observations could be most valuable to future researchers in this field.

Anode Condition

In the initial phases of the experimental work, several difficulties were experienced due to water leakages resulting from local melting at the anode surface. After the design of the anode had been improved and much higher water flow rates were used,

melting of anode surface was minimized but not completely eliminated. Hence, it was necessary to change the anode face disc after about ten (10) long runs. It was observed that the plasma created a crater at its axis on the anode face, and that the material removed from this part was carried towards the outer periphery of the plasma. Figure 16 shows a photograph of an anode surface, after about one-half hour of operation. The slight oxidation observed was suspected to occur primarily in the short time interval between the termination of the plasma and the cooling of the anode attachment spot, although the possibility of air entrainment into the arc could not be completely ruled out at that time.

Another important observation about the anode was that the high-frequency arc used to ignite the plasma, with the cathode in close proximity, caused serious damage on the anode surface in the form of streaks. Thus, it can be stated that the number of startups to which a particular anode has been subjected is as important in determining its life as the total time of operation.

Cathode Condition

The tungsten cathodes used in this work were ground to a sharp, conical tip. After a few minutes of operation, there was some material loss at the tip, causing it to assume a hemispherical shape. The cathode, however, maintained this "equilibrium"

FIGURE 16

PHOTOGRAPH OF THE ANODE SURFACE AFTER ≈30 MINUTES CONTINUOUS OPERATION (X3)

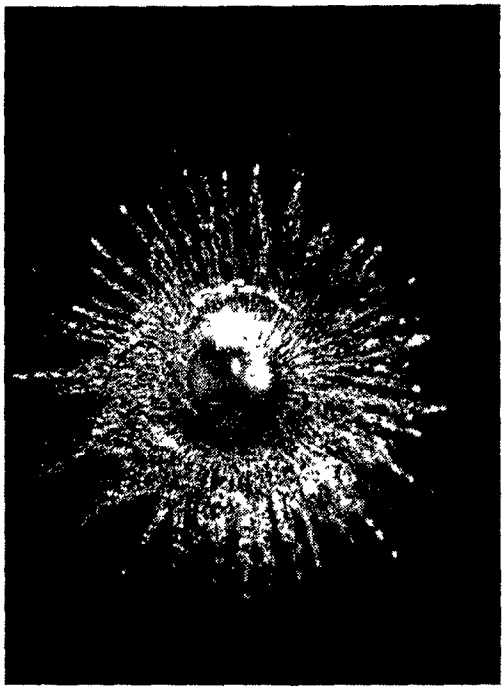

condition for many hours of operation. The photographs of a new tip and one after several hours of operation are shown on Figure 17. It was thus assumed that contamination of the plasma by tungsten vapors was negligible.

Electrode Concentricity

The concentricity of the cathode tip with the nozzle was found to be very critical in the operation of the transferred arc. If the conical tungsten cathode tip was not perfectly centered in the conical brass nozzle, very poor gas distribution was obtained at the exit plane of the nozzle. As a result, preferential attachment of the arc to a spot other than the centre of the anode (where maximum cooling rate was achieved) was observed and the anode lifetime was sharply reduced. At times, the arc made sporadic jumps from one position to the other. Thus, concentricity of the cathode was of paramount importance for stability and extended anode life. This was checked by using a mirror arrangement after each cathode tip replacement. Further, the plasma was closely observed from different angles and necessary adjustments were made via the retaining screws at the head of the cathode assembly. As a result, the photographs of the plasma revealed that, on average, the axis of the arc column coincided with the shortest path between the cathode tip and anode to within circa 0.5 mm, except for arc lengths > 10 cm, in which case the arc was not stable, regardless of concentricity of electrodes.

FIGURE 17

PHOTOGRAPHS OF THE CATHODE TIP
BEFORE AND AFTER OPERATION (X4)

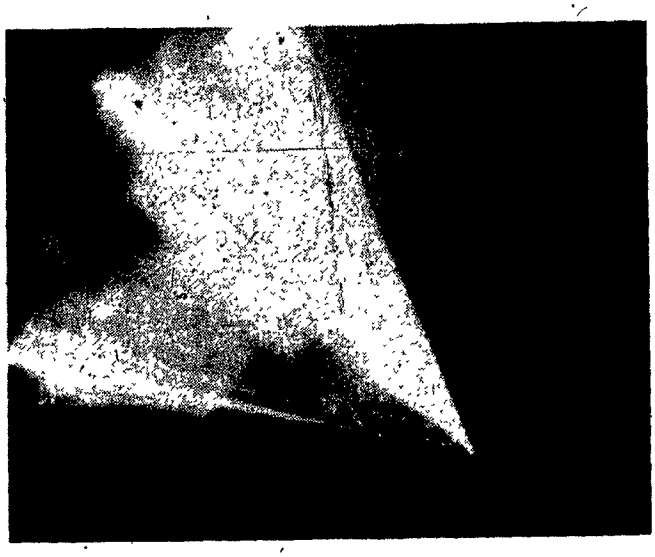

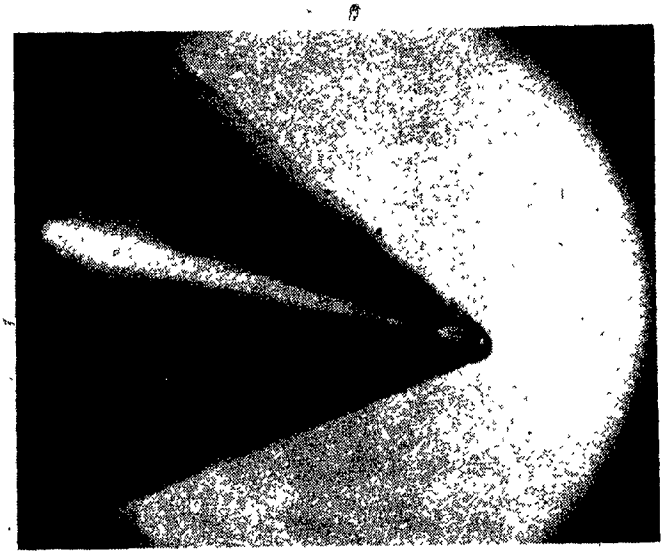

2 - Design of Experiments

The experimental work was carried out in two stages. The first was mainly devoted to the determination of the stable operating conditions and was used as a guide to determine the experimental conditions of the second stage. In the first stage, electrical, calorimetric and photographic measurements were carried out and because of the short time required to collect the data, the experimental design of this phase included all the possible combinations of the selected values of the operating conditions. The second stage involved temperature and impact pressure measurements. The more complex nature of these measurements necessitated a selective experimental design. Details of these experimental designs will be discussed in the appropriate sections.

3 - Total Arc Voltage Analysis

This phase of the experimental work was basically exploratory in nature. At the beginning of this stage, the effect of the applied current (I), the electrode separation (ℓ), the argon volumetric flow rate (Q) and the annular nozzle area (A) on the total arc voltage (V) was investigated. A 60° nozzle (with the horizontal) was used. No injection gas was fed. Following analysis of the results, it was hypothesized that the argon volumetric flow rate and the annular nozzle area could be combined into a single parameter, termed the "Inlet Gas Velocity" (v^*). A new set of

experiments were performed to substantiate this claim. Again, a 60° nozzle, but with two different nozzle diameters (D_n) without any injection gas, was used. Finally, the effect of the nozzle angle (θ) and the injection gas volumetric flow rate (q) on the total arc voltage was studied with a new experimental design. A three-variable Box-Behnken Design (Box and Behnken, 1960) was used for the last two sets, while all the possible combinations of the parameters were investigated for the first set.

The experimental conditions for Set I are shown in Table I. The particular ranges of parameters were chosen with the considerations of possible industrial applications (for ℓ), of electrode lifetime (for minimum Q and maximum I), of arc stability (for minimum I and maximum Q) and of cathode design (for A). The voltages recorded will be presented in two ways: (a) the sustained arc voltage versus electrode separation with gas flow rate as the third parameter and the applied current and/or the nozzle annular area varying between the graphs, (Figures 18 to 20 show three typical representations of the nine such graphs obtained; detailed data are given in Appendix E); (b) the sustained voltage versus the inlet gas velocity (ratio of the flow rate and the nozzle annular area) with the current as the third parameter. Here, four graphs, one for each electrode separation, would be obtained. Figures 21 to 24 show the results obtained in these cases.

As can be seen from Figures 18 to 20, it was not always

TABLE I

EXPERIMENTAL CONDITIONS FOR SET I

Annular Area	(A)	:	0.085, 0.07 and 0.055	cm^2
Current	(I)	:	150, 250 and 350	A
Electrode Separation	(ℓ)	:	4, 6, 8, 10	cm
Ar Volume Flow Rate	(Q)	:	14, 17, 20	L/min.
Nozzle Angle	(θ)	:	60°	
Nozzle Diameter	(D_n)	:	0.15"	(≃0.381 cm)
No Injection Gas Used				
Total Number of Experiments		:	108	

FIGURE 18

ARC VOLTAGE VARIATION WITH ELECTRODE SEPARATION

(Low Current, Large Area)

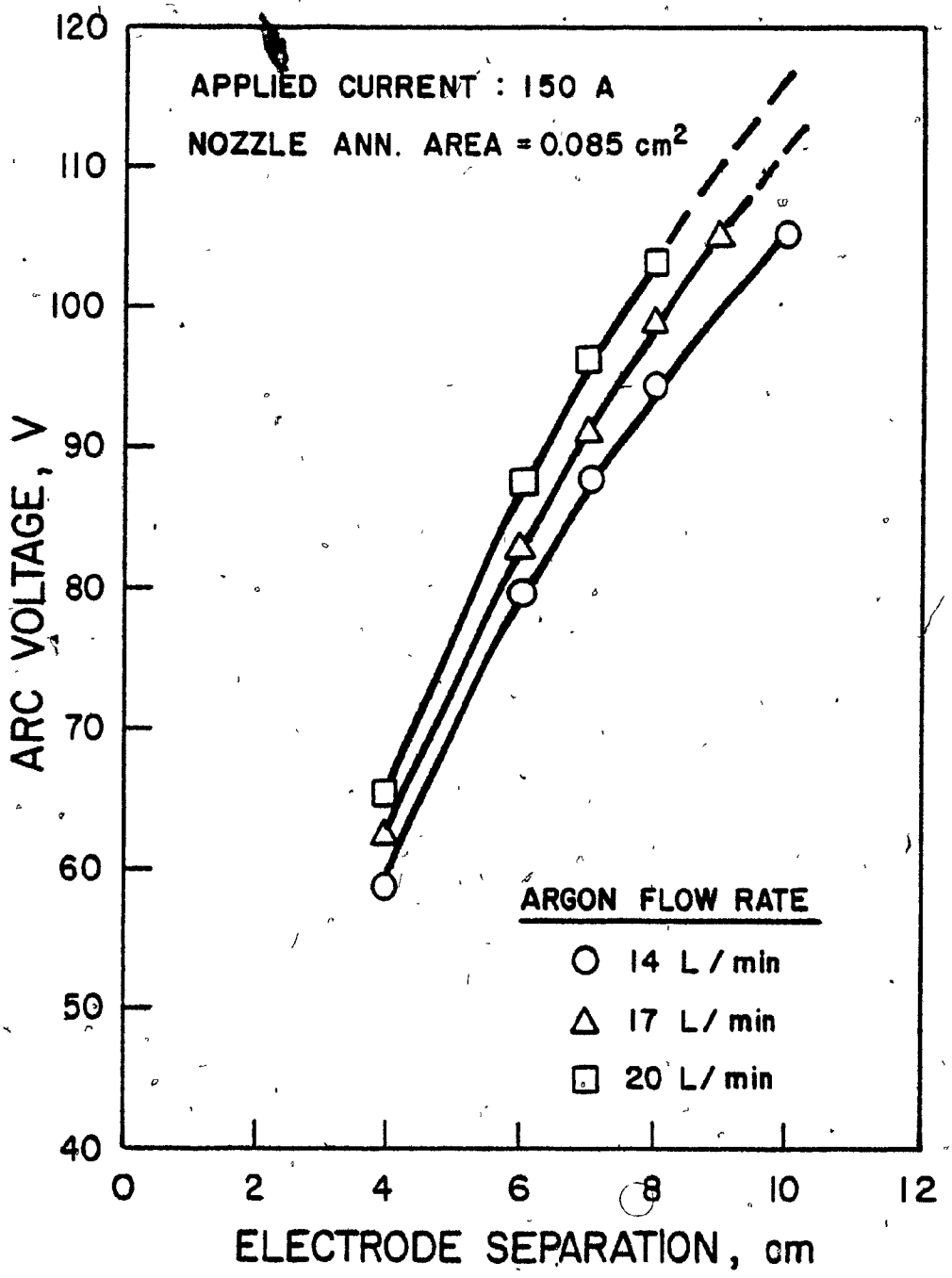
APPLIED CURRENT : 150 A
NOZZLE ANN. AREA = 0.085 cm²
ARC VOLTAGE, V
ELECTRODE SEPARATION, cm
ARGON FLOW RATE
14 L / min
17 L / min
20 L / min
120
110
100
90
80
70
60
50
40
0
2
4
6
8
10
12

FIGURE 19

ARC VOLTAGE VARIATION WITH ELECTRODE SEPARATION

(Medium Current, Medium Area)

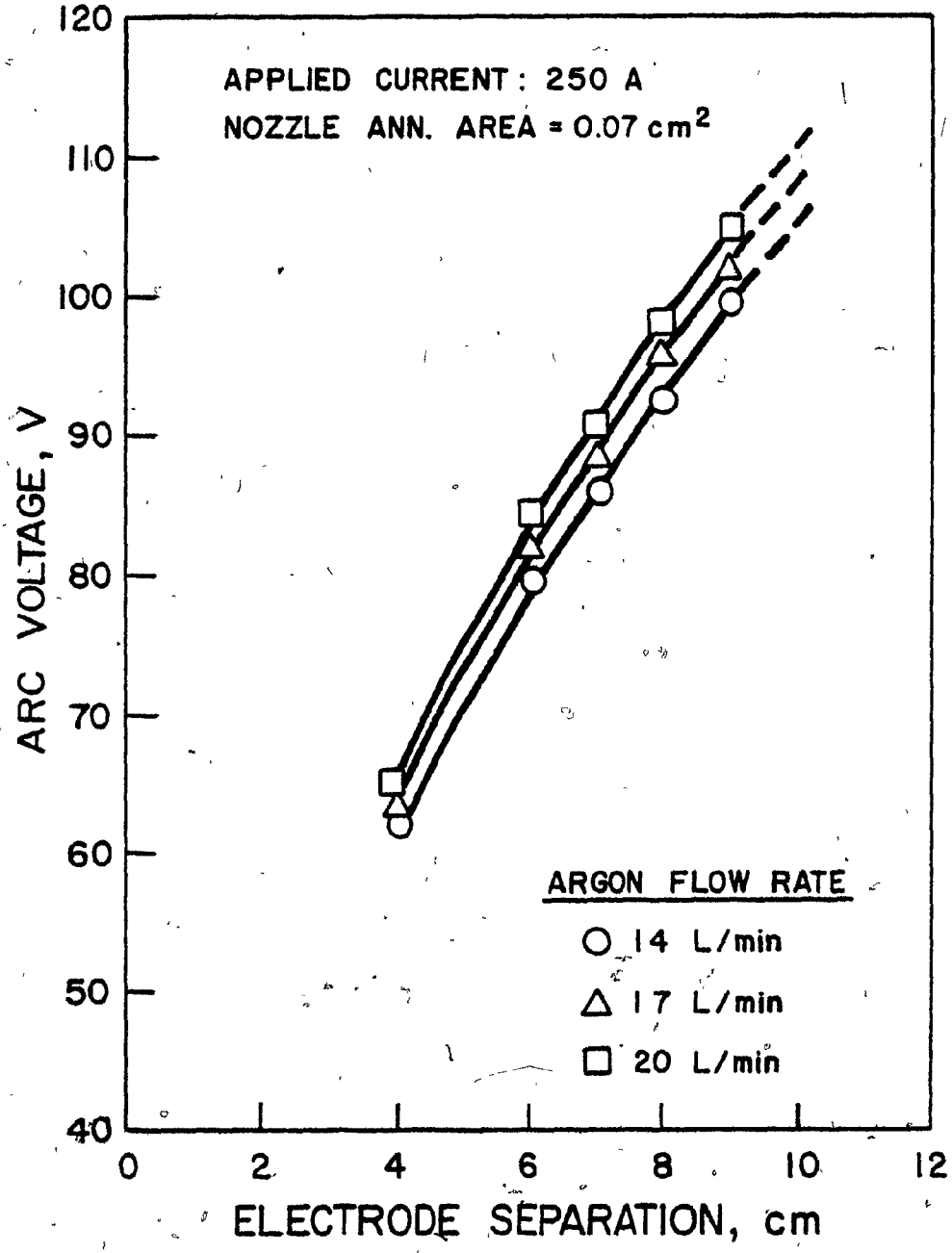
APPLIED CURRENT : 250 A
NOZZLE ANN. AREA = 0.07 cm²
ARC VOLTAGE, V
ELECTRODE SEPARATION, cm
ARGON FLOW RATE
14 L/min
17 L/min
20 L/min
120
110
100
90
80
70
60
50
40
0
2
4
6
8
10
12

FIGURE 20

ARC VOLTAGE VARIATION WITH
ELECTRODE SEPARATION

(High Current, Small Area)

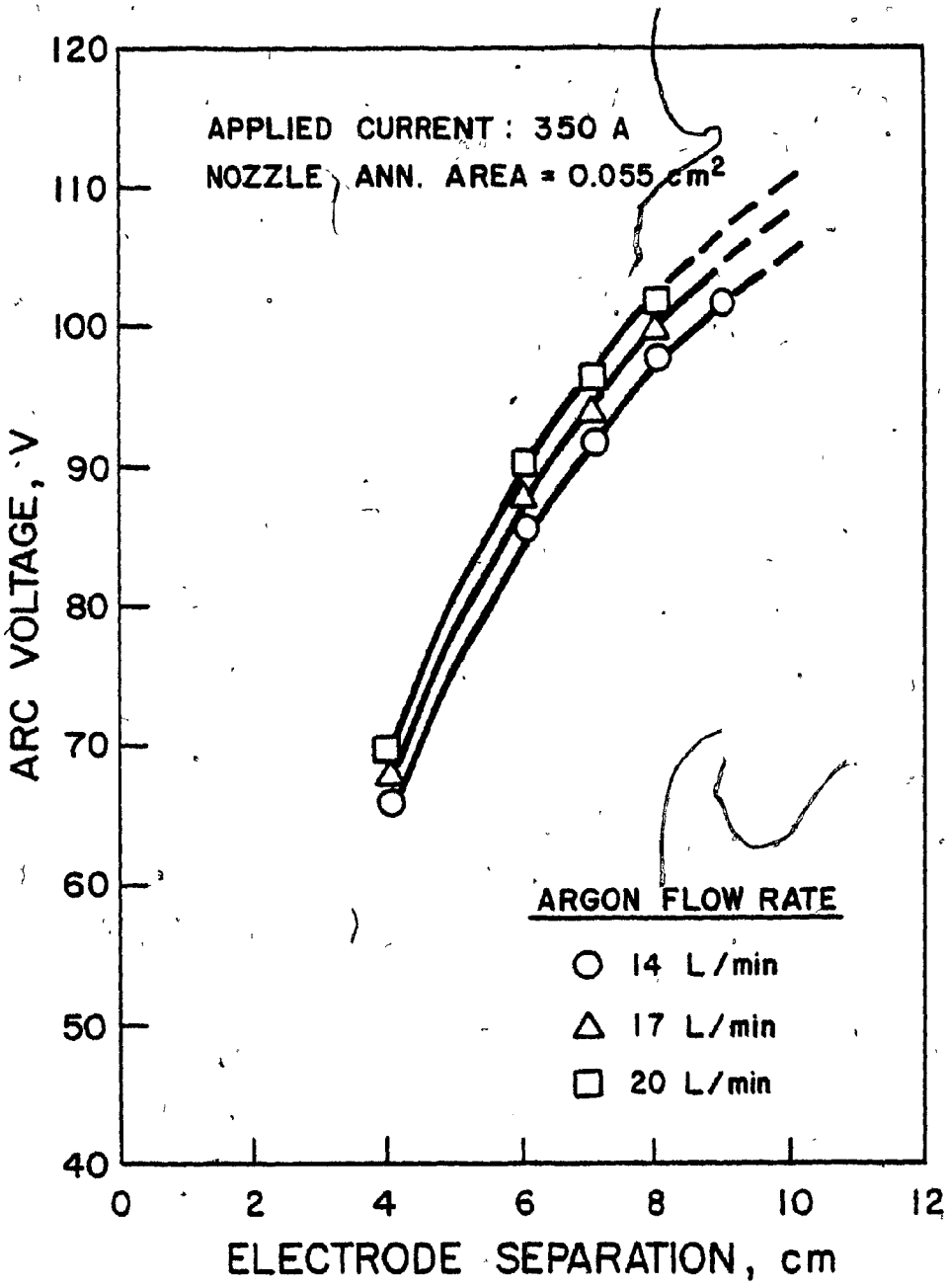
APPLIED CURRENT : 350 A
NOZZLE ANN. AREA = 0.055 cm²
ARC VOLTAGE, V
ELECTRODE SEPARATION, cm
ARGON FLOW RATE
14 L/min
17 L/min
20 L/min
120
110
100
90
80
70
60
50
40
0
2
4
6
8
10
12

FIGURE 21

ARC VOLTAGE VARIATION WITH
INLET GAS VELOCITY

(Electrode Separation: 4 cm)

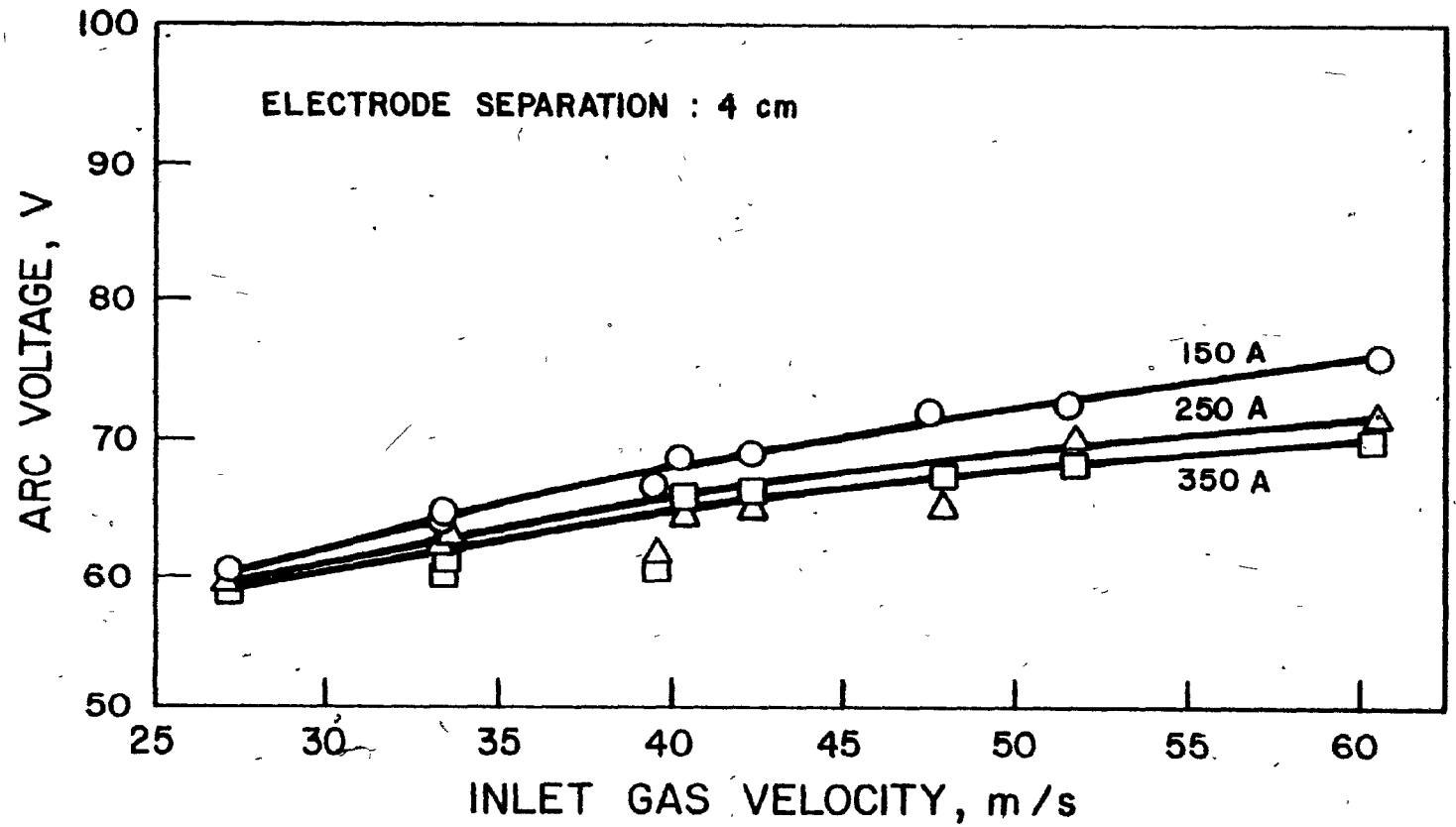
ELECTRODE SEPARATION : 4 cm
ARC VOLTAGE, V
INLET GAS VELOCITY, m/s
150 A
250 A
350 A
100
90
80
70
60
50
25
30
35
40
45
50
55
60

FIGURE 22

ARC VOLTAGE VARIATION WITH
INLET GAS VELOCITY

(Electrode Separation: 6 cm)

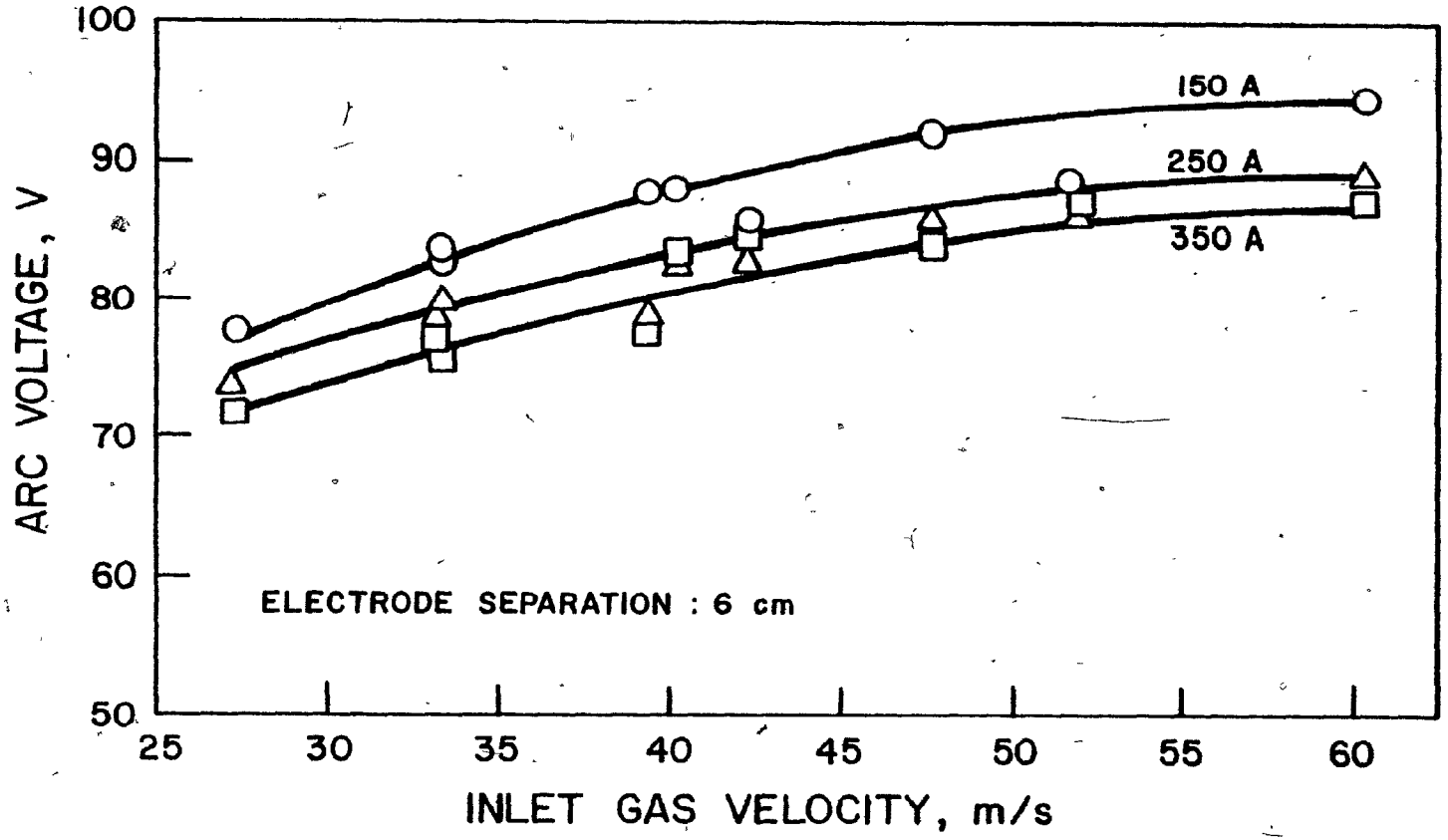
100
90
80
70
60
50
ARC VOLTAGE, V
150 A
250 A
350 A
ELECTRODE SEPARATION : 6 cm
25
30
35
40
45
50
55
60
INLET GAS VELOCITY, m/s

FIGURE 23

ARC VOLTAGE VARIATION WITH

INLET GAS VELOCITY

(Electrode Separation: 8 cm)

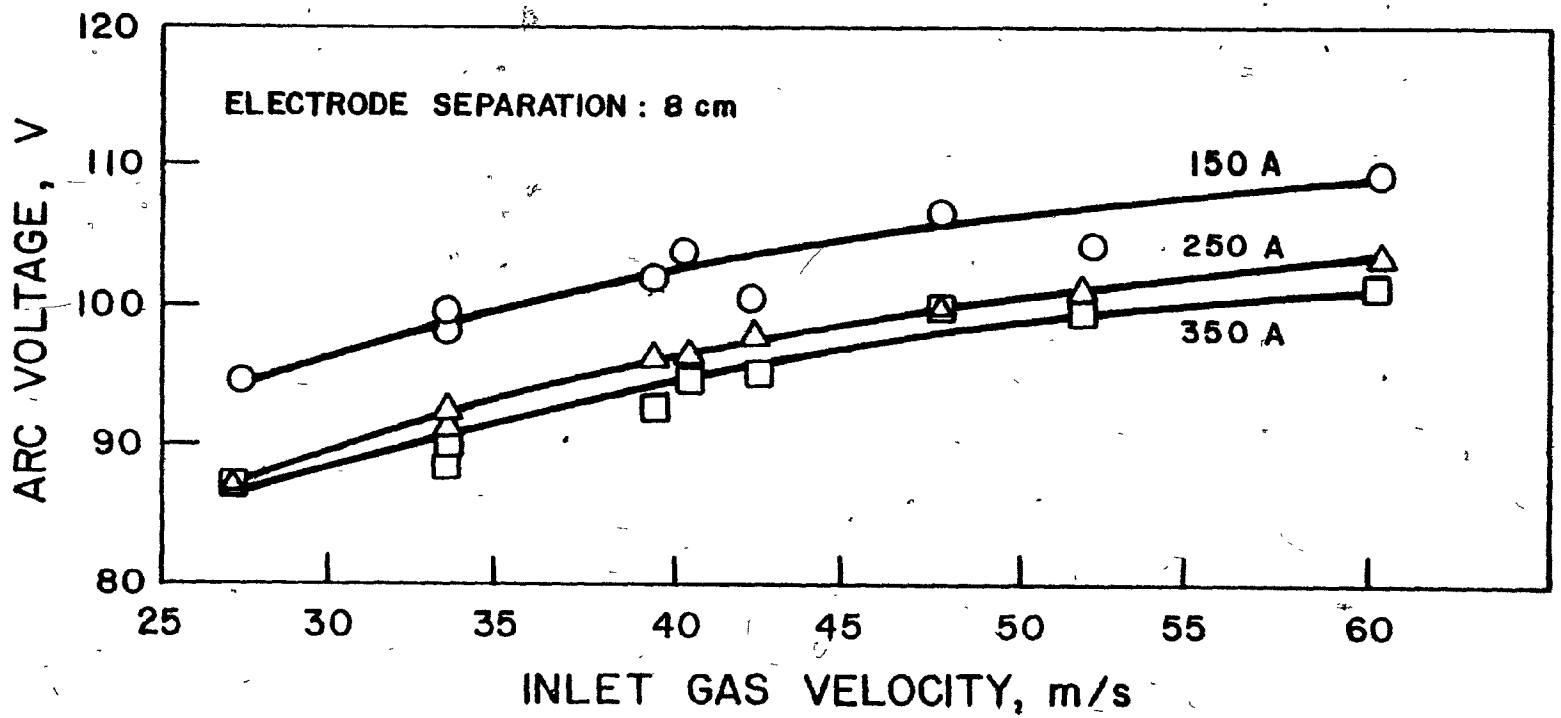
ELECTRODE SEPARATION : 8 cm
150 A
250 A
350 A
ARC VOLTAGE, V
120
110
100
90
80
25
30
35
40
45
50
55
60
INLET GAS VELOCITY, m/s

FIGURE 24

ARC VOLTAGE VARIATION WITH
INLET GAS VELOCITY

(Electrode Separation: 10cm)

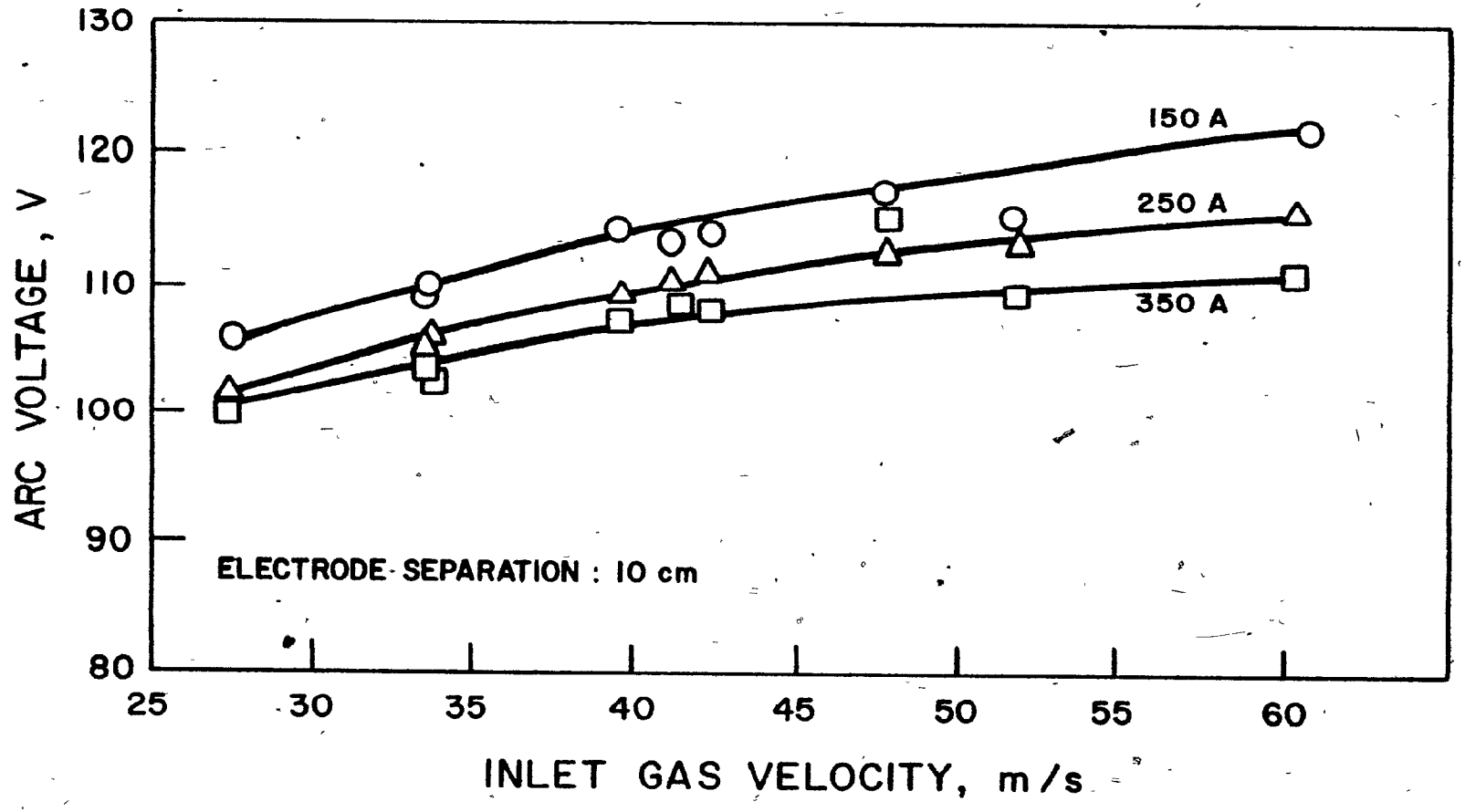
130
120
110
100
90
80
ARC VOLTAGE, V
150 A
250 A
350 A
ELECTRODE SEPARATION : 10 cm
25
30
35
40
45
50
55
60
INLET GAS VELOCITY, m/s

possible to operate at large electrode separations (due to an insufficient power supply) and for these conditions, additional experiments were done at 7 and 9 cm arc lengths to obtain enough data points so that extrapolation to 10 cm could be done. As a consequence, part of Figure 24 was drawn on the basis of the extrapolated data.

From the first set of figures, it can be seen that the sustained voltage increased significantly with increasing electrode separation. This is expected since the gas resistance is directly proportional to the arc length. This increase was more important for higher gas flow rates, probably due to temperature effects. The nozzle annular area did not affect the gradient of this increase; however, everything else being fixed, this gradient was higher for smaller currents, again most likely due to temperature effects.

The sustained arc voltage was relatively independent of the applied current. This statement was more correct for shorter arcs, for smaller gas flow rates, and for smaller nozzle annular areas. This is surprising at first glance; however, if the electrical conductivity versus temperature curve for argon is taken into consideration (shown in Appendix F), it can be seen that the electrical conductivity (and thus the resistance) of an argon plasma does not change too rapidly with temperature in the high temperature range. Thus, probably the plasmas generated for 150 to 350 A had average temperatures in this range.

The effect of the gas flow rate was almost negligible for short arcs, but was significant for long arcs. The nozzle annular area was observed to be an important parameter in the effect of the gas flow rate on the voltage. These effects can possibly be explained by the increase in convective losses from the plasma due to increase in gas velocity and surface area.

These conclusions could not be directly compared with the Literature due to lack of data in the range involved. However, relatively speaking, the trends observed agreed with the few data reported by Stojanoff (1968) for 3-cm arc length at 150 and 200 amperes.

The results obtained indicated that the gas flow rate and the annular nozzle area could be combined as one parameter, "inlet gas velocity," with the unit of m/sec. Figures 21 to 24 show the voltages recorded as a function of the inlet gas velocity, at different electrode separations. Different curves were drawn for each current. It must be noted that the combination of the fore-mentioned parameters at two of the operating conditions yielded the same inlet gas velocity (33.33 m/s) and the voltages recorded at these conditions were almost identical. As can be seen from the comparison of these figures with Figures 18 to 20, this new parameter (v*) was much more important, as far as affecting the sustained voltage was concerned, than the gas flow rate or the nozzle annular area taken alone.

In the light of these observations, it was decided to investigate the effect of the inlet gas velocity more systematically. It is evident that v* is directly related to the momentum of the convected gas at the moment of impingement on the column. Since the nozzle is a convergent one, the inwardly directed component of the gas momentum will exert a constricting effect on the column in the region just below the cathode tip. This constriction is expected to have a considerable influence on the arc behaviour. It must be noted here that the influence on an arc column of the gas flow controlled by an annular nozzle surrounding the cathode was also studied by Busz-Peukert and Finkelnburg (1956), Sheer et al (1969) and Stojanoff (1968). The main difference between their work and that of the present study lies in the use of different nozzle diameters in this case to change the nozzle annular area in addition to just changing the relative position of the tip with respect to the nozzle opening, as done in their systems. A new set of experiments was designed with a larger nozzle. (Diameter = 0.1875 in = 0.476 cm). It was expected that comparison of the results of this set and the previous set would show whether the inlet gas velocity could be considered as the single parameter describing the gas flow conditions (with respect to the sustained voltage) regardless of the nozzle diameter and nozzle annular area. The experimental conditions and the voltages recorded are shown as factorial plot in Figure 25. The nozzle annular area was fixed at 0.17 cm^2. The results of Set I (in which 0.15 in = 0.381 cm

FIGURE 25.

EXPERIMENTAL CONDITIONS AND RESULTS

FOR SET II

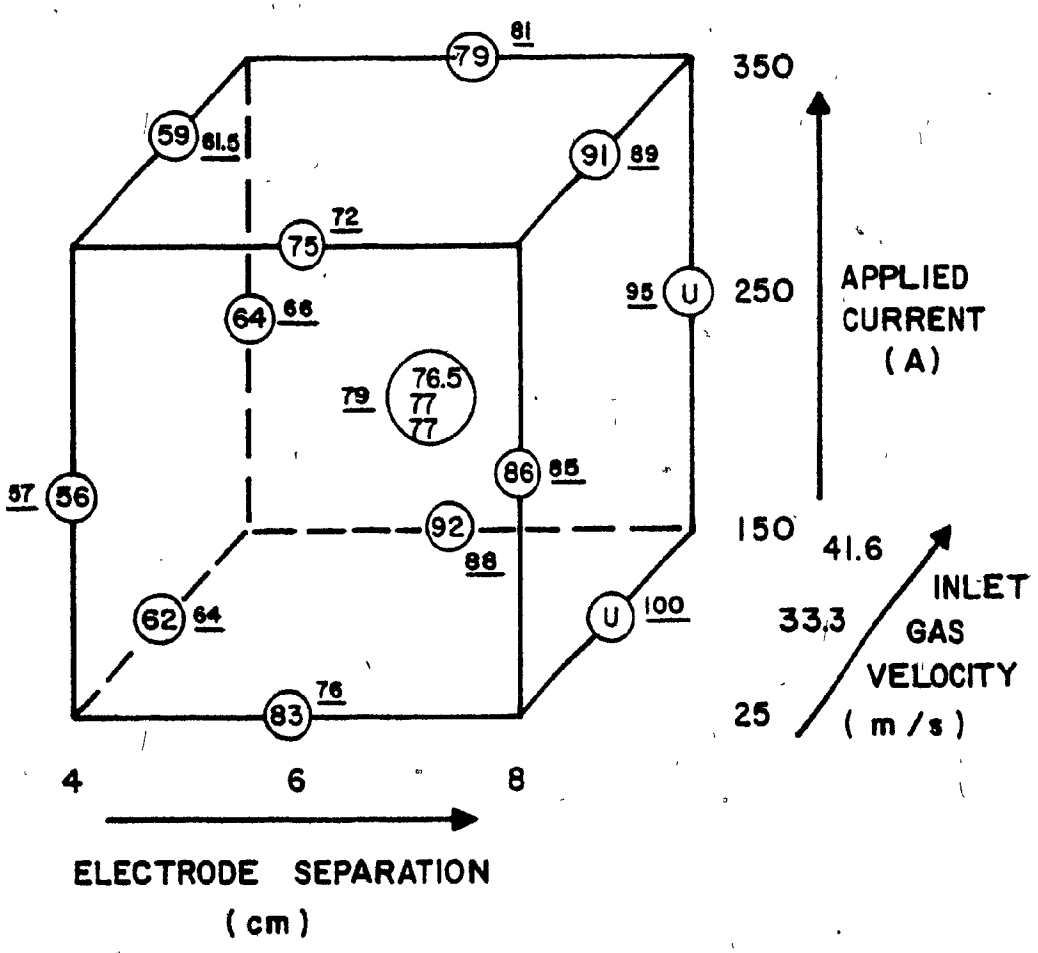

NOTES :

1. (V) VOLTAGE FOR SET II
2. V VOLTAGE FOR SET I
3. (U) UNSTABLE ARC

diameter nozzle was used) are also shown. The data for 25-m/s inlet gas velocity for Set I was obtained by extrapolation.

The reasonable agreement between the results of the two sets confirmed the assumption that the inlet gas velocity can be considered as the only parameter required to describe the influence of the flow conditions on the sustained voltage (and consequently, on the arc power). This conclusion was found important with respect to the selection of the experimental conditions for temperature and velocity measurements. Further evidence related to this conclusion will be given in the subsequent sections. It should be added that this conclusion has very important implications for the design of commercial plasma reactors, since it should permit considerable savings by cutting the volumetric flow rate of expensive plasma gas, as long as its velocity past the cathode is maintained.

To complete the study of the effect of the operating parameters on the arc voltage, it was decided to investigate the voltage variation with argon injection into the plasma column via the three injection channels. The effect of the nozzle angle was incorporated in this study by performing the injection experiments with 60° and 45° nozzle angles, with the same nozzle diameter (0.381 cm). As can be seen from the results presented as a factorial plot on Figure 26, gas injection near the cathode in addition to the plasma forming gas (termed "Sheath Gas" from here onwards to avoid confusion) lowered the sustained arc voltage. This effect was more

FIGURE 26

EXPERIMENTAL CONDITIONS AND

RESULTS FOR SET III (A & B)

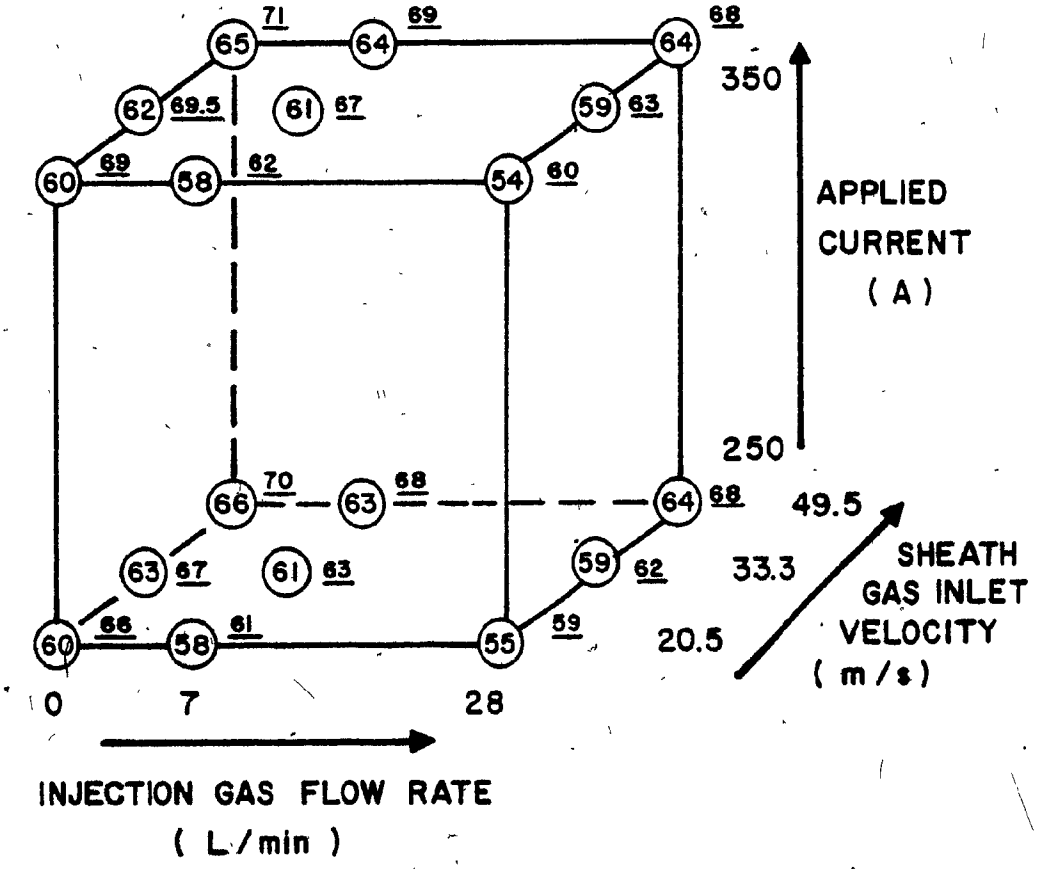

NOTES :

1. (V) VOLTAGE FOR 60° NOZZLE (SET III A)
2. V VOLTAGE FOR 45° NOZZLE (SET III B)

pronounced for lower sheath gas inlet velocities and for higher currents. A few experiments made with 6 and 8 cm arcs (not shown) gave identical results.

This phenomenon can be explained by the "Maecker Effect" (Somerville, 1969). As explained in the "MHD Streaming in Arc Plasmas" section of the Literature Survey, this effect results from the inwardly-directed pressure gradients that exist near the electrodes and it is directly proportional to the square of the applied current. Thus, it was argued that at low sheath gas inlet velocities, the entrainment requirement of the plasma (due to the Maecker Effect near the cathode root) was not completely satisfied with the amount of argon fed and consequently some ambient air was drawn into the plasma column. When injection gas was provided, it was drawn in instead of the ambient air and since the electrical conductivity of argon is higher than that of air above 10,000 K (Ahtye, 1965 and Devoto, 1978) this replacement caused a lowering of the sustained voltage for the same current. Obviously, less air was entrained when the sheath gas inlet velocity was high and the injection of additional gas caused little or no change in the sustained voltage. Similarly, for high currents, the amount of entrained air was higher and thus a greater difference was observed.

It must be noted that the above argument was further supported with the observations of lesser oxidation of the copper

anode surface. (This also meant that the earlier assumption that the slight oxidation at the anode attachment occurred primarily in the short time interval between the termination of the plasma and the cooling of the anode was not completely correct). One important consequence of the observation that the entrainment capacity changed with operating parameters was that one optimum condition existed where the plasma was 100% argon plasma. This optimum condition will exist where increasing the injection gas flow rate will not lower the sustained voltage any more but on the contrary, will increase it. (The same effect of increasing sheath gas inlet velocity). For the purpose of determining the experimental conditions of the temperature and velocity measurements, experiments to this effect were performed and these optimum values of the injection gas flow rates were determined. They will be shown at the beginning of the temperature measurements section. No study of this aspect appears in the literature.

Finally, the effect of the nozzle angle can be observed from Figure 26. For all the conditions studied, higher voltages were recorded for 45° nozzle. This difference could not be explained on the basis of voltage recordings only and the discussion of this subject will be postponed to the subsequent sections. Nevertheless, it will be noted that Sheer et al (1973) compared 30° and 45° nozzles and found that the plasmas generated by 30° nozzle were unacceptably unstable. They did not give any quantitative evidence to support their observations, however. If a

lower power requirement is to be taken as an indication of better stability, then the results of the present study are in accord with Sheer and his co-workers.

The accuracy of the voltage recordings was ±0.5 V, as read from the chart recorder. Considering that the accuracy of the gas rotameters was 2% and that of the current control about 5%, it was estimated that the accuracy of voltage results would be ±2 V.

4 - Voltage Gradient Study

The determination of the voltage gradient is important since it reflects the energy content of the column much more realistically than the total arc voltage (which includes the electrode potential drops). The standard method for obtaining a voltage gradient is to measure the potential distribution along the arc length by means of a sweeping wire. Since the difference between the floating probe potential and the plasma potential, although not directly determinable in dense plasmas, does not vary significantly along the column, the potential differences between relatively closely spaced points along the column axis will accurately reflect the voltage gradient. In this work, however, as a first approximation, the gradient of the linear portion in the graphs of the total arc voltage-versus-electrode separation (Figure 18, for example) was calculated at various currents and sheath gas inlet velocities. The inherent assumption in this calculation was that the electrode spacing did not significantly influence the magnitude of the

electrode falls. The results shown in Figure 27 indicate that the error due to this assumption is not very critical. It was observed that the best fit curves joining the experimental points at different applied currents indicated an assymptotic behaviour for high inlet gas velocities. To confirm this tendency, additional experiments were performed at 65 and 80 m/s inlet gas velocities. The voltage gradients calculated for the latter value of v* for the three currents were close enough to prove this particular point.

To further check the accuracy of this technique, actual measurements of the potential distribution along the column axis were performed at a few conditions (these conditions were the same as those used for the temperature and velocity measurements, as will be discussed later). A typical axial potential distribution is shown in Figure 28 (the full data are given in Appendix E). The gradients of the linear part of these graphs were calculated and are also shown on Figure 27. As can be seen from the latter, there is good agreement between the measured values of the voltage gradient and the curves drawn on the basis of the first approximation.

An examination of these results show that the column gradient increases with increasing inlet gas velocity which may be explained by a greater loss of energy. The indirect proportionality between the voltage gradient and the applied current is obviously due to the increase in the electrical conductivity with increasing current. On the other hand, it was not possible to explain the

FIGURE 27

VARIATION OF VOLTAGE GRADIENT

WITH INLET GAS VELOCITY AND CURRENT

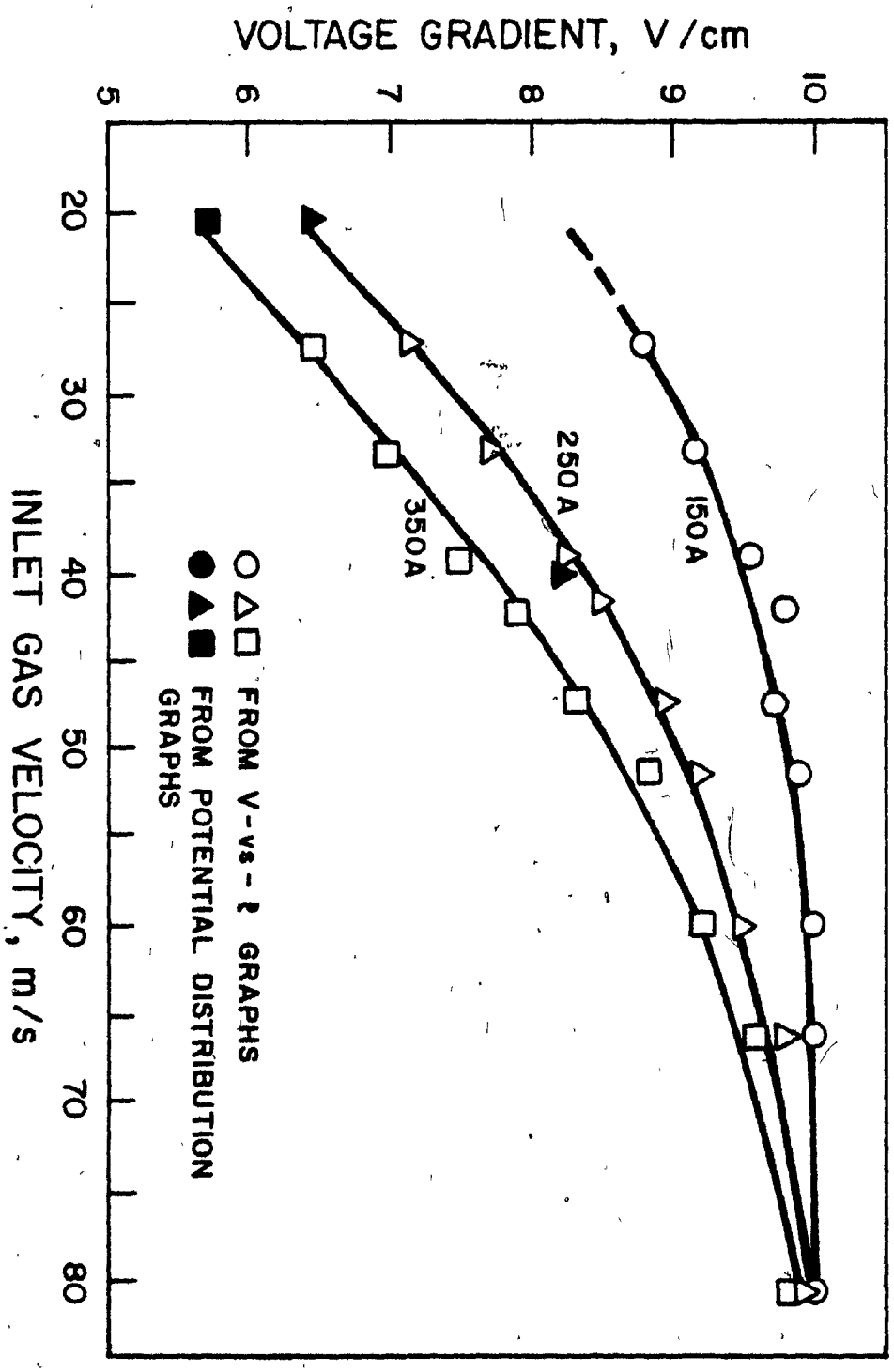
VOLTAGE GRADIENT, V/cm
5
6
7
8
9
10
20
30
40
50
60
70
80
INLET GAS VELOCITY, m/s
150A
250A
350A
○△□ FROM V-vs-ℓ GRAPHS
●▲■ FROM POTENTIAL DISTRIBUTION GRAPHS

FIGURE 28

AXIAL POTENTIAL DISTRIBUTION

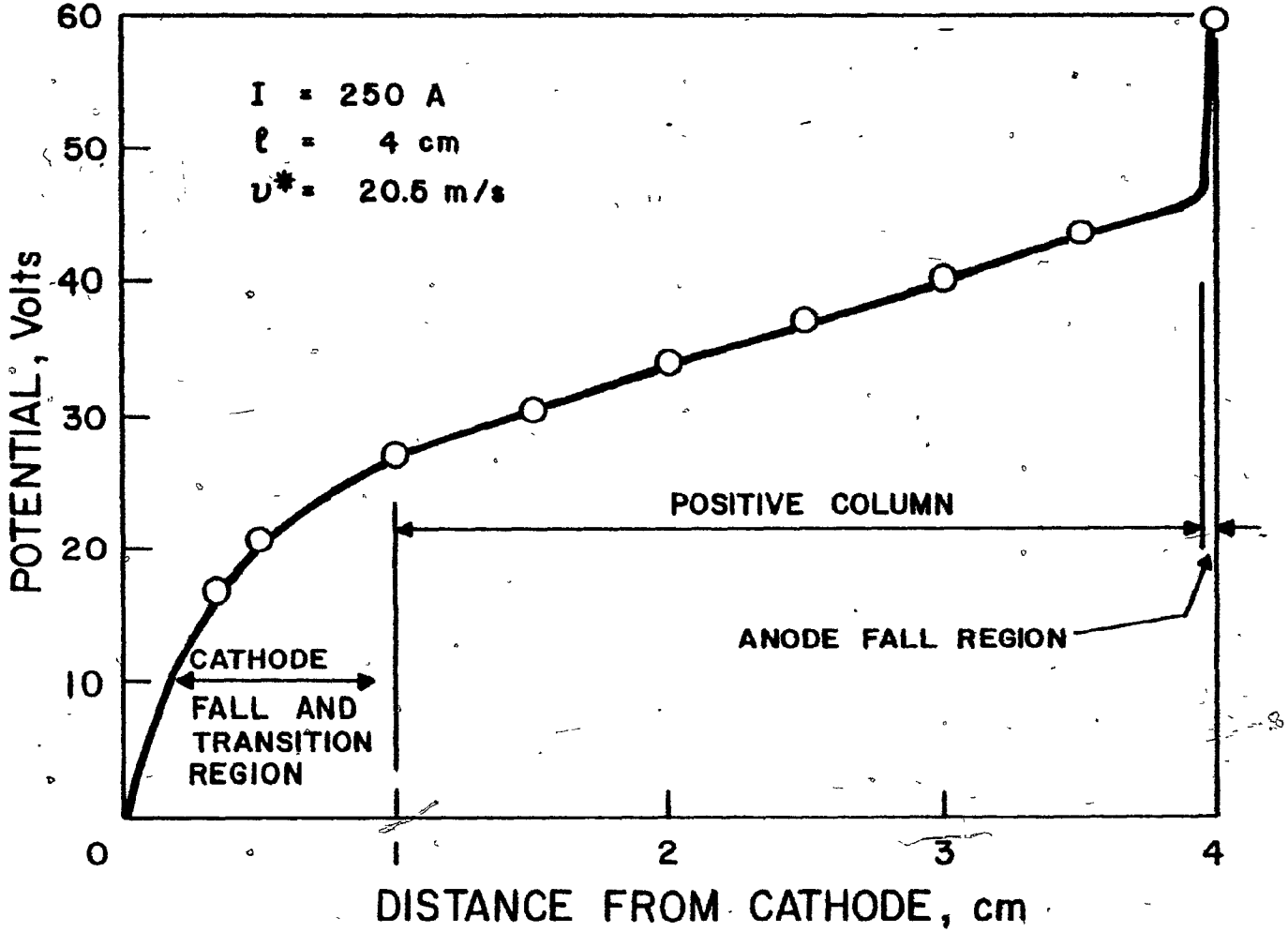
I = 250 A
ℓ = 4 cm
υ* = 20.5 m/s
POTENTIAL, Volts
60
50
40
30
20
10
0
1
2
3
4
DISTANCE FROM CATHODE, cm
POSITIVE COLUMN
ANODE FALL REGION
CATHODE
FALL AND
TRANSITION
REGION

convergence of all data points to 10 V/cm for high $\underline{v^*}$. At this point, it suffices to say that in case of turbulence, the column voltage gradient is determined by the heat dissipation.

The graphs of the potential distribution along the column axis (typical of which is Figure 28) revealed an interesting deviation of the transferred arc plasma from the other types of arc. The potential drop near the cathode was considerably higher and the transition between the cathode and the column was larger (about 10 to 20 V compared with about 5 V for a 5.6-cm arc at 200 A, given by Emmons, 1963). This was thought to be primarily due to the lower temperatures achieved in this region as a result of the convective cooling of the cathode. The magnitude of the anode fall seemed to be in accord with the other types of arc. Although different values for $\underline{V}_c$ and $\underline{V}_a$ for different conditions were obtained, an analysis for their variation with operating parameters was not attempted due to the inaccuracies involved in their determination.

Finally, it must be noted that the measurements of the potential distribution for 45° nozzle and for 6 and 8-cm electrode separations (with 60° nozzle) yielded almost identical voltage gradients with the ones already shown ($< \pm$ 0.3 V/cm deviation). Thus, the high total arc voltages recorded for 45° nozzle (Figure 26) can be attributed to the larger electrode potential drops.

5 - Calorimetric Study

General

The purpose of this phase of the work was twofold: firstly, to investigate the efficiency of the transferred-arc plasma in terms of the usable energy, and secondly, to check the assumption that the cathode assembly design used in this work resulted in an inhibition of cathode ablation, primarily due to the convective heat transfer to the high speed film of gas moving past the conical tip just prior to the entry to the plasma.

A large number of different heat transfer processes occur in a transferred arc system. A detailed analysis of these processes was the subject of another study carried in this laboratory (Choi, 1980). In the present work, however, only the net amount of the heat released at the anode, at the cathode tip and at the nozzle were measured. Assuming that the convective losses from the plasma column to the ambient as well as the sensible energy loss to the exit gas were small, the heat radiated could be determined by difference, from the total arc power.

Although calorimetric data were taken for all conditions of Set I, an error analysis indicated insufficient accuracies. On the other hand, the safety interlock of the control console imposed limitations on the cooling water flow rates and pressures. The solution was found by by-passing these safety interlocks for a new

set of experiments. The raw data and error analysis are presented in Appendix G, and derived results are shown in Table II.

Heat Transfer to Anode

It was observed that the anode heat fluxes increased with increasing current, increasing inlet gas velocity and also increasing electrode separation. The extensive anode heat transfer studies performed by Pfender and co-workers [Eckert and Pfender (1963), Smith and Pfender (1976), Pfender (1978), Liu and Pfender (1979), Johnson and Pfender (1979)], clearly indicate the positive effect of the current on the heat flux at the anode surface. The influence of the gas velocity (as the convective contribution to anode heat transfer) was also demonstrated by Eckert and Pfender (1967) and Wilkinson and Milner (1960). The effect of the electrode spacing on the anode heat flux is also very interesting. Although there was an increase in the absolute value of the heat transferred to the anode with increasing length, when the percentage of the arc energy transferred was considered, a steady decrease (from 44% at 4 cm to 38% at 8 cm) was observed. It is evident that the increase in the radiation loss was responsible for this decrease in the fraction of arc energy transferred to the anode.

Arc Radiation

As expected, arc radiation increased with the applied current. This is in complete agreement with several previous

TABLE II

CALORIMETRIC RESULTS

ℓ = 4 cm — I = 250 A

	Cathode Tip		Nozzle		Anode		Arc Power	Radiation	
v*	P_c	%	P_n	%	P_a	%	P	$P-(P_c+P_n+P_a)$	%
m/s	kW		kW		kW		kW	kW	
16.65	0.45	3.5	1.16	9.1	5.67	44.5	12.75	5.47	42.9
33.30	0.43	3.2	1.19	9.1	5.88	44.8	13.13	5.63	42.9
49.95	0.41	3.0	1.28	9.4	6.37	46.8	13.62	5.56	40.8
	ℓ = 4 cm							I = 350 A	
16.65	0.67	3.6	1.62	8.7	8.03	43.3	18.55	8.23	44.4
33.30	0.65	3.4	1.75	9.3	8.20	43.8	18.73	8.13	43.1
49.95	0.55	2.8	1.79	9.2	8.20	42.6	19.25	8.71	45.4
	v* = 33.30 m/s							I = 350 A	
ℓ	P_c	%	P_n	%	P_a	%	P	$P-(P_c+P_n+P_a)$	%
cm	kW		kW		kW		kW	kW	
6	0.66	2.6	1.90	7.8	10.22	41.7	24.50	11.72	47.9
8	0.66	2.3	1.95	6.7	10.98	37.8	29.05	15.46	53.2

workers. For example, Schoeck (1963) reported around 59% increase in the arc radiation (for a 10-mm arc) for 50% increase in current, while around 50% increase was observed in this work (for 4 cm) for a 40% increase in current. The inlet gas velocity, on the other hand, was observed to be less effective on the amount of heat lost by radiation. It should be emphasized that the radiation terms shown in Table II also contain convective contributions. Theoretically, increasing the gas inlet velocity should have two contradictory effects: lower temperatures and thus less radiation, and higher convective losses due to increased velocity. This complication prevents general conclusions from being drawn regarding the radiation balance of transferred-arcs. The increase in length caused higher arc radiation since the radiating volume increased.

Heat Transfer to Cathode Tip and Nozzle

As in the case of the anode, heat transfer to the cathode tip increased with current. This is obviously due to the increased current density which is the major contributor to the heat transfer to the cathode tip, (Guile, 1971). The increase in the heat transferred to the nozzle with increasing current was lower than in the case of the cathode tip. In this case, the heat transfer was basically due to radiation and hence the percentage change in the heat transfer followed that of radiation with current. This also explains why the heat transfer to the nozzle increased with increasing electrode separation while that to the cathode tip remained

almost constant. It is evident that the change in the electrode fall potential with the electrode separation was not sufficiently significant to show marked changes in the heat transfer to the cathode tip.

There was a small but persistent decrease in the cathode tip heat flux with increasing inlet gas velocity. This change, however, was not close to the experimental error predicted, especially for low current cases. It was thus decided to examine this behaviour with a more accurate and direct measurement, namely by measuring the cathode tip temperature with an optical pyrometer. A high-resolution pyrometer (Pyro Micro-Optical Pyrometer, The Pyrometer Instrument Co. Inc., Northvale, N.J.) was used. The interchangeable lenses permitted measurements to be made with object sizes as small as 0.01 cm in diameter.

The optical pyrometer reading may be influenced not only by the emissivity and reflectivity of the tungsten cathode tip, but also by the emissivity and transmissivity of the surrounding plasma. It was not possible to make a blackbody hole on the tungsten tip to check the emissivity and consequently a single value of 0.43 was used for the emissivity of tungsten. An effective wavelength of 6500 Å was used for brightness temperature correction. Since only the relative variations of the cathode tip temperature with the inlet gas velocity were of interest, no correction was made for the emissivity and the transmissivity of the surrounding plasma. It was expected

that due to the relatively low temperatures existing in the fall region, the effect of the surrounding plasma on the radiation of the tungsten tip would be reasonably constant in the temperature range of interest. Figure 29 shows the cathode tip temperatures versus the applied current for two different inlet gas velocities. The cooling effect of the gas flow is clearly demonstrated in this plot. It is interesting to note that this cooling effect stays constant with varying current. It is evident that, depending on the sheath gas velocity, there is an upper limit of the applied current for ablation-free operation. Although the absolute values of this limit as determined from Figure 29 are subject to reservation, it remains true that the current-handling capability of the cathode can be increased by increasing the gas flow rate alone.

6 - Photographic Study

This study was carried out to determine the effect of the operating conditions on the luminous plasma profile and to check the stability and the horizontal alignment of the plasma column. The former information was used in conjunction with the temperature and velocity data. To fulfil the second objective, the photographs of the plasma column taken at different times during an experimental run were compared. The runs that showed any variation were discarded.

Some of the photographs taken at different operating conditions are shown in Figure 30. An example of the luminous plasma

FIGURE 29

CATHODE TIP TEMPERATURES

VERSUS APPLIED CURRENT

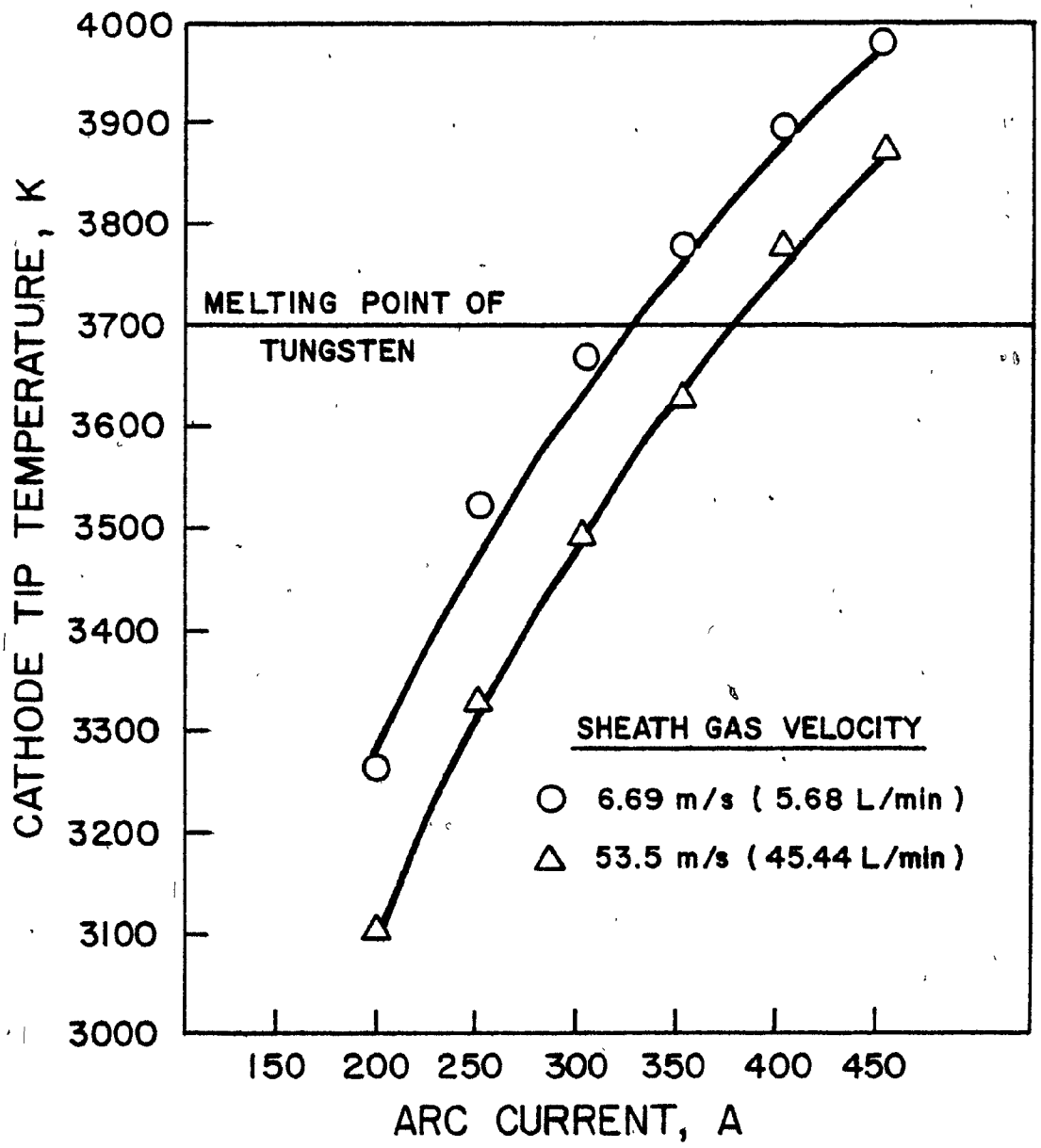
4000
3900
3800
3700
3600
3500
3400
3300
3200
3100
3000
CATHODE TIP TEMPERATURE, K
MELTING POINT OF
TUNGSTEN
SHEATH GAS VELOCITY
6.69 m/s (5.68 L/min)
53.5 m/s (45.44 L/min)
150
200
250
300
350
400
450
ARC CURRENT, A

FIGURE 30

PHOTOGRAPHS OF THE TRANSFERRED-ARC PLASMA

Legend

No. 1 : 4 cm, 250 A, 33.3 m/s

No. 2 : 4 cm, 350 A, 33.3 m/s

No. 3 : 6 cm, 350 A, 33.3 m/s

No. 4 : 8 cm, 350 A, 33.3 m/s

No. 5 : 4 cm, 350 A, 33.3 m/s, Gas Injection (28 L/min)

No. 6 : 4 cm, 350 A, 33.3 m/s, 45° Nozzle

No. 7 : 4 cm, 350 A, 20.5 m/s

No. 8 : 4 cm, 350 A, 49.5 m/s

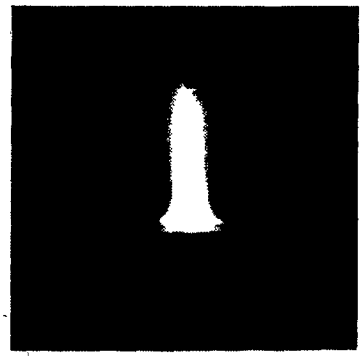

1

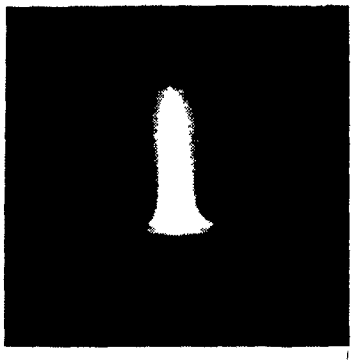

2

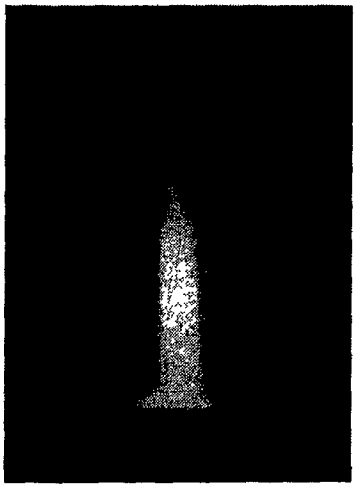

3

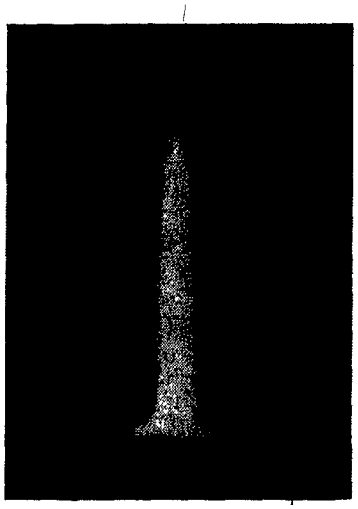

4

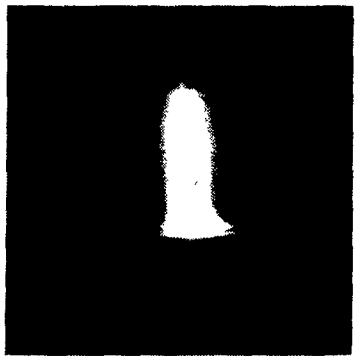

5

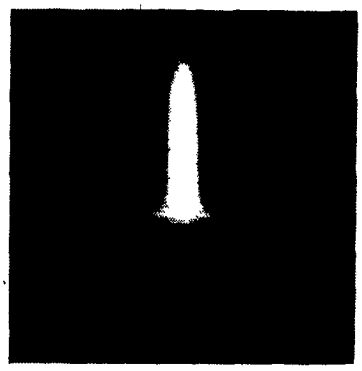

6

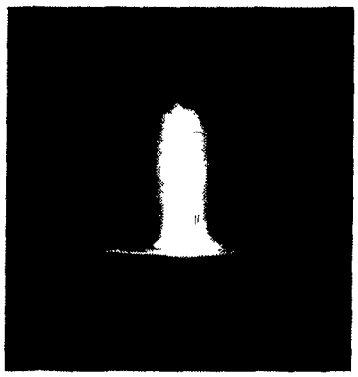

7

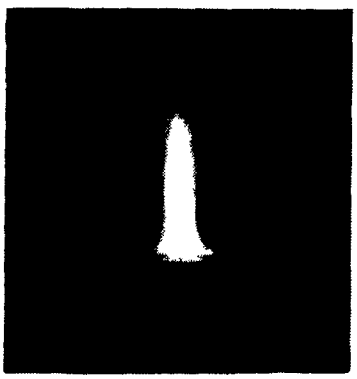

8

profiles drawn on the basis of such photographs is given in Figure 31.

The increase in the applied current had a positive effect on the plasma column diameter. This can be explained in terms of the increase in the current density and consequently in the Joule heating. Thus, it appears that for low currents, a certain fraction of the inlet gas does not receive enough energy and flows as a relatively cool envelope, outside of the visible arc column. As the current is increased, this surrounding gas becomes increasingly ionized due to the additional Joule heating, and contributes to the arc luminosity. Schoeck (1963) and Stojanoff (1968) are among the several workers who observed similar behaviours.

The above observation also helps to explain the fact that when the arc length was increased, the column diameter did not change. Hence, a fixed current implies a fixed diameter and as the length of the column is increased, the column surface area increases proportionally.

The most important information with respect to the column properties was obtained from the variation of the column diameter with the inlet gas velocity. The column luminous profile showed almost negligible variation with increasing inlet gas velocity from 16.5 m/s (photograph not shown) to 33.3 m/s. A decrease in the diameter was observed for 49.5 m/s. Such a behaviour was also

FIGURE 31

LUMINOUS PROFILE OF THE PLASMA COLUMN

(ℓ = 8 cm, 350 A, 33.3 m/s)

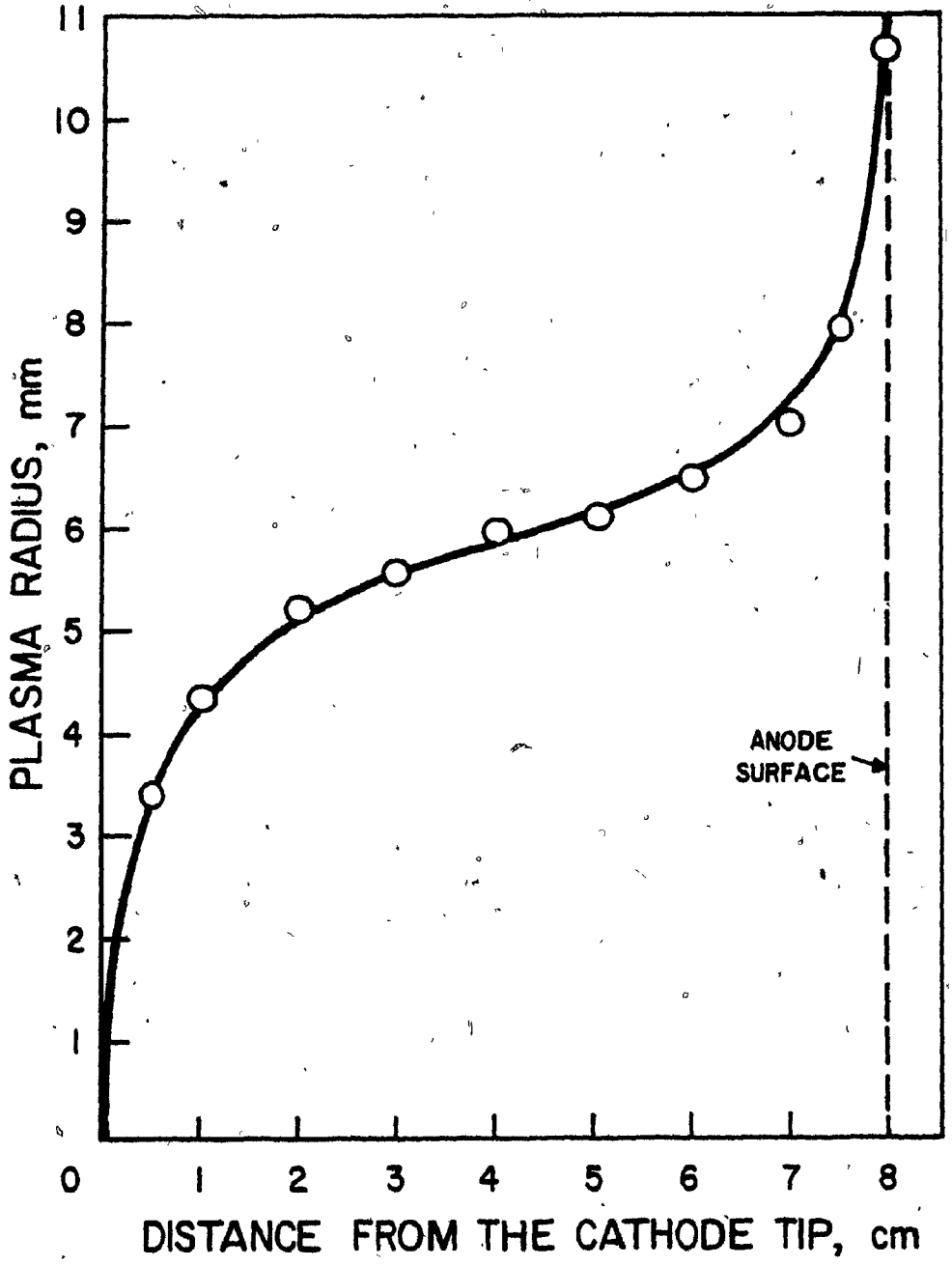
PLASMA RADIUS, mm
DISTANCE FROM THE CATHODE TIP, cm
ANODE SURFACE
0
1
2
3
4
5
6
7
8
9
10
11

reported by Sheer et al (1973) for a similar cathode design. Their explanation, which applies for this work also, was based on the favourable influence of the gas momentum on the column properties. The centrally-directed radial component of momentum exerts a fluid mechanical constriction on the column for a considerable axial distance from the cathode tip outward which, in turn, causes an increase in column temperature and voltage gradient (as shown in Figure 27). The latter raises the volume rate of Joule dissipation to a degree that more than compensates for the increased flow rate. This effect increases with flow until a counter effect sets in (probably caused by increasing convective losses as a result of increasing turbulence), such that a further increase in the inlet gas velocity cools the plasma and causes a decrease in the diameter. In this work, this transition was observed to be at 33.3 m/s for 350 A and ℓ = 4 cm, while the limit reported by Sheer et al (1973) corresponds to about 30.8 m/s for 200 A, and a 3-cm arc.

The gas injection via the three injection channels increased the column diameter, for all conditions studied. While this can be partly explained by the above argument, the fact that the arc voltage decreased and the voltage gradient remained constant with the injection requires additional explanations. Pfender (1979) observed that when a co-axial shroud flow was used around a d.c. plasma jet, a longer and wider jet was obtained. His explanation that the jet temperature increased due to the decrease in the relative velocity at the column boundary and consequently in the

net heat transfer could apply to the present work also.

Finally, the luminous profiles obtained for 45° nozzle showed no difference except for the region near the cathode tip, where a slightly narrower plasma was observed.

The accuracy of the above measurements was estimated to be around ±0.15 mm, with reproducibility, as checked by repeated runs of the same order of magnitude.

7 - Plasma Temperature Analysis

Preliminary Tests

Before the temperature profiles obtained with the new electro-optical technique are presented, it is appropriate for better understanding to explain the various tests performed to check the validity of this technique for measuring plasma temperatures.

Several questions arise due to the immersion of a blocking element in the plasma, and due to the assumptions used in the underlying principles. These questions can be categorized as follows:

1. Effect of the size and of the material of the blocking element?
2. Effect of the direction of the traverse?
3. Accuracy of the measurements with respect to the usual side-on spectroscopic technique?

4. Validity of the assumption of having a plasma that is optically thin at the wavelengths used?

The first question was investigated by using different sizes and different materials for the blocking element. The extent of the perturbations caused was determined by comparing the intensity profiles obtained and by observing the fluctuations in the sustained voltage during the traverse of the element, on the oscilloscope. In addition, the temperature that the blocking element reached in the plasma was also measured by connecting a tungsten/rhenium thermocouple to the element and recording the temperature decay curve after the plasma was turned off, so that the actual temperature could be obtained by extrapolation back to the time of the traverse.

For the blocking elements with the dimension (in the direction of the plasma) of 2 mm or less, no fluctuation in the sustained voltage was observed. The intensity profiles obtained for copper, tin and steel elements of 1 and 2-mm sizes, showed less than 1% variation. The maximum temperature the metal strip reached during its traverse through the plasma was determined to be around 90°C, including the heat effects before and after the traverse. Since the amount of plasma perturbation by the metal strip depends, in one sense, on the relative amount of energy absorbed by the strip, it can be safely assumed that the plasma will experience negligible perturbation due to heat effects.

The second question involves consideration of the fluid mechanics of the system. It was thought that the nature of the perturbations with respect to the stream lines would be different when the direction of the traverse of the blocking element was reversed. Various tests with varying current and inlet gas velocity were performed to check this effect. A sample of the results obtained is shown in Figure 32. The excellent match observed in this figure was considered as an indication that the recovery of the plasma from fluid mechanical perturbations was some order of magnitude faster than the speed of the traverse of the blocking element.

The accuracy of the temperature determination by this technique was checked by comparing the profiles with those obtained by the usual side-on spectroscopic technique. In order to obtain the lateral spectral intensity distribution of the plasma, the aperture system was mounted on a precision traversing mechanism which had an accuracy of ±0.05 mm. After the plasma was started, the aperture was manually moved along the side of the plasma, stopping for a short time period at the predetermined rest positions. The optical system was simultaneously moved in the same direction. Around 30 stops were used for a typical run. The values recorded on the oscilloscope were plotted and were smoothed by a curve. Then the Abel Inversion procedure was applied to this lateral distribution of the emission coefficients. A computer program using 20 intervals was utilized to obtain the radial distribution of

FIGURE 32

COMPARISON OF TEMPERATURE PROFILES OBTAINED BY

FORWARD AND BACKWARD MOTION AND BY THE "ABEL" INVERSION

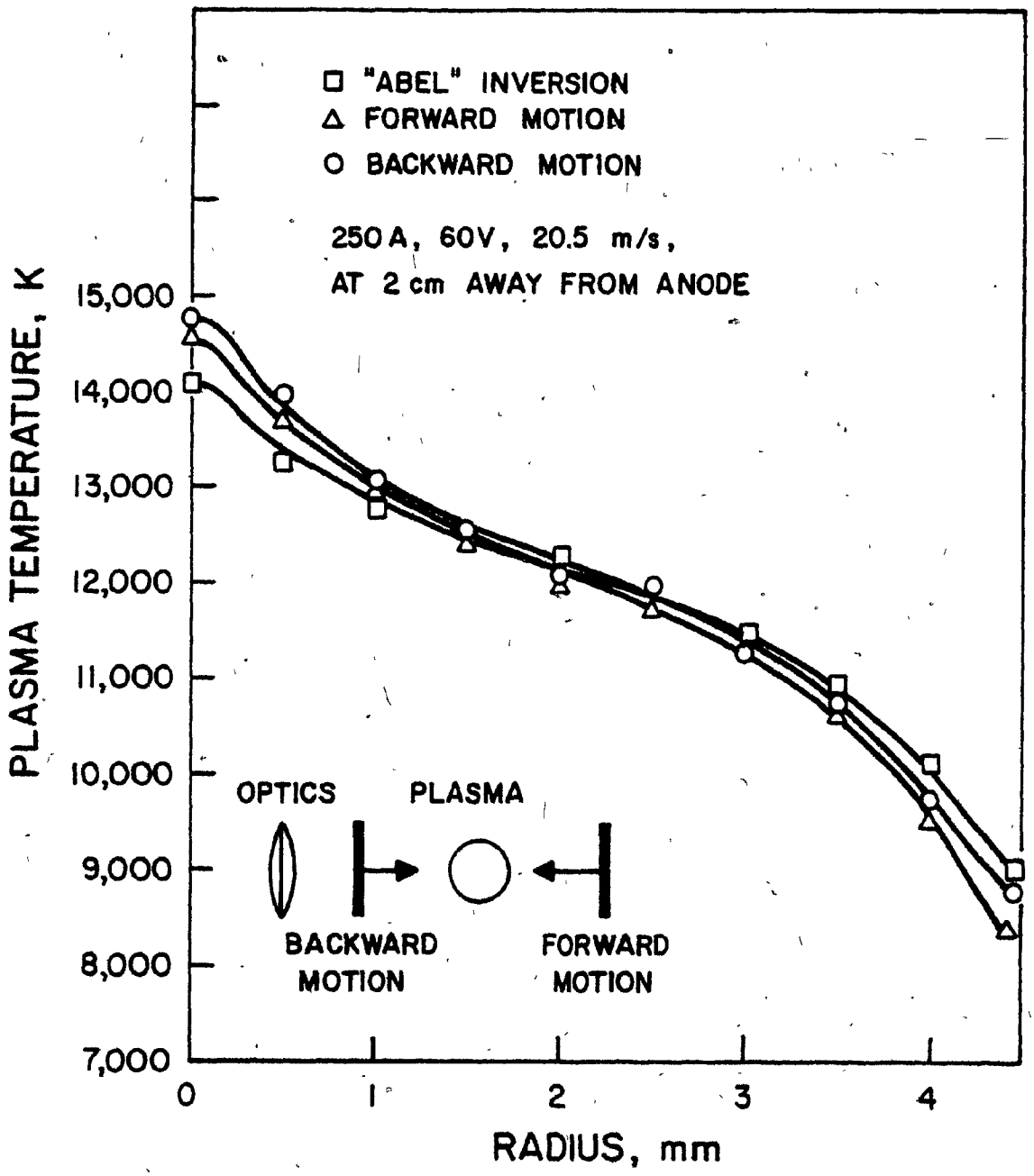
□ "ABEL" INVERSION
△ FORWARD MOTION
○ BACKWARD MOTION
250 A, 60V, 20.5 m/s,
AT 2 cm AWAY FROM ANODE
PLASMA TEMPERATURE, K
15,000
14,000
13,000
12,000
11,000
10,000
9,000
8,000
7,000
0
1
2
3
4
RADIUS, mm
OPTICS
PLASMA
BACKWARD MOTION
FORWARD MOTION

emission coefficients for 4806 Å and 6965 Å lines. The coefficients given by Barr (1962) (discussed in Appendix A) were used in the program. The temperatures obtained from the emission coefficients via Equation (1) or (2) (depending on the range) were compared with the values obtained by the "sweeping blocking element" technique.

This comparison was performed for different operating conditions to see the influence of increased current and increased inlet gas velocity. A typical representation of the results obtained is shown in Figure 32 from which it was concluded that the determination of arc temperature by the new technique is within the usual experimental accuracy required. The relative larger differences near the centreline implies that the plasma velocity has an effect on the accuracy of measurements. However, even for the highest sheath gas inlet velocity used in these tests (41 m/s), the two temperatures differed by only 6%.

To check the validity of the assumption of having a plasma that is optically thin for the wavelengths at which emission coefficients were measured, the standard method employed in the literature, namely using a reflecting concave mirror, was modified to suit the present electro-optical technique. Instead of a blackened metal blocking strip, a stainless steel piece with a perfect finish was swept through the plasma and the recorded values of the intensity were compared with that obtained with the blackened-strip. For the 4806 Å Ar II line, a ratio of 1.98 was obtained,

indicating negligible self-absorption. The ratio for 6965 Å Ar I line was 1.94 implying some minor self-absorption. Olsen (1962) also found a slight self-absorption for 6965 Å line, however, he claimed that this line can be used with an error of less than six per cent. Considering the reflection losses at the mirror, his argument was accepted for the measurements of temperature at 6965 Å line.

Experimental Design and Results

On the basis of the first phase of the experimental work (which involved electrical, calorimetric and photographic measurements), a new set of experimental conditions were selected for the temperature and impact pressure measurements as shown in Table III.

To observe the effect of the inlet gas velocity, the plasma was operated with a 4-cm electrode separation and at an applied current of 250 A. The inlet gas velocity was doubled from 20.5 m/s to 41 m/s under these conditions. In addition, the effect of the injection gas was investigated by operating the plasma under the above operating conditions, but with no injection gas and with the optimum flow rate of the injection gas. The effect of the current was studied by operating at 350 A for 20.5 m/s, again without and with injection gas. The last condition was repeated for 6 and 8-cm electrode separation, without any injection gas. Finally, the 45° nozzle was installed and the plasma was operated at 350 A and 20.5 m/s with a 4-cm electrode separation. Study of the effect of the

TABLE III

EXPERIMENTAL CONDITIONS FOR TEMPERATURE AND VELOCITY MEASUREMENTS

Run	ℓ	Position from Anode	I	v*	q
	cm	cm	A	m/s	L/m
60° Nozzle					
A-1	4	1	250	20.5	0
A-2		2			
A-3		3			
A-4		3.5			
A-5		1			25.0
A-6		2			
A-7		3			
A-8		3.5			
A-9	4	1	250	41.0	0
A-10		2			
A-11		3			
A-12		3.5			
A-13		1			20.0
A-14		2			
A-15		3			
A-16		3.5			
A-17	4	1	350	20.5	0
A-18		2			
A-19		3			
A-20		3.5			
A-21		1			31.0
A-22		2			
A-23		3			
A-24		3.5			
60° Nozzle					
A-25	6	1	350	20.5	0
A-26		2			
A-27		3			
A-28		4			
A-29		5			
A-30		5.5			
A-31	8	1	350	20.5	0
A-32		2			
A-33		3			
A-34		4			
A-35		5			
A-36		6			
A-37		7			
A-38		7.5			
45° Nozzle					
B-1	4	1	350	20.5	0
B-2		2			
B-3		3			
B-4		3.5			
B-5		1			31.0
B-6		2			
B-7		3			
B-8		3.5			

injection gas was also incorporated in this last phase.

The plasma temperature and velocity profiles were obtained at different vertical locations with 1 cm separation, except for the uppermost position which was 0.5 cm away from the cathode tip. No measurements were attempted for locations closer than 1 cm from the anode since it is well established that LTE does not hold close to the electrodes (Eddy et al, 1973). This experimental design resulted in 46 temperature and velocity profiles.

Before the results of the temperature measurements are presented, it must be mentioned that the results were obtained as full profiles, i.e., from one edge of the plasma column to the other. When these profiles were analyzed for symmetry it was observed that except for the edges of the plasma where the accuracy was low, the deviations between the two halves were negligible. The average values were used for the edges. The speed of the linear motor was kept around 100 cm/sec and showed a little variation from one run to the other due to lubrication conditions.

The results obtained will be presented as isothermal contours since they illustrate the thermal condition of the plasma more clearly. Figures 33 to 38 show the isothermal contours of the column for the experimental conditions shown in Table III. The axial centreline temperature distributions for these conditions are plotted in Figure 39. Finally, to demonstrate the effect of the operating parameters on temperature distribution, sample profiles

FIGURE 33

ISOTHERMAL CONTOURS OF THE

PLASMA FOR ℓ = 4 cm, I = 250 A

v^* = 20.5 m/s and q = 0 L/m and q = 25.0 L/m

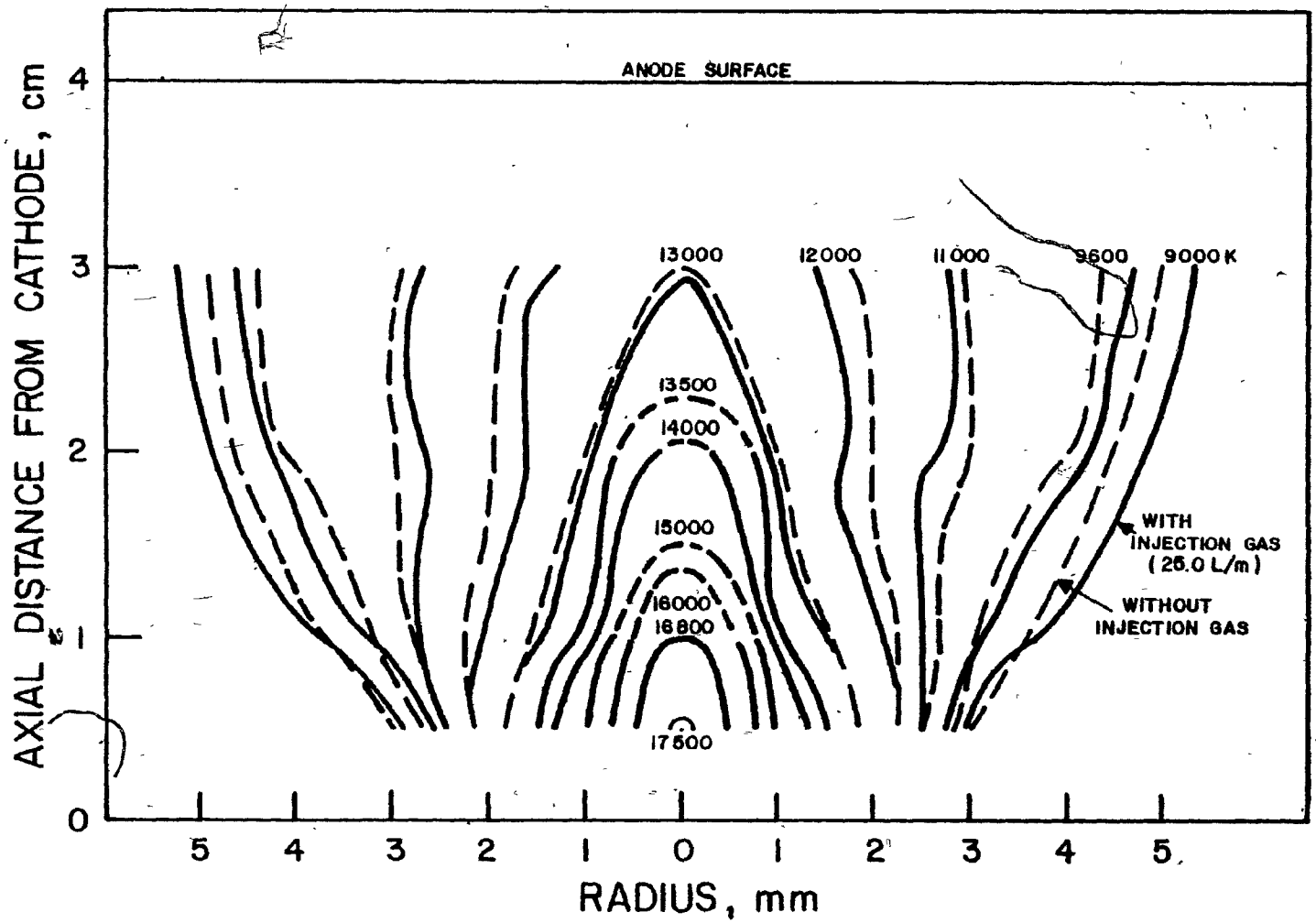
ANODE SURFACE
13000
12000
11000
9600
9000 K
13500
14000
15000
16000
16800
17500
WITH INJECTION GAS (25.0 L/m)
WITHOUT INJECTION GAS
AXIAL DISTANCE FROM CATHODE, cm
0
1
2
3
4
5 4 3 2 1 0 1 2 3 4 5
RADIUS, mm

FIGURE 34

ISOTHERMAL CONTOURS OF THE PLASMA FOR ℓ = 4cm, I = 250 A

v^* = 41 m/s and q = 0 L/m and q = 20.0 L/m

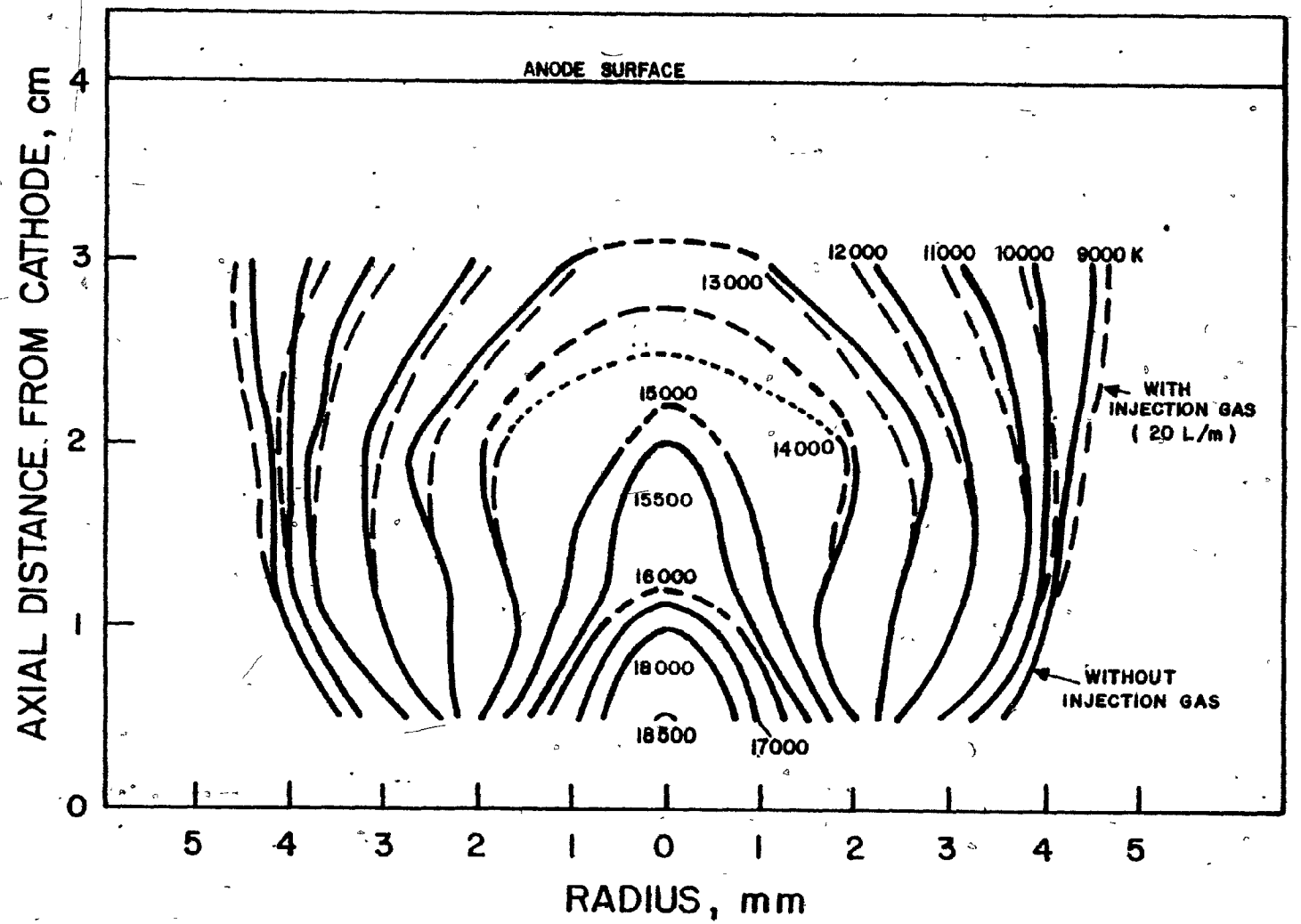
ANODE SURFACE
AXIAL DISTANCE FROM CATHODE, cm
0
1
2
3
4
RADIUS, mm
5 4 3 2 1 0 1 2 3 4 5
13000
12000
11000
10000
9000 K
15000
14000
15500
16000
18000
18500
17000
WITH INJECTION GAS (20 L/m)
WITHOUT INJECTION GAS

FIGURE 35

ISOTHERMAL CONTOURS OF THE
PLASMA FOR ℓ = 4 cm, I = 350 A
v^* = 20.5 m/s and q = 0 L/m and q = 31.0 L/m

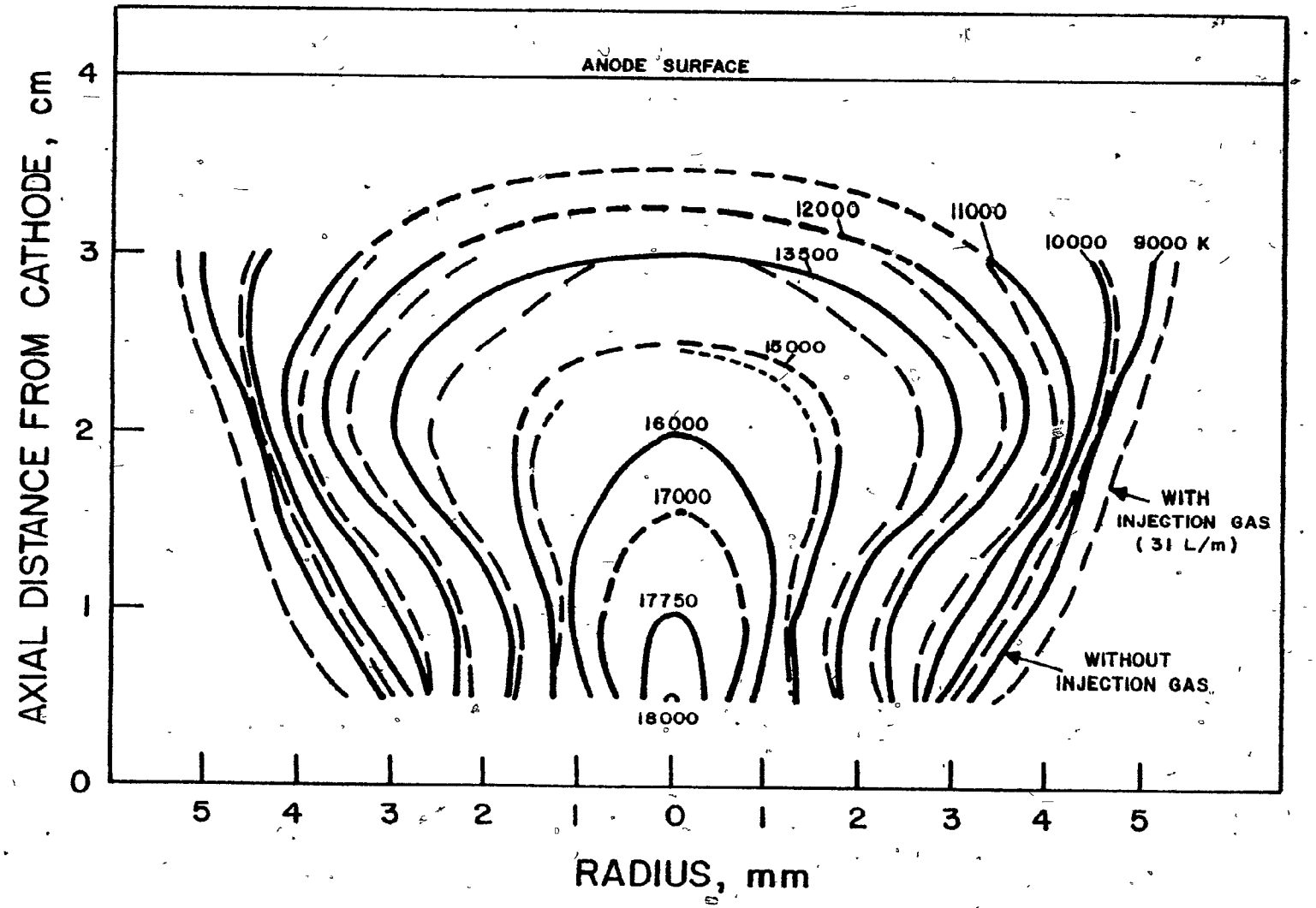
ANODE SURFACE
12000
11000
10000
9000 K
13500
15000
16000
17000
17750
18000
WITH
INJECTION GAS
(31 L/m)
WITHOUT
INJECTION GAS
AXIAL DISTANCE FROM CATHODE, cm
RADIUS, mm
0
1
2
3
4
5
4
3
2
1
0
1
2
3
4
5

FIGURE 36

ISOTHERMAL CONTOURS OF THE PLASMA FOR ℓ = 6 cm, I = 350 A v^* = 20.5 m/s and q = 0 L/m

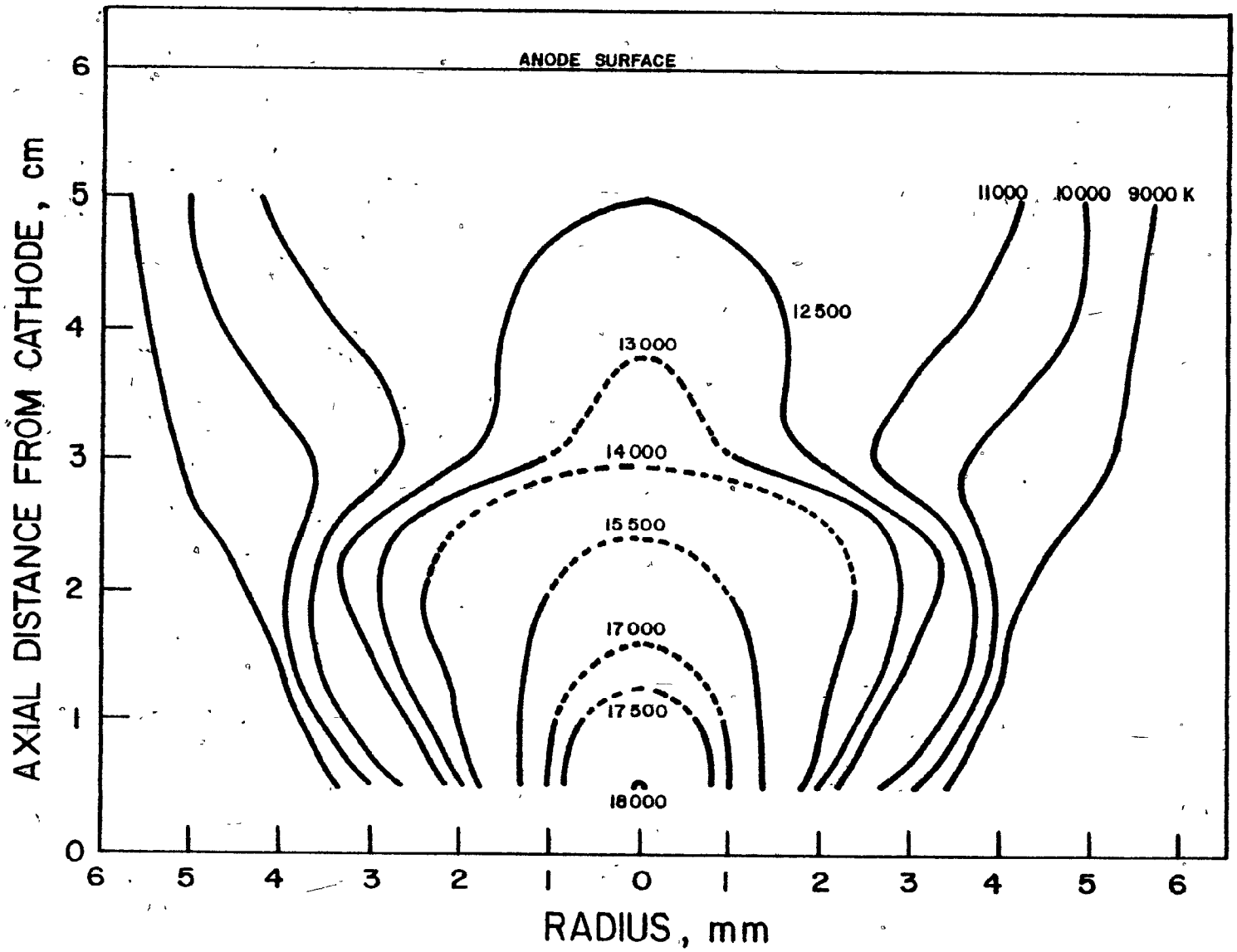
ANODE SURFACE
11000
10000
9000 K
12500
13000
14000
15500
17000
17500
18000
AXIAL DISTANCE FROM CATHODE, cm
RADIUS, mm
0
1
2
3
4
5
6

FIGURE 37

ISOTHERMAL CONTOURS OF THE PLASMA FOR ℓ = 8 cm, I = 350 A v^* = 20.5 m/s and q = 0 L/m

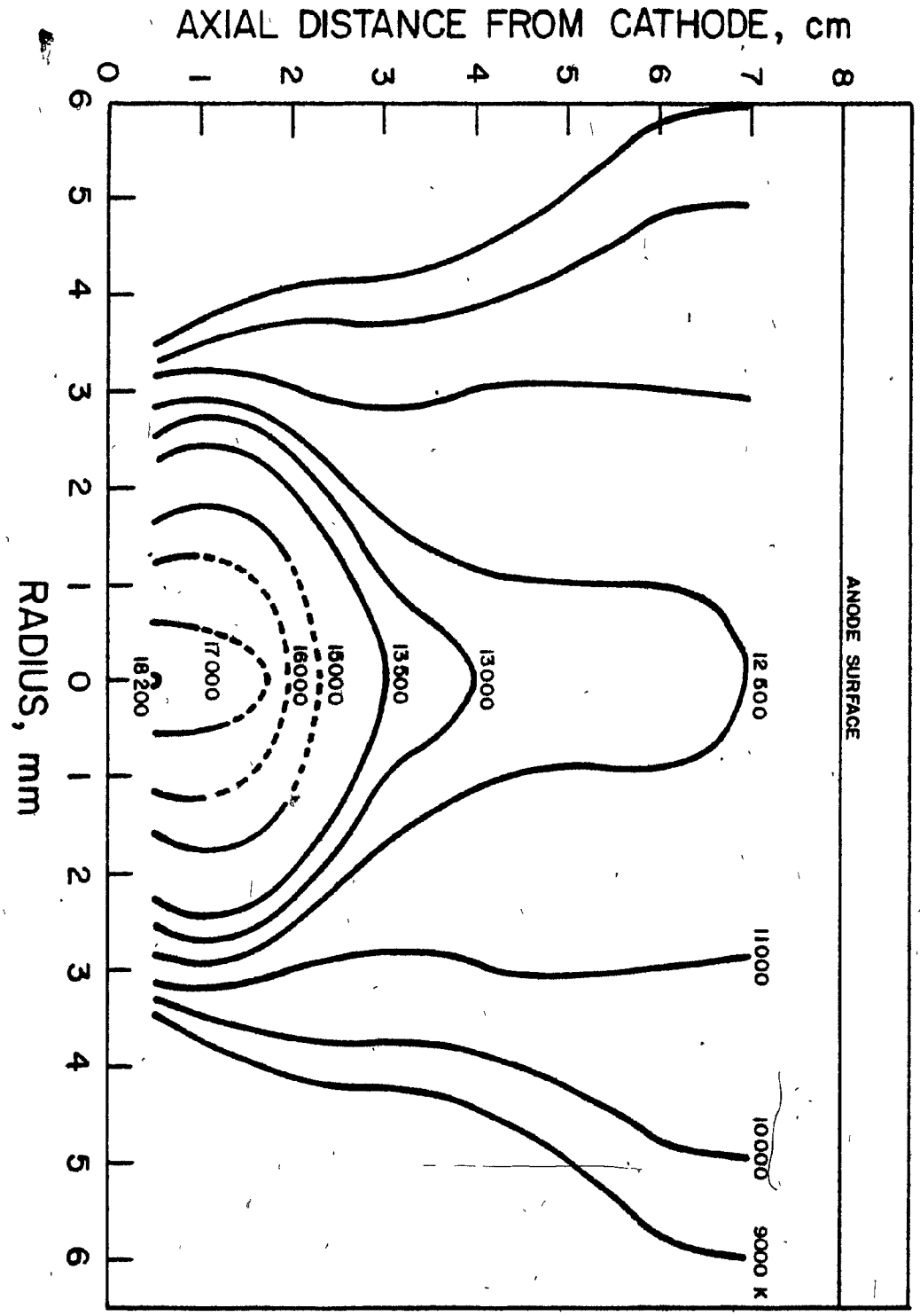
AXIAL DISTANCE FROM CATHODE, cm
0
1
2
3
4
5
6
7
8
RADIUS, mm
6
5
4
3
2
1
0
1
2
3
4
5
6
ANODE SURFACE
18200
17000
16000
15000
13500
13000
12500
11000
10000
9000 K

FIGURE 38

ISOTHERMAL CONTOURS OF THE
PLASMA FOR ℓ = 4 cm, I = 350 A
v^* = 20.5 m/s and q = 0 L/m and q = 31.0 L/m
(45° Nozzle)

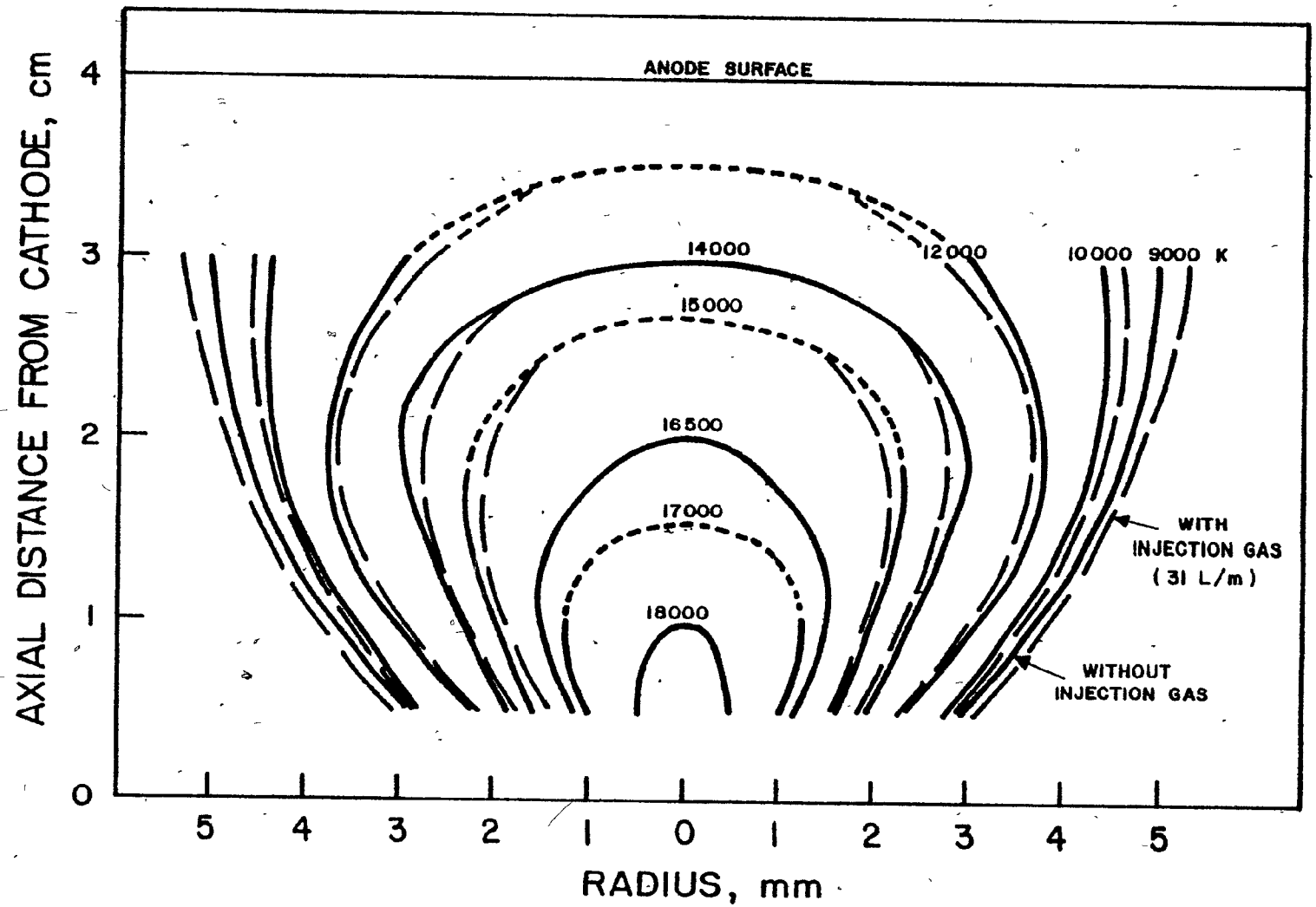
ANODE SURFACE
14000
12000
10000
9000 K
15000
16500
17000
18000
WITH
INJECTION GAS
(31 L/m)
WITHOUT
INJECTION GAS
AXIAL DISTANCE FROM CATHODE, cm
0
1
2
3
4
5 4 3 2 1 0 1 2 3 4 5
RADIUS, mm

FIGURE 39

AXIAL CENTRELINE TEMPERATURE

DISTRIBUTION IN PLASMA COLUMN

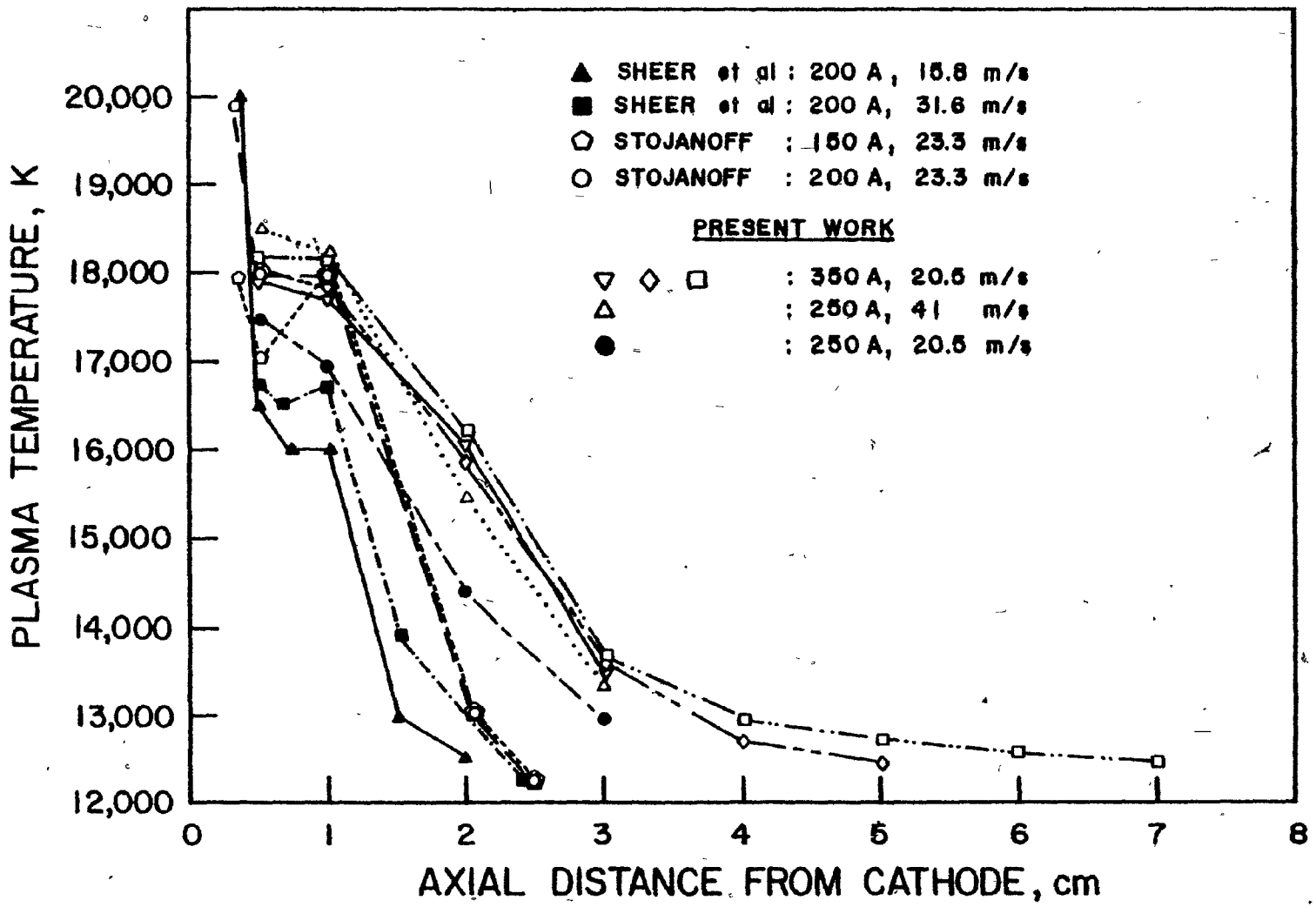
▲ SHEER et al : 200 A, 15.8 m/s
■ SHEER et al : 200 A, 31.6 m/s
⬠ STOJANOFF : 150 A, 23.3 m/s
○ STOJANOFF : 200 A, 23.3 m/s
PRESENT WORK
▽ ◇ □ : 350 A, 20.5 m/s
△ : 250 A, 41 m/s
● : 250 A, 20.5 m/s
PLASMA TEMPERATURE, K
20,000
19,000
18,000
17,000
16,000
15,000
14,000
13,000
12,000
0
1
2
3
4
5
6
7
8
AXIAL DISTANCE FROM CATHODE, cm

(obtained 3 cm away from anode) are plotted in Figure 40.

Examination of these curves shows that the axial temperatures increase near the cathode as the inlet gas velocity increases. This effect is considered to be due to the compression of the column exerted by the radial component of the fluid momentum as it enters the column. Both the current density (i.e., column diameter) and voltage gradient are increased with increased v*, resulting in an increased rate of heat transfer to the incoming fluid. It is interesting to note the rather flat portion of the axial temperature distribution for $0.5 < z < 1.0$ cm. It probably represents the section of the contraction zone where most of the gas is entering the column. The two previous investigators who used similar cathode designs (Sheer et al, 1973, and Stojanoff, 1968) also displayed similar distributions near the cathode, as shown on Figure 39.

The influence of the gas injection on the radial temperature distribution is also very interesting. Gas injection does not affect the temperature distributions near the cathode significantly, except for the high current case where slightly reduced temperatures were recorded. On the other hand, this additional flow has some effects downstream. While the 9,000 K isothermals move away from the axis (i.e., the luminous column profile increased), there is a cooling effect in the interior of the plasma. However, in all cases, a core region is present which maintained its temperature. This probably

FIGURE 40

RADIAL DISTRIBUTION OF TEMPERATURE

IN PLASMA COLUMN

(At 3 cm away from Anode for 4 cm total length)

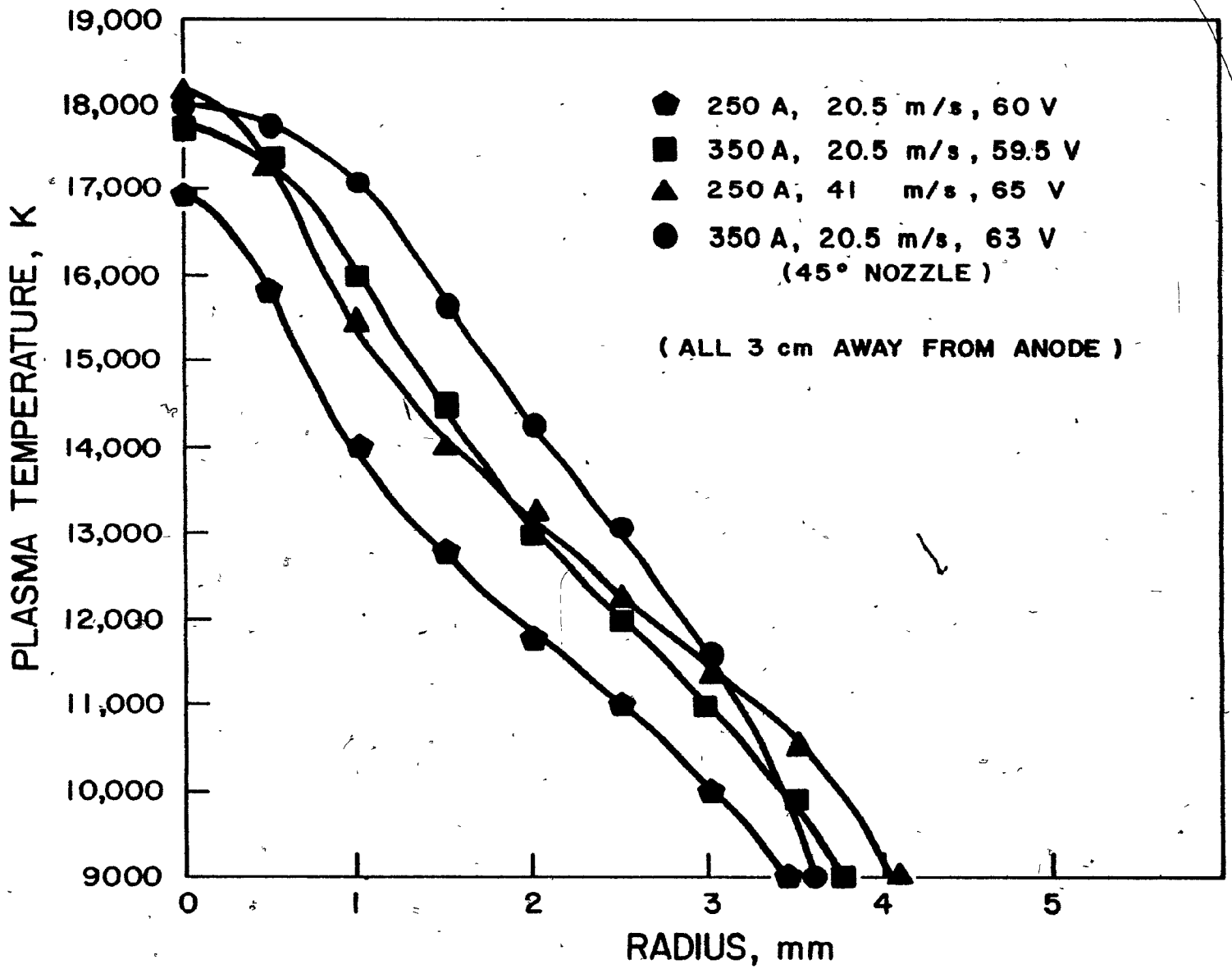
19,000
18,000
17,000
16,000
15,000
14,000
13,000
12,000
11,000
10,000
9000
PLASMA TEMPERATURE, K
0
1
2
3
4
5
RADIUS, mm
250 A, 20.5 m/s, 60 V
350 A, 20.5 m/s, 59.5 V
250 A, 41 m/s, 65 V
350 A, 20.5 m/s, 63 V
(45° NOZZLE)
(ALL 3 cm AWAY FROM ANODE)

reflects the fact that while the injection gas causes a slight expansion of the plasma, in general it cools the plasma. The axial temperature distribution does not vary with the gas injection.

The plasma temperature increases as the applied current increases. As can be seen from the axial temperature distribution, the magnitude of this increase does not change along the arc length. This effect had already been predicted by the calorimetric and photographic studies. Although the voltage gradient decreases with increasing current, the increase in the current density more than compensates this decrease. It is interesting to calculate the average power density in the column, given by the product of the current density and the voltage gradient. From Figure 27, the average voltage gradient of 6.3 and 5.7 volts per cm is obtained for 250 and 350 A columns, respectively. The average column diameter was calculated to be 0.7 and 0.8 cm, corresponding to 0.442 and 0.503 cm^2 for the cross-sectional area, for the 250 and 350 A cases, respectively. Thus, the ratio of the power densities for the 350 and 250 A columns averaged 1.11, showing 11% increase in the energy for the high current case.

The comparison of the axial temperature distributions for the 4, 6 and 8 cm columns shows that identical temperatures are obtained for the initial portion of the column included in these cases. The fact that the decay in axial temperature decreases considerably beyond a distance of 3 cm away from the cathode for the

6 and 8-cm arc lengths suggest that the phenomenon which is responsible for the loss of energy in the initial part of the plasma ceases to be important after 3 cm. Considering that radiative heat losses constitute a large percentage of the overall heat losses from the plasma column, the low temperatures encountered around z = 3 cm results in lower radiative heat losses and thus slower decay. This cause-effect relationship sets in for the rest of the plasma column. The results of Choi (1980), who measured arc radiation as a function of arc length for a transferred-arc plasma under similar conditions, also indicate a sharp change in the percentage of the arc energy lost by radiation beyond a 3-cm electrode separation. To complete this discussion, it must be stated that other factors such as the decreasing effect of the cathode jet are also probably responsible for the sudden drop in the axial temperature upstream of 3 cm. This decreasing effect of the cathode jet on the plasma energy with axial distance from the cathode has been reported by several workers, although generally for shorter arcs. The works of Schoeck (1963) and Reed (1960) are respresentative of such investigations.

Finally, the effect of the varying nozzle angle can be observed by comparison of Figures 35 and 38 and from Figure 40. The position of the 9000 K isotherms does not change between the two conditions, in agreement with the photographic observations. Higher temperatures result for 45° nozzle near the cathode. The magnitude of this difference decreases downstream from the cathode. The effect of the nozzle geometry on the energy content of the plasma in the

neighbourhood of the cathode can be attributed to the change in the electrode fall potentials.

Based upon the uncertainties in the transition probabilities of the lines used (±5%) and in the correction factors used for the continuum emission coefficients (±10%), fluctuations of the photo-diode signals (±3%), possible errors in the calibration of the optical system using the tungsten strip lamp as a reference (±2%), and errors arising from the approximations associated with the convolution integers method used in differentiation in the computer program (±2%), the maximum uncertainty in the temperature obtained is estimated to be ±8%. At 10,000 K this amounts to a range of ±800 K.

It should be mentioned that the above temperature distributions are based on the assumption of local thermal equilibrium (LTE) in the plasma. This assumption has been experimentally tested and found fully justified for transferred arc plasmas generated under similar conditions and with similar cathode design as used in this work (Stojanoff, 1968; Sheer et al, 1973). Busz and Finkelnburg (1954) obtained the following criterion for thermal equilibrium by comparing the energy gained by the electrons from the imposed electric field between collisions with the heavy particles, with that lost to the heavy atoms and ions during the collisions:

$$(T_e - T_g)/T = M(e\lambda_e E)^2/[4m(3kT/2)^2] << 1 \qquad (11)$$

where T_e, T_g are the temperatures of the electrons and heavy

particles, respectively, $\underline{E}$ is the applied electric field strength, $\underline{M}$ and $\underline{m}$ are the masses of the atoms and electrons, respectively, and $\underline{\lambda}_e$ is the electron mean free-path length.

Using the value of $\underline{\lambda}_e$ calculated by Olsen (1962), the measured temperatures and derived $\underline{E}$, $(T_e - T_g)/T$ was calculated to be (at the centre of the arc) 0.006 near the cathode and 0.01 near the anode, for 250 A and 20.5 m/s (conditions A-4 and A-1, respectively). In the light of this test, it can be claimed that the assumption of LTE throughout the measurement range of this work is very good.

A more restrictive condition for LTE pertains to the gradients in temperature along the radial coordinate in the arc. The perturbation of equilibrium may be considered small if the temperature difference in one mean-free path is small compared with the temperature itself (Olsen, 1962):

$$\lambda_e \text{ grad } T/T \ll 1 \qquad (12)$$

The maximum temperature gradient measured in the arc is around 10^5 °K /cm. Since $\underline{\lambda}_e$ is of the order of 10^{-4} cm with temperatures greater than 10^4 °K, the condition in the above equation is well satisfied, except possibly in the regions close to the electrodes, which is outside the scope of this thesis.

For completeness, it must be added that both the axial and radial distributions of temperature were found to deviate considerably from the ones predicted by the classic jet theory.

8 - Velocity Study

Method of Data Resolution

The experimental conditions given in Table III were also employed for the velocity study. The values of the impact pressures obtained from the continuous impact pressure profile together with the measured temperatures at the same radial positions permitted calculation of the plasma velocities at these points using Equation (10). The calculation was performed by a minicomputer. Since the viscosity and density in Equation (10) must be evaluated at the reference temperature, the probe wall temperature was estimated to be 400°K. The insensitivity of the reference temperature to the wall temperature justifies this choice. This particular wall temperature was chosen based on thermocouple measurements of the temperature of the probe after it completed a traverse. From the constant wall temperature and the given free stream temperature, the computer program internally calculated the reference temperature and evaluated the viscosity and density at this temperature. A regression fit to Ahtye's (1965) enthalpy, viscosity and compressibility factor was included in the program. The output from the velocity calculation included the actual velocity, the reference temperature, the Reynolds number for flow around the probe and the mass flow density. The computations were made at 18 equally-spaced positions along the diametrical pressure profile.

Results

Velocities measured by the sweeping pitot tube method are shown in Figures 41 to 46 in the form of constant velocity contours. This form of presentation was chosen as being consistent with that of the temperature results as well as providing better flow visualization. Figure 47 shows the axial distribution of the centreline velocity and in Figure 48, a sample of the radial velocity distributions is given, for the position 3 cm away from the anode, to assist in the discussions. Finally, Figure 49 contains a set of typical mass flow density distribution curves, for the cases A-1 through A-4. The limiting data points on the velocity profiles are determined by the limiting points on the temperature profiles which, in turn, are established by the luminous diameters of the column. Beyond these positions, impact pressures could be measured, but temperatures could not.

It can be seen that as in the case of temperatures, the velocity profiles are symmetric. The decay of the centreline velocity with the axial distance from the cathode is observed to be faster than that of centreline temperature. The primary reason of course is the superposition of the increase in density (due to cooling of the column) and the usual decay observed in isothermal jets. Cleaves and Boelter (1947) also noted a similar behaviour for their heated and unheated jets. Similarly, the radial distributions of velocity and momentum are found to decay faster than

FIGURE 41

CONSTANT VELOCITY CONTOURS
OF THE PLASMA COLUMN FOR
ℓ = 4 cm, I = 250 A, v* = 20.5 m/s
and q = 0 L/m and q = 25 L/m

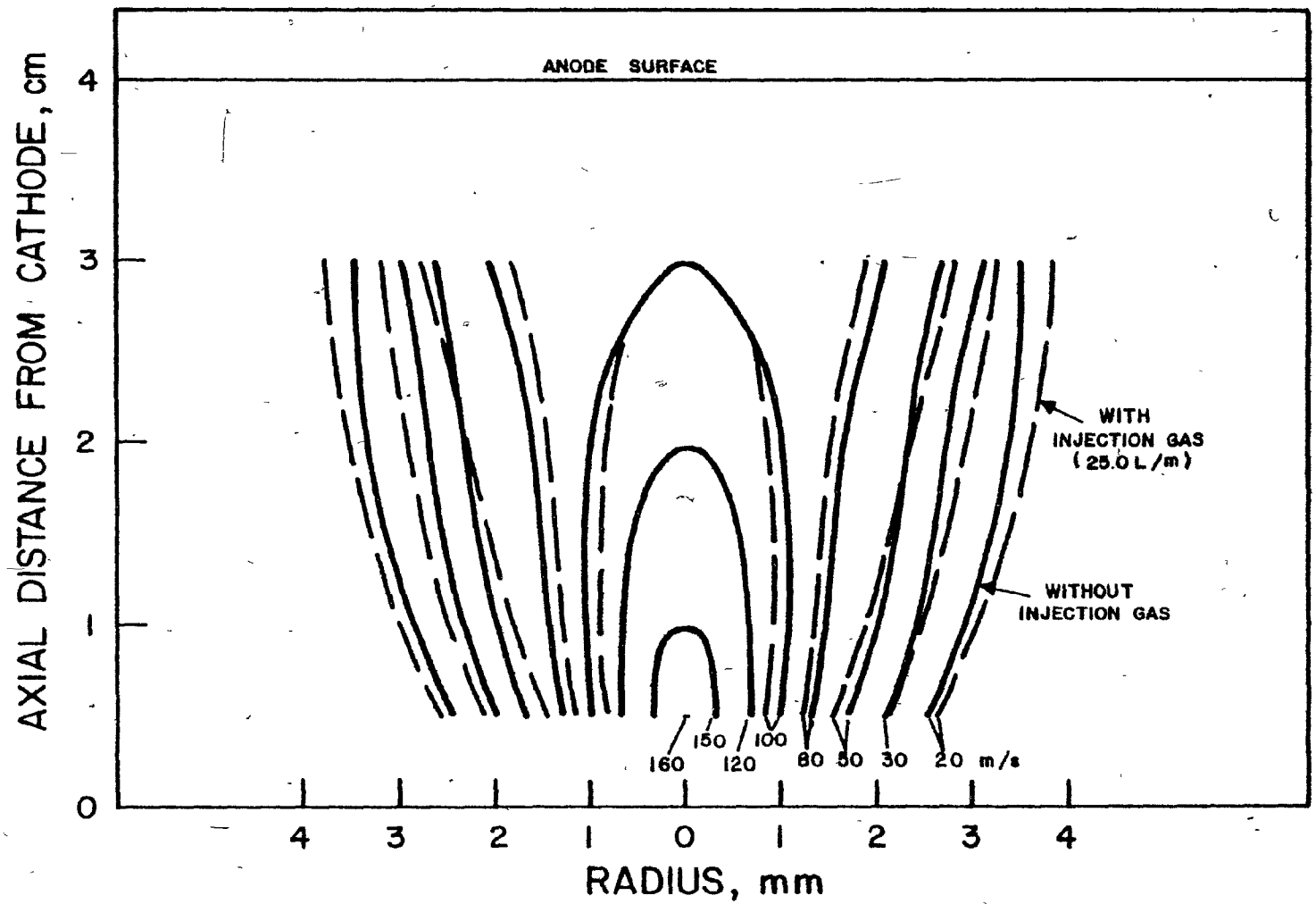
ANODE SURFACE
AXIAL DISTANCE FROM CATHODE, cm
0
1
2
3
4
RADIUS, mm
4 3 2 1 0 1 2 3 4
WITH INJECTION GAS (25.0 L/m)
WITHOUT INJECTION GAS
160 150 120 100 80 50 30 20 m/s

FIGURE 42

CONSTANT VELOCITY CONTOURS
OF THE PLASMA COLUMN FOR
ℓ = 4 cm, I = 250 A, v* = 41 m/s
and q = 0 L/m and q = 20 L/m

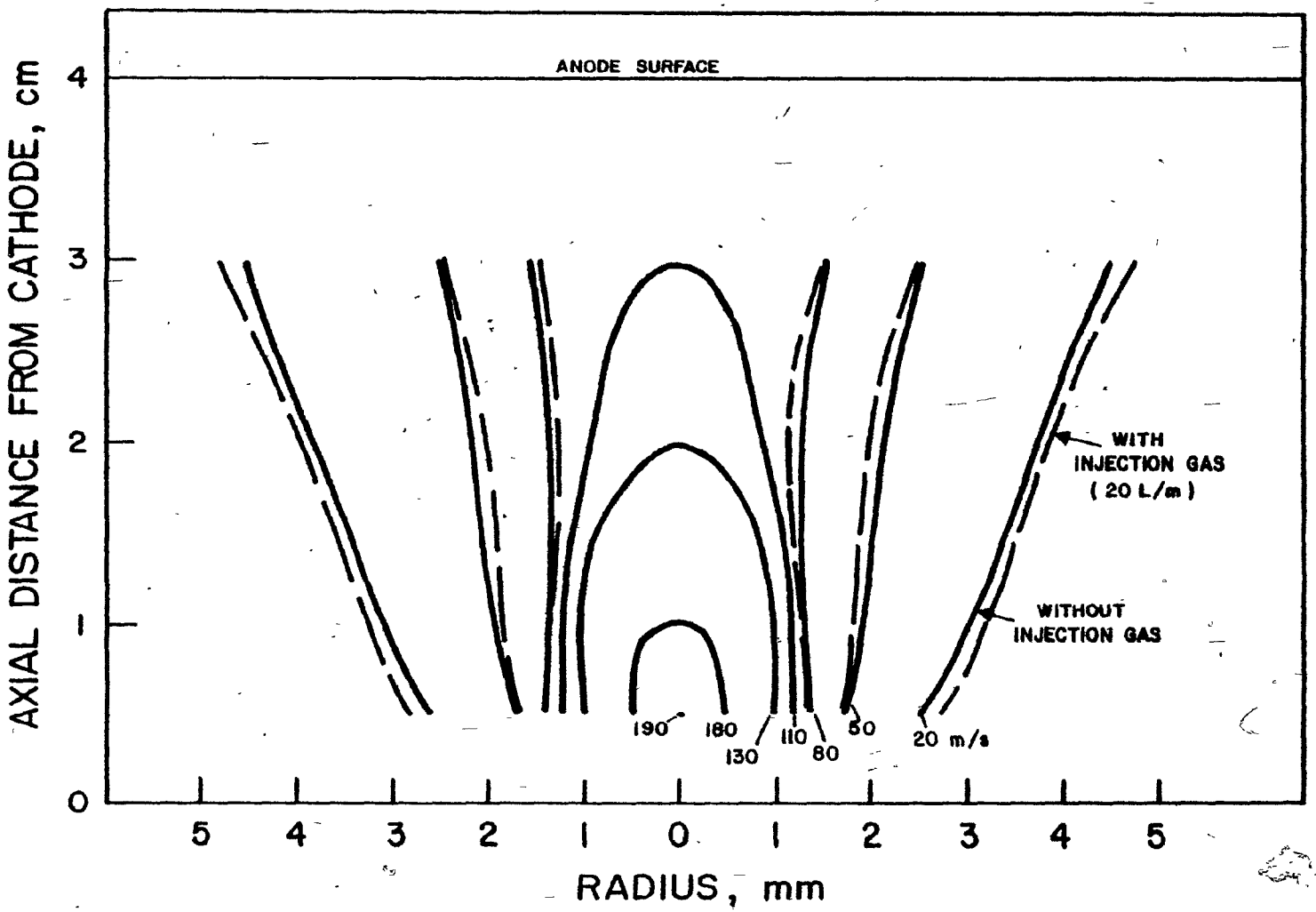
ANODE SURFACE
AXIAL DISTANCE FROM CATHODE, cm
0
1
2
3
4
5 4 3 2 1 0 1 2 3 4 5
RADIUS, mm
WITH INJECTION GAS (20 L/m)
WITHOUT INJECTION GAS
190
180
130
110
80
50
20 m/s

FIGURE 43

CONSTANT VELOCITY CONTOURS
OF THE PLASMA COLUMN FOR
ℓ = 4 cm, I = 350 A, v* = 20.5 m/s
and q = 0 L/m and q = 31 L/m

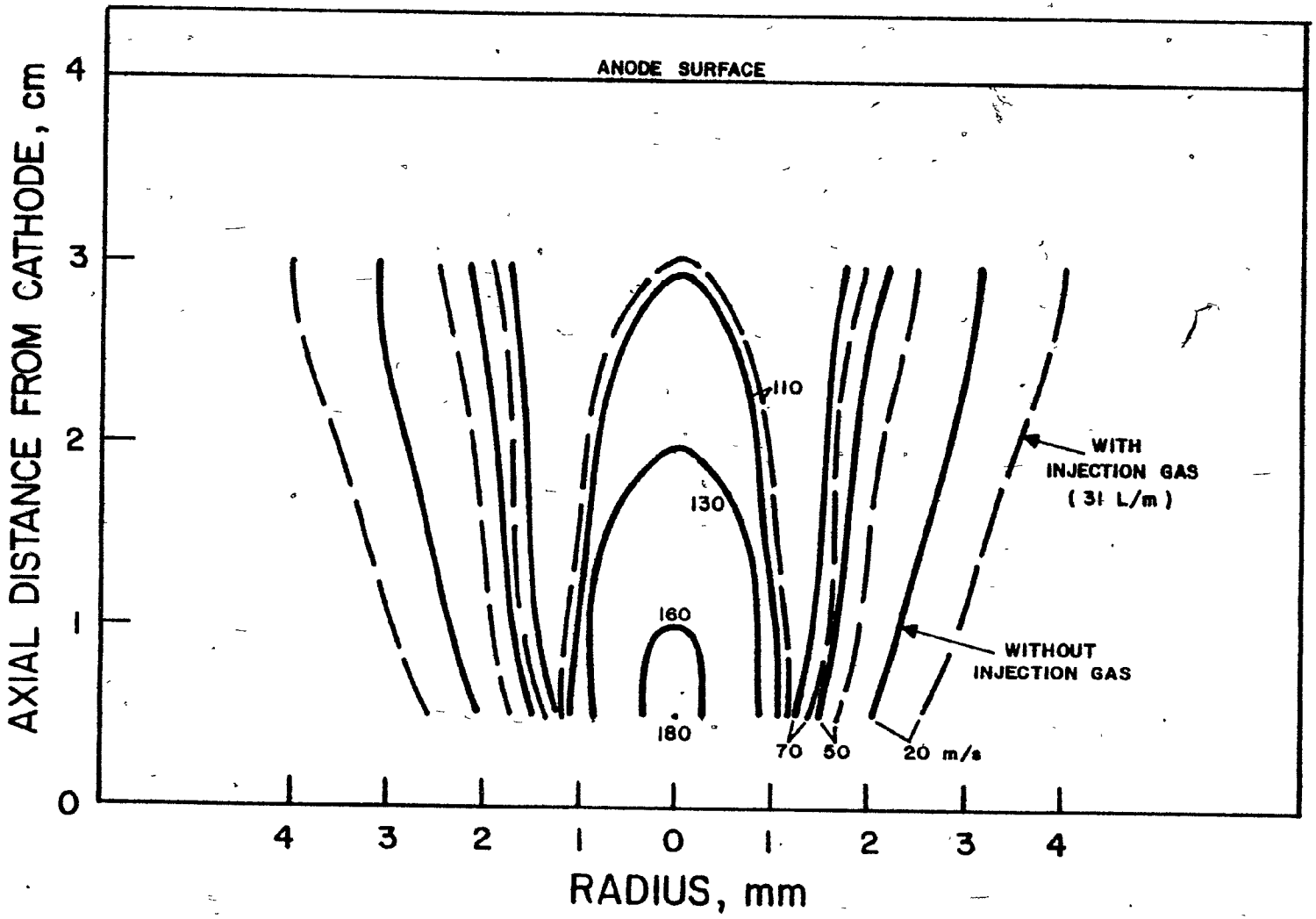
ANODE SURFACE
AXIAL DISTANCE FROM CATHODE, cm
RADIUS, mm
0
1
2
3
4
4 3 2 1 0 1 2 3 4
110
130
160
180
70
50
20 m/s
WITH INJECTION GAS (31 L/m)
WITHOUT INJECTION GAS

FIGURE 44

CONSTANT VELOCITY CONTOURS
OF THE PLASMA COLUMN FOR
ℓ = 6 cm, I = 350 A, v* = 20.5 m/s and q = 0 L/m

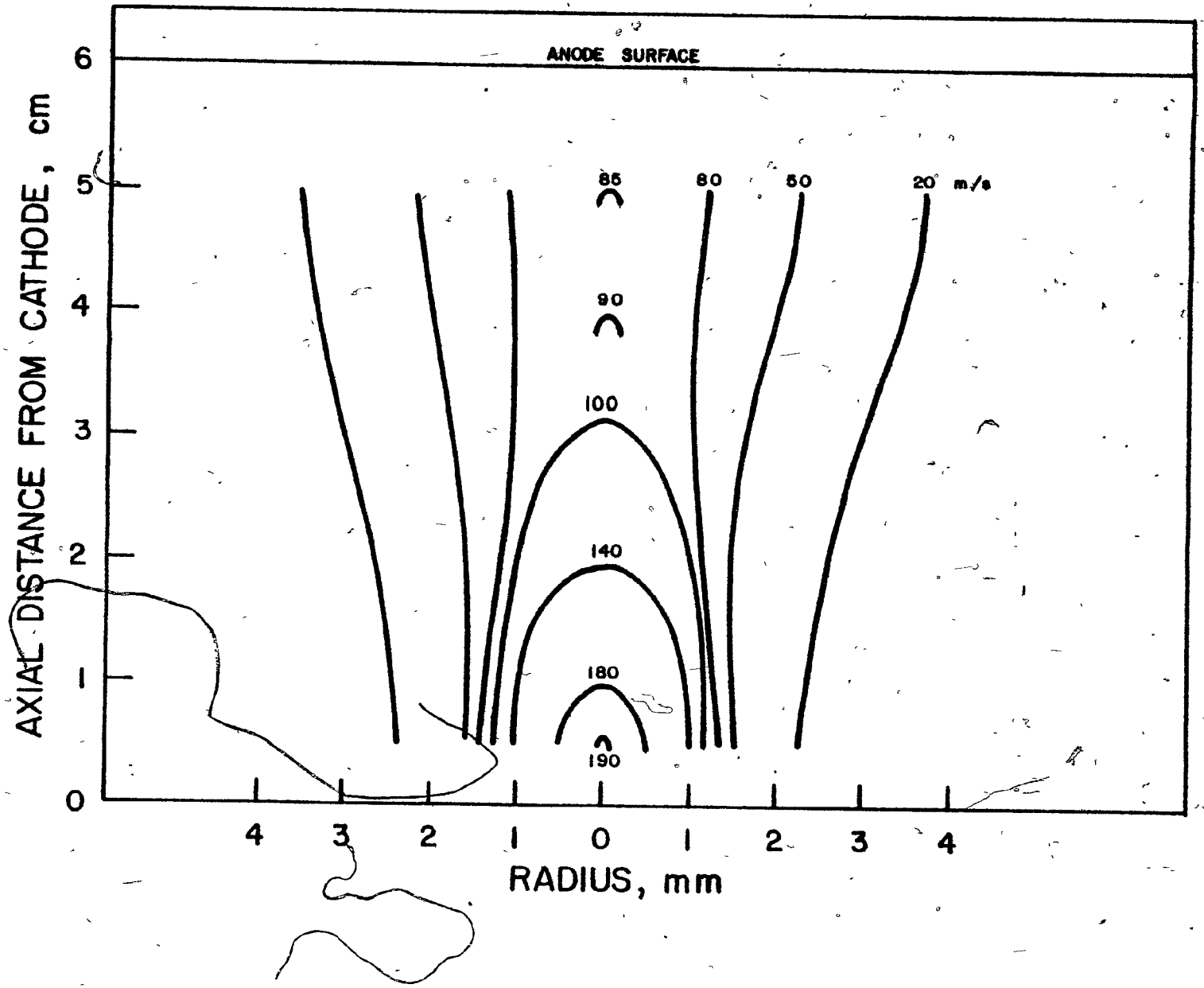
ANODE SURFACE
AXIAL DISTANCE FROM CATHODE, cm
RADIUS, mm
0
1
2
3
4
5
6
4
3
2
1
0
1
2
3
4
85
80
50
20 m/s
90
100
140
180
190

FIGURE 45

CONSTANT VELOCITY CONTOURS
OF THE PLASMA COLUMN FOR
ℓ = 8 cm, I = 350 A, v^* = 20.5 m/s and q = 0 L/m

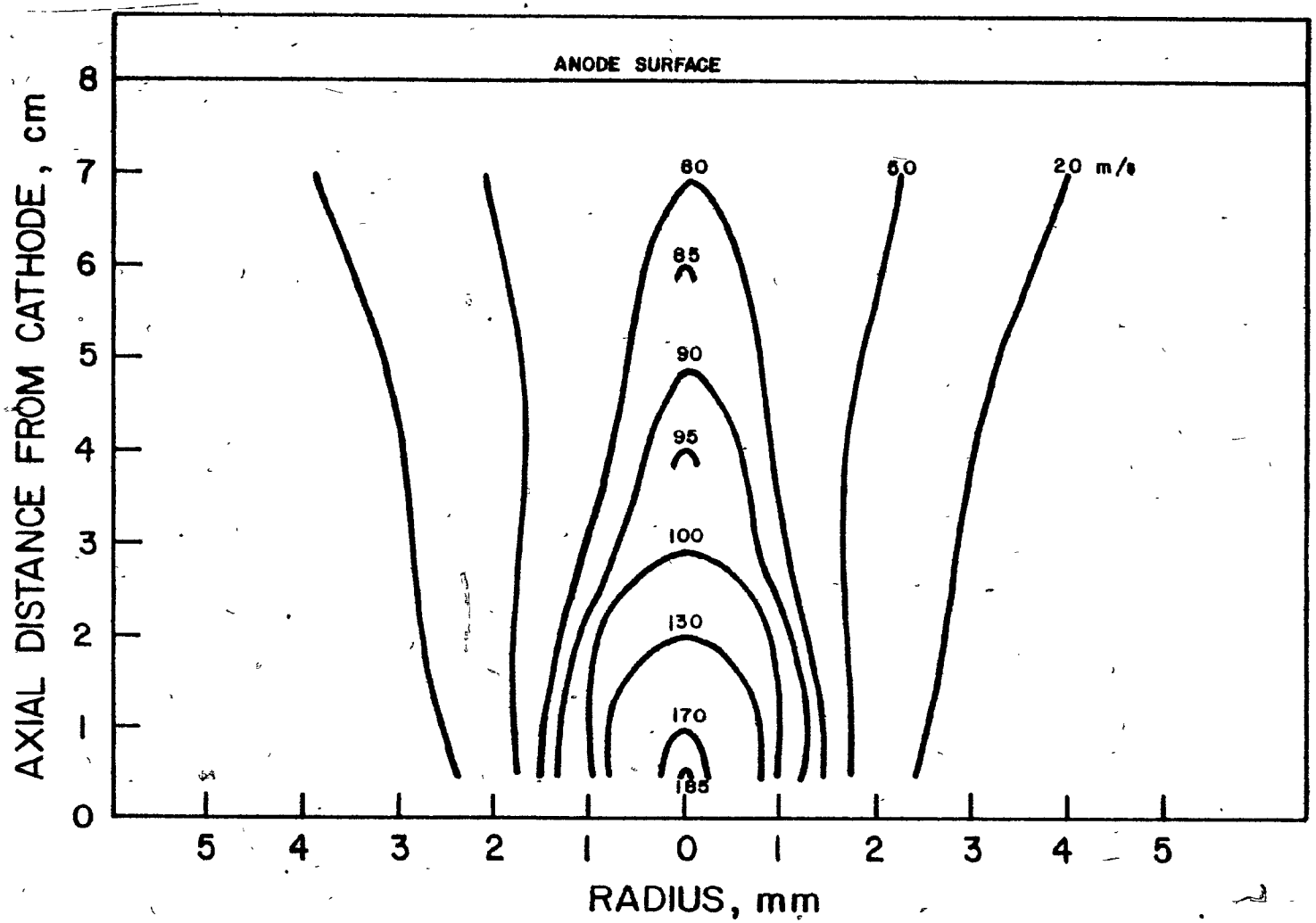
ANODE SURFACE
AXIAL DISTANCE FROM CATHODE, cm
RADIUS, mm
0
1
2
3
4
5
6
7
8
5
4
3
2
1
0
1
2
3
4
5
80
85
90
95
100
130
170
185
60
20 m/s

FIGURE 46

CONSTANT VELOCITY CONTOURS
OF THE PLASMA COLUMN FOR
$\ell = 4$cm, I = 350 A, $v^* = 20.5$ m/s
and q = 0 L/m and q = 31 L/m

(45° Nozzle)

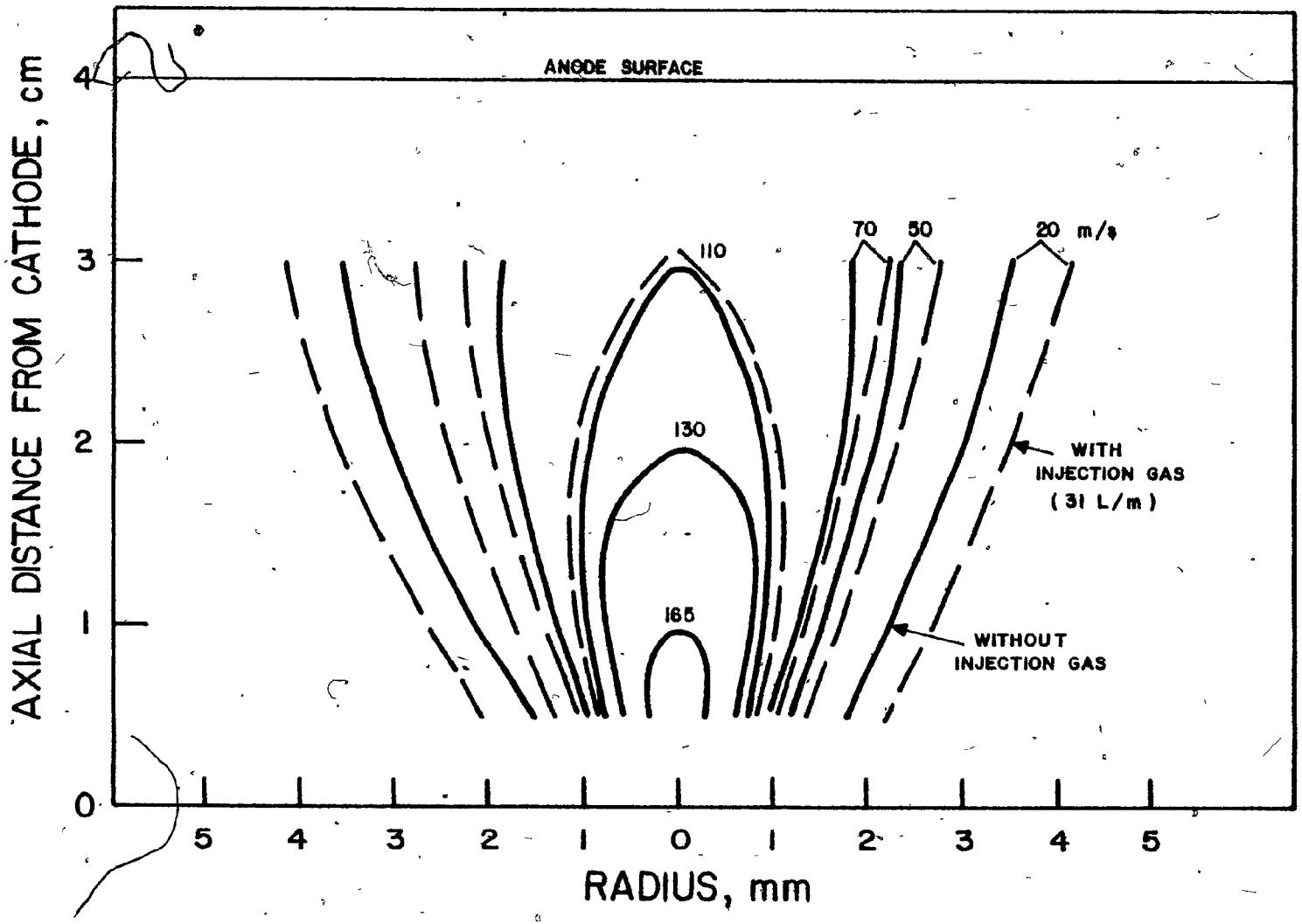
ANODE SURFACE
AXIAL DISTANCE FROM CATHODE, cm
RADIUS, mm
110
130
165
70
50
20 m/s
WITH INJECTION GAS (31 L/m)
WITHOUT INJECTION GAS
0
1
2
3
4
5

FIGURE 47

AXIAL CENTRELINE VELOCITY
DISTRIBUTION IN PLASMA COLUMN

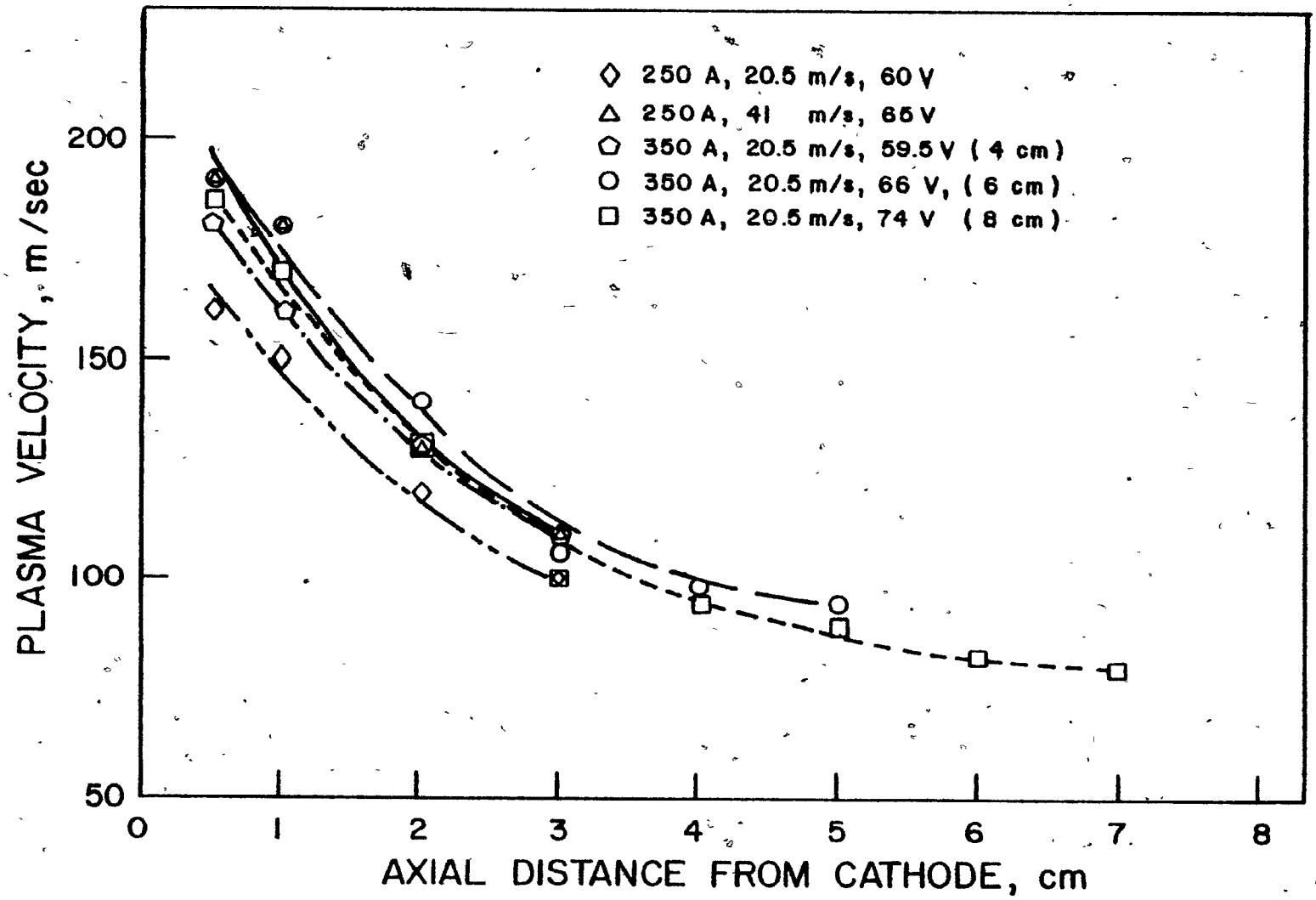
◇ 250 A, 20.5 m/s, 60 V
△ 250 A, 41 m/s, 65 V
⬠ 350 A, 20.5 m/s, 59.5 V (4 cm)
○ 350 A, 20.5 m/s, 66 V, (6 cm)
□ 350 A, 20.5 m/s, 74 V (8 cm)
PLASMA VELOCITY, m/sec
200
150
100
50
0
1
2
3
4
5
6
7
8
AXIAL DISTANCE FROM CATHODE, cm

FIGURE 48

RADIAL DISTRIBUTION OF VELOCITY

IN PLASMA COLUMN

(At 3 cm away from Anode
for 4 cm total length)

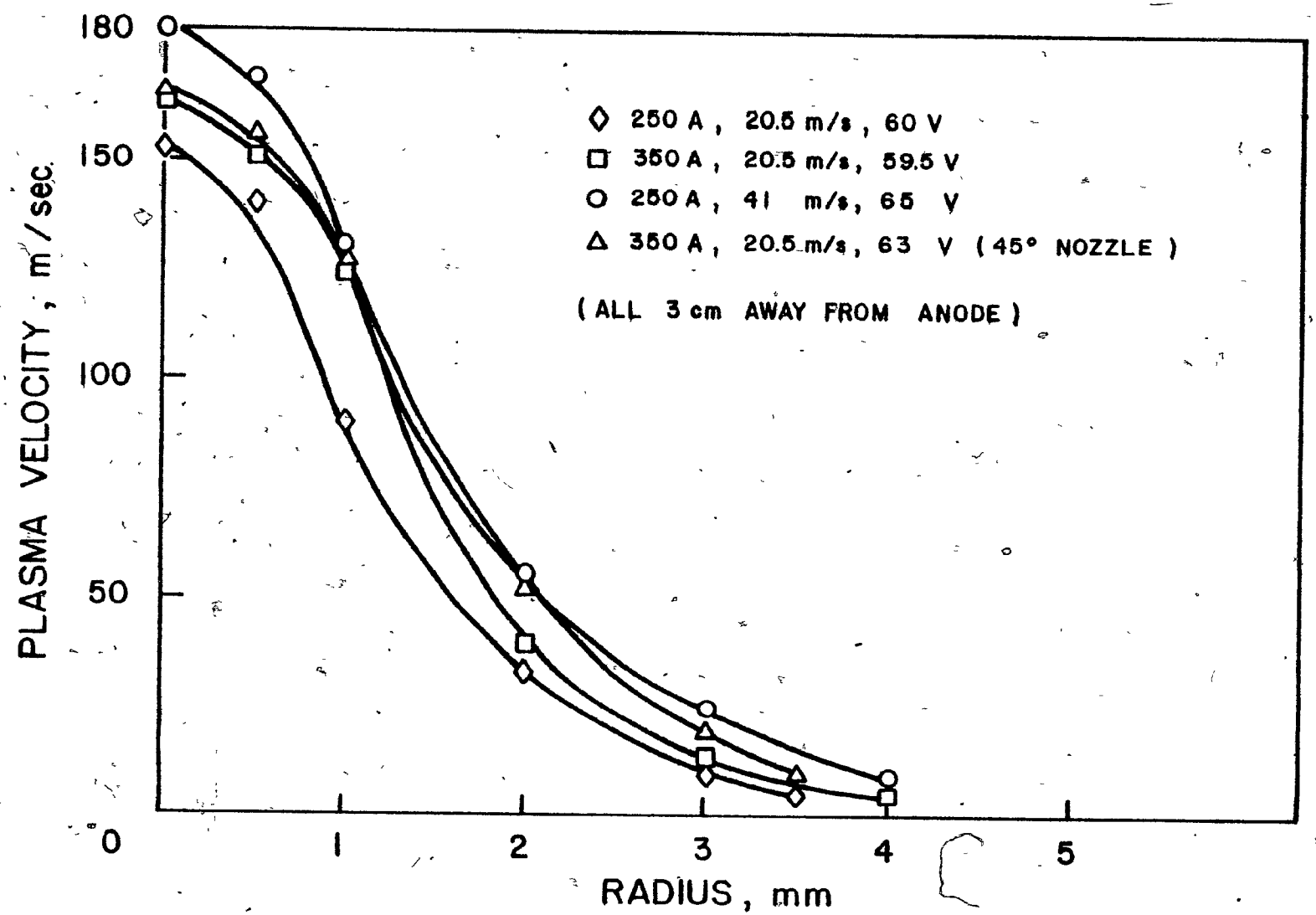
180
150
100
50
0
PLASMA VELOCITY, m/sec.
1
2
3
4
5
RADIUS, mm
◇ 250 A, 20.5 m/s, 60 V
□ 350 A, 20.5 m/s, 59.5 V
○ 250 A, 41 m/s, 65 V
△ 350 A, 20.5 m/s, 63 V (45° NOZZLE)
(ALL 3 cm AWAY FROM ANODE)

FIGURE 49

RADIAL DISTRIBUTION OF MASS FLOW DENSITY

FOR PLASMA COLUMN

(ℓ = 4 cm, I = 250 A, v* = 20.5 m/s)

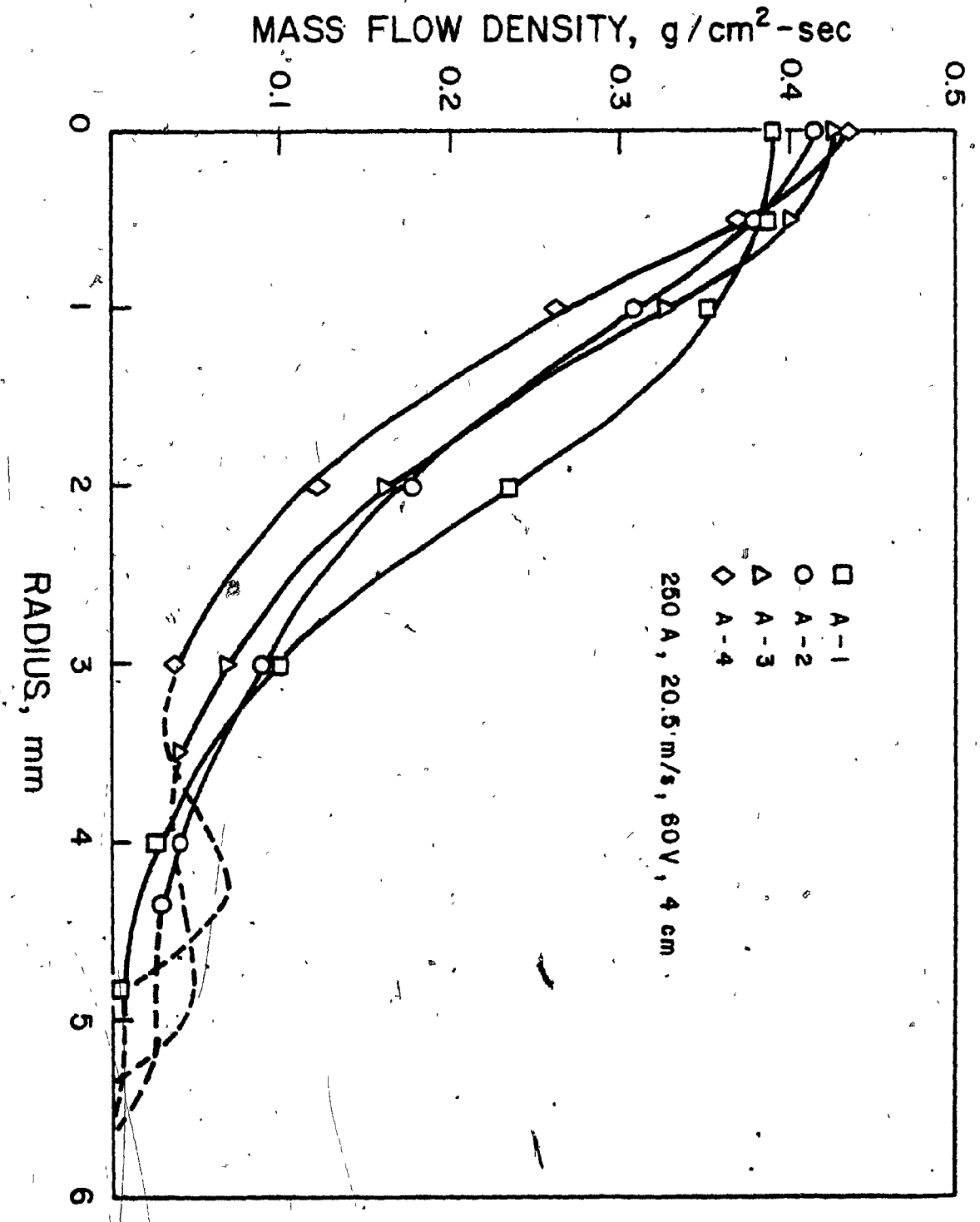
MASS FLOW DENSITY, g/cm²-sec
0.1
0.2
0.3
0.4
0.5
0
1
2
3
4
5
6
RADIUS, mm
A-1
A-2
A-3
A-4
250 A, 20.5 m/s, 60 V, 4 cm

that of temperature. This behaviour, however, is contrary to the behaviour observed in d.c. plasma jets as reported by Grey and Jacobs (1964), Kubanek and Gauvin (1968) and Katta and Gauvin (1973). It should be noted that the plasma column studied in this work was a conducting column which is expected to exhibit different behaviour than the d.c. plasma jets studied in these previous references. When compared with the limited data available for transferred arc plasmas (Reed, 1960; Stojanoff, 1968; Sheer et al, 1973), identical tendencies were observed.

Examination of these figures indicate that both the inlet gas velocity and the applied current have a positive effect on the centreline velocities. However, when the radial distributions are compared (Figure 48), it can be seen that towards the edges of the column, the effect of the applied current ceases to be significant. Since Reynolds numbers are quite low near the edges (around one compared to around 90 at the axis), the viscosity corrections are much more important; however, because the viscosity does not vary significantly with temperature below 10,000 K, it is normal that the applied current (which influences the temperature distribution near the edges) do not influence velocity profiles in these regions.

As in the case of the temperature profiles, the gas injection is effective basically for high current-low inlet gas velocity conditions. Again, it barely affects the inner core flow. The nozzle geometry does not seem to be a factor in the magnitude

of the injection gas effect on the flow field.

When the axial distributions of the centreline velocities for different electrode spacings are compared (see Figure 47), very close values are obtained over their respective lengths. This is of course to be expected since the temperatures and the luminous diameters do not show any deviation.

While the nozzle angle does not influence the axial distribution, it does have an effect on the radial velocity distribution in the form of a slower decay for 45° nozzle. This is predictable from the temperature profiles and is considered to be an important feature in favour of the selection of a 45° nozzle for industrial applications.

Since the column is cooling and increasing in density as the anode is approached, the product of density and velocity, or momentum, is of interest. Figure 49 shows a typical plot of the mass flow density ($\dot{m}$) versus radial distance. When the distributions of impact pressure were examined, it was observed that there existed a relatively cold gas flow outside the luminous boundaries of the column. The mass flow density distribution calculated for this flow is also shown in Figure 49, as dashed-lines. The temperature data used outside the luminous column were obtained by extrapolation from the temperature distributions inside the column and are therefore subject to considerable error. The curves were extended into this outer region to show qualitatively the changes in flow pattern

at various axial positions. The amount of gas that flows outside the column seems to decrease downstream. This undoubtedly indicates entrainment of the surrounding flow. It is interesting to note that although the presence of this flow can be deduced from their results, neither of the two investigators who worked with an annular nozzle orifice around a cathode (Stojanoff, 1968, Sheer et al, 1973) realized this occurrence. The theories of classical jet entrainment are found wholly inadequate to account for this change of entrainment with axial distance.

Radial velocity data of the type shown in Figure 48 are sometimes treated by plotting the velocity divided by the velocity at the centreline to see if a Gaussian distribution is followed. For the data presented here, no such indication was obtained because of the varying degrees of dependency of velocity on temperature, for different positions in the plasma. However, it was clearly seen that the classical jet theories on velocity distribution (both axial and radial) do not apply to transferred-arc plasmas.

Uncertainties in the velocity data arise from uncertainties both in the measured impact pressures and in the temperatures calculated from the measured emission coefficients. It will be recalled that the maximum uncertainty in plasma temperature was estimated to be ±8%. Uncertainties in the measured impact pressures occur because of possible errors in the calibration of the pressure transducer system, small fluctuations in the impact pressure itself,

and the error introduced by the time lag and the motion of the probe. The maximum error in the calibration of the pressure transducer unit with the alcohol manometer is ±0.98 Pa (0.00014 psi). Fluctuations in the impact pressure occur because of the changes in the input power and the random movements of the arc about its point of attachment. From repeated measurements, these variations were estimated to be ±5%. Since the probe moves through the plasma, there is a dynamic error in the measured impact pressure due to the time lag in the response of the transducer unit and to the small vibrations of the pitot tube. It will be recalled that the response time was measured to be around 0.002 second. The dynamic error including the time lag and the vibrations is found to be ±0.7% of the maximum pressure on the profile. The cumulative effect of these uncertainties is most significant near the edges of the column and least significant near the centreline. Thus, for the experimental conditions reported, the maximum uncertainty in the calculated velocity ranges from ±7.0% in the vicinity of the centreline to ±20.0% near the edges.

9 - Mass and Energy Balances

By using the experimentally-measured values of the temperature and velocity, mass and energy balances could be made for the plasma flows. The mass flow rate $\underline{M}$ and the energy flow rate $\underline{H}$ are calculated from:

$$M = \int_0^{2\pi} \int_0^{R} \dot{m}(r)\, r\, dr\, d\theta \tag{13}$$

and

$$H = \int_0^{2\pi} \int_0^{R} \dot{m}(r)\, h(r)\, r\, dr\, d\theta \tag{14}$$

where $\dot{m}$ is the mass flow density and h is the specific enthalpy.

A mini-computer was used to perform the calculations. Ahtye's (1965) data for compressibility and enthalpy were fitted numerically, and the required integrations across the plasma column were performed by using Simpson's rule. The integrations were first performed only out to the luminous profile of plasma column. The integration was then carried out to the fringes of the impact pressure profiles, using the extrapolated temperature values. The results of the mass and energy balances are shown in Table IV for the profiles obtained 1.0 cm away from the anode and 0.5 cm away from the cathode. The values in the brackets represent the results obtained by extrapolation. The profile designations correspond to the conditions given in Table III.

It can be seen that, away from the cathode, the mass flow rate inside the column increases while the energy rate decreases. This is in agreement with the cooling of the column since M is inversely proportional with temperature while H is directly proportional. The increased applied current has a positive effect on the amount of gas entering into the plasma, as predicted by the MHD equations describing the "Maecker Effect."

The mass input rates were determined from the rotameter

TABLE IV

RESULTS OF MASS AND ENERGY BALANCES

Profile Designation	Overall Mass Flow Rate (g/s)		Overall Energy Flow Rate (kW)		Profile Designation	Overall Mass Flow Rate (g/s)		Overall Energy Flow Rate (kW)	
A- 1	0.51	(0.51)	5.80	(5.80)	A-21	0.69	(1.10)	7.99	(8.25)
A- 4	0.36	(0.43)	6.00	(6.10)	A-24	0.43	(1.05)	9.05	(9.80)
Input Rate	0.50		6.30		Input Rate	1.35		7.98	
A- 5	0.52	(0.88)	6.07	(6.10)	A-25	0.50	(0.50)	7.29	(7.29)
A- 8	0.37	(1.00)	6.19	(7.00)	A-30	0.38	(0.48)	11.16	(13.05)
Input Rate	1.19		6.30		Input Rate	0.50		11.97	
A- 9	0.67	(0.90)	7.83	(8.20)	A-31	0.52	(0.52)	5.59	(5.59)
A-12	0.39	(0.89)	9.00	(9.62)	A-38	0.37	(0.42)	10.42	(10.85)
Input Rate	1.00		8.00		Input Rate	0.50		15.96	
A-13	0.70	(1.20)	7.55	(8.80)	B- 1	0.52	(0.52)	7.80	(7.80)
A-16	0.40	(1.30)	9.05	(10.0)	B- 4	0.30	(0.45)	8.32	(8.55)
Input Rate	1.53		8.00		Input Rate	0.5		7.98	
A-17	0.50	(0.50)	7.29	(7.29)	B- 5	0.69	(1.00)	8.33	(8.55)
A-20	0.38	(0.48)	8.11	(8.30)	B- 8	0.33	(1.22)	8.50	(8.72)
Input Rate	0.50		7.98		Input Rate	1.35		7.98	

readings. The energy input rates were calculated from the voltage gradients rather than the net electric power input rate to the plasma since electrode losses were considered not to contribute to the overall energy flow rate. Considering the uncertainty in the extrapolated temperature data, the agreement between the measured rates and the calculated values was found satisfactory, with an average error of ±15% for the mass flow and ±20% for the energy flow.

CONCLUSION

The basic characteristics of a transferred arc plasma and their variation with the operating parameters were studied experimentally. Argon was used as the plasma-forming gas. The plasma was operated between power levels of 8.4 and 38.5 kW.

A cathode assembly suitable for injection of fine particles and/or reactive gases into the column was designed. The experiments were carried out in open air, as it was discovered that no ambient air was admitted by entrainment in the cathode arc-root region as long as sufficient argon was supplied via the particle injection channels, in addition to the plasmagen argon flowing through the inner channel surrounding the cathode tip. The current was varied between 150 and 350 amperes and the arc length between 4 and 8 cm. It was observed that the inlet velocity of the plasmagen gas past the cathode tip (calculated as the cold gas flow rate divided by the free annular nozzle area) was an important parameter and should be

used instead of the volumetric gas flow rate alone, if the results are to be generalized.

Preliminary experiments which were carried out to establish the voltage characteristics under the major operating conditions showed that voltage depended strongly on the electrode separation and much less on the current and on the inlet gas velocity. It was observed that higher voltages were sustained for 45° nozzle compared to 60° nozzle. Additional argon feed from the injection channels decreased the sustained voltage by replacing the entrained ambient air in the plasma column.

The voltage gradient of the plasma column was calculated from the gradient of the linear portion of the voltage versus electrode spacing graphs. The experimental measurements of the potential variation along the length of the column by means of probes confirmed the above approximations.

Calorimetric measurements were carried out to determine the fractions of the power supplied: (a) lost to the cathode tip and nozzle cooling; (b) dissipated to the cold surrounding by radiation from the plasma; (c) released at the anode. The fraction of the power lost to the cathode and the nozzle was invariably small and almost constant with current and electrode separation. As the current was increased, substantial increase was observed in the amount of the power released at the anode. The electrode separation also had a positive effect in this respect. Depending on

the electrode separation, the power radiated by the arc could be varied between 41% and 53%, independently of the current. The inlet gas velocity was found to decrease the cathode tip temperature by convective cooling.

The temperature measurements were effected with a novel electro-optical system capable of measuring the temperature profile of plasmas above 8000° K with an accuracy of ±8%. The technique was based on measuring the variations in the intensity of the plasma (as viewed through an aperture) while a blocking element moves through the plasma. An interface-mini-computer assembly was used to process the signals recorded on the oscilloscope to yield the plasma temperature profiles. The results indicate higher centreline temperatures near the cathode. Increasing the current and the inlet gas velocity both increase the temperature of the plasma. Comparison of the axial temperature distributions obtained for different electrode separations showed that identical temperatures were obtained for the initial portion of the plasma included in all of them. Higher temperatures were obtained for a 45° angle nozzle as compared to a 60° angle nozzle. The validity of the LTE in the plasma was checked theoretically and its existence was confirmed. The maximum temperature measured in the work was 18,500 K for a 250 A arc with 4-cm electrode separation and 41 m/s inlet gas velocity.

A miniature, uncooled pitot tube connected to a high response-time differential pressure transducer was swept through the

plasma to determine the plasma gas velocity distribution. It was found that a sweep velocity of 20 cm/s was adequate for good resolution while avoiding ablation. Because of the low Reynolds numbers of the flow encountered under most of the plasma operating conditions, a correction for viscosity effects had to be included into the Bernoulli equation. The velocity profiles showed a strong decay in the radial direction. The velocities tended to increase with increasing current and inlet gas velocities. Additional gas feeding via the injection channels was found to be effective for high-current, low inlet gas velocity conditions. The nozzle with 45° inclusion angle was found to cause a slower radial decay. When mass flow densities were calculated, existence of a relatively cold flow outside the boundaries of luminous column was discovered. It was observed that this flow was decreasing downstream which was taken as an indication of entrainment. The maximum axial velocity measured with 190 m/s near the cathode with an accuracy of ±7%.

Mass and energy balances computed at various axial distances for various operating conditions agreed with the input rates and thus confirmed the accuracy of the temperature and velocity measurements.

NOMENCLATURE

NOMENCLATURE

a	-	Inside radius of the pitot tube
A	-	Annular nozzle area.
E	-	Voltage gradient
h	-	Specific enthalpy
H	-	Energy flow rate
I	-	Applied current
ℓ	-	Electrode separation
$\dot{m}$	-	Mass flow density
M	-	Mass flow rate
P	-	Pressure
P'	-	Increase in pressure due to viscosity
q	-	Injection gas flow rate
Q	-	Sheath gas volumetric flow rate
r	-	Radial position
R	-	Ratio of the total emission coefficients for 4806 Å and 6965 Å, respectively
R	-	Gas constant
T	-	Temperature
U	-	Gas velocity

V	-	Voltage
v*	-	Inlet gas velocity
z	-	Axial distance from cathode

Greek Letters

ρ	-	Gas density
μ	-	Viscosity of the plasma
ν	-	Kinematic viscosity
θ	-	Nozzle angle

REFERENCES

REFERENCES

Ahtye, W.F., "A Critical Evaluation of Methods for Calculating Transport Coefficients of Partially and Fully Ionized Gases," NASA TN D-2611, Washington, D.C., (1965).

Aubreton, J. and Fauchais, P., "Les Fours à Plasma," Rev. Gen. Therm. Fr. No. 200-201, p. 681, August-September (1978).

Barkan, P. and Whitman, A.M., "Stagnation Pressure Measurement in a Current Carrying Plasma," AIAAJ, Technical Notes, 4, (9), 1691, (1966).

Barker, M., (Miss), "On the Use of Very Small Pitot Tubes for Measuring Wind Velocity," Proc. Roy. Soc. of London, 101, 435, (1922).

Barr, W.L., "Method for Computing the Radial Distribution of Emitters in a Cylindrical Source," J. of Opt. Soc. of America, 52, (8), 885, (1962).

Box, G.E.P. and Behnken, D.W., "Some New Three Level Designs for the Study of Quantitative Variables," Technometrics, 2, 455-475, (1960).

Burns, J., "Research on Effects of Arc Fluctuations on Spectroscopically Determined Temperatures in Arc Plasmas," Air Force Materials Lab., Res. and Tech. Div., Air Force System Command, TDR ML - TDR - 64 - 243, (1964).

Busz-Peukert, G. and Finkelnburg, W., Z. für Physik, 140, 540-546, (1955).

Carleton, F.E., "Flow Patterns in a Confined Plasma Jet," Ph.D. Thesis, University of Michigan, (1970).

Chludzinski, G.R., "Energy Transfer to Solids in R.F. Generated Plasmas," Ph.D. Thesis, University of Michigan, (1964).

Choi, H.K., "Energy Distribution and Heat Transfer in an Argon Transferred-Arc Reactor," Ph.D. Thesis, McGill University, (1980).

Cleeves, V. and Boelter, E.M.K., "Isothermal and Non-Isothermal Air-Jet Investigations," Chem. Eng. Progress, 43, (3), 123, (1947).

Devoto, R.S., "Transport Coefficients of Partially Ionized Argon," The Physics of Fluids, 10, (2), 354, (1967).

Eckert, E.R.G. and Pfender, E., "Advances in Plasma Heat Transfer," Advances in Heat Transfer Vol. IV, 229, (1967), Academic Press, New York.

Eddy, T.L., Pfender, E. and Eckert, E.R.G., "Spectroscopic Mapping of the Nonequilibrium Between Electron and Excitation Temperatures in a 1 Atm Helium Arc," IEEE Trans. on Plasma Science, PS-1, (4), 31, (1973).

Emmons, H.W., "Recent Developments in Plasma Heat Transfer," Modern Dev. in Heat Transfer, ed. Ibele, p. 401, (1963).

Gauvin, W.H., Kubanek, G.R. and Irons, G., "The Plasma Production of Ferromolybdenum - Process Development and Economics," J. of Metals, (1980), (in press).

Grey, J., Jacobs, P.F. and Sherman, M.P., "Calorimetric Probe for the Measurement of Extremely High Temperatures," Rev. Sci. Instrum., 33, (7), 738, (1962).

Grey, J. and Jacobs, P.F., "Experiments on Turbulent Mixing in a Partially Ionized Gas," AIAAJ, 2, (3), 433, (1964).

Grey, J., "Thermodynamic Methods of High-Temperature Measurement," ISA Trans. 4, 102, (1965).

Grey, J., "Proposed Method for Measuring Gas Enthalpy using Calorimetric Probes," ASTM, Committee E-21 on Space Simulation, (1968).

Guile, A.E., IEE Reviews, 118, 1131, (1971).

Hamblyn, S.M.L., "A Review of Applications of Plasma Technology with Particular Reference to Ferro-Alloy Production," National Inst. for Metallurgy, Report No. 1895, (1977).

Johnson, D.C. and Pfender, E., "Modelling and Measurement of the Initial Anode Heat Fluxes in Pulsed High Current Arcs," IEEE Transac. on Plasma Science, PS-7, (1), 44, (1979).

Katta, S., Lewis, J.A. and Gauvin, W.H., "A Plasma Calorimetric Probe," Rev. Sci. Instrum. 44, (10), 1519, (1973).

Kubanek, G.R. and Gauvin, W.H., "Recent Developments in Plasma Jet Technology," The Can. J. of Ch. E., 45, 251, (1967).

Liu, C.H. and Pfender, E., "Heat Transfer in the Anode Region of High Intensity Arcs," published in Studies in Heat Transfer, A. Festschrift for E.R.G. Eckert, Hemisphere Publishing Corp., Washington, (1979).

Lochte-Holtgreven, W., "Plasma Diagnostics," North-Holland Publishing Co., Amsterdam, (1968).

Olsen, H.N., "Determination of Properties of an Optically Thin Ar Plasma," Temperature: Its Measurement and Control in Science, Vol. 3, p. 593, (1962).

Pfender, E., "Electric Arcs and Arc Gas Heaters," Chapter 5 in Gaseous Electronics, Vol. 1, Academic Press, (1978).

Pfender, E., Personal Communication, (December 1979).

Reed, T.B., "Determination of Streaming Velocity and the Flow of Heat and Mass in High-Current Arcs," J. of Appl. Physics, 31, (11), 2048, (1960).

Ruffino, G., "High Speed Radiation Pyrometry," High Temperatures - High Pressures, 8, 143-154, (1976).

Rykalin, N.N., "Plasma Engineering in Metallurgy and Inorganic Materials Technology," Pure and Appl. Chem., 48, 179-194, (1976).

Sayce, I.G., "Plasma Processes in Extractive Metallurgy," Advances in Extractive Metall. and Refining, 27, (1971).

Sayce, I.G., "Some Applications of Thermal Plasmas to Material Processing," paper 107, section 4A, World Electrotechnical Congress, Moscow, (July 1977).

Schoeck, P.A., "An Investigation of the Anode Energy Balance of High Intensity Arcs in Argon," Modern Developments in Heat Transfer, ed. by Ibele, p. 353, (1963).

Shapiro, A.H., "The Dynamics and Thermodynamics of Compressible Fluid Flow," V. 1, Ronald Press, New York, (1953).

Shaer, C., Korman, S., Stojanoff, C.G. and Tschang, P.S., "Diagnostic Study of the Fluid Transpiration Arc," Mechanical Division, Air Force Office of Scie. Res., AFOSR 70-0195 TR, (1969).

Sheer, C., Korman, S. and Kang, S.F., "Investigation of Convective Arcs for the Simulation of Re-entry Aerodynamic Heating," Aeromechanics Div., Air Force Office of Sci. Res., (1973).

Smith, J.L. and Pfender, E., "Determination of Local Anode Heat Fluxes in High Intensity Thermal Arcs," IEEE Transac. on PAS, PAS-95 (2), 704, (1976).

Smith, D.L. and Churchill, S.W., "Mass and Energy Transfer Between a Confined Plasma Jet and a Gaseous Coolant," Technical Report, University of MIchigan, (1965).

Somerville, J.M., "The Electric Arc," Butler and Tanner Ltd., G. Britain, (1959).

Stojanoff, C.G., "Characteristics of an Axially Flow Stabilized Arc and Its Application to the Determination of Transport Properties," Ph.D. Thesis, Stuttgart University, (1968), (in German).

Stojanoff, C.G., "A Transient Fiber Optics Probe for Space Resolved Diagnostics of Dense Plasmas," AIAAJ, 4, (10), 1766, (1966).

Wilkinson, J.B. and Milner, D.R., Brit. Welding, p. 115, (1960).

CONTRIBUTIONS TO KNOWLEDGE

1. A cathode assembly suitable for transferring an arc to a cooled anode or to a molten metal bath and for the injection of fine particles and/or reactive gases has been designed.

2. The electrical, calorimetric and photographic characteristics of the plasma were determined. It was found that the inlet gas velocity of the plasmagen gas past the cathode tip was an important operating parameter and should be used instead of the volumetric gas flow rate alone, if the results are to be generalized.

3. The variation of the voltage gradient in the plasma column with the applied current and gas inlet velocity was determined. It was found that the gradient of the linear portion of the voltage-arc length graphs can be used to calculate the voltage gradient with reasonable accuracy.

4. An electro-optical system capable of measuring the temperature profile of plasmas above 8,000 K with an accuracy of ±8% was developed. The primary advantages of this technique over

the conventional spectroscopic methods are its simplicity and lack of depencency on source symmetry.

5. The basic plasma characteristics, namely, the temperature and velocity, were measured under different operating conditions of current, electrode separation and inlet gas velocity.

6. Conditions under which a secondary gas can be introduced into the plasma have been studied. Lower sheath gas inlet velocities and higher currents encourage the entrainment of this secondary gas into the primary heat dissipation zone.

RECOMMENDATIONS FOR FUTURE WORK

The use of transferred arc plasmas in which the anode consists of a bath of the molten product has only received attention recently for the metallurgical processing of finely-divided materials. The present work constitutes the first published investigation on the diagnostics of a transferred-arc plasma in which the operating parameters have been chosen specifically for their direct applicability to industrial processes. In the light of the availability of simple diagnostic techniques capable of determining plasma characteristics in a short time and with good accuracy, as developed in this work, it is recommended that future research should concentrate on the following subjects:

1. Determination of the optimum conditions for the entrainment of the secondary gas (injection gas) into the plasma. These optimum conditions would probably be in the low main gas inlet velocity and high current range. The effect of the nozzle geometry is expected to be important in the light of the data obtained in this work. If the plasmagen gas and the secondary gas are chosen to be different, their respective temperatures can be

determined from their line intensities. If the concentration profiles can also be obtained (say by sampling through the anode centre hole) mass and energy transfer phenomena can be understood quite clearly.

2. Determination of the plasma characteristics while operating in a closed chamber. This should be compared with the present results to see the effect of the operation in confined conditions. It should be added that the techniques developed in this work can easily be applied to a closed system with some small modifications.

3. Study of the motion of particles entrained in the transferred arc plasma. It is expected that the size distribution of the particles will be an important factor in determining the efficiency of entrainment. Too large particles will not be feasible for industrial applications due to short residence times encountered. On the other hand, very small particles will be subjected to thermophoretic effects which will inhibit their penetration into the plasma column.

4. Investigation of the behaviour of the transferred arc plasmas with gases other than argon and with molten metal baths used as the anode. Diagnostic techniques should be developed to be used in the neighborhood of the anode.

APPENDICES

APPENDIX A

ABEL INVERSION TECHNIQUE

ABEL INVERSION TECHNIQUE

The Abel inversion is used whenever data obtained in integral form along a chord segment through an axissymetric medium must be resolved into the true radial distribution. The inversion in the case of plasma radiation is expressed analytically by:

$$\varepsilon(r,z) = -1/\pi \int_r^R (dI/dx)\, dx/(x^2-r^2)^{1/2} \qquad \text{(A-1)}$$

As noted in the Literature Review section, since $\underline{I}$ is obtained as numerical data, it is more convenient to use a numerical technique to perform the inversion. In this thesis, the method described by Barr (1962) is used when the results obtained by the "sweeping blocking element technique" were to be compared with the side-on spectroscopic measurements.

Since $\underline{I}$ is a set of numerical data, it is advantageous to reverse the order of differentiation and integration in Equation (A-1) if the functions are well behaved. This would smooth the data before differentiation and reduce amplification of noise in the data. Thus, if the functions are well behaved, Equation (A-1) can be written as:

$$\varepsilon(r,z) = -1/2\pi r \cdot dF(r,z)/dr \qquad \text{(A-2)}$$

where

$$F(r,z) = 2 \int_r^R I(x,z)x\, dx/(x^2-r^2)^{1/2} \qquad \text{(A-3)}$$

The x axis and hence r is divided into N equal intervals Δ so that:

$$x_n = n\,\Delta \tag{A-4}$$

and $$r_k = k\,\Delta$$

where $$\Delta = R/N \tag{A-6}$$

and n and k are integers between and including 0 and N. In each interval $I(x,z)$ is approximated by:

$$I(x,z) = a_n + b_n x^2 \tag{A-7}$$

The coefficients a_n and b_n are determined by requiring that:

$$I(x_n,z) = I(n,z) \tag{A-8}$$

and $$I(x_{n+1},z) = I(n+1,z) \tag{A-9}$$

where $I(n,z)$ and $I(n+1,z)$ are the measured numerical values at x_n and x_{n+1}, respectively.

For: $$r = r_k \tag{A-10}$$

Equation (A-3) can then be written as

$$F(k,z) = \Delta \sum_{n=k}^{N} \alpha_{kn}\, I(n,z) \tag{A-11}$$

where α_{kn} are positive, slowly varying functions of k and n only. The $F(k,z)$ are relatively insensitive to small random errors in the $I(n,z)$. In order to perform the differentiation of Equation (A-2),

a polynomial is fitted to each section of the $F(k,z)$ versus k curve. This process also smooths the data. Thus, the $F(k,z)$ are represented by:

$$F(k,z) = (A_k + B_k\, k^2 + C_k\, k^4)\, \Delta \qquad \text{(A-12)}$$

Equation (A-2) then takes the form:

$$\varepsilon(k,z) = -1/(2\pi\Delta^2 k) \cdot dF(k,z)/dk \qquad \text{(A-13)}$$

A least squares technique is used to determine the coefficients. As a result, a new set of coefficients β_{kn} is obtained such that:

$$\varepsilon(k,z) = 1/\pi\Delta \cdot \sum_{n=k-2}^{N} \beta_{kn}\, I(n,z) \qquad \text{(A-14)}$$

for $k > 2$, and:

$$\varepsilon(k,z) = 1/\pi\Delta \sum_{n=o}^{N} \beta_{kn}\, I\,(n,z) \qquad \text{(A-15)}$$

for $k \leq 2$.

The complete sequence of steps - integration, least squares fit, and final differentiation - is included in the β_{kn}, which have been evaluated and tabulated by Barr for N up to 20.

To check the accuracy of the inversion, a simple analytical distribution for $\varepsilon(r,z)$ was assumed and an analytic relationship for $I(x,z)$ determined. Discrete values of $I(n,z)$ were then calculated and used to evaluate the $\varepsilon(k,z)$ profile by means of the numerical method. The numerical values of $\varepsilon(k,z)$ are compared with those calculated from the analytic function $\varepsilon(r,z)$ in Table A-I for a

20-zone inversion. The assumed analytic distribution was:

$$\varepsilon(r,z) = 1600\ (1-x^2) \qquad \text{(A-16)}$$

for which the analytic chord distribution is

$$I(x,z) = 3200\ \pi^{-1}\ (1-r^2)^{1/2} \qquad \text{(A-17)}$$

It can be seen that the agreement between analytical and numerical values are satisfactory at all radial positions except the last.

TABLE A-I

ACCURACY TEST FOR ABEL INVERSION TECHNIQUE

$\varepsilon(r,z)$

Analytical	20 Zone
1018.592	1020.155
998.012	997.988
909.631	907.898
727.420	725.310
318.055	283.128
0.000	144.762

APPENDIX B

SPECIFICATIONS OF THE CATHODE ASSEMBLY COMPONENTS

SPECIFICATIONS OF THE CATHODE ASSEMBLY COMPONENTS

In actual industrial applications, especially when a molten-type of anode is to be used, it would be easier to move the cathode assembly rather than the anode. Since a closed reactor would be employed in such cases, the cathode assembly should have a length greater than the arc length expected to be achieved. This would also imply that the outer surface of the assembly has to be cooled to avoid over heating due to convective and radiative heat transfer.

The plasma-forming gas and the particles to be processed would have a greater chance of penetration into the primary energy dissipation zone if they are directed towards the cathode attachment of the arc, since an inwardly-directed pressure gradient exists here (Maecker, 1955). This is most easily achieved by employing an annular orifice surrounding the cathode tip and by providing inlet channels for the particles around the nozzle.

In the light of the above considerations, a cathode assembly suitable for operation in the transferred-arc mode and for injection of fine particles or of a secondary gas, other than the main plasma forming gas, has been designed. The assembly, shown in Figure B-1, consisted of four major parts: the lower distributor plate (nozzle), the upper distributor plate, the end caps and the cathode tip cooling and support piece. While the distributor plates direct the water and the primary and secondary

FIGURE B-1

DETAILED DRAWING OF THE

CATHODE ASSEMBLY

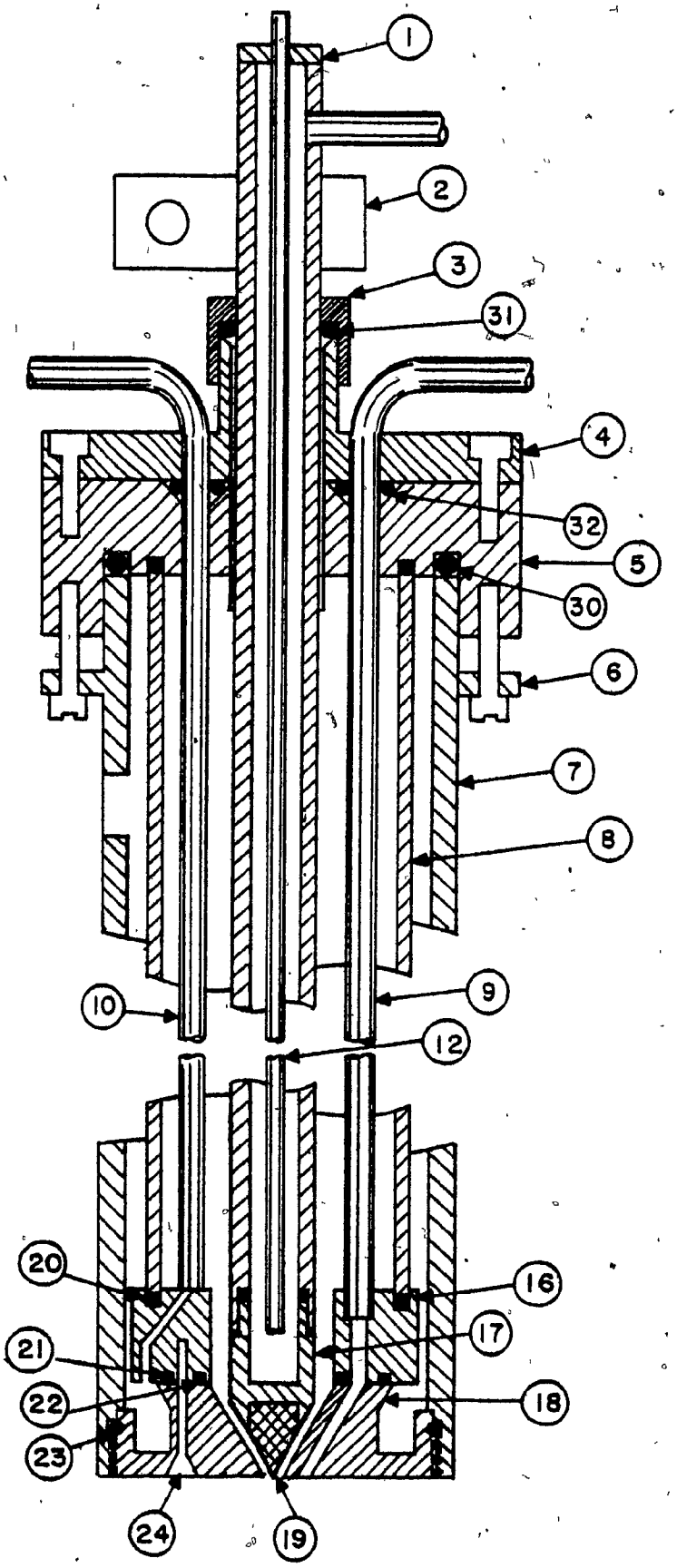
1
2
3
31
4
32
5
30
6
7
8
9
10
12
20
16
17
21
22
18
23
24
19

gas feeds, the end caps close the assembly at the top and help support the long feed tubes. The cathode-cooling system was designed to give maximum cooling in the form of an impinging water jet. The pressure drop calculations dictated the size of tube diameters to be used. Table B-I gives the materials of construction as well as the important dimensions of the parts of the cathode assembly shown in Figure B-1.

References

Maecker, H., "Plasma Streams Produced by Self-Magnetic Compression and Its Importance for the Mechanism of High Current Arcs," Appl. Sci. Res. 5, 231-236, (1955).

TABLE B-I

MATERIALS OF CONSTRUCTION OF THE CATHODE ASSEMBLY

Part*	Material
1. Cathode support	Copper tube (1.71 cm o.d., 1.07 cm i.d.)
2. Electrical connector	Copper strip
3. Sealing plate nut	Brass
4. Sealing plate	Phenolic board
5. End cap	Phenolic board
6. End cap support ring	316 stainless steel
7. Outer shell	316 stainless steel (2-½" sch. 40)
8. Inner shell	Copper tube (2" type K)
9. Powder feeding tube (3)	Copper
10. Water inlet tube (2)	Stainless steel
11. Spacer (2 - not shown)	Teflon
12. Cathode cooling tube	Stainless steel
13. Cathode assembly support nipple (not shown)	Teflon
14. Cathode assembly support ring (not shown)	Aluminum
15. Support ring centering screws (not shown)	
16. Upper distributor plate	Brass
17. Cathode	Brass
18. Lower distributor plate	Brass
19. Cathode tip	Tungsten
20. Inner shell 'O' rings (2) No. 033	
21. Outer distributor plate 'O' ring (1) No. 031	
22. Inner distributor plate 'O' ring (1) No. 024	

TABLE B-I

MATERIALS OF CONSTRUCTION OF THE CATHODE ASSEMBLY

- Continued -

Part *

23. Lower outer shell '0' ring (1) No. 143
24. Distributor plate retaining screws (3)
25. Cathode holder '0' ring (1) No. 013
26. End cap retaining screws (6)
27. Lift system connection to support ring (6) (not shown)
28. Wrench to tighten the lower distributor plate (not shown)
29. Water outlet connection to outer shell (not shown)
30. Upper outer shell '0' ring (1) No. 337
31. Sealing plate nut '0' ring (1) No. 116
32. Feed tube sealing '0' ring (6) No. 010

- - - - - -

* Numbers refer to Figure B-1

Note

All '0' rings - neoprene (National '0' rings)

APPENDIX C

TOTAL EMISSION COEFFICIENT CALCULATIONS

TOTAL EMISSION COEFFICIENT CALCULATIONS

The line emission coefficient for a spectral line is given by:

$$\varepsilon_{line} = hc/(4\pi\lambda) \cdot g_n A_{nm} \cdot (N_a/U_a) \exp(-E_n/kT) \qquad (C\text{-}1)$$

Table C-I below gives the characteristic constants for the lines 4806.90 Å and 6965.43 Å. The values presented were taken from Adcock and Plumtree (1964) who summarized the various determinations of argon transition probabilities. The values of Olsen (1959) are considered to be the most consistently reliable and are the ones listed in Table C-I.

Using these constants and the tabulated values of N_a and U_a as a function of temperature at one atmosphere given by Olsen (1959), the temperature variation of ε_{line} was calculated for 4806 Å and 6965 Å lines.

For the continuum emission coefficients the following equation was used:

$$\varepsilon(\nu,T_e) = C_1 N_e/(T_e)^{1/2} \Sigma z^2 N_z [G_z(\nu,T_e)\exp(-h\nu/kT_e) + \zeta_z(\nu,T_e) g_z/U_z \, (1-\exp(-h\nu/kT_e))] \qquad (C\text{-}2)$$

The tabulated values of n_e cited above were used together with the correction factors obtained from Schlüter (1965) and Schnapauff (1968) to calculate the variation with temperature of the continuum emission coefficients at 4806 Å and 6965 Å (for 20 Å

TABLE C-I

SPECTRAL LINE CONSTANTS

Line Å	g_m	A_{nm} 10^5 sec^{-1}	g_m A_{nm} 10^5 sec^{-1}	E_n ev
4806.90	6	786	4716	19.22
6965.43	3	53.1	159.3	13.33

bandwidth).

The line emission coefficients and continuum emission coefficients were used to calculate the dependency of the total emission coefficients which is shown in Figure C-1.

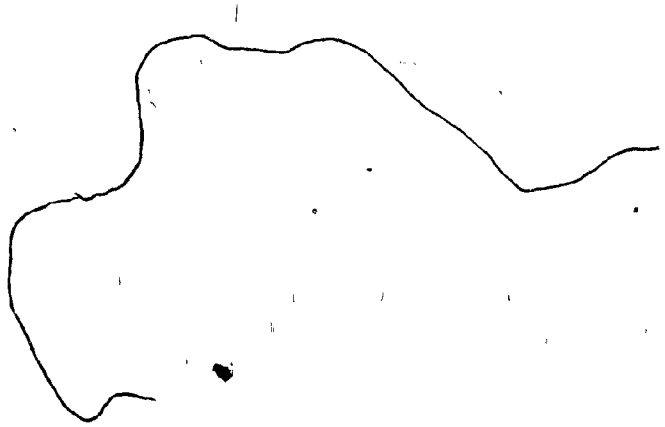

FIGURE C-1

TOTAL EMISSION COEFFICIENT OF ARGON
FOR 4806 Å AND 6965 Å LINES AS
A FUNCTION OF TEMPERATURE

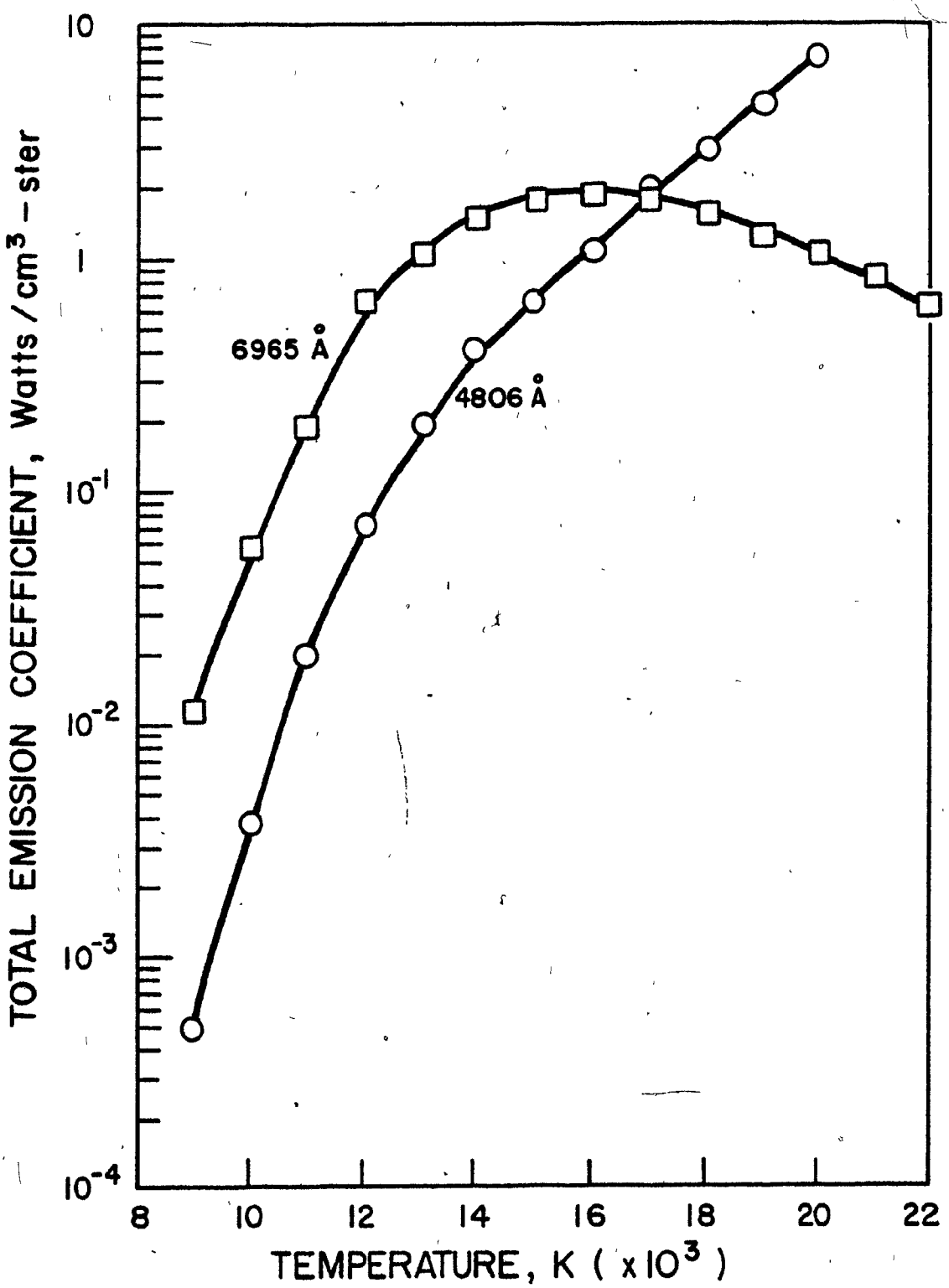
10
1
10^{-1}
10^{-2}
10^{-3}
10^{-4}
TOTAL EMISSION COEFFICIENT, Watts / cm^3 – ster
6965 Å
4806 Å
8
10
12
14
16
18
20
22
TEMPERATURE, K (x 10^3)

A P P E N D I X D

EXPLANATION AND LISTING OF THE COMPUTER PROGRAM FOR TEMPERATURE DATA ANALYSIS

EXPLANATION AND LISTING OF THE COMPUTER PROGRAM FOR TEMPERATURE DATA ANALYSIS

General

A computer program written in ASSEMBLER and BASIC was used to process the data by a Commodore PET minicomputer. The object of the program was:

a. Transfer data as stored in memory on a GOULD model OS4000 oscilloscope to read/write memory locations 6912 to 7935 in the PET minicomputer.

b. Reproduce graphically the transferred data.

c. Differentiate and smooth the data by using the Convolution Integers Method (described at the end of this Appendix section).

e. Calculate the temperature at each data point using the regression equation previously described.

f. Plot and tabulate the temperature profiles.

Only the part of the program which describes the data transfer will be described below and the listing of the computer program will be given afterwards.

Transfer of Data

An ASSEMBLER routine is responsible for the transfer of data from the oscilloscope to the minicomputer. The program is

loaded and executed via the BASIC program "GOULD-TEMP."

Line number 1 of the program requests if new data are to be transferred from the oscilloscope or if data previously transferred are to be manipulated. If new data are to be transferred, then line 100 of "GOULD-TEMP." loads the assembler language instructions given as data in lines 10 to 40 into the second cassette buffer (locations 826 to 885 of the PET's memory). Line 120 then transfers control to the assembler program at memory address 826.

The assembler program transfers data into memory addresses 6912 to 7935 (BASIC text random access memory). A datum is transferred when PET senses a low state on the IEEE - EOI line of the "parallel user port" (the high-low state is achieved through a pulse shaping interface between the oscilloscope and the user port). A high state resets the assembler routine for transfer of the next datum.

Data transfer alternates between channels one and two of the oscilloscope. The BASIC program decodes the data after transfer to separate two channels.

LISTING OF "GOULD-TEMP."

```
1  DIM A(72), W(10), D(66), T(36): ? "CLEAR" : INPUT "NEW
   DATA Y/N"; A1$:INPUT" EXP. NO"; E$
2  INPUT "LIMITS OF CALC. AS CM ON OSC"; LL, UL
```

```
  3 INPUT "DECREASE (-1) OR INCREASE (+1)"; S:INPUT "PLOT OF THE
    DERIVATIVES Y/N"; A3$
  7 INPUT "OSC SPEED, MS/CM & LIN. MOTOR SPEED, CM/SEC"; O, L1
  8 INPUT "RANGE TO PLOT FOR TEMP."; RL, RH:PRINT" PRESS OSC
    BUTTON"
  9 IF A1$ <> "Y" GO TO 140
 10 DATA 162, 27, 160, 0, 76, 104, 3, 234, 234, 234, 234,
 20 DATA 234, 234, 205, 80, 232, 16, 3, 76, 71, 3, 173, 79, 232,
    141, 0, 27
 30 DATA 200, 140, 83, 3, 192, 0, 240, 3, 76, 104, 3, 232, 142,
    84, 3, 224, 31, 240, 13
 40 DATA 169, 200, 205, 80, 232, 48, 3, 76, 106, 3, 76, 69, 3, 96
100 FOR I = 826 to 885 : READ N : POKE I, N : NEXT I
120 SYS (826)
140 LL = LL * 51 : UL = UL x 51 : A = 6912 : G$ = "plotting graphics":
    DX = INT (UL - LL) / 36)
170 XH = LL + DX * 36 : IF x H > UL THEN DX = DX - 1 : GO TO 170
180 XL = INT (DX/2)
190 ? "CLEAR"; XL + LL; "(XL ="; XL;"): TAB (16); "DX ="; DX;
    "EXP #"; E$; TAB (34); XH
195 FOR I = 1 TO 36: K = 0: P = ((I - 1) * DX + INT (LL/2) *2) *2
200 PRINT "HOME"; TAB (I);: N =0: V =0; FOR J =0 TO DX *2 - 2 STEP
    2: V = V + 1
210 N = N + PEEK (A + P + J + K) : NEXT J
220 A ( I + K * 36) = N/V : N = N/11/V: R = N - INT (N)
240 FOR J = 1 TO N : ? "down"; : NEXT J
```

```
250 ? MID $ (G$, R*8 + 1, 1) : K = -1 * (K = 0) : IF K = 1
    GOTO 200
260 NEXT I : C$ = TIME $
265 GET H$ : IF H$ <>" "GO TO 280
270 IF (-VAL (C$) + VAL (TIME $)) <30 GOTO 265
280 IF A1$ = "Y" GO TO 310
290 FOR I = 1 TO 60 : READ X : NEXT I
310 D(1)=0 : FOR I = 1 TO 5 : READ W (I) : NEXT I : READ F :
    (D(1) = 0 : D(34) = 0
320 ? "CLEAR";"DIFFERENTIATION IN PROGRESS"; "-"; K1 + 1 : FOR I
    = 1 TO 32 : P = 0
330 FOR J = 0 TO 4: LJ = I + J + K1 *36: P = P + W (J + 1) *
    A(LJ) : NEXT J : B = I + K1 * 33 + 1 : B1 = B - 1
340 D(B) = -S * P/F : IF P * S > 0 THEN D(B) = D(B1)
350 NEXT I : K1 = -(K1 = 0) : IF K1 = 1 GO TO 320
360 IF A3$ = "N" GO TO 460
370 ? "CLEAR"; XL + LL; TAB (16); "DX ="; DX; "EXP.#"; E$;
    TAB (34); XH; FOR I = 1 TO 32 : K=0
380 ? "HOME"; TAB (I + 2) : N = (255 - INT(D(I + 1 + K * 33) *25)
    /22 : IF N < 0 THEN N = 0
390 FOR J = 1 TO n - 12 * (K = 0) : ? "DOWN"; : NEXT J
400 ? MID $ MID $ (G$, R * 8 + 1, 1) : "DOWN" : K = -1 * (K = 0)
    : IF K = 1 GO TO 380
410 NEXT I : R$ = TIME $
420 GET Q$ : IF Q$ <> "" GO TO 460
430 IF (VAL (TIME $) - VAL (R$)) <0 GO TO 420
```

```
460  ? "CLEAR";"TEMP. CALC. IN PROGRESS"
470  FOR I = 1 TO 32 : IF D (I + 1) * D(I + 33)=<0 GO TO 490
475  R = D(I + 33) / (1.5345 * D(I +1)) : IF R < = 0.322 GO TO 485
480  T(I) = 10  (4.22836 + 0.08902 *LOG (R) / LOG (10)) : GO TO 490
485  T(I) = 10   (4.30055 + 0.24978 * LOG (R) / LOG (10))
490  NEXT I
500  NT = INT ((RH - RL) *51 *32 / (UL - LL)) : IF INT (32/NT)
     < = 1 GO TO 549
510  ? "CLEAR"; RL; TAB (16); "DX="; DX; "EXP #"; E$; TAB(34);
     RH : Q = 0
515  Z = INT (0 * L1 * (RH - RL)/32) : FOR I = 1 TO 32: ? "HOME";
     TAB (I + 1)
516  IF (I - 1) / INT (32/NT) = INT ((I - 1) / INT (32/NT)) GO TO
     525
520  N1 = T (1 + INT ((RL * 51 - LL) *32 / (UL - LL)) + Q) / 100 :
     IF N1 < 0 THEN N1 = N
521  IF N1 < 220 THEN N1 = 220
522  N = (N1 + N)/2 : GO TO 530
525  N = T(1 + INT (RL *51 - LL) *32/(UL - LL)) + Q)/100 :
     Q = Q + 1 : N = -(N > 0) * N : IF N > 220 THEN N = 220
530  M = (220 - N) /6.5 : R1 = M - INT (M) : IF M > 22 THEN M = 22
535  FOR J = 1 TO M + 1 : ? "DOWN"; : NEXT J
540  ? MID$ (G$, R1 * 8 + 1, 1) : NEXT I
542  ? "HOME"; : FOR K = 0 TO 22 STEP 2 : ? "DOWN"; (220 - K * 65):
     NEXT K
543  ? "HOME"; : FOR I = 1 to 24 : ? "DOWN"; : NEXT I
```

```
544  FOR J = 0 TO 32 STEP 8 : ? TAB (J + 1 + (J > 0)) : J * Z / 100;
     : NEXT J
545  GET Q$ : IF Q$ = "" GO TO 545
546  GO TO 565
549  Z = INT (0 * L1 * (XH - (XH + LL)) / 32 / 51)
550  ? "CLEAR"; XL + LL; TAB (16); "DX=" ; DX ; "EXP#"; E$; TAB
     (34); XH : FOR I =1 TO 32
552  ? "HOME"; TAB (I + 1) : N = (220 - T(I)/100)/6.5 : R1 = N -
     INT (N) : IF N = > 22 THEN N = 22
553  FOR J = 1 TO N + 1 : ? "DOWN"; : NEXT J
555  ? MID $ (G$, R * 8 + 1, 1); "UP" : NEXT I
556  ? "HOME"; : FOR K = 0 TO 22 STEP 2 : ? "DOWN"; (220 -K * 6.5):
     NEXT K
557  ? "HOME"; : FOR I = 1 TO 34 :   ? "DOWN" ; : NEXT I
558  FOR J = 0 TO 32 STEP 8 : ? TAB (J + 1 + (J > 0)) ; J * Z/100 :
     NEXT I
560  GET Q$ : IF Q$ = "" GO TO 560
565  ? "CLEAR" ; TAB (15); "EXP.#" ; E$ ; "RL= " ; RL; "RH="; RH;
566  ? INT (RL * 51 - LL) * 32 / (UL - LL)) : ? TAB (2) ; "R, MM
     T °K" ; TAB (16) ; "R, MM T°K"
580  FOR L = 0 TO 32 : R = Z x L / 100 : IF L > 21 GO TO 600
590  ? TAB (2) ; R ; TAB (6) ; INT (T(L)) : GO TO 650
600  ? "HOME" ; : FOR N = 1 TO L - 19 ? "DOWN"; : NEXT N : ? TAB
     (16); R; TAB (20); INT (T(L))
650  NEXT L
660  GET J$ : IF J$ = "" GO TO 660
```

```
670  ? "CLEAR" : INPUT "NEW RANGE FOR PLOTTING TEMPERATURE"; RL,
     RH : GO TO 500
700  DATA - 2, -1, 0, 1, 2, 10
```

Convolution Integers Method

The Convolution Integers Method is a generalized form of the Moving Average Method in which the average of a certain set of data points is assigned to the centre abscissa. Then, the set moves one data point in one direction and the procedure is repeated. In the Moving Average Method, the same weight is given to all the data points, however, in the Convolution Integers Method, the weight given to each point is different. This technique resembles the least square fit procedure, applied to the central point only. If the evaluation of the function only at the centre point of a set of equally spaced observations is considered, then there exists sets of convoluting integers for the first derivative as well. A complete set of tables for derivatives up to the fifth order, for polynomials up to the fifth degree, using from 5 to 25 points, has been given by Savitzky and Golay (1964). In the present work, the integers for first derivative for a quadratic fit and for a set of five points was used.

References

Savitzky, A. and Golay, M.J.E., "Smoothing and Differentiation of Data by Simplified Least Squares Procedures," Analytical Chemistry, 36 (8), 1629 (I964)

APPENDIX E

TOTAL ARC VOLTAGE DATA

TOTAL ARC VOLTAGE DATA

TABLE E-I

VOLTAGE RECORDINGS FOR SET I

Annular Area : 0.0085 - (0.070) - 0.055 cm^2

Q L/m	I A	ℓ cm	V v	Q L/m	I A	ℓ cm	V v
14	150	4	58-(64) - 68	14	350	4	59.5-(65)- 66
17	150	4	62-(68) - 72	17	350	4	60-(66)- 67
20	150	4	66-(72) - 76	20	350	4	60.5-(67)- 68
14	150	6	80-(84) - 85	14	350	6	72-(81)- 86
17	150	6	82-(88) - 88	17	350	6	76-(83)- 88
20	150	6	88-(92) - 94	20	350	6	78-(84.5)- 90
14	150	8	95-(100) -101	14	350	8	88-(94)- 98
17	150	8	98-(104) - 96*	17	350	8	90-(98)-100
20	150	8	103-(107) -100*	20	350	8	93-(100)-102
14	150	10	110-(92) - 59*	14	350	10	100-(115) ?
17	150	10	110-(9.4) - 62*	17	350	10	103-(?) ?
20	150	10	?-(96) - 64*	20	350	10	107-(?) ?
14	250	4	59-(62) - 68				
17	250	4	60-(63) - 70				
20	250	4	61-(64) - 71.5				
14	250	6	74-(80) - 82				
17	250	6	76-(82) - 84				
20	250	6	78-(84) - 86				
14	250	8	87-(92) - 98				
17	250	8	90-(96) -100				
20	250	8	94-(98) -102				
14	250	10	102-(100)*-110*				
17	250	10	105-(102)*-114*				
20	250	10	110-(105)*-116*				

* value taken for a shorter arc length

TABLE E-II

POTENTIAL DISTRIBUTION vs ARC LENGTH DATA

Condition	z cm	V v	Condition	z cm	V v	Condition	z cm	V v
1	0.4	17	5	0.4	18	8	0.4	22
	0.5	22		0.5	23		0.5	24
	1.0	26.5		1.0	28		1.0	29
	2.0	33.5		2.0	36.5		2.0	36
	3.0	41		3.0	43.5		3.0	44
	3.5	45		3.5	47.5		4.0	50
	4.0	60		4.0	59.5		5.0	51
							6.0	64
							7.0	71
							7.5	74
							8.0	84
2	0.4	16	6	0.4	17	9	0.4	27
	0.5	20		0.5	21		0.5	30
	1.0	24		1.0	24		1.0	35
	2.0	31.5		2.0	33		2.0	42
	3.0	38		3.0	39		3.0	50
	3.5	42		3.5	42.5		3.5	53
	4.0	58		4.0	58.5		4.0	63
3	0.4	19	7	0.4	22	10	0.4	25
	0.5	23		0.5	25		0.5	27
	1.0	29		1.0	28		1.0	30
	2.0	36.5		2.0	35		2.0	40
	3.0	44		3.0	42.5		3.0	47.5
	3.5	48		4.0	50		3.5	52
	4.0	65		5.0	58		4.0	61
				5.5	62.5			
				6.0	76			
4	0.4	18						
	0.5	22						
	1.0	27.5						
	2.0	35						
	3.0	42.5						
	3.5	46						
	4.0	63						

APPENDIX F

PROPERTIES OF ARGON

PROPERTIES OF ARGON

In Figures F-1, F-2 and F-3, the Electrical Conductivity (stat mho/cm), the compressibility and dimensionless enthalpy of argon as a function of temperature are given. The values are that given by Ahtye (1965).

FIGURE F-1

ELECTRIC CONDUCTIVITY OF ARGON

versus

TEMPERATURE

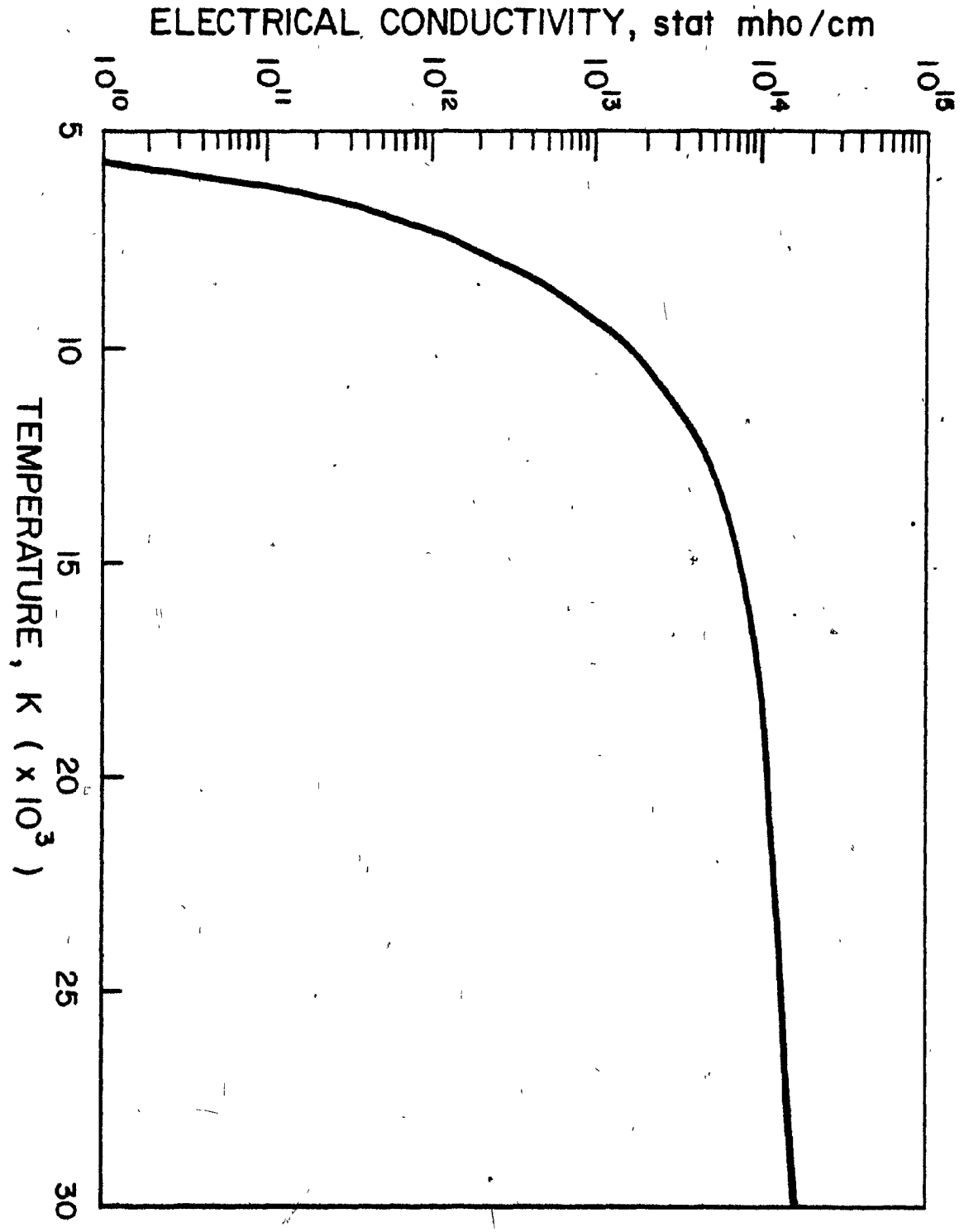
ELECTRICAL CONDUCTIVITY, stat mho/cm
10^{10}
10^{11}
10^{12}
10^{13}
10^{14}
10^{15}
5
10
15
20
25
30
TEMPERATURE, K (x 10^3)

FIGURE F-2

COMPRESSIBILITY OF ARGON

versus

TEMPERATURE

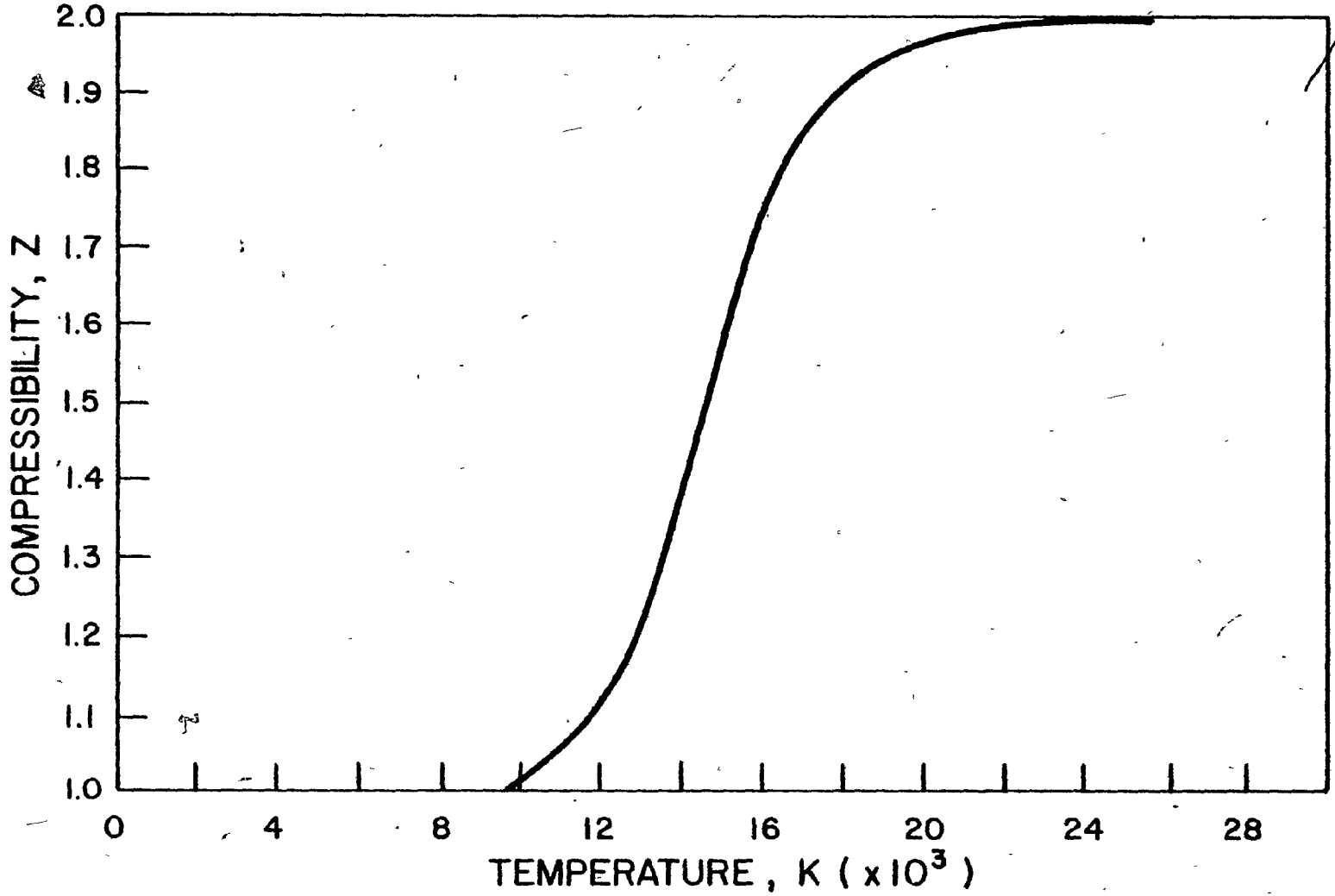
2.0
1.9
1.8
1.7
1.6
1.5
1.4
1.3
1.2
1.1
1.0
COMPRESSIBILITY, Z
0
4
8
12
16
20
24
28
TEMPERATURE, K (x10³)

FIGURE F-3

DIMENSIONLESS SPECIFIC ENTHALPY OF ARGON

versus

TEMPERATURE

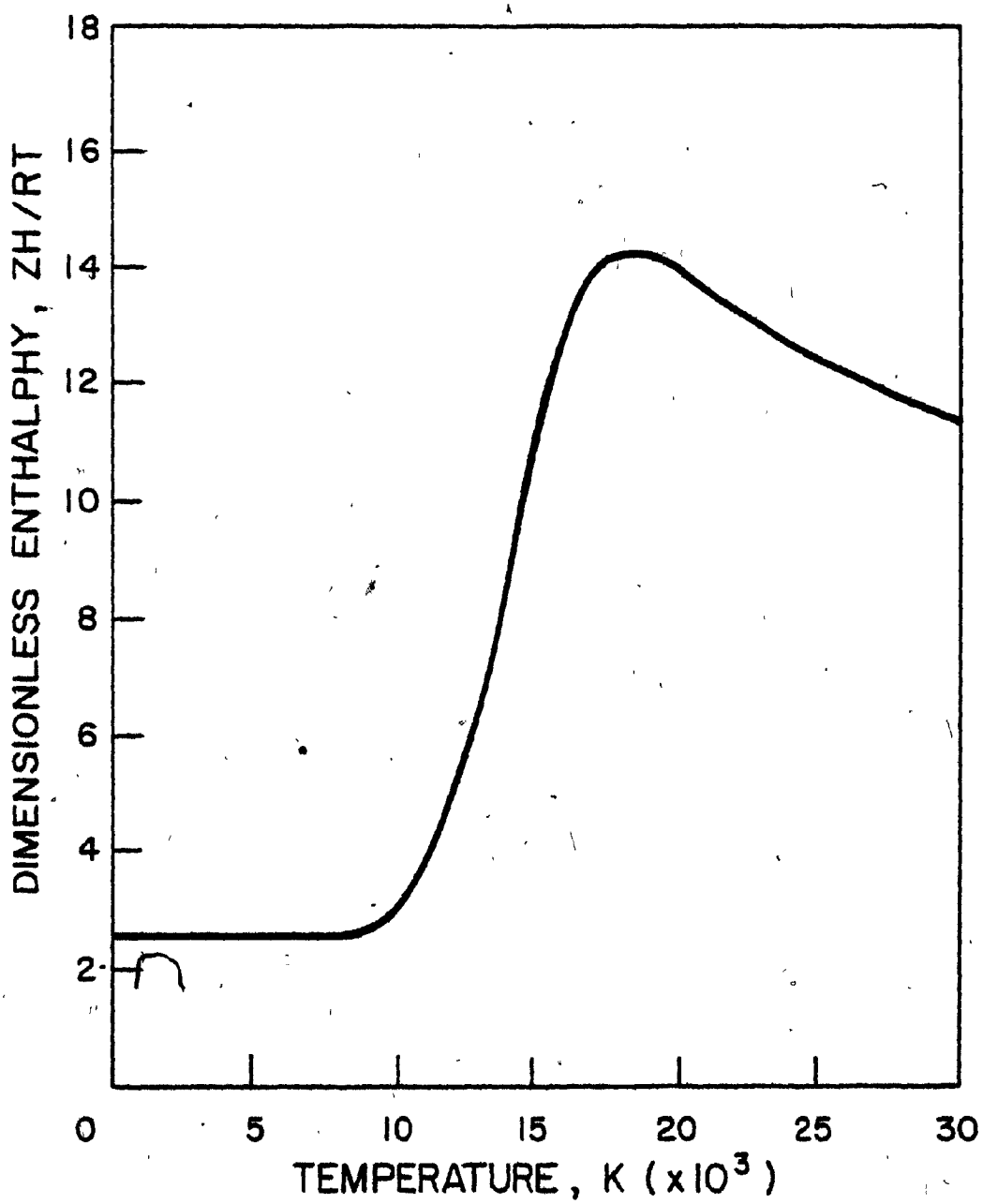
DIMENSIONLESS ENTHALPHY, ZH/RT
18
16
14
12
10
8
6
4
2
0
5
10
15
20
25
30
TEMPERATURE, K (x10³)

APPENDIX G

CALORIMETRIC RESULTS

TABLE G-I

RAW CALORIMETRIC DATA

Run	v* m/s	Cathode Tip Water ΔT °C	Cathode Tip Water Flow Rate g/m x 10^{-3}	Nozzle Water ΔT °C	Nozzle Water Flow Rate g/m x 10^{-3}	Anode Water ΔT °C	Anode Water Flow Rate g/m x 10^{-3}
Electrode Separation: 4 cm					**Applied Current: 250 A**		
1	16.65	5.0	1.30	9.1	1.79	5.2	15.89
2	16.65	5.5	1.18	8.6	1.95	15.0	5.28
3	33.30	2.4	2.59	9.0	1.95	4.7	18.13
4	33.30	5.0	1.29	8.5	2.04	10.0	8.52
5	49.95	5.0	1.18	9.5	1.95	7.5	12.27
6	49.95	5.0	1.18	9.1	2.04	17.5	5.28
Electrode Separation: 4 cm					**Applied Current: 350 A**		
7	16.65	3.8	2.59	14.0	1.68	9.5	12.27
8	16.65	6.0	1.62	14.8	1.59	9.5	12.27
9	33.30	3.6	2.59	14.3	1.77	6.5	18.29
10	33.30	7.5	1.25	13.0	1.95	22.5	5.28
11	49.95	6.4	1.25	14.7	1.77	9.7	12.27
12	49.95	6.3	1.25	13.3	1.95	13.9	8.52
Inlet Gas Velocity: 33.30 m/s					**Applied Current: 350 A**		
	L, cm						
13	6	7.7	1.25	14.8	1.86	12.1	12.27
14	6	8.0	1.18	15.3	1.77	17.4	8.52
15	8	8.0	1.18	16.8	1.68	13.0	12.27
16	8	7.9	1.18	17.3	1.63	12.9	12.27

Error Analysis

The amount of heat released at a component of the transferred-arc assembly was calculated from the equation:

$$P = \dot{m}_w C_{pw} \Delta T_w \qquad \text{(G-1)}$$

The error in such a measurement can be expressed by:

$$dP = C_{pw} \Delta T_w \, d\dot{m}_w + \dot{m}_w C_{pw} \, d\Delta T_w + \dot{m}_w \Delta T_w \, dC_{pw} \qquad \text{(G-2)}$$

where $d\dot{m}_w$ refers to the error in the measurement of the water flow rate and so forth. Typical values of the variables and the estimate of the maximum error in the measurements are given below.

Cathode Tip

$$\Delta T_w = 6.3\ ^\circ C\ , \quad d\Delta T_w = 0.25\ ^\circ C$$

$$\dot{m}_w = 0.999\ cal/g^\circ C\ , \quad dC_{pw} = 0.001\ cal/g^\circ C$$

Nozzle

$$\Delta T_w = 13.3^\circ C\ , \quad d\Delta T_w = \text{same as above}$$

$$\dot{m}_w = 1.95 \times 10^3\ g/m\ , \quad d\dot{m}_w = \text{same as above}$$

Anode

$$\Delta T_w = 13.9^\circ C\ , \quad d\Delta T_w = \text{same as above}$$

$\dot{m}_w = 8.52 \times 10^3$ g/m , $d\dot{m}_w = 20$ g/m

From these values, the following results were obtained:

Cathode Tip

P = 0.54 kW; dP = 0.025 kW; % Error = 4.78%

Nozzle

P = 1.79 kW; dP = 0.0468 kW; % Error = 2.62%

Anode

P = 8.17 kW; dP = 0.165 kW; % Error = 2.02%

In all cases, the major source of error was due to errors in the measurement of temperature.

Nomenclature

Symbol	Meaning	Units
C_p	heat capacity	cal/g°C
$\dot{m}$	mass flow rate	g/m
ΔT	temperature difference	K
P	power	cal/s or kW

Subscripts

w	water